The Occurrence and Mobility of Arsenic in Soils and Sediments: Assessing Environmental Controls

A thesis submitted to the University of Manchester for the degree of Doctor of Philosophy in the Faculty of Engineering and Physical Sciences

2012

Aimee Fleur Hegan

School of Earth, Atmospheric and Environmental Sciences

Table of Contents

Final Word Count: 78,352 words

List of Tables

List of Figures

Abstract

Elevated levels of arsenic (As) in soils and water around the world are both a significant human health and environmental hazard. With increasing global water demands, there is a requirement to further the understanding of the biogeochemical cycling of As from soils and sediments. This thesis focussed on exploring the environmental controls on the occurrence and subsequent mobility of As in a range of natural environments. Arsenic was found to undergo mobilisation from both river sediments and upland peats under changing environmental conditions. The transport of As was found to be correlated with both iron (Fe) and organic carbon (OC), however temporal changes in both sediment/soil composition and movement of water through catchments have a important role in controlling the ultimate transport of As within the environment. A range of investigative methods were employed to study the occurrence and mobility of As within the river sediments of the Allier and Loire Rivers (France), including sequential extraction procedures and batch incubation studies. Arsenic was associated with the reducible phases of sediments, indicating the major role of Fe(oxy)hydroxides in the storage of As in river sediments. In addition to the presence of labile As, the rapid release of As was dependent on the initial sediment composition. Temporal changes in sediment composition may therefore play an important role in controlling the movement of As within fluvial systems.

The combination of lead (Pb) and strontium (Sr) isotopic analysis with sequential extraction studies of sediments from the Loire and Allier Rivers was able to determine the relative dominance of granites and basalts within the sediments. This approach provided a first order study on which to better understand the mineral origins of the sediments. The analysis of multiple Pb isotopes was able to eliminate possible anthropogenic contribution to contamination within the sediments, confirming the importance of geogenic cycling of As within the rivers. Information on the origin of mineral formation was obtained through $^{87}Sr/^{86}Sr$ isotopic analysis, with the formation of Fe-minerals not occurring uniformly along the course of the rivers. While the Sr within the sediment phase targeting well-crystallised Fe(oxy)hydroxides was in equilibrium with the sampled river water, the formation of amorphous Fe minerals was likely occurring in waters upstream of the study sites, within the Massif Central.

Total concentration profiles peat from two subcatchments within the Peak District (United Kingdom) provided evidence for both the retention and post depositional movement (PDM) of As within the solid phase, dependent on local conditions. For the first time, the partitioning of As was determined within ombrotrophic peat, and found to be in contrast to Pb, with oxidisible As (likely associated with organic matter) dominating, while Pb was found predominantly within the reducible sediment phase. High temporal resolution monitoring of the organic-rich streamwater draining the peat showed the transport of As was variable, with As found largely in the soluble form despite extensive peat erosion. The evidence for PDM, and the subsequent soluble transport of As demonstrated the importance of biogeochemical processes in releasing As from the solid phase. Once mobilised, both the ratio of Fe:OC and the form of Fe were found to be factors controlling transport of As, with the flushing of stored porewaters an important contribution to As transport from the peat. Despite OC-rich waters, the occurrence of high concentrations of Fe may dominate control of As within the aqueous phase. At relatively high (>0.2) Fe:OC ratios, the particle size distribution of As was closely correlated with that of >1um Fe, although the presence of dissolved and colloidal As was found even within these waters. Given the temporal variability of As transport within the streams, knowledge of the mixing order and ratio between Fe, OC, and As within natural waters may be required for prediction of the mobility and ultimate fate of As.

Declaration

No portion of the work referred to in the thesis has been submitted in support of an application for another degree or qualification at this or any other university or other institute of learning

Copyright Statement

Acknowledgements

This work was funded by aquaTRAIN (AquaTRAIN MRTN-CT-2006-035420), Marie Curie Actions, European Commission Sixth Framework.

I would first like to thank my academic supervisor, and coordinator of AquaTRAIN, Prof David Polya, for the support, and significantly, the opportunity to work within the network. The whole aquaTRAIN experience has, from the outset, been an engaging, challenging but thoroughly rewarding experience that I will carry with me. To my French supervisory team Dr Romain Millot and Dr Philippe Négrel, thank you for making my stay in Orléans so wonderful and for teaching me about the fundamentals of isotopic measurements. The support of Gilles Braibant and Catherine Guerrot was also invaluable in obtaining and analysing the Loire samples. I am also indebted to Geerke Floor for her friendship & assistance throughout my time in Orléans. During my stay at the JRC, everyone at the Soils Unit, especially Dr Luis Rodriquez Lado made me very welcome.

In Manchester, I am also extremely grateful to have worked within the Env Hydro team, with my supervisor Dr Stephen Boult, and post doc Dr John Gaffney. There are not enough words to thank you for making me one of the env hydro team, and for always being there to talk through the possibilities. John: sci-ence!

The technological knowhow and cheerful nature of Cath Davies made the chem lab a much brighter place. Thanks also to Paul Lythgoe for chemical analyses over the years. A special mention to my friends in Manchester; Vicky & John, Stu, Enoma, Natalie and Mike for the support, chat, and (ever so) occasional drink.

Within the aquaTRAIN network, I have met some amazing young researchers and being able to regularly follow their progress has been a highlight of the whole experience. The support and friendship of Julia Leventon, Enoma Omoregie, Naresh Rawat within the network and Magali Cave & Francesca Spagnuolo at the JRC was especially significant, and I am so happy to have been able to share the journey.

To my family; Bernard, Marguerite, Emma, Harry, Zach, Spike & George I am extremely grateful for the support from afar in my time overseas. Thanks for always being there, on email, googlechat and also for our wonderful trips around Europe over the last four years. Thanks also for letting Turangi become a thesis-haven. And finally, Matthew, you didn't blink when I asked you to set up home 18000km away in Manchester; and even though we have spent more time apart in the last four years than I care to recall- you have always, always been there for me. You are my person.

The Author

The author graduated from The University of Auckland in 2005 with a First Class honours MSc. Degree in Environmental Science. Between 2005-2007, she worked as an environmental scientist within Auckland's private engineering sector. Since October 2007, the author has been engaged in the research reported in this thesis.

CHAPTER 1

Introduction

1.1 Arsenic in the natural environment

Elevated concentrations of arsenic (As) in water, sediments and soils pose both a human health risk and an environmental hazard on a global scale. The contamination of groundwater aquifers with high concentrations of As in South East Asia is one of the greatest humanitarian disasters of our time (Mandal and Suzuki, 2002; Smedley and Kinniburgh, 2002). Long term exposure to elevated levels of As has been linked to a number of adverse health conditions, including cancers of the skin, lung, kidney and bladder and the non carcinogenic conditions arsenicosis and melanosis (Berg et al., 2007; Gebel, 1997; Mandal and Suzuki, 2002; Tollestrup et al., 2005). Because of its toxicity, there is a need to understand the distribution and cycling of As in the natural environment. In response to the human health threat resulting from geogenic contamination of groundwaters, and the anthropogenic contamination of other sites, a vast body of research has been conducted characterizing the occurrence of As within a range of surface and groundwaters, soils and sediments, (Bauer et al., 2008; Blute et al., 2009; Harvey et al., 2002; Oremland and Stolz, 2005; Polizzotto et al., 2006; Rothwell et al., 2010; Smedley and Kinniburgh, 2002; Swartz et al., 2004; Webster-Brown and Lane, 2005) as well as establishing the mobilisation mechanism responsible for solid-aqueous phase transfer (Ahmann et al., 1997; Bauer and Blodau, 2006; Islam et al., 2004; Linge and Oldham, 2004; Nickson et al., 2000). Although an extensive amount of work has recently been carried out involving sediments and aquifers, linking the biogeochemical cycling of As to that of iron (Fe) (Warren and Haack, 2001), there is still debate over the mineral source (McArthur et al., 2004; Ravenscroft et al., 2009; Rowland et al., 2005).

Without an identified mineralogical source, investigations of the occurrence of As within a solid phase commonly utilise sequential extraction techniques to investigate the partitioning of As (Hudson-Edwards et al., 2004; Wenzel et al., 2001) and provide useful insights into the associations of As within different phases of the sediment. Recently, the use of isotopic analysis has developed as a tool to provide information on the origin of elements such as lead (Pb), and strontium (Sr) in the characterisation of both sediment and water samples (Aberg, 1995; Bacon and Hewitt, 2005; Grosbois et al., 2000; Millot et al., 2004; Négrel and Grosbois, 1999). Previous work combining isotopic analysis with single-step digests obtaining the labile part of the sediment; known as acid extractable material (AEM); has highlighted the potential for investigating different phases within a sediment sample (Négrel and Roy, 2002). The combination of sequential extraction and isotopic analysis (Bacon and Davidson, 2008) is

therefore a potentially powerful technique to be able provide information on the origin of the trace elements within a sediment.

In addition to the questions over the source of As, mechanisms of As release are also not understood comprehensively, with a range of possible triggers including the role of carbon sources, microbially mediated pathways and redox triggers all being investigated (Bauer and Blodau, 2006; Buschmann et al., 2006; Chatain et al., 2005; Islam et al., 2004; Miao et al., 2006; Signes-Pastor et al., 2007; Solaiman et al., 2009). River sediments typically contain higher concentrations of As than the overlying waters which has been attributed to the coprecipitation and adsorption of arsenate (As(V)) with Fe(oxy)hydroxides in the sediment (Ahmann et al., 1997). These sediments have the potential to act as a source of As under certain environmental conditions (Ahmann et al., 1997; Chaillou et al., 2003).

Several studies have observed seasonal trends in dissolved As concentrations in rivers (La Force et al., 2000; Masson et al., 2007; McLaren and Kim, 1995). High levels of dissolved As are typically seen in the spring and summer months, where temperatures are high and dissolved oxygen levels are low. Dilution of the As inputs during the higher flows of the winter months cannot entirely explain the patterns observed (Aggett and O'Brien, 1985; Masson et al., 2007). A lack of a seasonal trend in particulate As concentrations has been attributed to the importance of As mobilisation from sediment through reduction processes instead of As release from the water column (Masson et al., 2007). Despite an increased understanding of the behaviour of As in freshwater (Aggett and O'Brien, 1985; Chow and Taillefert, 2009; Linge and Oldham, 2004; Masson et al., 2007; McLaren and Kim, 1995; Nicholas et al., 2003), including investigations of the behaviour of As at the source of anthropogenic pollution, and at the estuary/ocean interface (Michel et al., 2000; Mucci et al., 2000; Seyler and Martin, 1990), little work has focused on understanding the behaviour of As in the river sediments downstream of the As inputs (Masson et al., 2007) and on understanding the processes that control its distribution and mobility in unpolluted rivers.

The behaviour of As is more complex than other trace elements due in part to its existence as a redox sensitive anionic species (Bissen and Frimmel, 2003). In aqueous environments, under oxic conditions, the inorganic arsenate ion (As(V) pK_{a1} =2.2, $H_2AsO_4^-$ and/or $HAsO_4^{2-}$) dominates, changing to the reduced species arsenite (As(III) pK_{a1} = 9.2, $H_3AsO_3^0$ and $H_2AsO_3^-$) under oxygen depleted reducing conditions through the action of either chemical or microbial reduction (Smedley and Kinniburgh, 2002). Although organic As species are documented

(Anderson and Bruland, 1991), inorganic As is generally more prevalent, with As(III) more mobile than As(V) due to its adsorptive preferences and competition for binding sites with other ions. The adsorptive behaviour of different species once mobilised has been the focus of a significant body of laboratory based studies, with the adsorption/desorption and dissolution of As fairly well understood (Smedley and Kinniburgh, 2002). Iron minerals are thought to be amongst the most important controls in the retention of As within the solid phase, due to the affinity of As for Fe(oxy)hydroxides (Dixit and Hering, 2003). In addition to the research focused solely on the unique conditions posed by groundwater aquifers, there is an emerging awareness of the behaviour of As in other natural environments; notably fluvial systems and organic-rich environments, and on how the variability of these environments affects As mobility.

Further to the well established adsorption behavior of As (Bowell, 1994; De Vitre et al., 1991; Dixit and Hering, 2003; Ghosh and Yuan, 1987; Raven et al., 1998), there is increasing awareness of the dynamic interaction of As with both Fe and organic matter (OM). Organic matter has been previously recognised as an electron donor in reductive dissolution of Fe-minerals (Islam et al., 2004), but has recently been highlighted in a number of As-OM interactions affecting adsorption, and aqueous complex formation (Bauer and Blodau, 2009; Redman et al., 2002; Ritter et al., 2006; Sharma et al., 2011). As an organic rich material that experiences a range of redox conditions due to its close relationship to the water table, peats can play an important role in the storage and cycling and trace elements in the natural environment (Steinmann and Shotyk, 1997; Tipping et al., 2003). Within sediments of low organic composition, As has a strong affinity for Fe(oxy) hydroxide minerals, as well as aluminium (Al) and manganese (Mn) hydroxides (Dixit and Hering, 2003; La Force et al., 2000). Mobilisation of As has therefore been closely linked to the redox cycles of Fe (Ahmann et al., 1997; Masscheleyn et al., 1991; Smedley and Kinniburgh, 2002), although minor roles for surface bound and OM-bound As have also been established (Jay et al., 2005; Linge and Oldham, 2002). The partitioning of As within the solid phase is of significance as it ultimately affects the processes which will mobilise As and therefore its long term storage. Despite a paucity of studies on the partitioning of As in ombrotrophic peat, recent partitioning work on minerotrophic peats found a strong role for OM-bound As in the accumulation of As within the solid phase (Gonzalez et al., 2006). This finding indicates that assumptions of partitioning of As need to consider the environmental matrix, and that extrapolation across different sediment types may not be appropriate.

Increasingly, recognition of the presence of differently sized As species is shaping the way As transportation, and in turn mobility is considered (Bauer and Blodau, 2009; Garnier et al., 2011). The occurrence of colloidal species has been noted to have important implications for contaminant transportation (Buffle, 1990; Doucet and Lead, 2007; Gschwend and Reynolds, 1987), with the stability of colloids highly dependent on temporal physicochemical conditions (Liang and Morgan, 1990). The occurrence and role of colloids in the transport of As in natural systems is not currently fully understood. Analysis of <1 μm size classes have shown As, Fe and organic carbon (OC) concentrations to be correlated (Astrom and Corin, 2000; Davis and Atkins, 2001; Puls and Powell, 1992; Ritter et al., 2006), suggesting the binding of As to colloids rich in OM and Fe (Astrom and Corin, 2000; Bauer and Blodau, 2009). In streamwaters there is a relatively high proportion of total Fe and OC in the colloidal fraction, each component mutually stabilising the other (Gaffney et al., 2008; Pédrot et al., 2011; Pullin and Cabaniss, 2003; Ritter et al., 2006). Therefore, it seems likely that given its affinity for Fe-minerals, As will also be concentrated within this colloidal fraction (Fritzsche et al., 2011; Guo et al., 2011; Sharma et al., 2010). Recent work by Rothwell et al.,(2011) has highlighted that As transported from organic-rich catchments is mainly found to be in the aqueous phase, rather than transported in particulate form, highlighting the potential role colloids may play in the long term transport of As.

The interaction of As, Fe and OC in the natural environment is complicated due to a number of factors involving the inherent variability of natural systems. Previous work conducted on the association of As with OC is largely restricted to laboratory based studies. Whilst in the natural environment there is significant variation in the forms of OC and Fe-minerals present in the system, within laboratory studies, only one form of Fe or OC is often selected. For Fe, this is typically a synthesised ferrihydrite mineral (Grafe et al., 2002), and for OC; humic acid (HA) or fulvic acid (FA) is commonly synthesised (Liu et al., 2011) or obtained through extensive purification methodologies (Bauer and Blodau, 2006). Such methods ignore the potential for stabilisation of Fe minerals though the presence of OC (Gaffney et al., 2008; Pédrot et al., 2011; Pullin and Cabaniss, 2003; Ritter et al., 2006), and any changes to structure or reactivity of the colloidal material. In addition to the nature of the Fe and OC, stream systems are inherently 'flow through' systems, meaning that there is a dependency on discharge to mobilise the stored material within the system, with the possible interactions also dependent on the time available within the system. Recent studies have sought to address these issues through the use of natural sourced minerals and OC in laboratory studies (Fritzsche et al.,

2011; Sharma et al., 2011), finding the type and condition of OC influences the aqueous complexes formed. Despite this, little data is available on the interaction of As, Fe and OC in the natural environment.

With increasing pressures on water resources, and the likely environmental variability brought about through global climactic changes (Blodau et al., 2008; IPCC, 2001; Tipping et al., 2003; Worrall et al., 2004), there is a requirement to further to the understanding of the occurrence and behaviour of As within the natural environment.

1.2 Aims and objectives

Previous investigations on the occurrence and mobility of As in groundwaters (Nickson et al., 2000; Polya et al., 2005; Swartz et al., 2004; van Geen et al., 2003), deltaic systems (Berg et al., 2007; Islam et al., 2004; Meharg et al., 2006), marine systems (Chaillou et al., 2003; Munksgaard and Parry, 2002; Seyler and Martin, 1990), and geothermal (McLaren and Kim, 1995; Webster-Brown and Lane, 2005) has highlighted the complex biogeochemical behaviour of As, and the linked dynamics with local environmental conditions. With increasing awareness of the dynamic interaction of As and OC (Bauer and Blodau, 2009; Redman et al., 2002; Ritter et al., 2006; Sharma et al., 2011), and the roles of fluvial systems as transport vectors for As transport (Chaillou et al., 2003; Masson et al., 2009; Michel et al., 2000; Mucci et al., 2000), the aim of this research is to further our understanding of the environmental controls governing the occurrence of As within the solid-phase in both dynamic fluvial and organic-rich upland systems. This research seeks to make a significant contribution to our knowledge of the biogeochemistry of As, and provide an incremental improvement in our knowledge of the mobility and ultimately transport of As within the natural environment.

To achieve this aim, investigations were conducted at study sites within Europe that presented a range of natural environments, involving both geogenic and anthropogenic As contamination. Selection of field sites was in part contributed to by the placement of the author throughout Europe. As part of the research training network AquaTRAIN (MRTN-CT-2006-035420, Marie Curie Actions, European Commission Sixth Framework), placements in addition to the University of Manchester were held for six months at both the Bureau de recherches géologiques et minières (brgm), Orléans (France), and the Soils Unit of the Joint Research Centre (JRC), European Commission, Ispra (Italy).

In France, the Loire and Allier Rivers, draining the Massif Central, were chosen to study the role of river bed sediments on the cycling of As within fluvial systems. The Massif Central is known to contain As concentrations higher than average world background values due to the presence of a variety of hydrothermal and mining-related sources (Cances et al., 2005; Roussel et al., 2000; Smedley and Kinniburgh, 2002). The Allier River is also known to pass through the areas of Margeride, Auvergne and Echassieres, which are known to contain anomalously high As levels in the sediment (Barbier and Chery, 1997; Morin et al., 2002). The bedrock and waters of both rivers has been previously well characterised both chemically and isotopically, allowing for the application of further isotopic analysis in the field area.

Within the United Kingdom, the upland peats of the Peak District National Park were used to investigate the behaviour of As in organic-rich environments. The study area, Crowden Great Brook, is located within the Peak District National Park which is part of the southern Pennine uplands, situated between Manchester and Sheffield in the UK. The position of the Peak District has resulted in years of atmospheric contamination from historic mining, smelting and industrial activity in neighbouring areas. Concentrations of contaminants such as As, Pb and other trace elements are known to be elevated in the surface peat (Lee and Tallis, 1973; Rothwell et al., 2007).

The following specific objectives relating to the upland peats of the Peak District, UK, and the river sediments of the Loire and Allier Rivers, France, have been included:

1. To determine the retention and binding mechanisms of As within contrasting soils and sediments

2. Examine the potential for the use of Sr and Pb isotopes to provide insight into the mineralogical source of trace elements including As within riverbed sediment

3. Identify environmental processes contributing to the mobilisation of As from within both riverbed sediment and upland peat.

4. Assess transportation of As within organic-rich stream environments in order to understand the factors controlling size and therefore mobility of As in the aqueous phase.

1.3 Approach and thesis structure

This thesis has been written in a scientific paper format. Whilst this may lead to some repetition between chapters, this format will allow for a more efficient transfer of PhD thesis chapters for submission for publications. It should be noted that separate literature reviews are included in the introduction of each chapter, specific to the nature of each paper. With the exception of Chapter One, Two and Seven, all chapters are either intended to be or are in the process of being submitted for publication, lead by the author. Chapters One and Two provide the context for this thesis, and Chapter Seven gives the overall conclusions. In addition to the work presented in the following thesis chapters, additional work was completed in the early stages of this PhD project whilst at the JRC, Ispra (Italy), focusing on the geostatistical modelling of As in groundwaters of Cambodia. Scientific papers and presentations resulting from work completed during the duration of this PhD are outlined in Appendix 1. Analytical and experimental data, where necessary, are provided as appendices.

CHAPTER TWO

This chapter presents and discusses the experimental and analytical methods used to collect and analyse the data presented in the following four chapters that is not included in the individual chapters. Chapter Two includes sampling techniques, analytical procedures, and specific details of experimental processes.

CHAPTER THREE

This chapter presents the results of water and sediment chemistry over contrasting seasons at the study sites in the Loire and Allier Rivers, France. Batch incubation studies were used to assess the physicochemical controls on As release. Results from both solid phase partitioning of As in the river sediments, both pre- and post-batch experiment, were used to discuss the role of environmental conditions in the retention and release of As from river bed sediments.

Contributors to this chapter include Dr Romain Millot and Dr Philippe Négrel (BRGM), and Prof David Polya (SEAES) who assisted in project overview and planning. Additional technical assistance was also received from Gilles Braibant (BRGM) for sample collection, Thibauld Conte for chemical analysis at BRGM, and Paul Lythgoe for chemical analysis at Manchester. This chapter is in preparation for the journal Applied Geochemistry.

CHAPTER FOUR

This chapter presents the results of the combination of isotopic analysis and sequential extraction in an effort to constrain the mineralogical source of As within sediments. This chapter discusses the application of Sr and Pb isotopic analysis to sequential extractions, with the data presented here used to describe the implications for As mobility. An assessment of the isotopic changes in the aqueous and solid phase as a result of changes in physicochemical conditions is also made.

Contributors to this chapter include Dr Romain Millot and Dr Philippe Négrel (BRGM), who assisted in project overview and planning, sample collection and methodology. Additional technical assistance was also received from Gilles Braibant (BRGM) for sample collection, Thibauld Conte for chemical analysis at BRGM, Michele Robert and Catherine Guerrot for technical assistance in Sr and Pb isotope measurements (BRGM). Prof David Polya (SEAES) provided project planning and review. This chapter is in preparation for the journal Chemical Geology.

CHAPTER FIVE

Chapter five presents the results of the extensive peat chemical characterisation studies conducted at the study site in the Peak District, United Kingdom. This chapter describes the variability of the profiles of As, Fe and Pb and discusses the process of post-depositional movement of As in the context of As transport from the catchment. The role of peat degradation on the storage of contamination is also explored. The solid phase partitioning of Pb and As are investigated, with the implications on As transport discussed.

Contributors to this chapter include Dr Stephen Boult and Dr John Gaffney who assisted in project overview and planning, sample collection and discussion of results. Additional technical assistance was also received from Cath Davies and Paul Lythgoe for chemical analysis at Manchester. Prof David Polya assisted in project overview and review. This chapter is in preparation for the journal Geochimica et Cosmochimica Acta.

CHAPTER SIX

Chapter six builds upon the findings of Chapter five, presenting the results from an extensive field sampling campaign from streams draining the studied peat subcatchments within the

Peak District, United Kingdom. This chapter describes the flux of As from both vegetated and degraded peat areas and assesses the role of discharge, OC and Fe in the transport of As. Particle size distribution and detailed analysis of a discharge event are used to assess the controlling variables in the transport and mobility of As within organic-rich aqueous systems.

Contributors to this chapter include Dr Stephen Boult and Dr John Gaffney who assisted in project overview and planning, sample collection and discussion of results. Additional technical assistance was also received from Paul Lythgoe for chemical analysis at Manchester. Prof David Polya assisted in project overview and review. This chapter is in preparation for the journal Applied Geochemistry.

CHAPTER SEVEN

Finally, chapter seven revisits the aims and objectives of the thesis, presenting the overall conclusions of this research. In addition to providing an overall summary of the thesis, future research directions are recognised.

1.4 References

Aberg G. The use of natural strontium isotopes as tracers in environmental studies. Water, Air, & Soil Pollution 1995; 79: 309-322.

Aggett J, O'Brien G. Detailed Model for the Mobility of Arsenic in Lacustrine Sediments Based on Measurements in Lake Ohakuri. Environmental Science & Technology 1985; 19: 231-238.

Ahmann D, Krumholz LR, Hemond HF, Lovley DR, Morel FMM. Microbial mobilization of arsenic from sediments of the Aberjona Watershed. Environmental Science & Technology 1997; 31: 2923-2930.

Anderson LCD, Bruland KW. Biogeochemistry of arsenic in natural waters: The importance of methylated species. Environmental Science & Technology 1991; 25: 420-427.

Astrom M, Corin N. Abundance, Sources and speciation of trace elements in humus-rich streams affected by acid sulphate soils. . Aquatic Geochemistry 2000; 6: 367-383.

Bacon J, Davidson CM. Is there a future for sequential chemical extraction? The Analyst 2008; 133: 25-46.

Bacon JR, Hewitt IJ. Heavy metals deposited from the atmosphere on upland Scottish soils: Chemical and lead isotope studies of the association of metals with soil components. Geochimica et Cosmochimica Acta 2005; 69: 19-33.

Barbier J, Chery L. Relationships between natural geochemical background and high heavy metal levels in waters (Sb, As, Ba, Cr, Ni, Pb, Zn). Application to Auvergne and Limousin, and validation. BRGM report R 39544, Orleans, 1997, pp. 1-51.

Bauer M, Blodau C. Mobilization of arsenic by dissolved organic matter from iron oxides, soils and sediments. Science of the Total Environment 2006; 354: 179-190.

Bauer M, Blodau C. Arsenic distribution in the dissolved, colloidal and particulate size fraction of experimental solutions rich in dissolved organic matter and ferric iron. Geochimica et Cosmochimica Acta 2009; 73: 529-542.

Bauer M, Fulda B, Blodau C. Groundwater derived arsenic in high carbonate wetland soils: Sources, sinks, and mobility. The Science of The Total Environment 2008; 401: 109-120.

Berg M, Stengel C, Trang PTK, Viet PH, Sampson M, Leng M, et al. Magnitude of arsenic pollution in the Mekong and Red River Deltas — Cambodia and Vietnam. Science of the Total Environment 2007; 372: 413-425.

Bissen M, Frimmel FH. Arsenic- a Review. Part 1: Occurrence, Toxicity, Speciation, Mobility. Acta Hydrochimica et Hydrobiologica 2003; 31: 9-18.

Blodau C, Fulda B, Bauer M, Knorr K-H. Arsenic speciation and turnover in intact organic soil mesocosms during experimental drought and rewetting. Geochimica et Cosmochimica Acta 2008; 72: 3991-4007.

Blute NK, Jay JA, Swartz CH, Brabander DJ, Hemond HF. Aqueous and solid phase arsenic speciation in the sediments of a contaminated wetland and riverbed. Applied Geochemistry 2009; 24: 346-358.

Bowell RJ. Sorption of arsenic by iron oxides and oxyhydroxides in soils. Applied Geochemistry 1994; 9: 279-286.

Buffle J. Complexation Reactions in Aquatic Systems: An Analytical Approach. New York: Ellis Horwood, 1990.

Buschmann J, Kappeler A, Lindauer U, Kistler D, Berg M, Sigg L. Arsenite and arsenate binding to dissolved humic acids: Influence of pH, type of humic acid, and aluminum. Environmental Science & Technology 2006; 40: 6015-6020.

Cances B, Juillot F, Morin G, Laperche V, Alvarez L, Proux O, et al. XAS evidence of As(V) association with iron oxyhydroxides in a contaminated soil at a former arsenical pesticide processing plant. Environmental Science & Technology 2005; 39: 9398-9405.

Chaillou G, Schafer J, Anschutz P, Lavaux G, Blanc G. The behaviour of arsenic in muddy sediments of The Bay of Biscay (France). Geochimica et Cosmochimica Acta 2003; 67: 2993-3003.

Chatain V, Bayard R, Sanchez F, Moszkowicz P, Gourdon R. Effect of indigenous bacterial activity on arsenic mobilization under anaerobic conditions. Environment International 2005; 31: 221-226.

Chow SS, Taillefert M. Effect of arsenic concentration on microbial iron reduction and arsenic speciation in an iron-rich freshwater sediment. Geochimica et Cosmochimica Acta 2009; 73: 6008-6021.

Davis A, Atkins D. Metal distribution in Clark Fork River sediments. Environmental Science & Technology 2001; 35: 3501-3506.

De Vitre R, Belzile N, Tessier A. Speciation and adsorption of arsenic on diagenetic iron oxyhydroxides. Limnology and Oceanography 1991; 36: 1480-1485.

Dixit S, Hering JG. Comparison of Arsenic(V) and Arsenic(III) Sorption onto Iron Oxide Minerals: Implications for Arsenic Mobility. Environmental Science & Technology 2003; 37: 4182-4189.

Doucet FJ, Lead JR. Colloid-trace element interactions in aquatic systems In: Wilkinson KJ, Lead JR, editors. Environmental Colloids and Particles. 10. John Wiley & Sons, 2007, pp. 95–158.

Fritzsche A, Rennert T, Totsche KU. Arsenic strongly associates with ferrihydrite colloids formed in a soil effluent. Environmental Pollution 2011; 159: 1398-1405.

Gaffney JW, White KN, Boult S. Oxidation state and size of Fe controlled by organic matter in natural waters. Environmental Science & Technology 2008; 42: 3575-3581.

Garnier JM, Hurel C, Garnier J, Lenoble V, Garnier C, Ahmed KM, et al. Strong chemical evidence for high Fe(II)-colloids and low As-bearing colloids (200 nm-10 kDa) contents in groundwater and flooded paddy fields in Bangladesh: A size fractionation approach. Applied Geochemistry 2011; 26: 1665-1672.

Gebel T. Arsenic and antimony: comparative approach on mechanistic toxicology. Chemico-Biological Interactions 1997; 107: 131-144.

Ghosh MM, Yuan JR. Adsorption of inorganic arsenic and organoarsenicals on hydrous oxides. Environmental Progress 1987; 6: 150-157.

Gonzalez Z, Krachler M, Cheburkin A, Shotyk W. Spatial distribution of natural enrichments of arsenic, selenium, and uranium in a minerotrophic peatland, Gola di Lago, Canton Ticino, Switzerland. Environmental Science & Technology 2006; 40: 6568-6574.

Grafe M, Eick M, Grossl P, Saunders A. Adsorption of arsenate and arsenite on ferrihydrite in the presence and absence of dissolved organic carbon. Journal of Environmental Quality 2002; 31: 1115-1123.

Grosbois C, Négrel P, Fouillac C, Grimaud D. Dissolved load of the Loire River: chemical and isotopic characterization. Chemical Geology 2000; 170: 179-201.

Gschwend PM, Reynolds MD. Monodisperse ferrous phosphate colloids in an anoxic groundwater plume. Journal of Contaminant Hydrology 1987; 1: 309-327.

Guo H, Zhang B, Zhang Y. Control of organic and iron colloids on arsenic partition and transport in high arsenic groundwaters in the Hetao basin, Inner Mongolia. Applied Geochemistry 2011; 26: 360-370.

Harvey CF, Swartz CH, Badruzzman B, Keon-Blute N, Yu W, Ali MA, et al. Arsenic Mobility and Groundwater Extraction in Bangladesh. Science 2002; 298: 1602-1606.

Hudson-Edwards KA, Houghton SL, Osborn A. Extraction and analysis of arsenic in soils and sediments. TrAC Trends in Analytical Chemistry 2004; 23: 745-752.

IPCC. Climate Change 2001. In: Third Assessment Report. Intergovernmental Panel on Climate Change, 2001.

Islam FS, Gault AG, Boothman C, Polya DA, Charnock JM, Chatterjee D, et al. Role of metal-reducing bacteria in arsenic release from Bengal delta sediments. Nature 2004; 430: 68-71.

Jay J, Blute N, Lin K, Senn D, Hemond H, Durant J. Controls on arsenic speciation and solid-phase partitioning in the sediments of a two-basin lake. Environmental Science & Technology 2005; 39: 9174-9181.

La Force MJ, Hansel CM, Fendorf S. Arsenic speciation, seasonal transformations, and co-distribution with iron in a mine waste-influenced palustrine emergent wetland. Environmental Science & Technology 2000; 34: 3937-3943.

Lee JA, Tallis JH. Regional and historical aspects of lead pollution in Britain. Nature 1973; 245: 216-218.

Liang L, Morgan JJ. Chemical aspects of iron oxide coagulation in water: laboratory studies and implications for natural systems. Aquatic Sciences 1990; 51: 32-55.

Linge K, Oldham C. Arsenic remobilization in a shallow lake: The role of sediment resuspension. Journal of Environmental Quality 2002; 31: 822-828.

Linge K, Oldham C. Control mechanisms for dissolved phosphorus and arsenic in a shallow lake. Applied Geochemistry 2004; 19: 1377-1389.

Liu G, Fernandez A, Cai Y. Complexation of Arsenite with Humic Acid in the Presence of Ferric Iron. Environmental Science & Technology 2011; 45: 3210-3216.

Mandal BK, Suzuki KT. Arsenic round the world: a review. Talanta 2002; 58: 201-235.

Masscheleyn PH, Delaune RD, Patrick WH. Effect of redox potential and pH on arsenic speciation and solubility in a contaminated soil. Environmental Science & Technology 1991; 25: 1414-1419.

Masson M, Schäfer J, Blanc G, Dabrin A, Castelle S, Lavaux G. Behavior of arsenic and antimony in the surface freshwater reaches of a highly turbid estuary, the Gironde Estuary, France. Applied Geochemistry 2009; 24: 1747-1756.

Masson M, Schafer J, Blanc G, Pierre A. Seasonal variations and annual fluxes of arsenic in the Garonne, Dordogne and Isle Rivers, France. Science of the Total Environment 2007; 373: 196-207.

McArthur JM, Banerjee DM, Hudson-Edwards KA, Mishra R, Purohit R, Ravenscroft P, et al. Natural organic matter in sedimentary basins and its relation to arsenic in anoxic ground water: the example of West Bengal and its worldwide implications. Applied Geochemistry 2004; 19: 1255-1293.

McLaren S, Kim N. Evidence for a seasonal fluctuation of arsenic in New Zealands longest river and the effect of treatment on concentrations in drinking water. Environmental Pollution 1995; 90: 67-73.

Meharg AA, Scrimgeour C, Hossain SA, Fuller K, Cruickshank K, Williams PN, et al. Codeposition of Organic Carbon and Arsenic in Bengal Delta Aquifers. Environmental Science & Technology 2006; 40: 4928-4935.

Miao S, DeLaune R, Jugsujinda A. Influence of sediment redox conditions on release/solubility of metals and nutrients in a Louisiana Mississippi River deltaic plain freshwater lake. The Science of The Total Environment 2006; 371: 334-343.

Michel P, Boutier B, Chiffoleau JF. Net fluxes of dissolved arsenic, cadmium, copper, zinc, nitrogen and phosphorus from the Gironde Estuary (France): Seasonal variations and trends. Estuarine Coastal and Shelf Science 2000; 51: 451-462.

Millot R, Allegre CJ, Gaillardet J, Roy S. Lead isotopic systematics of major river sediments: a new estimate of the Pb isotopic composition of the Upper Continental Crust. Chemical Geology 2004; 203: 75-90.

Morin G, Lecocq D, Juillot F, Calas G, Ildefonse P, Belin S, et al. EXAFS evidence for sorbed arsenic-(V) and pharmacosiderite in a soil overlying the Echassieres geochemical anomaly, Allier, France. Bulletin de la Societe Geologique de France 2002; 173: 281-291.

Mucci A, Richard LF, Lucotte M, Guignard C. The differential geochemical behavior of arsenic and phosphorus in the water column and sediments of the Saguenay Fjord estuary, Canada. Aquatic Geochemistry 2000; 6: 293-324.

Munksgaard NC, Parry DL. Metals, arsenic and lead isotopes in near-pristine estuarine and marine coastal sediments from northern Australia. Marine and Freshwater Research 2002; 53: 719-729.

Négrel P, Grosbois C. Changes in chemical and 87Sr/86Sr signature distribution patterns of suspended matter and bed sediments in the upper Loire river basin (France). Chemical Geology 1999; 156: 231-249.

Négrel P, Roy S. Investigating the sources of the labile fraction in sediments from silicate-drained rocks using trace elements, and strontium and lead isotopes. Science of the Total Environment 2002; 298: 163-181.

Nicholas DR, Ramamoorthy S, Palace V, Spring S, Moore JN, Rosenzweig RF. Biogeochemical transformations of arsenic in circumneutral freshwater sediments. Biodegradation 2003; 14: 123-137.

Nickson RT, McArthur JM, Ravenscroft P, Burgess WGA, K.M. Mechanism of arsenic release to groundwater, Bangladesh and West Bengal. Applied Geochemistry 2000; 15: 403-413.

Oremland RS, Stolz JF. Arsenic, microbes and contaminated aquifers. Trends in Microbiology 2005; 13: 45-49.

Pédrot M, Boudec AL, Davranche M, Dia A, Henin O. How does organic matter constrain the nature, size and availability of Fe nanoparticles for biological reduction? Journal of colloid and interface science 2011; 359: 75-85.

Polizzotto ML, Harvey CF, Li G, Badruzzman B, Ali A, Newville M, et al. Solid-phases and desorption processes of arsenic within Bangladesh sediments. Chemical Geology 2006; 228: 97-111.

Polya DA, Gault AG, Diebe N, Feldman P, Rosenboom JW, Gilligan E, et al. Arsenic hazard in shallow Cambodian groundwaters. Mineralogical Magazine 2005; 69: 807-823.

Pullin MJ, Cabaniss SE. The effects of pH, ionic strength, and iron-fulvic acid interactions on the kinetics of photochemical iron transformations. I. Iron(II) oxidation and iron(III) colloid formation. . Geochimica et Cosmochimica Acta 2003; 67: 4067-4077.

Puls RW, Powell RM. Transport of inorganic colloids through natural aquifer material: implications for contaminant transport. Environmental Science & Technology 1992; 26: 614-621.

Raven KP, Jain A, Loeppert RH. Arsenite and Arsenate Adsorption on Ferrihydrite: Kinetics, Equilibrium, and Adsorption Envelopes. Environmental Science & Technology 1998; 32: 344-349.

Ravenscroft P, Richards K, Brammer H. Arsenic Pollution: A Global Synthesis. Chichester, UK: Wiley-Blackwell, 2009.

Redman A, Macalady D, Ahmann D. Natural organic matter affects arsenic speciation and sorption onto hematite. Environmental Science & Technology 2002; 36: 2889-2896.

Ritter K, Aiken G, Ranville J, Bauer M, Macalady D. Evidence for the aquatic binding of arsenate by natural organic matter-suspended Fe(III). Environmental Science & Technology 2006; 40: 5380-5387.

Rothwell JJ, Evans MG, Daniels SM, Allott TEH. Baseflow and stormflow metal concentrations in streams draining contaminated peat moorlands in the Peak District National Park. Journal of Hydrology 2007; 341: 90-104.

Rothwell JJ, Taylor KG, Chenery SRN, Cundy AB, Evans MG, Allott TEH. Storage and Behavior of As, Sb, Pb, and Cu in Ombrotrophic Peat Bogs under Contrasting Water Table Conditions. Environmental Science & Technology 2010; 44: 8497-8502.

Rothwell JJ, Taylor KG, Evans MG, Allott TEH. Contrasting controls on arsenic and lead budgets for a degraded peatland catchment in Northern England. Environmental Pollution 2011; 159: 3129-3133.

Roussel C, Neel C, Bril H. Minerals controlling arsenic and lead solubility in an abandoned gold mine tailings. Science of the Total Environment 2000; 263: 209-219.

Rowland HAL, Gault AG, Charnock JM, Polya DA. Preservation and XANES determination of the oxidation state of solid-phase arsenic in shallow sedimentary aquifers in Bengal and Cambodia. Mineralogical Magazine 2005; 69: 825-839.

Seyler P, Martin JM. Distribution of arsenite and total dissolved arsenic in major French estuaries - dependence on biogeochemical processes and anthropogenic inputs. Marine Chemistry 1990; 29: 277-294.

Sharma P, Ofner J, Kappler A. Formation of Binary and Ternary Colloids and Dissolved Complexes of Organic Matter, Fe and As. Environmental Science & Technology 2010; 44: 4479-4485.

Sharma P, Rolle M, Kocar B, Fendorf S, Kappler A. Influence of Natural Organic Matter on As Transport and Retention. Environmental Science & Technology 2011; 45: 546-553.

Signes-Pastor A, Burlo F, Mitra K, Carbonell-Barrachina AA. Arsenic biogeochemistry as affected by phosphorus fertilizer addition, redox potential and pH in a west Bengal (India) soil. Geoderma 2007; 137: 504-510.

Smedley PL, Kinniburgh DG. A review of the source, behaviour and distribution of arsenic in natural waters. Applied Geochemistry 2002; 17: 517-568.

Solaiman ARM, Meharg AA, Gault AG, Charnock JM. Arsenic mobilization from iron oxyhydroxides is regulated by organic matter carbon to nitrogen (C:N) ratio. Environment International 2009; 35: 480-484.

Steinmann P, Shotyk W. Chemical composition, pH, and redox state of sulfur and iron in complete vertical porewater profiles from two Sphagnum peat bogs, Jura Mountains, Switzerland. Geochimica et Cosmochimica Acta 1997; 61: 1143-1163.

Swartz CH, Blute NK, Badruzzman B, Ali A, Brabander D, Jay J, et al. Mobility of arsenic in a Bangladesh aquifer: Inferences from geochemical profiles, leaching data, and mineralogical characterization. Geochimica et Cosmochimica Acta 2004; 68: 4539-4557.

Tipping E, Smith EJ, Lawlor AJ, Hughes S, Stevens PA. Predicting the release of metals from ombrotrophic peat due to drought-induced acidification. Environmental Pollution 2003; 123: 239-253.

Tollestrup K, Frost F, Cristiani M, McMillan G, Calderon R, Padilla R. Arsenic-induced skin conditions identified in southwest dermatology practices: an epidemiologic tool? Environmental Geochemistry and Health 2005; 27: 47-53.

van Geen A, Zheng Y, Versteeg R, Stute M, Horneman A, Dhar R, et al. Spatial variability of arsenic in 6000 tube wells in a 25 km2 area of Bangladesh. Water Resources Research 2003; 39: 1140-1155.

Warren LA, Haack EA. Biogeochemical controls on metal behaviour in freshwater environments. Earth-Science Reviews 2001; 54: 261-320.

Webster-Brown JG, Lane V. Modeling Seasonal Arsenic Behavior in the Waikato River, New Zealand. In: O'Day P, Vlassopoulos D, Meng X, Benning L, editors. Advances in Arsenic Research: Integration of Experimental and Observational Studies and Implications for Mitigation. 915. American Chemical Society, Washington, 2005, pp. 253-266.

Wenzel WW, Kirchbaumer N, Prohaska T, Stingeder G, Lombi E, Adriano DC. Arsenic fractionation in soils using an improved sequential extraction procedure. Analytica Chimica Acta 2001; 436: 309-323.

Worrall F, Burt T, Adamson J. Can climate change explain increases in DOC flux from upland peat catchments. Science of the Total Environment 2004; 326: 95-112.

CHAPTER 2

Analytical Procedures and Experimental Techniques

This chapter outlines the sampling protocols and analytical techniques that were employed in this research, in addition to the basic detail provided within each chapter. Detailed description of field sites and sampling rationale is presented within the subsequent chapters, as required.

2.1 Field collection techniques

2.1.1 Sample Collection Loire and Allier Rivers (France)

Within the Loire and Allier Rivers (France), collection of waters was made on a point sample basis. River water samples were collected in 100 ml polypropylene containers, filtered through pre-cleaned 0.45 µm cellulose nitrate filters (Whatman, UK) using a pre-cleaned Nalgene filter apparatus. Each sample was acidified to pH< 2 with trace element grade HNO_3 on site, and stored at 4^{o}C during transportation. Prior to collection, all plastic-ware was cleaned by soaking in 10% (v/v) HNO_3 for >24hr followed by rinsing with Milli-Q water. Measurements of temperature, pH, Eh and electrical conductivity standardized to 25^{o}C, were taken *in-situ* at each site using calibrated meters. The discharge of the Loire and Allier Rivers at the point of sampling was obtained from the continuous measurements of the Environmental Agency DIREN-Agence de l'Eau, from gauging stations located in the vicinity of each sampling point.

Sediments from the top 50 cm of the riverbed were initially collected using a sediment corer; however use of a spade was also required due to the loose nature of the sediment at the Loire-Imphy site. All sediment samples were taken from 1 m into the sampled rivers flow path (i.e. with respect to the flow on the day of sampling). After transportation back to the laboratory, the samples were sieved through a 2 mm sieve to remove large stones and vegetal debris from the samples. In order to minimise disturbance to the samples, each sample was stored anaerobically, in a sealed glass jar, in the dark at 10^{o}C. Prior to analysis a subsample of sediment was weighed and oven-dried at 70^{o}C to obtain the dry-weight. Dried sediments were then size fractionated using sieving. Prior to total digests, samples were oven-dried at 70^{o}C, ground in a ball-mill, homogenized, quartered and dry-sieved through a 165 µm nylon mesh.

2.1.2 Sample Collection Crowden Great Brook, Peak District (United Kingdom)

Collection of water samples was achieved through a combination of point sampling and regular automatic sampling. Two automatic sampling systems (SIGMA 900) were triggered by manual sample programming in order to capture samples of varying discharge (Q) condition. Each sampler inlet was located as close as practicable to the centre of the stream channel and above the channel bed. The water sampler was programmed to extract 500 ml samples with an inlet rinse between each sample. Sampling of the discharge event was achieved through manual triggering of the automatic samplers and timing of samples to cover the forecast event. At a minimum, upon returning to the laboratory, each water sample was divided into two subsamples: an unfiltered (UF) sample was kept, and a portion was filtered through Milli-Q water-rinsed 0.2 µm cellulose nitrate membranes to produce a soluble (<0.2 µm) fraction. More thorough filtration, as outlined in section 2.1.3 was undertaken on selected samples. A portion of each filtered sample was acidified using concentrated HNO_3 (Analar grade, Fisher chemicals, UK) to pH< 2. Sample handling was achieved within 12 hrs of return from field. Prior to collection, all plastic-ware was cleaned by soaking in 10% (v/v) HNO_3 for >24 hr followed by rinsing with Milli-Q water.

In addition to measurements of pH, conductivity (EC) and temperature (^oC) made on point sample collection, continuous *in situ* data was collected as part of an ongoing catchment study. Data was collected using Sentry II loggers (Intelisys, UK). At each site, attached to each logger are a pressure transducer (Intelisys, UK), pH probe (Russell, Fife, Scotland) and turbidity cell (Partech, St Austell, UK). At site 50 a barometer (Intelisys, UK) is additionally positioned to adjust for atmospheric pressure when considering stage and discharge (Q). The sampling interval on each logger was set to 15 minutes. Prior to placing the equipment in the field all probes were calibrated using known standards and Sentry II software (Intelisys, UK). Data was periodically downloaded, with spot samples of pH taken using calibrated field probes and measurements of discharge taken to check and correct for drift in the probes. Discharge was determined by dilution gauging on each site visit. Subsequently, stage measurements were converted into a continuous discharge record using a discharge relationship developed for each site with ongoing data collected since 2003 (Gaffney, 2008).

Dilution gauging utilises the dissolution of a conservative tracer (most commonly NaCl) into stream water; calculating discharge through the known relationship between EC, mass of NaCl

and time. Following Gaffney (2008), a four pole conductivity probe (range 0-2500 µS) was calibrated using a 3 point calibration with NaCl standards. The EC probe was then attached to a Sentry II data logger (Intelisys, UK) and positioned in the stream. The logger was set to record data at a 3 second time interval. A known weight of NaCl (g) was subsequently mixed in a plastic container of river water until fully dissolved; the container was then emptied into the stream approximately 10m upstream of the EC probe. EC was measured with a hand held meter above the point where the NaCl was emptied into the stream and below the measurement point throughout gauging, ensuring all the NaCl had passed the recording point. If both readings were consistent the gauging was considered complete. This process usually took approximately 10 minutes (Figure 2.1).

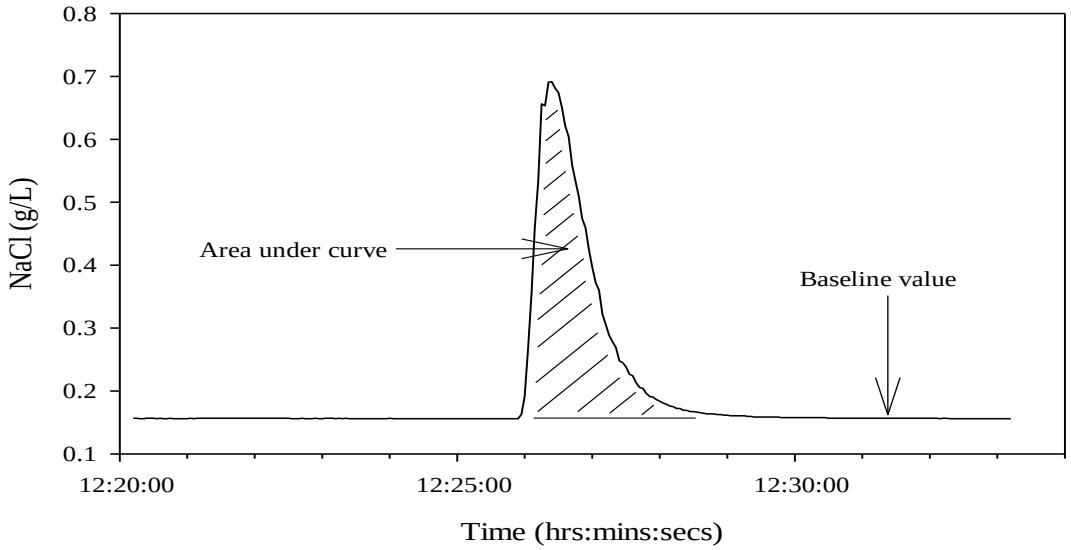

Figure 2.1 Example of dilution gauging curve (from Gaffney, 2008).

In the laboratory the data was downloaded from the logger. As the amount of total dissolved solids (TDS) is known above the baseline value, the area under the conductivity curve can be used to calculate the volume of water passing the recording point on the river in a known time, and thus discharge can be quantified using the two equations below.

Discharge (m^3s^{-1}) = Mass of NaCl (g) / Area under curve ($gl^{-1}s$) (Figure 2.1) *Equation 1*

Area under curve ($gl^{-1}s$) = (time interval (s) x NaCl (gl^{-1})) – (time interval (s) x baseline value (gl^{-1}) x n (Figure 2.1). *Equation 2*

n = Number of data points.

Peat cores were collected at a number of locations with a stainless steel peat corer (5 cm diameter, 50 cm length). Due to the consistency of the peat, cores of varied length were obtained from each site, with a standard length of 33 cm obtainable from each core location. In order to obtain enough material for analytical determinations, a number of cores had to be obtained from multiple adjacent cores within one core location. Surface vegetation was carefully removed and each core was sectioned in the field every 3 cm by use of a plastic ruler, resulting in a total of 88 individual samples. Samples were transported in paper sediment bags, each contained within a plastic bag to ensure samples were sealed. Upon returning to the laboratory the peat was stored at 10^{o}C prior to sample handling, which was undertaken within 24 hrs of collection. The peat was carefully divided into two subsamples, one was maintained in its original condition and stored in at 10^{o}C in sealed polypropylene containers. The second subsample was weighed, dried and weighed again to determine the moisture content of each sample. The dried peat was subsequently milled to a fine powder using an agate planetary ball mill (Pulverizette 5, Fritsch, Idar-Oberstein, Germany).

2.1.3 Filtration

Two methods of filtration, corresponding to desired pore size, were utilised throughout this thesis. For pore sizes of 0.2 µm and above (1 µm, 5 µm), filter membranes composed of cellulose nitrate (Whatman), housed in acid-rinsed filter unit were utilised. Prior to use, each filter membrane was rinsed with Milli-Q water (18MΩ). Where measurements of total organic carbon (TOC) were to be made on a filtered sample, each filter membrane was rinsed with excess of 200 ml of Milli-Q water to ensure that any unfixed carbon from the membrane was removed (tested by repeated TOC measurements).

The analytical technique used for particle size determination at a high resolution (<0.2 µm) was tangential flow ultrafiltration (TFU). While pressure filtration involves forcing sample through a membrane under pressure, the design of TFU is such that particles pass tangentially over the membrane and if of the correct size they are filtered by gravity (Figure 2.2).

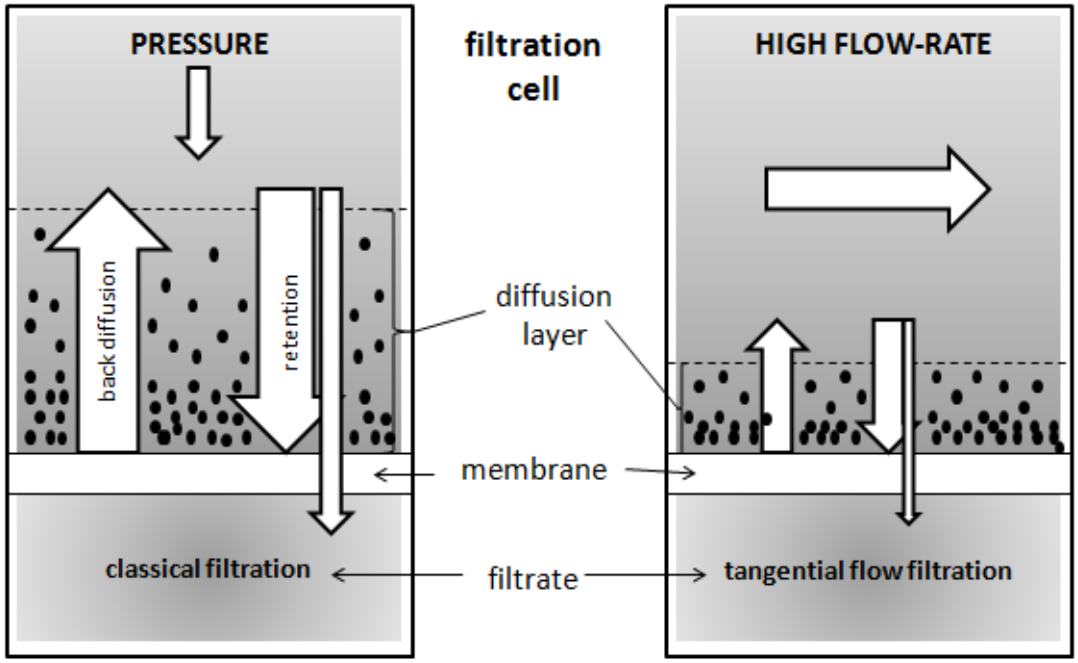

Figure 2.2 **Comparison between pressure filtration and tangential flow ultrafiltration (Figure adapted from Buffle and Leppard (1995)).**

The design of TFU applies less force than pressure filtration, meaning that distortion of particle shape during filtration is minimised. Also, the height of the diffusion layer at the membrane surface is reduced, minimising slow back diffusion which creates a high concentration of particles at the membrane surface, facilitating coagulation (Buffle and Leppard, 1995) (Figure 2.2). TFU has been shown to be an effective technique for previously in the Peak District field area (Gaffney, 2008) and other marine (Wen et al., 1996) and freshwaters (Pokrovsky et al., 2005).

Prior to sample analysis, TFU and cellulose filter membranes were always ensured blank by first flushing with Milli-Q water (18 MΩ) and subsequent filtrates and retentates analysed for OC concentrations. Flushing was repeated until the OC concentration was comparable to that of Milli-Q water. Samples were first filtered through 1 µm and 0.2 µm cellulose nitrate membranes (Whatman, UK) in order to obtain large (>1 µm) and small (<1 µm, 0.2 µm) particulates and then sequentially filtered through paired 1000 kDa, 50 kDa and 10 kDa TFU membranes in order to obtain large (<0.2 µm, >1000 kDa), medium (<1000 kDa, >50 kDa) and small (<50 kDa, >10 kDa) colloids. Once the sample separation was complete, 100 ml of pH 2

Milli-Q water and then 100 ml of Milli-Q water were recirculated through each membrane in order to recover any remaining material.

2.2 Sequential extraction

Sequential extraction protocols were employed in order to determine the distribution of As within both the solid phase sediment in the Loire and Allier Rivers (Chapter 3), and the peat at Crowden Great Brook (Chapter 5). There are currently a range of SEPs being utilised to investigate the partitioning of both trace elements and As in sediment samples (Hudson-Edwards et al., 2004; Wenzel et al., 2001), with the variation in followed protocol being one of the principal reasons for lack of comparability between studies (Hall and Pelchat, 1999). Despite a desire to maintain consistency within this thesis, changes in utilised protocol were unavoidable due to sample and analytical considerations.

The protocols used in each study are outlined in Table 2.1. The protocol used on the sediment from the Loire and Allier Rivers (Chapter 3) is a six-step extraction based on the Wenzel et al., (2001) and Tessier (1979) extractions, and used regularly within As studies on sediments (Gault et al., 2003; Haque et al., 2008; Yolcubal and Akyol, 2008). In order to differentiate between different mineralogical stores, this protocol uses two separate steps to differentiate between amorphous and more crystalline minerals (Wenzel et al., 2001). Difficulties were encountered analysing the residual phase of this protocol, due to the high total dissolved solids (TDS) associated with the boric acid needed to complex HF precluding the use of inductively coupled plasma- mass spectrometry (ICP-MS). The concentrations of As within the sediments were not elevated (> 20ppm), leading to a lack of reliable analysis by inductively coupled plasma- atomic emission spectrometry (ICP-AES). Furthermore, reactions of organic-rich material with the oxidisible step utilising $KClO_4$ would also be too vigorous to use safely within the laboratory, leading to a need to alter at least two of the protocol steps for use on peat. As previous work with organic-rich peat samples had found that As was not associated with the mineral content of the sample (Gonzalez et al., 2006), use of a simpler protocol was identified as a means of increasing the number of analysed samples. For this reason, the protocol used in the study by Gonzalez et al., (2006) on minerotrophic peat was employed for use on the Crowden Great Brook peat samples.

The main difference between the two protocols stems from the different ionic strengths used in the first step. Both protocols use anion exchange as a means of extracted adsorbed As, with the ionic strength used by Gonzalez et al., (2006) significantly higher than in the Wenzel et al., (2001) extraction (1 M vs. 0.05 M respectively). Use of higher ionic strength phosphate solutions has been found to release both non-specifically sorbed and specifically sorbed As, as well as breaking the bonds between inner sphere complexes of As and Fe-minerals (Wenzel et al., 2001). Consequently, the exchangeable fraction of As in this protocol may represent As associated with amorphous iron (Fe) as well as other surface sorbed species. The subsequent step targeting Fe-minerals, although using a lower strength reagent than the Wenzel (2006) extraction, is therefore solely targeting As co-precipitated with Fe/Mn- minerals and not also extracting strongly adsorbed As.

As typical sediment preparation techniques such as drying and grinding are known to affect the partitioning of trace elements including As (Anawar et al., 2010; Einax and Nischwitz, 2001; Vasile et al., 2010), all sequential extraction work was undertaken using moist peat that had not been processed in any way. The same reagent: sample ratio was employed in both protocols, with 1 g (dry weight) sample used for 25 ml of reagent (unless otherwise specified). After each stage, the sediment–extractant mixture was centrifuged (1700 x g for 20 min) and the supernatant decanted, filtered at 0.45 µm and refrigerated until analysis. All chemicals were analytical reagent grade or equivalent analytical purity. Due to logistical considerations, the reproducibility of our sequential extraction method was examined with duplicate analyses for the Crowden peat samples and triplicate analyses for the Loire/Allier River sediments.

Table 2.1 Outline of sequential extraction protocols

Environmental process	Loire and Allier River sediment			Crowden Great Brook peat		
	Extractant	Conditions	Target phase	Extractant	Conditions	Target phase
Desorption	0.05 M $(NH_4)_2SO_4$	end-over-end shaking, 25°C, 4 hrs	non-specifically sorbed	25 ml 1M NaH_2PO_4 (pH 5)	24 hrs, 25°C [one repetition] water wash (25 ml, 24 hrs)	strongly adsorbed
	0.05M $NH_4H_2PO_4$	end-over-end shaking, 25°C, 16 hrs	specifically sorbed			
Reduction	25 ml 0.2 M NH_4 -oxalate buffer (pH 3.0)	end-over-end shaking, 25°C dark, 4 hrs, wash step (12.5 ml NH_4 -oxalate 10 mins)	poorly crystalline hydrous oxides of Fe/Al	25 ml 1N HCl	1 hr, 25°C [one repetition] water wash (25 ml, 1 hr)	co-precipitated with Fe/Mn hydroxides
	25 ml 0.2 M NH_4 -oxalate buffer (pH 3.0) and 0.1 M ascorbic acid	occasional shaking, 90°C, 4 hrs, wash step (12.5 ml NH_4 -oxalate 10 mins)	well crystallised hydrous oxides of Fe/Al			
Oxidation	1g $KClO_4$ / 20 ml HCl	45 min standing, dilute with 15 ml DIW	organics and sulphides	3 ml 0.02M HNO_3 + 8 ml 30 % H_2O_2 / 5 ml 3.2 M NH_4OAc in 20% (v/v) HNO_3	heated at 85 ±2°C 5hrs. After cooling NH_4OAc added and sample diluted to 20ml with DIW	organics
Not available	HF-H_3BO_3-HNO_3	microwave- closed vessel, diluted to 50ml DIW	Residual	16 N HNO_3 + 30% H_2O_2	microwave- closed vessel, diluted to 50ml DIW	residual

2.3 Analytical procedures

2.3.1 Aqueous chemistry analysis

Arsenic (As) and other trace elements in water samples were measured using a Plasmaquad 2 ICP-MS, (VG Elemental) with a detection limit of < 1 µg l^{-1}. Major element concentrations of water samples, and trace elements in sample digests with high total dissolved solids (TDS) were determined by ICP-AES, (Horizon, Fisons). Quality control standards were used throughout the course of analysis to monitor analytical performance. External calibration standards were used to prepare standard calibration curves from which measured concentrations can be corrected for deviation from using weighted ordinary least squares linear regression, with analytical errors calculated using the methods of Miller and Miller (2005).

Arsenic speciation was analysed by IC-ICP-MS using the method of Gault et al. (2005). Samples (1 ml) were passed through a 0.45 µm filter. As(V) and As(III) were separated on a Hamilton PRP-X100 anion exchange column using a 20 mM $NH_4H_2PO_4$ (BDH, UK) (adjusted to pH 8.1 using NH_4OH (BDH, UK)) mobile phase, housed in a Metrohm 790 Personal IC unit, which was interfaced to a VG PlasmaQuad II ICP-MS. Peak integration and drift-corrected calibration were performed using in-house Turbo Pascal programs TRPEAK (Polya, 1998) and DBSCORR (Polya, 1999), respectively. Standard reference materials were included in each analytical run; the As concentrations determined were found to agree well with those certified.

A ferrozine assay based on a method adapted from Lovley and Phillips (1986) was utilised to determine Fe(II). The ferrozine solution was made by adding 11.96 g HEPES (Sigma Aldrich, UK) and 1.0 g ferrozine (Sigma Aldrich, UK (2-Pyridyl)-5,6-bis(4-phenylsulfonic acid)-1,2,4-triazine) to 1 l of Milli-Q water (18MΩ) producing a 2mM ferrozine in 50mM HEPES solution. This solution was then adjusted to pH 7 using 1 M NaOH (Fisher chemicals, UK) and stored at 4°C. Initially, Fe (II) was determined by addition of 0.1 g slurry (weight determined) to 5 ml 0.5 M HCl and mixed vigorously for 30 s. After 1 hr, 50 µl of sample was then added to a cuvette with 2.45 ml of ferrozine solution and inverted to achieve complete mixing. The absorbance was then read at 562 nm; at this wavelength the visible absorption spectrum of the ferrous complex of ferrozine exhibits a sharp peak (Stookey, 1970). Total Fe was measured though the addition of 0.1 g (weight determined) of sediment slurry to 5 ml of 0.25 M hydroxylamine hydrochloride in 0.25 M HCl, with the exception that the slurry was left to react for 24 hrs.

Under acidic conditions hydroxylamine reduces Fe(III) to Fe(II) allowing for its determination by absorption spectrometry at 562 nm (Lovley and Phillips, 1986). The UV visible spectrophotometer was calibrated prior to each sample analysis with Fe(II) standards of 1, 5 and 10 mg l^{-1} adjusted to pH 2 (1M HCl, Analar Grade, Fisher chemical, UK) to inhibit oxidation.

Total Organic Carbon (TOC) was performed using a Shimadzu 5050A TOC analyser (Shimadzu, Japan). Total carbon (TC) stock solutions were prepared using 2.125 g potassium hydrogen phthalate (Shimadzu, Japan) in 1 l of 18 MΩ ultra violet (UV) treated Milli-Q water (Elga, Option 4, water purifier), and inorganic carbon (IC) stock solutions were prepared using 3.5 g sodium hydrogen carbonate (Shimadzu, Japan) and 4.41 g sodium carbonate (Shimadzu, Japan) in 1 l of UV treated Milli-Q water(Elga, Option 4, water purifier). Standards were prepared daily by diluting the stock solution using 18 MΩ UV treated Milli-Q water (Elga, Option 4, water purifier) and were analysed at the start and end of each period of analysis. TC was calibrated using 0, 1, 5 and 20 mgl^{-1} standards. A 50 mgl^{-1} standard was analysed in the event of a sample containing >20 mgl^{-1} TC. Samples >50 mgl^{-1} were diluted into the range of the TC standards to avoid sample carryover associated with high TC concentrations. Every 5 samples a standard closest to the concentration of the samples was analysed as a check standard. IC was calibrated using 0, 0.5 and 5 mgl^{-1} standards with a 10 mgl^{-1} standard being analysed in the event of a sample containing >5 mgl^{-1} IC. Every 5 samples a standard closest to the concentration of the samples was analysed as a check standard. Linear drift of the instrument was corrected using a linear drift correction programme (Boult, 2000) which corrects data according to standard concentration and time; assuming that the time and therefore drift between each sample measurement is equal. In effect the programme draws a polygonal surface between standard concentration and between sets of standards (time); assuming that sample values can be corrected to a point somewhere on this surface by linear interpolation between known standard concentrations (Gaffney, 2008).

2.3.2 Isotopic chemistry

Strontium separation was achieved through the use of a column separation protocol (Deniel and Pin, 2001; Négrel et al., 2007). All sample handling was performed in Class 10 vertical laminar flow hoods. A portion of each sample was evaporated on a hotplate and subsequently resuspended in 150 µl 2M HNO_3. Difficulty in obtaining a clear solution was experienced for some samples. In this case, additional HNO_3 was added to dissolve formed solids and the evaporation repeated. If a residue was observed post evaporation, the purification process was repeated. The extraction chromatographic material (ECM) Sr.Spec (particle size 50–100 µm), consists of a solution of the crown ether di-*tert*butyl- cis-dicyclohexano-18-Crown-6 (DtBuCH18-C6) in 1-octanol sorbed on the inert support Amberchrom CG-71ms (Deniel and Pin, 2001). Microcolumns (2 ml reservoir and 12mm long) were assembled out of plastic pipettes (Fisherbrand), with a porous polyethylene frit at the bottom used for the separation work. A small amount of Sr.Spec ECM in 6M HCl was loaded onto the columns, to give a 0.15 ml bed. Each sample used new Sr.Spec, whereas the columns were thoroughly cleaned after each elution. Each sample (150 µl) was loaded onto the column, and rinsed with 4 x 0.1 ml HNO_3 to remove rubidium (Rb), rare earth elements (REE), uranium (U) and thorium (Th). Barium was subsequently removed through addition of 1 ml 7M HNO_3, and 2 x 0.1 ml 2M HNO_3. Strontium sample elution was then eluted with 1 ml 0.05M HNO_3. After chemical separation, approximately 150 ng of Sr was loaded onto a tungsten filament with tantalum activator and analyzed with a Finnigan MAT 262 multi-collector mass spectrometer. The $^{87}Sr/^{86}Sr$ ratios were normalized to an $^{86}Sr/^{88}Sr$ ratio of 0.1194. An average internal precision of about ±10 ppm (2 σ_m) was obtained. Reproducibility of the $^{87}Sr/^{86}Sr$ ratio measurements was tested through repeated analyses of the NBS987 standard (accepted value 0.710248), for which we obtained a mean value of 0.710230 ± 20×10^{-6} (2σ, n=17) during the period of analysis.

Lead (Pb) isotopic ratios were determined on the solutions from the SEP and total digests of sediment by using a Neptune Multi Collector-ICP-MS with Faraday Cups (Figure 2.3) (Thermo Fischer Scientific) in operation at the BRGM Isotopic Geochemistry Laboratory. According to the recent protocol developed in BRGM and presented by Cocherie and Robert (2007), the key parameter for the analysis of solutions by the means of the MC-ICP-MS is the Pb concentration and the cation matrix of the water sample. The high sensitivity of the Multi-Collector ICP-MS allows direct measurements at Pb concentration levels as low as 10 ng ml^{-1}, with no matrix effects where the ion charge is lower than 400 mg l^{-1}.

The required set of Faraday cups simultaneously collects the following masses: ^{201}Hg or ^{202}Hg, ^{203}Tl, ^{204}Pb+^{204}Hg, ^{205}Tl, ^{206}Pb, ^{207}Pb and ^{208}Pb.

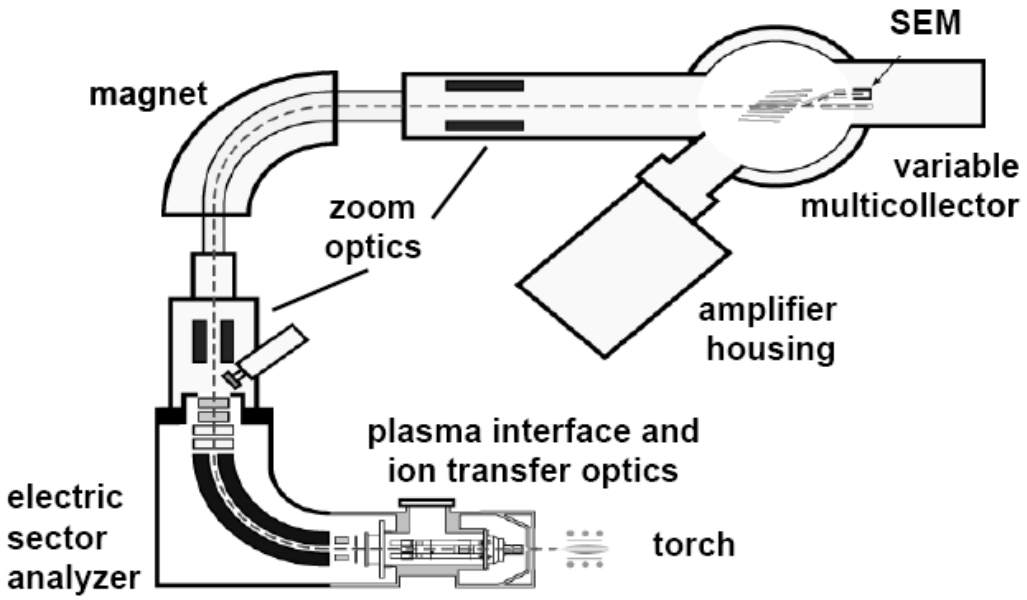

Figure 2.3 Schematic of Neptune Multi Collector-ICP-MS (Thermo Fischer Scientific)

Volumes of sample were prepared to a final concentration of 10 ppb Pb with a mix of HNO_3, H_2O and Tl standard (used for "in-run" instrumental mass bias correction) and analysed by direct measurement by MC-ICP-MS. At the beginning of each analytical session, a pure Pb standard solution (SRM-981) was run to optimize the signal. A gain calibration of all the Faraday cups was carried out to determine the correction coefficients between all the Faraday cups, after having determined the most efficient instrumental settings. Then, the peak shape at all masses of interest was checked. For a given analysis, 5 blocks of 10 cycles with 8 seconds integration time per peak were recorded in static mode for common samples over 7min.

The dead time of the detector is optimised prior to the analyses by measuring the $^{208}Pb/^{204}Pb$ ratio of the NIST SRM 981 standard at various concentrations (10, 20, 50 and 100 ppb). When using this method, a Tl correction technique is used for mass discrimination calculation following an exponential correction to $^{205}Tl/^{203}Tl = 2.3871$. In such conditions, 2σ standard errors of 0.10% are achieved for $^{206}Pb/\ ^{204}Pb$, $^{207}Pb/^{204}Pb$, $^{208}Pb/^{204}Pb$ ratios, and errors of 0.01% are achieved for both $^{207}Pb/^{206}Pb$ and $^{208}Pb/^{206}Pb$ ratios. A "blank" solution of 3 % v/v HNO_3 added to MilliQ water (18 MΩ) similar to that used to adjust the sample solutions was

prepared. The blank solution was systematically measured between each sample, after careful washing out of the instrument. The blank subtraction involved measurement of a real blank solution. The following sequence was followed: blank1, 981–1, blank2, sample1, blank3, sample2, blank4, sample3, blank5, 981–2, blank6,…, etc. Long term measurement of SRM981 standard material gave mean values of 16.932 ± 0.015, 15.486 ± 0.014 and 36.679 ± 0.030 respectively for $^{206}Pb/^{204}Pb$, $^{207}Pb/^{204}Pb$ and $^{208}Pb/^{204}Pb$ ratios (2s, n = 38).

Where the concentration of Pb was too low to enable the dilution required for detection by Faraday Cups, the use of multi-ion-counters system (MIC)-ICP-MS was employed to optimise peak shape (Figure 2.4) (Négrel et al., 2010). Only five counters are available on our instrument at low mass, therefore the "Tl spike" technique cannot be used in static mode. Due to the lack of stability of the ion beam generated by the ICP and due to the more difficult calibration of ion counters compared to Faraday cups, a static mode acquisition sequence was used. This detection method achieved 2σ standard errors of between 0.5-1.3 % for $^{206}Pb/^{204}Pb$, $^{207}Pb/^{204}Pb$, $^{208}Pb/^{204}Pb$ ratios and 0.08-0.15 % for $^{207}Pb/^{206}Pb$ and $^{208}Pb/^{206}Pb$ ratios. Measurements were carried out for solutions having 0.1 µg l^{-1} of Pb. In that case, the method of sample-standard bracketing was used for the mass discrimination effect correction (normalization to the SRM-981 standard solution), similar to that used for other stable isotope measurements in the BRGM Neptune laboratory (Millot et al., 2004). For Pb isotope analysis, we performed the direct measurement of a solution containing 0.1 µg l^{-1} of Pb without any sample preparation beforehand (i.e., without chemical separation of the matrix). Only dilution or pre-concentration by evaporation (on a hot plate) of the sample were used to adjust the concentration of the solution to 0.1 µgl^{-1} of Pb in 3 % v/v sub-boiling HNO_3. The major advantage of this method is that all Pb isotopes (including the minor isotope ^{204}Pb) are measured in a static mode; reducing significantly the uncertainty of measurement. For mass discrimination correction, the method of sample-standard bracketing was used and the reference standard (NIST standard SRM981: $^{204}Pb/^{206}Pb$ ratio 0.059042 ±0.000037, $^{207}Pb/^{206}Pb$ ratio 0.91464 ±0.00033, $^{208}Pb/^{206}Pb$ ratio 2.1681 ±0.0008) must be adjusted to the same concentration as the samples (0.1 µg l^{-1}). At the beginning of each analytical session a pure Pb standard solution (SRM-981) at 100 pg ml^{-1} was run to determine the most efficient instrumental settings. The peak shape was optimized by adjusting the optic zoom lenses to control the peak shape and to optimize the peak superposition of all masses. The dark noise was measured for each counter: usually it does not exceed a few counts per minute. The plateau calibration of all counters was also optimized and then the yield could be determined

and loaded in the computer. For a given analysis, 5 blocks of 10 cycles with 8 integrations of one second integration time per peak were recorded in static mode. The total acquisition time was 7 min for each analysis. The available set of counters allowed the following masses to be collected simultaneously: ^{202}Hg, ^{204}Pb+^{204}Hg, ^{206}Pb, ^{207}Pb and ^{208}Pb. Blank subtraction was systematically undertaken and the raw value of each sample was normalised with the average of the two standards analysed before and after according to following sequence: blank1, 981–1, blank2, sample1, blank3, 981–2, blank4, sample2, blank5, 981–3, blank6,…etc.

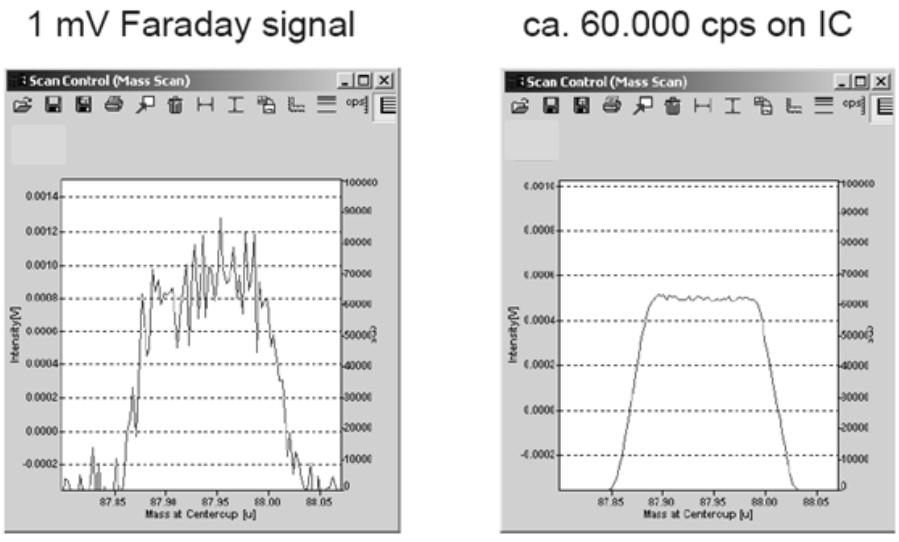

Figure 2.4 Optimisation of peak shape on MIC-ICP-MS relative to Faraday cups signal. (Image from presentation by Thermo Electron Corporation)

Use of the sample–standard technique can have a slightly adverse effect on the reproducibility because the instability of the sample or standard cannot "internally" be corrected during acquisition as it is done using the Tl standardisation technique. Despite this, in the case of very low sample Pb levels (i.e. 100 pg), the sample–standard bracketing technique, associated with a MIC system, allows Pb-isotope ratios to be accessed without purification stages, thus avoiding contamination relating to additional sample handling. Furthermore, as both the

sample and the standard are recorded at the same count rate level, the potential lack of linearity of the counters is not a significant problem

2.4 References

Anawar H, Mihaljevic M, Garcia-Sanchez A, Akai J, Moyano A. Investigation of Sequential Chemical Extraction of Arsenic from Sediments: Variations in Sample Treatment and Extractant. Soil & sediment contamination 2010; 19: 133-141.

Boult S. Sub ICP Drift Corrector. School of Earth Sciences (now SEAES). University of Manchester, UK, 2000.

Buffle J, Leppard GG. Characterisation of Aquatic Colloids and Macromolecules. 2. Key role of physical structures on analytical results. Environmental Science & Technology 1995; 29: 2176-2184.

Cocherie A, Robert M. Direct measurement of lead isotope ratios in low concentration environmental samples by MC-ICP-MS and multi-ion counting. Chemical Geology 2007; 243: 90-104.

Deniel C, Pin C. Single-stage method for the simultaneous isolation of lead and strontium from silicate samples for isotopic measurements. Analytica Chimica Acta 2001; 426: 95-103.

Einax JW, Nischwitz V. Inert sampling and sample preparation - the influence of oxygen on heavy metal mobility in river sediments. Fresenius Journal of Analytical Chemistry 2001; 371: 643-651.

Gaffney JW. Role of natural organic matter in controlling the behaviour of Fe in natural waters. School of Earth, Atmospheric and Environmental Science. University of Manchester, 2008.

Gault AG, Jana J, Chakraborty S, Mukherjee P, Sarkar M, Nath B, et al. Preservation strategies for inorganic arsenic species in high iron, low-Eh groundwater from West Bengal, India. Analytical and Bioanalytical Chemistry 2005; 381: 347-353.

Gault AG, Polya DA, Charnock JM, Islam FS, Lloyd JR, Chatterjee D. Preliminary EXAFS studies of solid phase speciation of As in a West Bengali sediment. Mineralogical Magazine 2003; 67: 1183-1191.

Gonzalez Z, Krachler M, Cheburkin A, Shotyk W. Spatial distribution of natural enrichments of arsenic, selenium, and uranium in a minerotrophic peatland, Gola di Lago, Canton Ticino, Switzerland. Environmental Science & Technology 2006; 40: 6568-6574.

Hall GEM, Pelchat P. Comparability of results obtained by the use of different selective extraction schemes for the determination of elements forms in soils. Water Air and Soil Pollution 1999; 112: 41-53.

Haque S, Ji JF, Johannesson KH. Evaluating mobilization and transport of arsenic in sediments and groundwaters of Aquia aquifer, Maryland, USA. Journal of Contaminant Hydrology 2008; 99: 68-84.

Hudson-Edwards KA, Houghton SL, Osborn A. Extraction and analysis of arsenic in soils and sediments. TrAC Trends in Analytical Chemistry 2004; 23: 745-752.

Lovley DR, Phillips EJP. Availability of Ferric Iron for Microbial Reduction in Bottom Sediments of the Fresh-Water Tidal Potomac River Applied and Environmental Microbiology 1986; 52: 751-757.

Miller JN, Miller JC. Statistic and Chemometrics for Analytical Chemistry. Harlow, England: Pearson Education Limited, 2005.

Millot R, Guerrot C, Vigier N. Accurate and high-precision measurement of lithium isotopes in two reference materials by MC-ICP-MS. Geostandards and Geoanalytical Research 2004; 28: 153-159.

Négrel P, Guerrot C, Millot R. Chemical and strontium isotope characterization of rainwater in France: influence of sources and hydrogeochemical implications. Isotopes in Environmental and Health Studies 2007; 43: 179-196.

Négrel P, Millot R, Roy S, Guerrot C, Pauwels H. Lead isotopes in groundwater as an indicator of water-rock interaction (Masheshwaram catchment, Andhra Pradesh, India). Chemical Geology 2010; 274: 136-148.

Pokrovsky O, Dupre B, Schott J. Fe-Al-organic colloids control of trace elements in peat soil solutions: Results of ultrafiltration and dialysis. Aquatic geochemistry 2005; 11: 241-278.

Polya D. TRPEAK, Unpublished Turbo Pascal Programme. Department of Earth Sciences (now SEAES). University of Manchester, UK, 1998.

Polya D. DBSCORR, Unpublished Turbo Pascal Programme. Department of Earth Sciences (now SEAES). University of Manchester, UK, 1999.

Stookey LL. Ferrozine – A new spectrophotometric reagent for iron. Analytical Chemistry 1970; 42: 779-781.

Tessier A, Campbell PGC, Bisson M. Sequential Extraction Procedure for the Speciation of Particulate Trace-Metals. Analytical Chemistry 1979; 51: 844-851.

Vasile G, Tanase I, Dinu C. The Influence of the Air-drying Pretreatment of Sediment Samples for Metallic Element Mobilities. Analytical letters 2010; 43: 1199-1206.

Wen LS, Stordal MC, Tang D, Gill G, A , Santschi PH. An ultraclean cross-flow ultrafiltration technique for the study of trace metal phase speciation in seawater. Marine Chemistry 1996; 55: 129-152.

Wenzel WW, Kirchbaumer N, Prohaska T, Stingeder G, Lombi E, Adriano DC. Arsenic fractionation in soils using an improved sequential extraction procedure. Analytica Chimica Acta 2001; 436: 309-323.

Yolcubal I, Akyol NH. Adsorption and transport of arsenate in carbonate-rich soils: Coupled effects of nonlinear and rate-limited sorption. Chemosphere 2008; 73: 1300-1307.

CHAPTER 3

Mobilisation of arsenic from Loire and Allier River sediments (France): changes in solid phase partitioning

3.1 Introduction

Elevated concentrations of arsenic (As) in water, sediments and soils pose both a human health risk and an environmental hazard on a global scale. A growing global demand for water resources has highlighted the temporal variability of surface waters for a range of trace elements including As. In addition to the elevated concentrations observed in streams and rivers due to anthropogenic contamination, unpolluted waters can also show a large range of concentrations. Rivers are dynamic systems, where the interaction of surface water and groundwater, soils and sediments all influence the availability of contaminants. Whilst the processes controlling the mobilisation of As from anoxic aquifer and lake sediments have been the focus of numerous studies, increasingly there is an appreciation for the lack of understanding of As behaviour in the sediments of fluvial systems.

Rivers transport large quantities of solid phase, particulate and dissolved trace elements including As to estuaries and ultimately oceans (Howard et al., 1984; Masson et al., 2007; Michel et al., 2000). Within rivers, dissolved As concentrations have been found to vary on both a diurnal and seasonal timescale (La Force et al., 2000; Masson et al., 2007; McLaren and Kim, 1995; Michel et al., 2000), with elevated water temperatures and low DO levels linked to occurrence of higher concentrations in summer months. While in some cases a link to the dilution of an input (e.g. geothermal discharges) can be found responsible for lower winter concentrations, it is not thought to be the only contributing factor (Aggett and O'Brien, 1985; Masson et al., 2007; McLaren and Kim, 1995; Webster-Brown and Lane, 2005). With changing flow regimes, complex sediment transport and seasonal variations in pH, temperature and DO, rivers experience a range of environmental conditions that have the potential to influence As mobilization (Masson et al., 2007; McLaren and Kim, 1995).

Much recent research has focused on explaining seasonal trends in dissolved As concentrations using As behavior once in the water column. Increased understanding of the changing nature of suspended particulate matter (SPM) in the Waikato River, New Zealand, has allowed for explanation of changes in seasonal adsorption/desorption processes in the removal and release of As within the water column. The As-adsorption capacity of SPM was found to increase in proportion to the amount of iron (Fe) mineral phases present in the SPM (Webster-Brown and Lane, 2005). While the interaction of particulate and dissolved As phases is an important process affecting As transportation, it is more important in understanding the

behaviour of dissolved As downstream from a known source e.g. geothermal inputs. Determination of the origin of As is unable to be made from adsorption/desorption processes between dissolved and particulate As, as these can only occur once As is already in the water column. This issue is reinforced by the observations of Masson et al. (2007), where conversion of particulate As could not be used to explain the observed dissolved As concentrations in the Garonne, Dordogne and Isle rivers during summers.

In addition to SPM, sediments have a major role to play in the removal and mobilisation of As in the aqueous environment (Figure 3.1). Sediments have the ability to act as both a source and a sink of As under certain environmental conditions (Ahmann et al., 1997; Chaillou et al., 2003), due to the release of As from the underlying sediments, or from suspended particulate matter that has settled to the bottom sediments (Mucci et al., 2000). River sediments are well known to contain higher concentrations of As (along with other trace elements) than the overlying waters; this has been attributed to the coprecipitation and adsorption of arsenate (As(V)) with/onto Fe(oxy)hydroxides in the sediment (Ahmann et al., 1997; Jung et al., 2009; Négrel and Roy, 2002). Sediments are therefore able to act as reservoirs for the release of As under favourable environmental conditions.

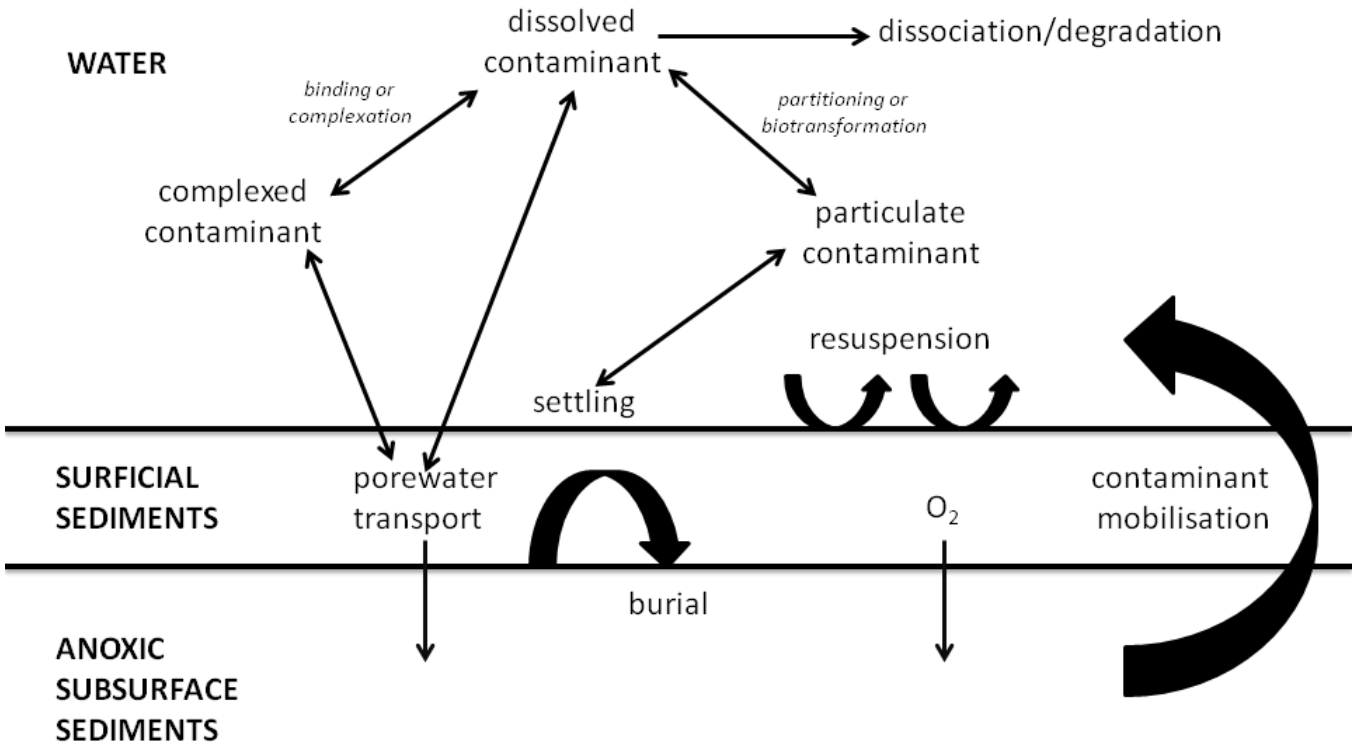

Figure 3.1 Transportation of contaminants in sediments (modified from Lyman (1995))

While numerous studies have highlighted the release of As from mining or industrially contaminated sediments (Bird et al., 2003; Cances et al., 2005; Espinosa et al., 2009; Harrington et al., 1998; Klarup, 1997; Mok and Wai, 1989; Roussel et al., 2000; Turner et al., 2008) few investigations have taken place into the cycling of As in uncontaminated sediments of rivers. Several studies into the behaviour of As at the estuary/ocean interface have been conducted (Michel et al., 2000; Mucci et al., 2000; Seyler and Martin, 1990), highlighting the importance of rivers in the transportation of As in the natural environment. Numerous studies on lake sediments have provided insight into likely mobilization mechanisms in the reducing conditions experienced at the bottom of lakes, and subsequent release during lake turnover events (Freeman et al., 1986). However, results from lake sediments are not directly transferable to processes occurring within rivers due to the different environmental conditions obtained from the movement of water within the river. Rivers are unique environments with physical and chemical conditions changing on both short and long timescales. Both diurnal and seasonal DO and pH changes have been observed in a number of rivers, reflecting temporal changes in factors such as erosional inputs and biological activity (Barringer et al., 2007; Grosbois et al., 2000; Jones et al., 2004; McLaren and Kim, 1995). The movement of sediment within a river basin is complex, with changing river dynamics leading to the flooding of river banks and subsequently increasing the contact of sediment with river water (Kalnejais et al., 2007). The dynamics of moving sediment can lead to the rapid burial of sediment or suspended material, causing sudden changes in redox conditions within the sediment. The hyporheic zone, where sediment is in contact with both ground and surface water is known to experience changing redox conditions, with reducing conditions known to exist within the top 30 cm of sediment (Nagorski and Moore, 1999) and within adjacent wetland areas (Blute et al., 2009). Because of the temporal variations experienced by river sediments, it is important to understand how the storage of As within the sediment is affected.

A number of biogeochemical processes have been used to explain the release of As from sediments. The onset of anaerobic conditions can lead to the reductive dissolution of metal oxide mineral phases within the sediments, possibly as a microbially driven process (Ahmann et al., 1997; McArthur et al., 2004). Microorganisms present in the sediment are thought to catalyse the release of As through assisting Fe(oxy)hydroxide dissolution. Direct microbial arsenate reduction through the use of As(V) as an electron acceptor in anaerobic respiration has also been observed in freshwater sediments and mining environments (Ahmann et al.,

1997). Microbial activity is thought to be dependent on water temperature, with increased activity observed in warmer seasons. Under less turbulent flow conditions, or in ponded areas, As that is adsorbed to the surface of minerals, or settled suspended material may also be reduced, and subsequently released (Masson et al., 2007). While the effect of pH on the adsorption and desorption of trace metals and As in aqueous environments is well established in both laboratory experiments for simple solid Fe(oxy)hydroxides and natural aquatic sediments (Bourg et al., 2000; Fuller and Davis, 1989; Manning and Goldberg, 1997; Swedlund and Webster, 1999), some studies have failed to find a link between pH and dissolved As concentrations (Masson et al., 2007). In addition to the changes in the composition of the sediment with river flow, temporal variation of these biogeochemical factors will also influence the retention or release of As from river sediments.

The mobilization of As from the solid phase is dependent on its partitioning within the sediment. A common tool to investigate the mobility of trace elements including As within a soil or sediment is to utilise a sequential extraction procedure (SEP) to provide useful insights into the associations of As within different phases of the sediment. The solid phase partitioning of As is one factor in the potential mobility of As within the sediment, with SEPs distinguishing between adsorbed or coprecipitated As. While the exact steps of each SEP typically vary with each study, As in sediments is frequently found to be strongly associated with Fe-oxides (or oxyhydroxides) and other mineral phases including Mn-oxides and Fe-sulphides, although contributions from adsorbed or organic associated As are not uncommon (Blute et al., 2009; Devesa-Rey et al., 2008; Gonzalez et al., 2006; Haque et al., 2008). While there are a number of recognised limitations to the use of SEPs (Wenzel et al., 2001), an understanding of the chemical processes removing As during the SEP and the likely similarity to the environmental processes occurring within the sediments allows for description of the SEP in terms of the operational processes used.

Distribution of As between the aqueous and solid phases is controlled by both removal and mobilization processes. While partitioning between the different solid phases is primarily controlled by redox conditions, a close association with Fe is well known (Nagorski and Moore, 1999; Sherman and Randall, 2003). The association of As with more labile phases influences the availability of As by desorption processes, while As found within the mineral phases may be released by the reductive dissolution of Fe-oxides. Because of the different release mechanisms influencing the phases of As within the sediment, seasonal changes in the

distribution of As within the sediment may provide information on the mobilisation mechanisms occurring within the sediment. In addition to in-situ changes in sediment As partitioning, insight into the mechanisms controlling As remobilisation may also be gained by looking at changes in partitioning before and after an incubation study (Linge and Oldham, 2002).

The Massif Central (France) is known to contain As concentrations higher than average world background values due to the presence of a variety of hydrothermal and mining-related sources (Cances et al., 2005; Roussel et al., 2000; Smedley and Kinniburgh, 2002). Both the Loire and Allier Rivers have their origins within the Massif Central, however the geology, along with path, of each river differs. The older volcanic and plutonic rocks drained by the Loire River are not known to be high in As, while the Allier River is known to pass through the areas of the Margeride, Auvergne and Echassieres, which are known to contain anomalously high As levels in the sediment (Barbier and Chery, 1997; Morin et al., 2002). Both rivers undergo strong seasonal discharge variations, with flooding of riverbanks and seasonal pH cycles also observed. The aim of this study was to further understand the cycling of As within the riverbed sediments under seasonal environmental conditions. For this purpose, the objectives of this study were:

- To determine the solid phase partitioning of As within Loire and Allier riverbed sediment under contrasting seasonal conditions.

- To establish, through the use of incubation studies, if changes in pH and/or anaerobic conditions increase As mobility from riverbed sediments.

- Determine the likely phases contributing to release of As through combination of both dissolved As release and changes in solid phase partitioning, and therefore elucidate seasonal mobilisation mechanisms occurring in riverbed sediment.

3.2 Field Area

3.2.1 Site location

Surface sediment samples were collected during November 2008 and August 2009 from two sites within the Bec d'Allier region near Nevers, France (Figure 3.2). Surface water samples were also collected at the point of sediment sampling, with additional water samples collected from a third site (Marzy), after the confluence of the Loire and Allier Rivers. One sediment collection site was located on the Loire River, at Imphy, before the confluence with the Allier River. The second site was located on the Allier River, at Apremont (Figure 3.2).

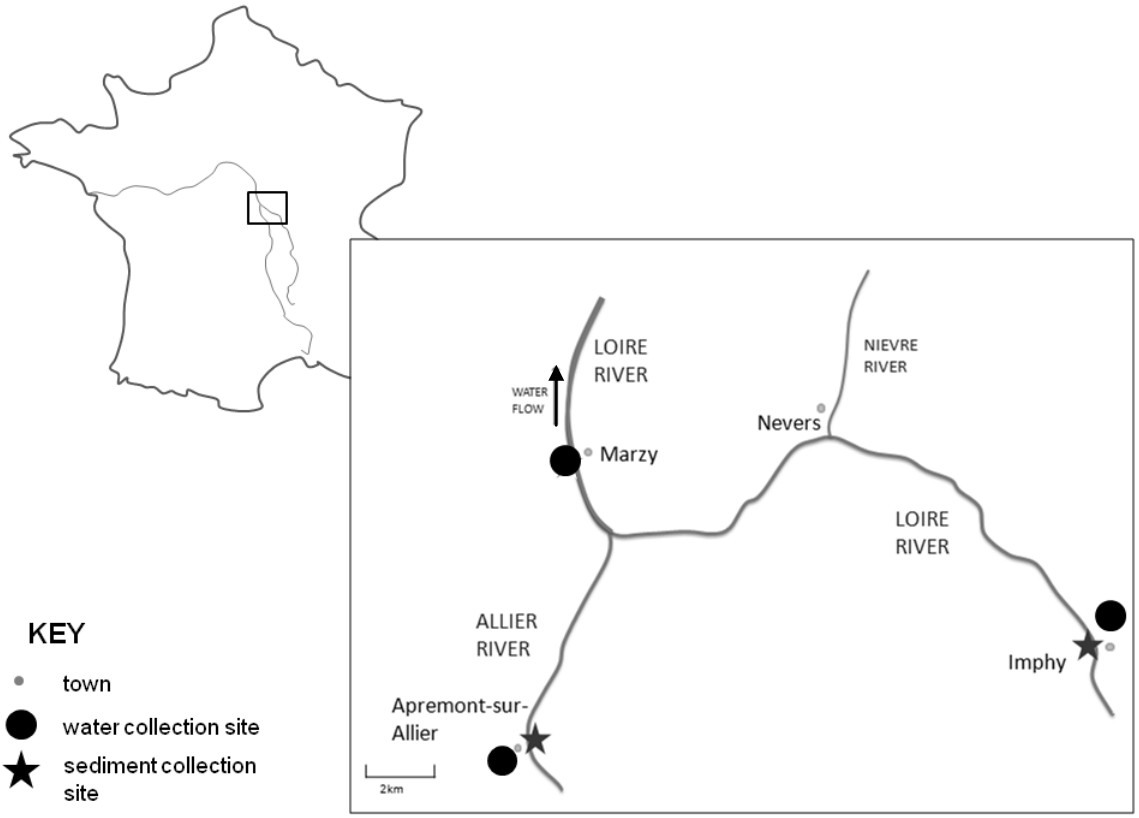

Figure 3.2 **Location map of sampling sites. Sediment (indicated by stars) was collected from Allier-Apremont and Loire-Imphy, with water samples collected from all three marked sites (indicated by circular marks).**

3.2.2 Site Description

The rivers investigated in this study both flow from the French Massif Central, forming part of the Loire River Catchment. The Loire in central France is approximately 1010 km long and drains an area of 117,800 km^2, while the Allier is a tributary of the Loire, and is approximately 400 km long, draining an area of 14,320 km^2. Initially, the Loire and Allier both flow in a south to north direction originating in the Massif Central, they join near the town Nevers (Figure 3.2) and continue as the Loire up to the city of Orléans, 650 km from the source. The Loire River then follows a general east to west direction to the Atlantic Ocean, entering the Bay of Biscay at St Nazaire. The Loire River is one of the main European river inputs to the Atlantic ocean (Négrel, 1997).The oceanic receiving environment, the Bay of Biscay, is enriched in As due to the presence and exploitation of As-bearing ores in the drainage catchments (Chaillou et al., 2003).

The bedrock composition of the rivers has been well characterized with both rivers sharing the silicate dominated basement of the upper Loire River Catchment (Figure 3.3). The upstream section of the Loire includes older plutonic rocks, granite, gneiss and mica schist; and a large volcanic area which represent 46 % of the total basin surface (Négrel et al., 2000). The intermediate section of the Loire features the sedimentary series of the Paris Basin, consisting primarily of carbonate deposits (Négrel and Grosbois, 1999). The geology of the Allier differs slightly to the Loire, with the main gravel and sand components being of granitic–gneissic and basaltic origin from the Massif Central; carbonates from the Limagne d'Allier can also be a source of material (Négrel and Roy, 2002).

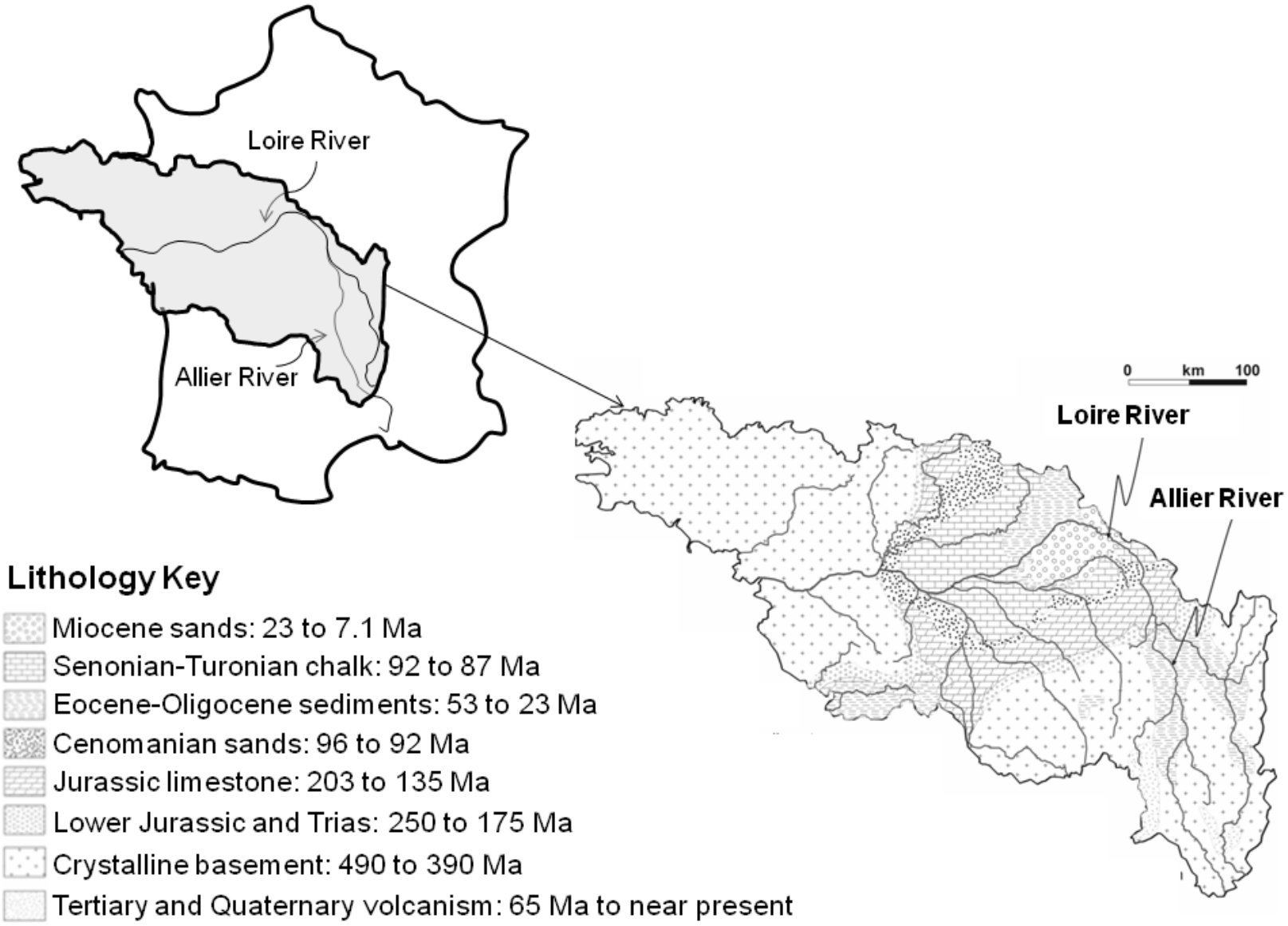

Figure 3.3 **Simplified geological map of the Loire and Allier River catchment(s). Lithology map and information provided by R. Millot (brgm)**

3.3 Methods

3.3.1 Sample Collection

River water samples were collected from Loire-Imphy, Loire-Marzy and Allier-Apremont sites (Figure 3.2) in November 2008 (Winter), April 2009 (Spring) and August 2009 (Summer). Samples were collected in 100 ml polypropylene containers, filtered through precleaned 0.45 µm Whatman cellulose nitrate filters using a precleaned Nalgene filter apparatus. Each sample was acidified to pH< 2 with trace element grade HNO_3 on site, and stored at 4°C during transportation. Prior to collection, all plastic-ware was cleaned by soaking in 10 % (v/v) HNO_3 for >24 hr followed by rinsing with Milli-Q water ($18M\Omega$). Measurements of temperature, pH, Eh and electrical conductivity standardized to 25°C, were taken *in-situ* at each site using calibrated meters. The discharge of the Loire and Allier Rivers at the point of sampling was obtained from the continuous measurements of the Environmental Agency DIREN-Agence de l'Eau, from gauging stations located in the vicinity of each sampling point.

Sediments from the top 50 cm of the riverbed were initially collected using a sediment corer, however use of a spade was also required due to the loose nature of the sediment at the Loire-Imphy site. Due to logistical constraints, sediment samples were only collected from the Loire-Imphy and Allier-Apremont sites during the Winter 2008 and Summer 2009 period, with all sediment samples taken from 1 m into the sampled rivers flowpath (i.e. with respect to the flow on the day of sampling). After transportation back to the laboratory, the samples were sieved through a 2 mm sieve to remove large stones and vegetal debris from the samples. In order to minimise disturbance to the samples, each sample was stored anaerobically, in a sealed glass jar, in the dark at 10°C. As typical sediment preparation techniques such as drying and grinding are known to affect the partitioning of trace elements including As (Anawar et al., 2010; Einax and Nischwitz, 2001; Vasile et al., 2010), all sequential extraction work was undertaken using sediment that had not been processed in any way. Prior to analysis a subsample of sediment was weighed and oven-dried at 70°C to obtain the dry-weight. Dried sediments were then size fractionated using sieving. Prior to total digests, samples were oven-dried at 70°C, ground in a ball-mill, homogenized, quartered and dry-sieved through a 165-µm nylon mesh. Mineral identification was undertaken on a portion of both sediments collected in the winter only, using a combination of density, magnetic character and microscopy.

3.3.2 Sequential extraction

There are currently a range of SEPs being utilised to investigate the partitioning of both trace elements and As in sediment samples (Hudson-Edwards et al., 2004; Wenzel et al., 2001). As an anion, the behaviour of the adsorbed As species differs from metallic cations and so recent work by Wenzel (2001) has altered the standard SEP used in metals analysis (Tessier et al., 1979) to allow for the removal of anions during the first two steps. Because of the lack of a standard protocol for As (e.g. the Bureau Communitaire de Reference (BCR) protocol for metals) and the ongoing issues around the need for comparability between studies, a previously used SEP specific to the evaluation of As was chosen for this study based on the Wenzel (2001) and Tessier (1979) extractions (Table 3.1). The extraction steps used are outlined in Table 3.1, along with the key used to describe the different phases. Briefly, portions of sediment (1 g dry weight, no physical processing/drying), were carefully weighed into screwcap polypropylene centrifuge tubes (Fisher Scientific, Loughborough, UK). All reagents were of analytical reagent grade (Fisher Scientific, 99+% Certified AR grade).

The non-specifically sorbed As (F1) was extracted in the first step by end-over-end shaking with 25 ml of 0.05 M $(NH_4)_2SO_4$ For 4 h.

Specifically sorbed As (F2) was then removed by end-over-end shaking with 25 ml of 0.05M $NH_4H_2PO_4$ for 16 h.

Poorly crystalline hydrous oxides of Fe/Al (F3) were leached using 25 ml of 0.2 M NH_4 -oxalate buffer (pH 3.0), with end-over-end shaking in the dark for 4 h. The supernatant was removed and a further 12.5 ml of NH_4-oxalate buffer was added and shaken in the dark for 10 min. The supernatant from this wash step was combined with that withdrawn from the main extraction step.

Well-crystallized hydrous oxides of Fe/Al (F4) used the addition of 25 ml of 0.2 M NH_4 -oxalate buffer (pH 3.0) and 0.1 M ascorbic acid, followed by incubation at 90° C in the light with occasional shaking for 30 min. After the supernatant was removed, a wash step using 12.5 ml of the NH_4-oxalate buffer was utilised as in previously extraction step.

The removal of organics and sulphides (F5) present in the sample, was achieved by the addition of 1 g of $KClO_4$ to the residue followed by the careful addition of 20 ml of

concentrated HCl. The tubes were then left to stand for 45 min (with occasional shaking) before dilution with 15 ml of deionized water.

The residual material (F6) was dried and then microwave digested using a mixture of HF-H_3BO_3-HNO_3 to bring any recalcitrant As into solution.

After each stage, the sediment–extractant mixture was centrifuged (1700 x g for 20 min) and the supernatant decanted, filtered at 0.45 µm and refrigerated until analysis. All chemicals were analytical reagent grade or equivalent analytical purity. High-purity Milli-Q deionised water (18 MΩ, Millipore) was used for all solutions. The reproducibility of the sequential extraction method was examined with triplicate analyses. Procedural blanks were also run in duplicate over the SEP simultaneously and found to be below detection levels for Steps 2, 3 and 5, with Step 1 reagents contributing up to 1.7% (0.00038 µg) of the detected As, and Step 4 contributing up to 2.3% (0.042 µg) As.

Table 3.1 Key for extraction steps, targeted As phases, and environmental process controlling removal of each phase for the SEP

	Extractant	Target phase	Environmental process
F1	0.05 M $(NH_4)_2SO_4$	Non-specifically sorbed	Desorption
F2	0.05M $NH_4H_2PO_4$	Specifically sorbed	Desorption
F3	0.2 M NH_4 -oxalate buffer (pH 3.0)	Poorly crystalline hydrous oxides of Fe/Al	Reduction-dissolution
F4	0.2 M NH_4 -oxalate buffer (pH 3.0) and 0.1 M ascorbic acid	Well crystallised hydrous oxides of Fe/Al	reduction - dissolution (less readily)
F5	$KClO_4$ /HCl	Organics and sulphides	Oxidation
F6	HF-H_3BO_3-HNO_3	Residual	not available

3.3.3 Sediment Incubations

i) pH stat leaching experiment details

The effect of changing river water pH on As release from river sediments was determined through the use of a simplified pH_{stat} leaching test. To maintain an ionic strength similar to river water, 20 g sediment (no physical handling/drying) was mixed with a solution of 0.01 M $NaNO_3$ to obtain a slurry at a water/sediment ratio of 3:1 (weight: weight). The experiment was carried out in 200ml plastic bottles. All glass and plastic-ware was cleaned by soaking in 10 % (v/v) HNO_3 for >24 hr followed by rinsing with Milli-Q water ($18M\Omega$). Each slurry was adjusted with NaOH or HNO_3 to obtain a pH of 7, 8, 9 and 10 respectively, and were mixed aerobically, end-over-end over a period of two weeks. To assess the variability of the observed release, duplicate slurries were produced using the Allier-Apremont winter sediment, for pH 9 and 10. The pH of each sample was monitored twice daily, and adjustments made to maintain each desired pH. At each sampling point, a sample of the aqueous phase was taken and pH determined prior to filtration at 0.45 μm and acidification with HNO_3 prior to analysis. A sequential extraction was run on the residual winter sediments from both the Allier-Apremont and Loire-Imphy sites for the pH 8 and pH 10 incubations to determine the changes to partitioning caused by the incubation.

ii) Microcosm details

To mimic the rapid burial of river sediments, anaerobic conditions were imposed on incubations of sediment samples in parallel to aerobically maintained samples. Sediment (3 ± 0.1 g) was mixed with N_2-degassed, filtered (0.45 μm) river water from the Loire-Marzy sample site, at a water/sediment ratio of 3:1 (weight:weight). River water was used instead of a synthetic solution to allow for similar competitive displacement reactions as would occur in the river. In an anaerobic cabinet (under N_2 atmosphere), each anaerobic slurry was placed in a 20 ml serum bottle, fitted with butyl rubber stoppers, sealed with an aluminium clamp, and incubated at 20^{o}C. The aerobic samples were prepared using river water that had not been degassed, and the manipulations were carried out on a lab bench in normal aerobic conditions. Over the period of incubation the samples were periodically shaken to mix the sediment and aqueous phases. For each sampled timepoint, a separate sacrificial slurry was created in order to avoid the possible contamination associated with sampling the same vessel multiple times. After sampling, each vessel was discarded. Aerobic conditions were maintained by piercing the

butyl stoppers with a hypodermic syringe to allow the free passage of oxygen into the microcosm. All experiments were performed in triplicate using sterile, acid-washed equipment. To evaluate changes in partitioning of As within the sediment, a sequential extraction was performed on the residual winter sediment from both Allier-Apremont and Loire-Imphy sites for both aerobic and anaerobic conditions after 14 days incubation.

3.3.4 Total digests & XRF

The total metal concentrations in the sediment were determined by a total digestion procedure, using a microwave digestion. A mixture of HF- HNO_3 was left with 0.3 g sediment in a Teflon microwave vessel overnight to allow dissolution of silicate material. The sediment was then digested in a MARS Xpress microwave (CEM, Kamp-Lintfort, Germany) over two hours. After cooling, boric acid (H_3BO_3) was then added to complex the HF, as removal of HF by volatilisation is also thought to also remove the volatile AsF_5 species, giving low concentrations (Gault et al., 2003).

The total solid phase elemental concentrations were also determined for each sediment by X-ray fluorescence (XRF). Ground, homogenised sediment samples (12 g) are mixed with a wax binder (3 g) and pressed into sediment pellets. The pellets were analyzed using a wavelength separation XRF Spectrometer (Axios) for a range of elements including As , Fe, Mn, Pb and Zn.

3.3.5 Metal concentration analysis

Trace element concentrations were determined in all river water samples, with As and Fe measured in the non-residual SEP solutions and incubation studies using inductively coupled plasma – mass spectrometry (ICP-MS) with a detection limit of < 1 µg l^{-1}. Because of high total dissolved solids (TDS) in solutions from the HF-H_3BO_3-HNO_3 total digestion analysis using the ICP-MS was not possible. Instead, the trace element contents were determined by inductively coupled plasma – atomic emission spectroscopy (ICP-AES, Horizon, Fisons) using matrix matched standards. Quality control standards were used throughout the course of analysis for both instruments to monitor analytical performance. Commercial multi-element standards were used to prepare standard calibration curves which were used to correct measured concentrations using weighted ordinary least squares linear regression, with analytical errors calculated using the methods of Miller and Miller (2005).

i) As and Fe speciation

The Fe(II) concentration of the sediment slurry was determined spectrophotometrically using a ferrozine assay after extraction with 0.5 M HCl on a CamSpec (CamSpec Ltd, Cambridge, UK) M330 UV-Visible Spectrophotometer (Lovley and Phillips, 1986). Values of Fe are represented throughout as total concentrations mobilized per gram of adjusted dry weight sediment from the start of the experiment.

Aqueous As speciation was measured on field site water samples by ion chromatography inductively coupled plasma-mass spectrometry (IC-ICP-MS) (Gault et al., 2005; Rowland et al., 2007). A strong anion exchange column (PRP-X100, Hamilton, Switzerland), housed in a Metrohm Personal IC 790 unit (Metrohm AG, Herisau, Switzerland), was interfaced with an ICP-MS. A 20-M $NH_4H_2PO_4$ mobile phase, adjusted to pH 8.1, and containing 50 µg l^{-1} rubidium (Rb) and germanium (Ge) internal standards, was passed through the column at a flow rate of 1.5 ml min^{-1} and then into the ICP-MS. Samples were injected onto the column via a 100-µl sample loop. Arsenic species peak integration and drift correction were calculated using the in-house Turbo Pascal programs TRPEAK (Polya, 1998) and DBSCORR (Polya, 1999), respectively. Certified reference materials (CRM) (National Water Research Institute, Canada) were included in each analytical run to monitor accuracy.

3.4 Results and Discussion

3.4.1 River water chemistry

In the surface water of both the Loire and Allier River, the temperature, DO, conductivity and pH showed large variation over the three sample periods at all three sites (Table 3.2). Temperature showed strong seasonal variation, with minimum values in winter (~6 ^{o}C) and maximum values in summer (~26^{o}C). Measured pH values ranged from near-neutral to slightly alkaline. Consistent with previous studies (Grosbois et al., 2000), variation in pH with season was observed at all sites, with minimum values obtained in winter (≈7.8 - 7.9) for all three sites. Higher pH values appear to be related to increased temperatures and lower flows, with maximum values seen in the Allier-Apremont sediment during summer (8.3), and at the two Loire sites during spring (8.6 - 8.7). Previous work in the Loire River, downstream of this study site has recorded the pH of the river water to be both above pH 9 (May-September 1995), and below pH 7 (January-April 1996) (Grosbois et al., 2000), indicating significant seasonal variation within the water column.

Dissolved Fe concentrations are variable at the sampled sites, with maximum concentrations (0.14- 0.16 mg l^{-1}, 2x higher than lowest observed) at Allier-Apremont and Loire-Imphy respectively during winter, with lowest values seen during the low flows in summer. Loire-Marzy does not show the same trend, with spring concentrations the highest observed. Increasing Fe concentrations with increased flow is suggestive of a source of Fe-material related to flow. Increased erosion inputs were identified as a source of particulate mineral material in the Loire River during high flows by Négrel et al., (2000). Using strontium (Sr) isotopes, the likely source of Fe oxide minerals in suspended particulate matter (SPM) in the Loire River during high flows was found to be material that had been transported from the river source (the Massif Central).

Dissolved As concentrations are variable in both the Loire and Allier Rivers (Table 3.2), with maximum concentrations observed during the summer sampling at the Loire-Imphy and Allier-Apremont sites, while at the Loire-Marzy site the maximum As concentration was seen in winter. Decreased dissolved As concentrations at the Loire-Imphy and Allier-Apremont sites during the higher flows of winter suggest that dissolved As concentrations may be affected by dilution. However despite increased flows, the increase in concentration seen from spring to winter, indicate that factors other than dilution are also important in understanding As

mobility within rivers. While these results are only spot samples, and do not offer a complete picture of seasonal As variation, they do generally support the observation of summer maximum As concentrations observed in other rivers (Masson et al., 2007; McLaren and Kim, 1995), suggesting that changing environmental conditions during the summer season increase dissolved As concentrations. The observation of ~10 % As(III) (1.1 µg l^{-1}) coinciding with lower DO levels, at the Allier-Apremont site during the warmer summer sampling period also provides evidence of a link with changing environmental conditions observed at the Allier site in summer, including increased pH, temperature and reduced DO. Release of As(III) indicates mechanisms of As release such as the reductive dissolution of As, or bacterial As(v) reduction could be occurring either in the particulate or solid phase, with the mixing of released As(III) with oxygenated river waters causing a reduction in the observed concentrations.

Whilst dissolved As concentrations are highest in summer, a simplified calculation of flux utilising the flow ($m^3 s^{-1}$) at the point of sampling (Table 3.2), indicates that greater dissolved As transport is achieved during the higher flows. If the variability in amount of dissolved As transported by each river was due to dilution only, then the absolute amount carried by each river would remain constant. The observed variability in flux, seen from our limited data set of three sample points, indicates that processes introducing As to the rivers are likely affected by seasonal environment conditions (McLaren and Kim, 1995), such as the flooding and erosion of riverbank sediments (Taylor et al., 2008). These results are in keeping with the findings of Masson et al (2007), where >50 % of As flux was found to be transported due to sediment resuspension during the high flows of flood events.

As seen in the Isle River (Grosbois et al., 2009), the observed dissolved As/Fe ratios are variable, generally increasing in low flow. In line with this observation, the proposed selective retention/mobilisation outlined by Grosbois et al., (2009) may be valid for the Allier and Loire Rivers, whereby loss of Fe to Fe(oxy)hydroxides, or gain of As relative to Fe (due to e.g. competitive sorption with organic matter(OM)) could be responsible for higher summer (low flow) As/Fe ratios. In addition to the reasons for increases in As/Fe ratio during summer months outlined by Grosbois et al., (2009), the increased concentrations of Fe in higher flows can also be considered. While increased inputs of Fe minerals relating to erosion during high flows increase the dissolved Fe concentration, the lack of a corresponding increase in dissolved As indicates that the environmental conditions required for As mobilisation are not met during the winter months.

Table 3.2 **Mean results for aqueous samples collected from the Loire and Allier Rivers November 2008-August 2009.**

		Allier-Apremont			Loire- Marzy			Loire-Imphy		
		Winter	Spring	summer	Winter	Spring	Summer	Winter	Spring	Summer
Date		24/11/2008	11/04/2009	4/08/2009	24/11/2008	11/04/2009	4/08/2009	24/11/2008	11/04/2009	4/08/2009
pH		7.9	8.0	8.3	7.9	8.7	8.2	7.8	8.6	8.1
Temp	^{o}C	6.7	13.4	22.6	6.2	14.3	22.2	6.5	14.4	26.1
DO	$mg\ l^{-1}$	11.3	12.5	9.2	11.2	16.6	9.3	10.7	14.4	14.2
Conductivity (at 25°C)	$\mu S\ cm^{-1}$	256	174	324	245	189	257	97	181	246
Eh	mV	281	266	218	249	258	224	182	280	195
Flow	$m^3\ s^{-1}$	180	140	36	530	264	73	350	135	36
As_{tot}	$\mu g\ l^{-1}$	4.6	4.0	10.3	3.7	1.4	3.3	2.0	1.4	4.0
As(III)	$\mu g\ l^{-1}$	0.2	0.2	1.1	0.2	< 0.1	0.3	< 0.1	< 0.1	0.2
As(V)	$\mu g\ l^{-1}$	4.4	3.8	9.2	3.4	1.4	3.2	1.8	1.4	3.4
As flux	$g\ s^{-1}$	0.8	0.6	0.4	2.0	0.4	0.2	0.7	0.2	0.1
Fe	$mg\ l^{-1}$	0.14	0.07	0.01	0.02	0.07	0.03	0.16	0.08	0.05
Cu	$\mu g\ l^{-1}$	1.5	1.0	1.0	2.1	1.4	1.0	1.9	1.3	3.1
Zn	$\mu g\ l^{-1}$	1.8	1.0	0.9	3.3	1.5	0.4	1.4	3.2	1.4
Pb	$\mu g\ l^{-1}$	0.2	0.1	0.04	< 0.01	0.1	0.06	0.3	0.1	0.1
Mg	$mg\ l^{-1}$	6.2	4.8	8.9	3.7	3.8	4.6	3.8	3.8	4.6
Sr	$\mu g\ l^{-1}$	163	116	217	115	100	138	112	99	138

3.4.2 General sediment characteristics- Mineralogy

The silicate dominated basement of the Loire River Catchment is reflected in the mineralogy of sediments from both the Allier-Apremont and Loire-Imphy sites. The sediment at the Loire-Imphy was silicate-dominated, with quartz, feldspars and micas making up 95 % of the sediment. Rock debris made up a component of the sediment, with the other minerals present including Fe(oxy)hydroxides, zircon, apatite, pyrite and clays. The Allier-Apremont sediment was similar in make-up to the Loire sediment, with clays making up a larger proportion of the sample and rutile and pyroxene also present. Although sediment mineralogy was only able to be determined for the sediment collected in November 2008, the nature of the silicate dominated basement rocks in the catchment means that any seasonal alterations to the mineralogy are likely to be minor.

3.4.3 General sediment characteristics- Physical and Chemical composition

Sediment particle size (Figure 3.4a&b) reveals the complex nature of sediment transport within riverbeds. The general absence of fine particles (<63 µm) is typical of dynamic water conditions where finer particles are carried further along the river course, combined with the mid-way location of the sampling points relative to the river courses. During summer sampling, the sediment particle size distribution was found to be similar between the Loire-Imphy and Allier-Apremont sites (Figure 3.4a) with 500 µm - 1 mm grains dominating, however the distribution during the winter sampling was more variable. The presence of a larger proportion of finer particles at the Allier-Apremont site during the winter sampling likely reflects the changing seasonal nature of the river system, with the increased winter flows causing the channel to widen to include riverbank sediments (Taylor et al., 2008).

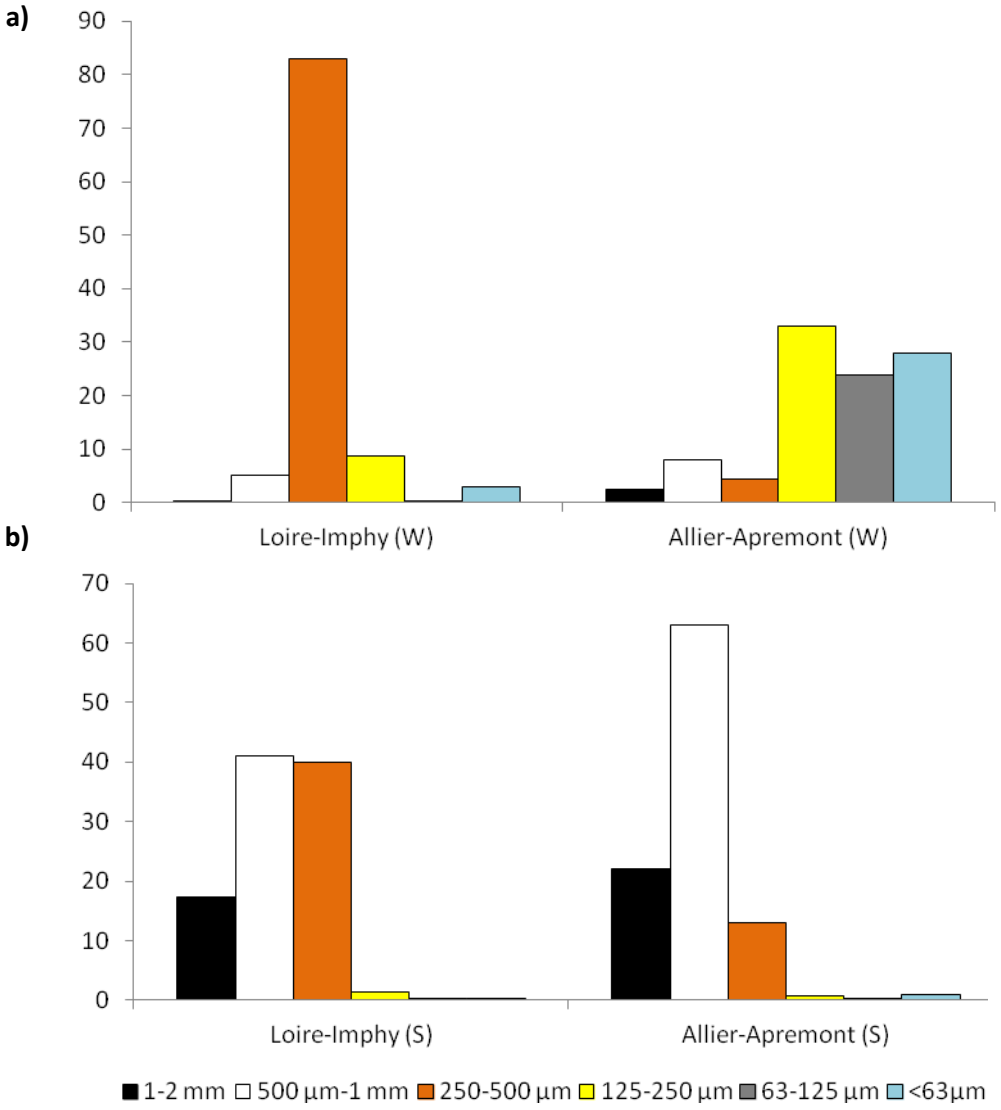

Figure 3.4 **Particle size distribution of <2 mm bed sediment in a) winter (November 2008) and b) summer (August 2009)**

Further evidence of the complex nature of riverbed sediments is provided by the changing chemical composition, as determined by XRF (Table 3.3). Corresponding to the increased proportion of fine particles during winter at the Allier-Apremont site, the concentration of Fe within the sediment is higher during winter (20.1 mg g^{-1}) than summer (5.5 mg g^{-1}). Although not as high as the Allier-Apremont sample, the concentration of Fe is also higher during winter at the Loire-Imphy site, likely indicating the increased erosion inputs during higher flows observed for particulates in the Loire River (Négrel et al., 2000). The concentration of As within sediment is also variable between seasons and sites, with As concentrations exceeding world average river sediment concentrations at the Allier-Apremont site (12-15 mg kg^{-1}) (Smedley and Kinniburgh, 2002), reflecting the elevated As concentrations found along the Allier river course (Gautier et al., 2000; Morin et al., 2002). Unlike Fe, the possible role of riverbank erosion contributing to elevated As concentrations within the seasonal sediment samples is not as clear. While the Allier-Apremont winter sediment contains higher As than the summer sample, the reverse is true for the Loire-Imphy site, indicative of the heterogeneity inherent in riverbed samples.

Table 3.3 **General sediment data, including average trace element composition, as determined by XRF**

		Allier-Apremont		**Loire-Imphy**	
		Nov-08 winter	Aug-08 summer	Nov-08 winter	Aug-08 summer
	pH (river)	6.6	8.0	7.8	7.3
Fe	mg g^{-1}	20.1	5.5	5.1	2.8
As	µg g^{-1}	15.8	12.4	6.4	9.4
Mn	µg g^{-1}	387	267	224	153
Pb	µg g^{-1}	43	21	29	25
Zn	µg g^{-1}	110	17	28	17

Variation could be attributable to a number of factors including variation in transported sediment loads, the transport and storage of sediments along the riverbanks and environmental processes removing As from within the solid phase. A similar increase is seen in other trace element concentrations in the winter sampling of the Allier-Apremont sediment

(Table 3.3), reinforcing the variability in river sediment composition, and the likely contribution of riverbank sediments. At the Loire-Imphy site, while As is higher within the summer sediment, the other trace elements including Fe and Mn are higher within the winter sediment. However, the difference observed between seasons is not as great as observed for the Allier site, possibly due to the presence of a number of dams and reservoirs along the length of the upper Loire removing a large proportion of suspended material and subsequently decreasing the transport of trace elements within the water column. The pH of the sediments was generally found to be slightly alkaline (Table 3.3), however the winter Allier-Apremont sediment was an exception, having a more acidic pH than the summer sediment, possibly due to the increased presence of humic acids within the sediment.

3.4.4 Solid phase partitioning of As and Fe

The partitioning of As and Fe was determined in all four sediments prior to the incubation studies to gain insight into the storage of both elements in the bed sediment (Figures 3.5 & 3.6). Good agreement was found for the sum of extraction steps and the XRF As content of each sediment, indicating minimal loss of As during the experimental procedure. In all of the sediments, over half of the total As extracted was found within the reducible fractions F3 and F4, targeting amorphous and crystalline hydrous oxides of Fe/Al respectively. This observation is consistent with the findings of previous studies, where the geochemistry of As has been found to be closely coupled to the cycling of Fe(oxy)hydroxides within sediments (Blute et al., 2009; Dixit and Hering, 2003; Haque et al., 2008; Linge and Oldham, 2002; Masscheleyn et al., 1991). It is interesting to note that whilst the concentration of As found within the reducible fractions (F3 and F4) of the Allier-Apremont sediments does not significantly vary between season, the amount of each respective fraction does alter. During winter there is more As associated with the amorphous Fe(oxy)hydroxide minerals, while in summer there is more As found within the crystalline Fe(oxy)hydroxide minerals. In the Loire-Imphy sediments a similar relationship is evident, with the amount of As associated with crystalline mineral phases increasing in summer (Figure 3.5).

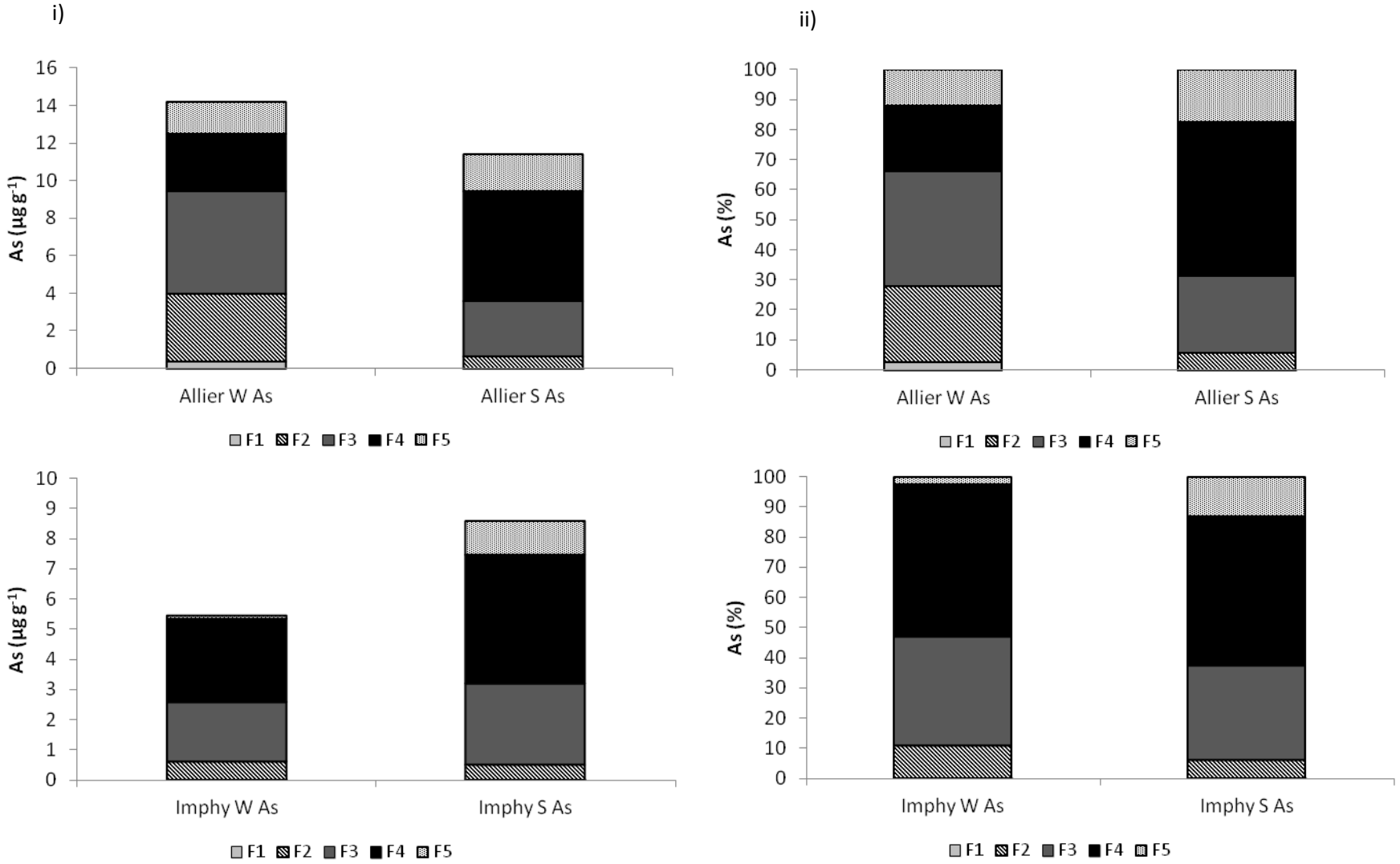

Figure 3.5 **Arsenic extraction results for winter and summer sediments including (i) As concentrations and (ii) percentages in each extractant pool, described in more detail in Table 3.1.**

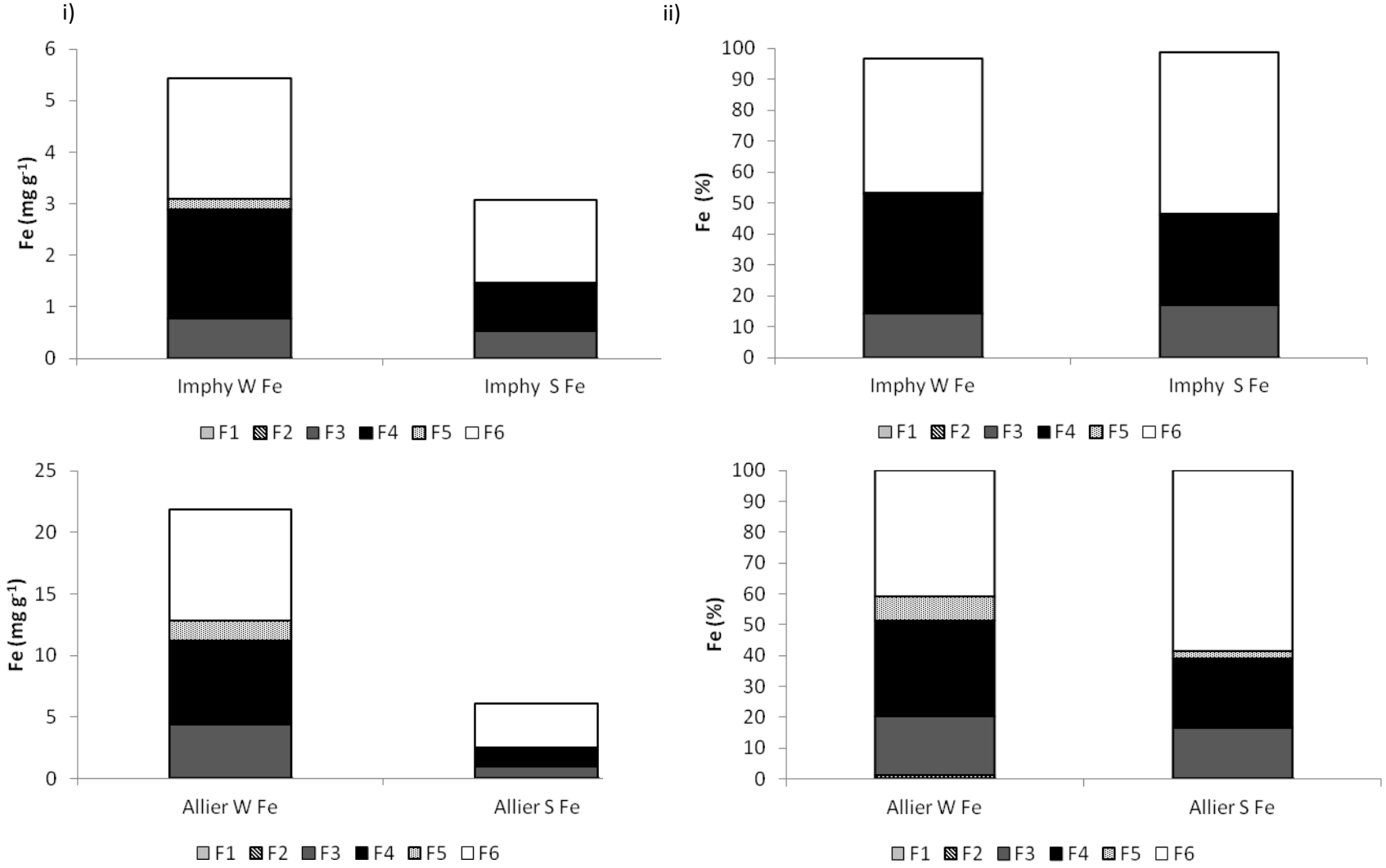

Figure 3.6 **Iron extraction results for winter and summer sediments including (i) Fe concentrations and (ii) percentages in each extractant pool, described in more detail in Table 3.1.**

The results of the SEP (Figure 3.5) for all of the studied sediments demonstrate that the easily exchangeable (anion exchange by SO_4) As is a minor component of total As within the riverbed sediment, with only nominal (< 3%) amounts found within the sediments. Specifically sorbed (PO_4 exchangeable) As plays a more important role within the sediment, with a significant decrease in the proportion of F2 present in the summer Allier-Apremont sample relative to the winter sample. While the total amount of F2 is similar between seasonal Loire-Imphy sediment samples, the proportion of F2 is higher in the winter sample. These results suggest that the environmental conditions responsible for desorption processes are more prevalent during the summer months. The amount of As associated with the oxidisable fraction targeting sulphides and OM appears to be similar between seasons in the Allier-Apremont sediment, with a slightly higher proportion associated in the summer sediment. The storage of As within the oxidisable fraction of the Loire-Imphy summer sample is significantly higher than the winter sediment, which could be explained by either increased removal of this fraction of As during the higher flows of the winter conditions, or by enrichment of sulphide and OM within the sediment during the summer months.

Despite the total concentration of Fe being considerably higher in the Allier-Apremont winter sediment, the distribution of Fe within each sediment is not as variable, with approximately 40-60 % found within the residual fraction of the sediment (Figure 3.6). This Fe is likely incorporated into silicate minerals and therefore resistant to mobilisation by changes in environmental conditions. The remaining extractable Fe is found primarily in the reducible fractions F3 and F4, which are targeting amorphous and crystalline Fe(oxy)hydroxide minerals. The concentration of Fe found within F3 and F4 is higher in both winter sediments, however the proportion found within each fraction is similar between seasonal samples for each sediment. Within both the Allier-Apremont and Loire-Imphy sediments the proportion of Fe in the crystalline Fe/Al mineral fraction is higher than the amorphous fraction (Figure 3.6). The partitioning of As generally follows that observed for Fe, with the reducible fraction F4 representing the largest pool of As within the sediments, with the exception of the Allier-Apremont winter sample. However, despite higher amounts of Fe within the reducible fractions of the winter sediments at both sites, the association of As within F4 is actually higher during summer. Clearly environmental conditions as well as the occurrence of Fe within the sediment are important in the geochemical cycling of As within river sediments. The contrast

in partitioning of As relative to Fe at the Allier suggests different controls on these trace elements in the Allier-Apremont sediment under the winter environmental conditions.

No significant amount of Fe was found in the exchangeable fraction of any of the sediments, suggesting that there is little adsorption of Fe onto the bed sediment from the water column under differing seasonal conditions in both rivers. In contrast to the storage of As, there is a greater proportion of Fe associated with the oxidisable fraction F5 in both the Allier-Apremont and Loire-Imphy winter samples, with only nominal amounts of Fe found within F5 in summer. This finding confirms that the As associated with the oxidisable fraction is not related to the presence of Fe minerals.

3.4.5 Mechanisms of arsenic remobilisation

i) Alteration of pH

The release of dissolved As over time at different pH values for each sediment is illustrated in Figure 3.7. Results are presented as amount of As released per gram of dry sediment. Fluctuations in slurry pH are inherent to the methodology used, and is represented in Figure 3.7. To enable a clear discussion, each slurry is referred to hereafter by the initial pH. Related to the mobility of the anionic species of As occurring under alkaline conditions (Smedley and Kinniburgh, 2002), increased As release is observed at higher (>8) pH values for all sediments, with neutral pH values releasing only nominal amounts of As from the sediment (<30 ng g^{-1}). While there appears to be a general relationship between the amount of released As and the total concentration of As present within each sediment, with release above pH 8 highest from the Allier-Apremont winter sediment (As content: 15.8 µg g^{-1}), the variation in total concentration does not completely explain the similarity of the observed release for the remaining sediments. As pH affects the protonation of surface ligand groups and therefore the availability of surface binding sites for aqueous ions, mobilisation of As caused by changes in pH is likely due to release from surface adsorbed sites, although changes in crystallinity of minerals present and subsequent As release have also been documented (Cornell and Schwertmann, 1996). Evaluation of the partitioning of the As within each sediment can help to explain the observed release pattern. According to the initial sediment partitioning (Figure 3.5), the Allier-Apremont winter sediment contained the highest amount of surface sorbed As with

F1 + F2 comprising of 3.96 μg g^{-1}, with the remaining three sediments containing similar amounts of F1 + F2 between 0.51-0.65 μg g^{-1} despite having different total concentrations of As. Grain size analysis has indicated that the Allier-Apremont winter sediment contained the highest proportion of <63 μm particles (Figure 3.4). Given that the availability of surface binding sites is related to the surface area of particles, the higher level of sorbed As found within the Allier-Apremont winter sediment is likely a function of the sediment grain size.

An initial rapid release of dissolved As is evident in all sediments at pH 9 and 10, however the degree of release appears to be variable. At pH 10, over 50 % of the total released As is in solution after 5hrs of incubation of the Allier-Apremont winter sediment compared with 27-32 % for the other sediments. Whilst the increased rapid release seen in the Allier-Apremont winter sediment is most likely due to the increased presence of easily exchangeable As within the sediment, seen within F1 of the SEP (Figure 3.5), lack of As within F1 for the other sediments suggest that As associated with other fractions is also contributing to the observed release. After 5hrs, 29 - 40 % of the total released As is in solution from the winter sediments, with a steady increase in concentration occurring with time. A different pattern of release is observed for the summer sediments with 71- 92 % of the total released As in solution from the summer sediments after 5hrs. Following the initial rapid release from the summer sediments, there is a subsequent decrease observed at 24 hrs, followed by a steady increase up to the end of incubation at day 14 (Figure 3.7). The variation does not appear to be related to minor fluctuations (±0.3) in pH during the incubations, with maximum pH values not observed in either 5 hr incubation.

a)

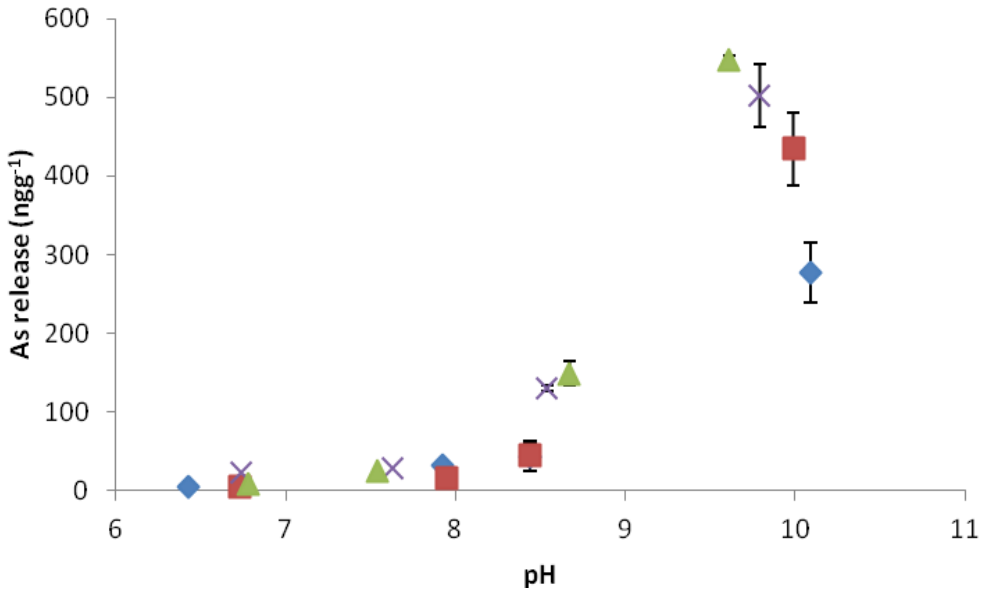

b)

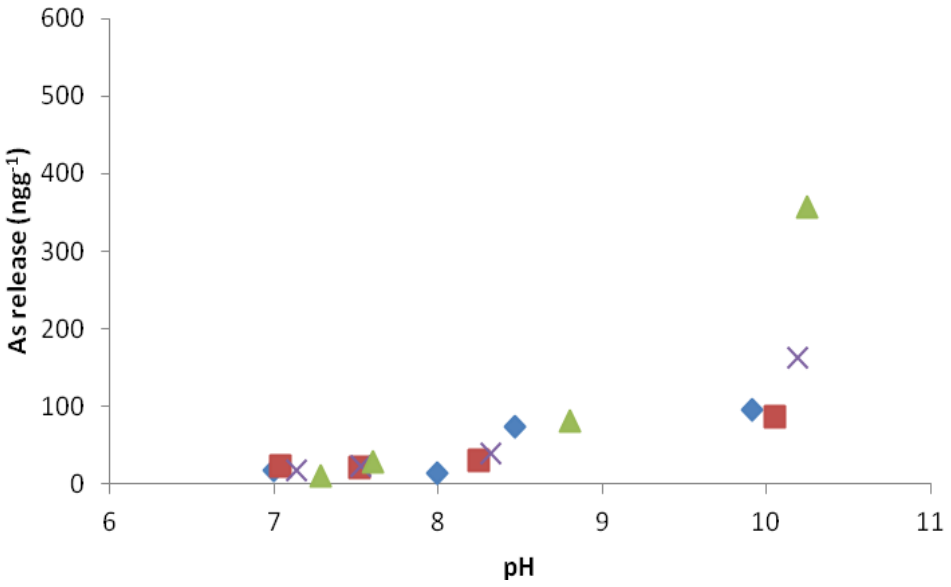

Figure 3.7 **Release of As (ng g^{-1}) from sediment under varying pH conditions. Using a) Allier-Apremont Winter sediment b) Allier-Apremont Summer sediment. Time is indicated by symbol, ◆ 5 hrs , ■ 1 day (24 hrs), × 7 days (168 hrs), and ▲ 14 days (336 hrs). Error bars represent 2SD on duplicates run for pH 9 and 10 Allier-Apremont winter sediment. Data in Table S3-1, Appendix 2**

c)

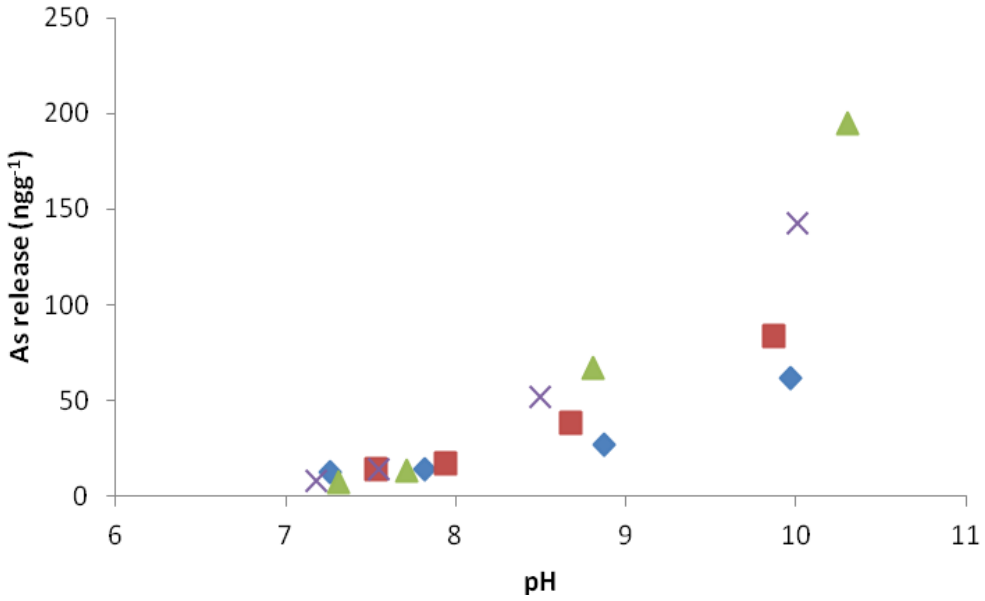

d)

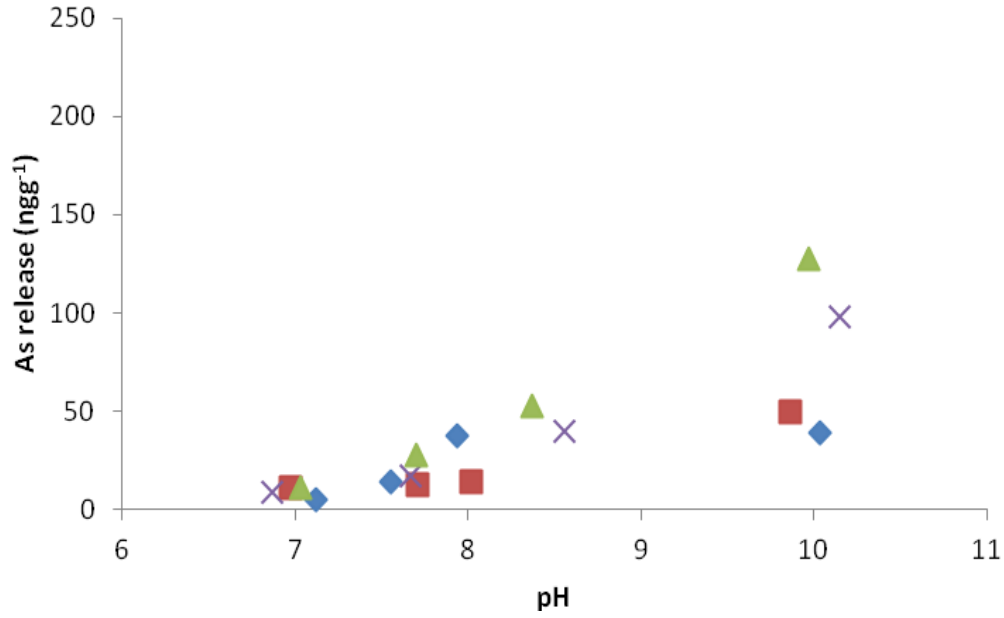

Figure 3.7 (cont) **Release of As (ng g^{-1}) from sediment under varying pH conditions. Using c) Loire-Imphy Winter sediment d) Loire-Imphy Summer sediment. Time is indicated by symbol, ◆ 5 hrs , ■ 1 day (24 hrs), × 7 days (168 hrs), and ▲ 14 days (336 hrs).**

After the initial rapid release, it is evident that for the slurries at pH 9 and 10, there is a clear relationship between As release and time (Figure 3.7), with sediments generally displaying increasing As release with increasing time. This is most evident for the pH 10 slurries, where dissolved concentrations increase up to 4-fold from those measured at 7 days to 14 days. Despite this, evaluation of peak concentrations of dissolved As at pH 10 reveal that only 3.0 - 3.6 % of total As is released from the Allier-Apremont sediments, and 1.4 - 2.9 % from the Loire-Imphy sediments. The continual increase in dissolved As concentrations observed for all sediments at alkaline pH's indicates that equilibrium has not been reached even after 14 days. It appears that the desorption of As from bed sediments is not a short term phenomenon, and that bed sediments remain a significant store of releasable As over longer time periods. Shorter equilibration times (24 hrs) have been noted for desorption from other sediments, notably by Linge & Oldham (2002), who found that 19 % of sediment As was released in 24 hours. This increased release is likely related to the contaminated nature of the lake sediment used in incubations, however the reasons for the difference in equilibration time are not as clear.

Comparison of the initial sediment partitioning with the residual winter sediment obtained from the pH 8 and pH 10 slurries after 14 days incubation allows for the determination of the phases contributing to As release. It should be noted that the sum of the extraction steps were in some cases higher for the post-extraction sediment than for the initial sediment reflecting both the small fraction of the total pool of As released under experimental conditions and the uncertainty relating to SEPs (Table S3-2, Appendix 2). Overall, clear changes in partitioning were observed amongst the measured fractions, allowing for comment on the likely phases contributing to the release of As. As expected for desorption caused by changes in pH, it is clear that loss of As is seen in both exchangeable fractions of the sediment, F1 and F2 (Figure 3.8). In addition to losses of exchangeable As, there is also a clear reduction in oxidisable As within the Allier-Apremont winter sediment for both pH incubations. Rapid release of As from within this fraction could explain the increased release observed in the summer sediments, with both summer sediments containing a higher proportion of F5 As than their corresponding winter sediments. The reduction in As associated with F5 in the incubations of Allier-Apremont winter sediment is possibly related to the dissolution of humic acids. An orange colour was observed in the leachates of the pH 9 and 10 incubations, which produced a precipitate upon acidification. A similar observation has been made by Linge and Oldham (2002), where lake

sediments were suspended with deionised water at pH >11. Despite possible removal of dissolved As from solution due to the precipitate, a low pH was maintained in the leachate after formation of the precipitate to desorb any As associated with the precipitate.

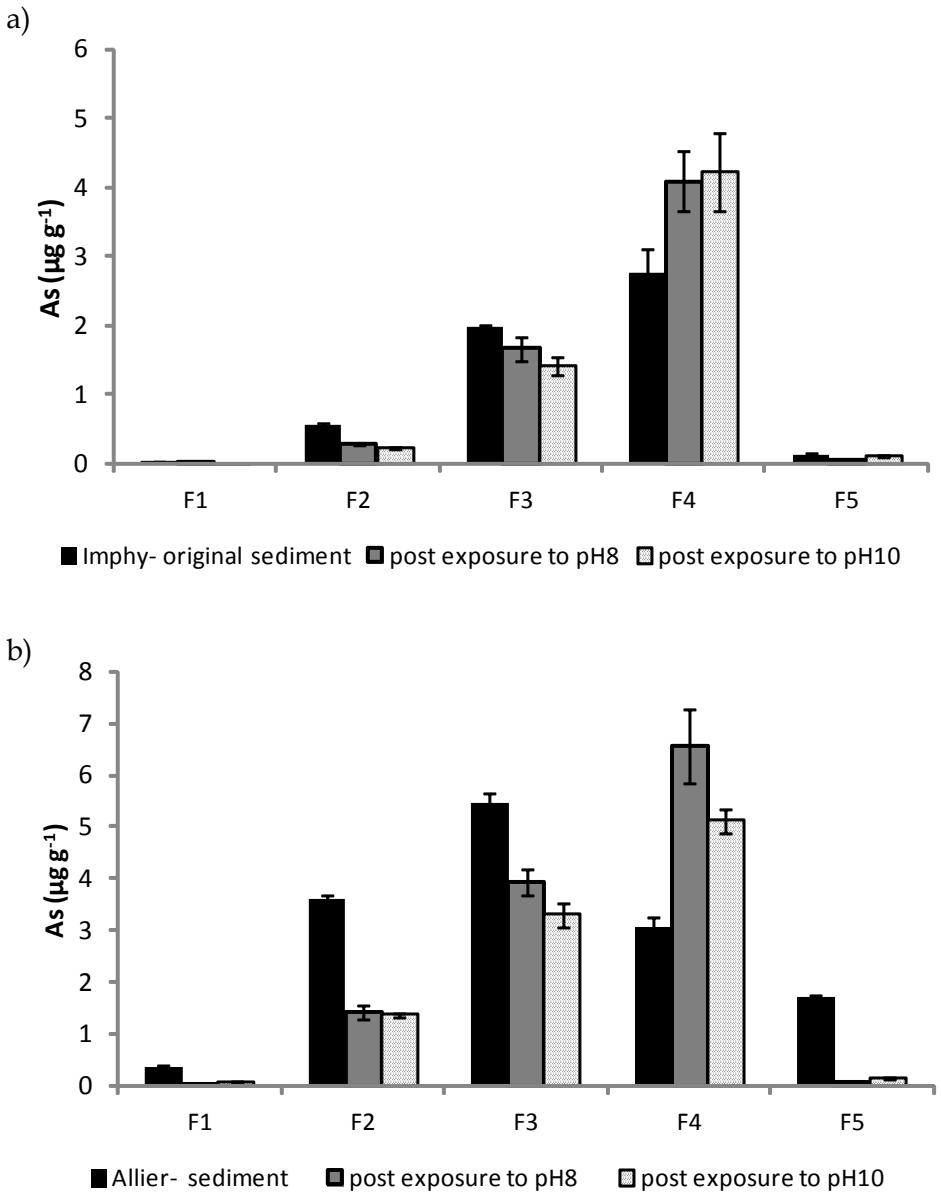

Figure 3.8 **The effect of incubation under varying pH conditions (pH 8, pH10) on sediment As partitioning (a) Imphy winter sediment (b)Allier winter sediment. Comparison is made between initial sediment partitioning and partitioning in sediment after 14 days incubation. Bars represent standard errors from triplicate measurements. Data in Table S3-2, Appendix 2**

In addition to the losses in exchangeable and oxidisable As, changes in the storage of reducible As in F3 and F4 are also observed, with decreases in F3 and corresponding increases in F4 in both sediments. Such a shift in As storage could be due to changes in Fe-mineralogy occurring during incubation, with the Fe minerals present becoming progressively more crystalline, and therefore more thermodynamically stable, with time under the alkaline conditions. In addition to a range of environmental factors including temperature, time, competing ions and microbial activity, the transformation of ferrihydrite to the more crystalline hematite and goethite has been found to be accelerated by increased pH in a number of previous studies (Baltpurvins et al., 1996; Cornell and Schwertmann, 1996). This observation could explain why increased levels of As are found within the more crystalline Fe(oxy)hydroxide (F4) fraction within the summer sediments (Figure 3.8), when the rivers are typically experiencing higher pH's (Table 3.2). The pH experiments indicate that exposure to elevated pH affects both As release and storage of As within the sediment, having important implications for the ongoing mobility of As within river sediments undergoing seasonal fluctuations in pH.

It is apparent that the seasonal pH variations experienced by both rivers (Table 3.2) fall within the range where As desorption was found to increase. The higher pH values found typically in the summer period, combined with the lower flows and increased water-sediment contact time should allow for increased desorption occurring within the riverbed sediments. Evidence of this removal is apparent in the sediments collected from both sites, with lower exchangeable As (F1 and F2) present in the summer sediments. These observations indicate that both Loire-Imphy and Allier-Apremont bed sediments contain significant pools of As that are able to be mobilised under changing environmental conditions. Rivers are complex hydrosystems, experiencing changing flowpaths on a seasonal basis. Fresh riverbank sediments are inundated under increased flows, especially in the middle reaches of both the Loire and Allier rivers (Gautier et al., 2000), providing additional trace element inputs. The ongoing release of As from the exchangeable fraction of the bed sediment is therefore an important mobilisation pathway occurring on an environmentally significant timescale.

ii) Anaerobic conditions

Release of As from sediments under anaerobic conditions has been found to occur by a number of pathways including reductive desorption and reductive dissolution of As-bearing

Fe(III) minerals (Smedley and Kinniburgh, 2002). The process of reductive dissolution of Fe(oxy)hydroxides is thought to be microbially mediated, whereby Fe(III) is used as an electron acceptor to facilitate growth, possibly driven by the microbial oxidation of organic carbon (Akai et al., 2004; Islam et al., 2004; van Geen et al., 2004). The direct use of As(V) as an electron acceptor by microorganisms has also been noted (Lloyd and Oremland, 2006; Zobrist et al., 2000). The effect of anaerobic conditions on the release of As and Fe from the river bed sediment was investigated through the use of microcosm incubations under both aerobic and anaerobic conditions. Experiments were conducted utilising filtered, sterilised river water collected from the Loire River at Marzy to investigate the reductive dissolution of As and Fe from within the sediments using an aqueous matrix similar to natural river conditions.

The release of Fe(II) into the aqueous phase was not detected in any of the aerobic incubations (Figure 3.9), indicating that oxidative conditions were maintained during the incubation, and reductive dissolution of Fe minerals did not occur. After 14 days incubation, the concentration of As within the sediments reached a mean ± SD of 5.1 ± 1.0 ng g^{-1}, 24.0 ± 0.7 ng g^{-1}, for Allier-Apremont winter and summer sediments respectively, and 22.5 ± 1.5 ng g^{-1} and 12.7 ± 1.1 ng g^{-1} for Loire-Imphy winter and summer sediments respectively. These concentrations are within the range expected to occur through dissolution processes, as evidenced in the pH experiments. Due to the lower sediment pH of the Allier-Apremont winter sample, the resulting pH of the Allier-Apremont winter incubations were approximately 1.5 pH units below those of the other incubations. Because of the lower incubation pH, the release of As seen in the aerobic incubation (up to 8.9 ng g^{-1}) is lower than the other incubations, and falls within the range (4-20 ng g^{-1}) expected from the corresponding pH 7 experiments. Therefore release under aerobic conditions appears to be controlled by adsorption/desorption processes.

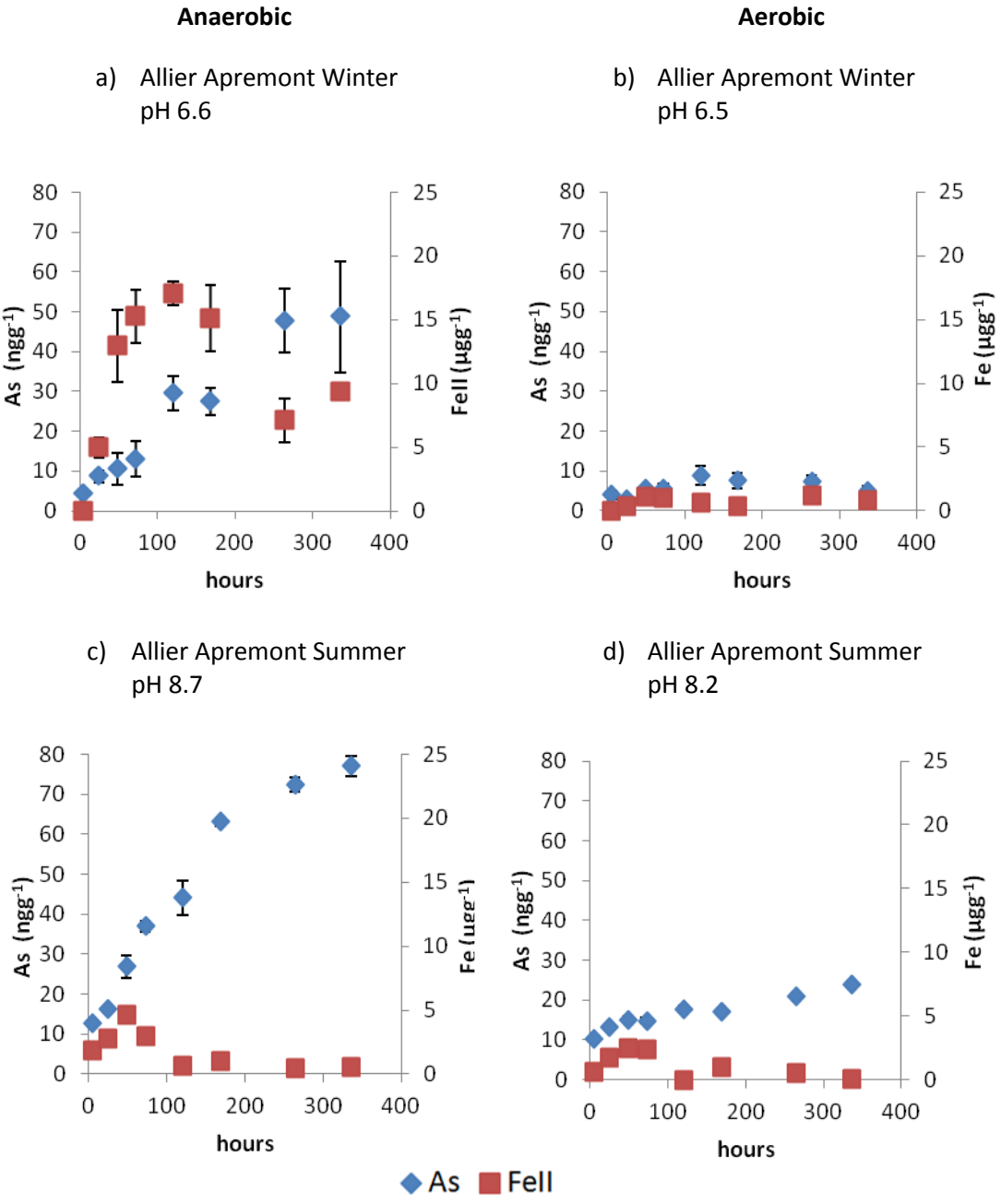

Figure 3.9 **Arsenic (As_{tot}, and Fe(II) release during anaerobic and aerobic incubations for Allier-Apremont winter (a,b) and summer (c,d) bed sediments. Anaerobic incubations are displayed in the left-hand column, aerobic in the right-hand column. The pH of each incubation is noted on the graph. Bars represent standard errors from triplicate measurements, where not visible, errors are within the icon. Data for As release in Table S3-3, Appendix 2**

Anaerobic **Aerobic**

e) Loire-Imphy Winter pH 8.5

f) Loire-Imphy Winter pH 8

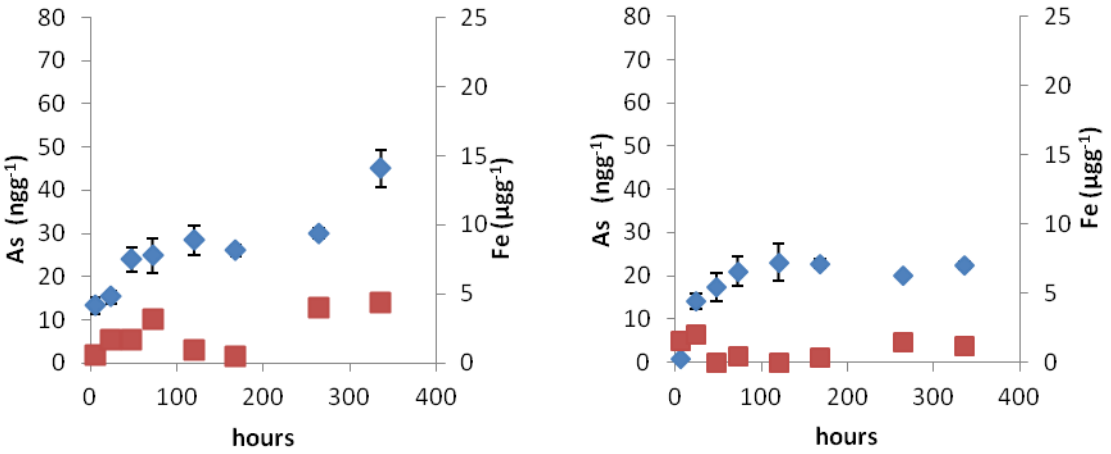

g) Loire-Imphy Summer pH 8.5

h) Loire-Imphy Summer pH 8.2

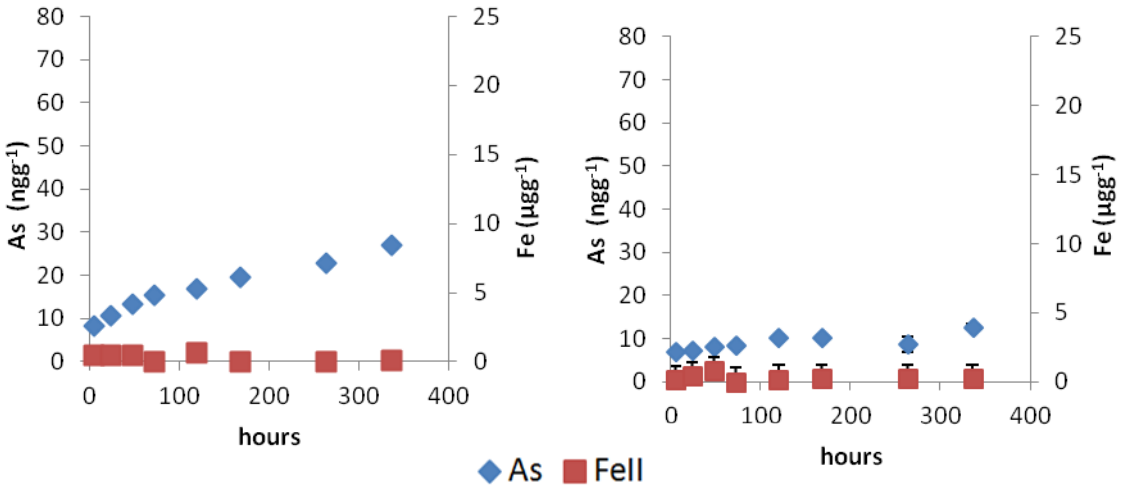

Figure 3.9(cont) **Arsenic (As_{tot}, and Fe(II) release during anaerobic and aerobic incubations for Loire-Imphy winter (e, f) and summer (g, h) bed sediments. Anaerobic incubations are displayed in the left-hand column, aerobic in the right-hand column. The pH of each incubation is noted on the graph. Bars represent standard errors from triplicate measurements, where not visible, errors are within the icon. Data for As release in Table S3-3, Appendix 2**

Release of As was found to increase over time in the anaerobic incubations of all four sediments, with the pattern of release of Fe(II) found to coincide for all sediments (Figure 3.9). Rapid release of Fe(II) was not observed, with concentrations found to peak at 4 days (120 hours) from the Allier-Apremont winter sediment, and 2 days (48 hours) from the Allier-Apremont summer sediment. Release of Fe(II) in the Loire-Imphy winter sediment showed two distinct peaks, occurring at 3 days (72 hours) and again towards the end of the incubation at 14 days (336 hours) (Figure 3.9).

The release Fe(II) under anaerobic conditions suggests that release is due to the reductive dissolution of Fe(oxy)hydroxide minerals (Duan et al., 2009; Masscheleyn et al., 1991; Pedersen et al., 2006). It appears that the increased release of Fe(II) is related to the level of Fe found within the amorphous and crystalline Fe(oxy)hydroxide mineral fractions of the sediment. Levels of Fe(II) release are significantly higher in the Allier-Apremont winter sediment (17.0 µg g^{-1}), correlating to the higher amount of Fe associated within F3 and F4 of the SEP (11.0 mg g^{-1}), while the lower release of Fe(II) (4.3 µg g^{-1}) in the Loire-Imphy winter sediment is in similar proportion with the Fe associated with F3 and F4 (2.9 mg g^{-1}) as observed in the Allier sediment.

Dissolved oxygen levels were measured at the end of each incubation and found to be <1 mg l^{-1}. Analysis of the partitioning of As in the sediments indicated that both summer sediments had a higher proportion of As within F5 (Figure 3.5), indicating that this is a potential source of the released As.

Field water quality data indicated that As(III) concentrations were higher in the summer (Table 3.2), when DO levels were lower, suggesting that reductive dissolution of Fe(oxy)hydroxides is occurring in the bed sediments, or in riverbank aquifers. Despite rivers being generally accepted as aerobic aqueous environments, low levels of DO have been noted in sediments as shallow as 20-30 cm in a region termed the hyporheic zone (Nagorski and Moore, 1999). Anaerobic conditions are also more likely to occur in during the periodic saturation of riverbank sediments, during low flows, or in ponded areas such as those experienced during the summer drought months. In the river water, the reduced As(III) will quickly be oxidised by the turbulent flow in the channel, accounting for the lower proportion of As(III) observed in the water column.

Aqueous concentrations of As increased in all incubations over the 14 day incubation period, to a maximum of 77.0 ± 4.2 ng g^{-1} in the Allier-Apremont summer sediment incubation. However despite the lower pH, release of As in the anaerobic Allier-Apremont winter sediment was found to exceed release seen in equivalent pH experiment, increasing over the course of incubation to 48.7 ± 14.0 ng g^{-1}. Clearly under anaerobic conditions desorption processes alone cannot explain the observed release, indicating the importance of dissolution processes when considering As mobilisation (Pedersen et al., 2006).

Both amorphous and crystalline Fe minerals were found to be significant stores of As within the sediments collected at both sites (Figure 3.5). While release of Fe(II) from the summer sediments has indicated that Fe-minerals play a important role on As mobilisation under anaerobic conditions, the importance of other factors must also be considered. The behaviour of the Loire-Imphy summer sediment differs from the others, with no evidence of reductive dissolution occurring in either aerobic or anaerobic incubations (Figure 3.9). The release of As observed in both incubations (12.7 - 26.9 ng g^{-1}) is lower than, or within the range of expected release from desorption processes, as estimated from the pH experiments (27 – 53 ng g^{-1}). Lower than expected release from the aerobic incubation could be due to the different methods of mixing employed in the microcosm vs. pH experiments (regular shaking vs. end-over end mixing) because of logistical restraints. However lower As release combined with the lack of Fe(II) release, despite the similarity of Fe content within the sediment indicates that factors other than the presence of Fe within the sediment are important in the mobilisation of both Fe and As.

Although the activity of native microorganisms was not measured during these incubations, the reduction of Fe(III)-(oxy)hydroxide minerals is generally accepted to be microbially mediated (Bhattacharyya et al., 2007; Jones et al., 2000; Pearcy et al., 2011; Rowland et al., 2007). Therefore factors contributing to the activity of the microbial community e.g. nutrient sources and other environmental conditions (Ehrlich, 2001) may be responsible for differences observed in reductive dissolution in the Loire-Imphy summer sediment.

Changes in As partitioning were evaluated by post incubation SEP of the two winter sediments. It should be noted that the sum of the extraction steps were in some cases higher for the post-extraction sediment (but within acceptable error limits) than for the initial sediment, as seen for the pH experiments. This is not unexpected given the released dissolved As accounts for as

little as 0.3 - 0.6 % and 0.1 - 0.7 % of solid-phase As within the Allier-Apremont and Loire-Imphy sediments respectively. Despite the lack of a difference in measured total concentrations post incubation, clear changes in partitioning were observed amongst the fractions. Loss of exchangeable As (F1 and F2) was observed in all extractions, with greater losses of F2 seen in the aerobically incubated sediment (Figure 3.10). The higher amount of As in the Allier-Apremont winter sediment exchangeable fraction (F2) post incubation relative to that seen for the pH experiment (Figure 3.8) is attributable to the decreased pH of the microcosm experiment. Desorption appears to be the primary release process occurring within the aerobic incubations, with the observed small differences between the partitioning of As between the amorphous and crystalline Fe(oxy)hydroxide minerals (F3 and F4), similar to those seen in the pH experiments.

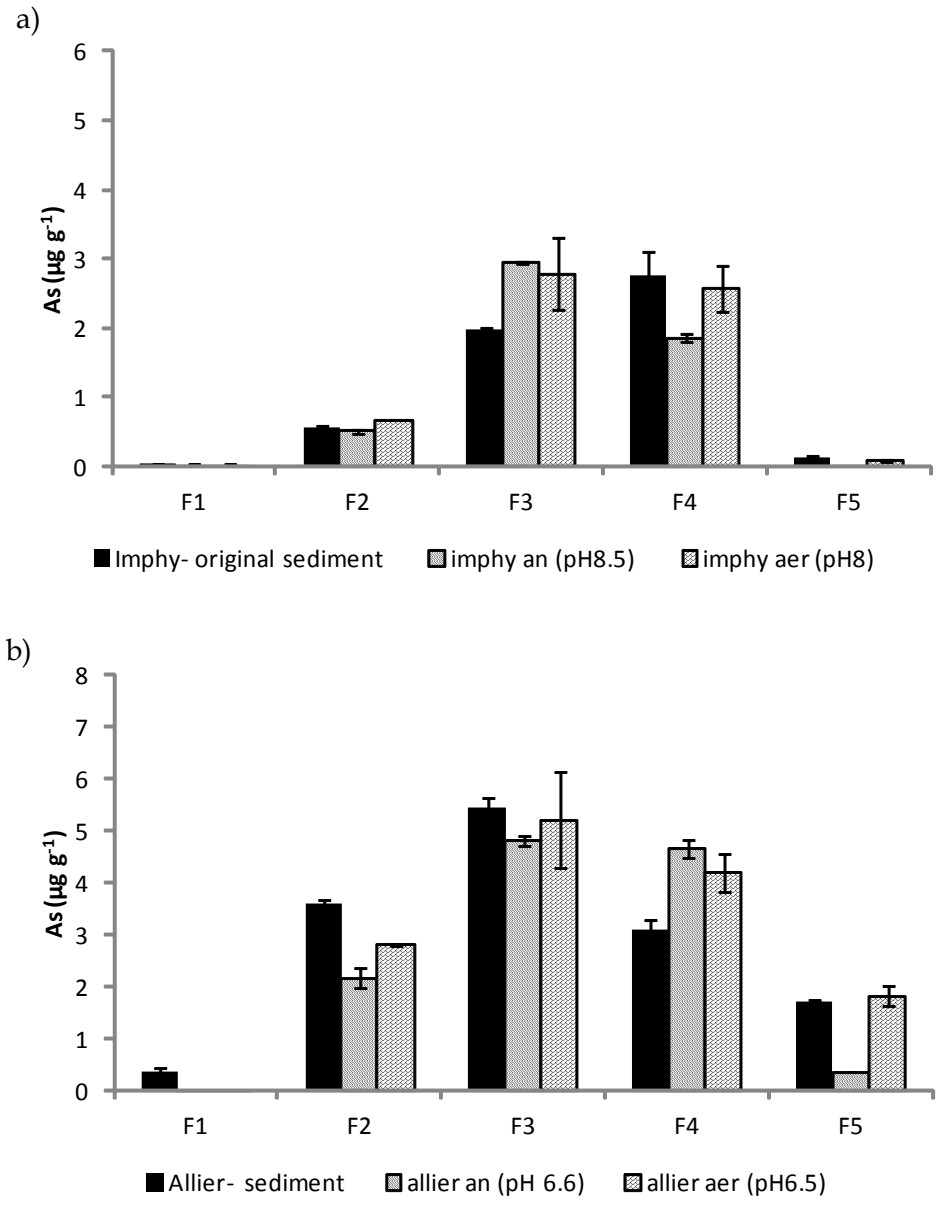

Figure 3.10 **The effect of anaerobic incubation on sediment As partitioning. a) Imphy (winter) sediment, b) Allier (winter) sediment. Comparison is made between initial sediment partitioning (black bar) and partitioning in sediment incubated anaerobically (diagonal lines) and aerobically (block fill) after 14 days incubation. Note that the pH of the incubations varies. Error bars represent the SD on triplicate samples. Data in Table S3-2, Appendix 2.**

Under anaerobic conditions there is evidence of loss of As from the reducible fraction targeting crystalline Fe(oxy)hydroxide minerals in both the Loire-Imphy and Allier-Apremont winter sediments, supporting the loss of As through reductive dissolution (Figure 3.10). Loss of reducible As from the Allier-Apremont winter sediment was also seen, with a decrease in As found in F3 after anaerobic incubation (Figure 3.10). Release of OM-associated As (F5) was also found to vary with incubation conditions. The relatively high amount of As within F5 for the Allier-Apremont sediment was removed in both aerobic incubations at pH 8 and 10 (Figure 3.8) and in the anaerobic pH 6.6 incubation (Figure 3.10), whilst no removal was evident in the aerobic pH 6.5 incubation. Previous work on the behaviour of OM using a series of wetland soil incubations found its solubility to be dependent on both pH and redox conditions (Grybos et al., 2009). They found that reducing conditions resulted in an increase in aqueous dissolved organic carbon (DOC) and pH, whilst aerobic incubation at lower (~5.5) pH was not found to release DOC. Under aerobic conditions at pH 6.5, the lack of As release from the OM-associated fraction of the Allier-Apremont winter indicates that the release of As is dependent on the release of OM from within the sediment. These results indicate that whilst there is a strong correlation between the storage of As and the Fe mineral content of sediments, other contributing factors including the activity of native microbial communities, and the OM content of the sediment could also be controlling factors in the mobilisation of As.

3.5 Conclusions

Concentrations of dissolved As were found to be highest during summer months, with increased occurrence of As(III). Variability in the total amount of As transported by each river indicated that dilution of a single source of As is not responsible for changes in concentration. Bed sediments clearly have an important role in the cycling of As within the Allier and Loire Rivers. Concentrations of As in the bed sediment of the Allier-Apremont and Loire-Imphy Rivers were above global averages for sediment, with the As content of the Allier-Apremont sediment found to reflect the increased As sources within the upper reaches of the Allier River. While no overall link was found between season and total concentrations of As, total concentrations of Fe were found to be higher in both rivers during winter, suggesting erosion of riverbank sediments as a source of Fe into the river. Variability in total As likely reflects the complexity of river flows and sediment transport in the two rivers. Iron was found to play a key

role in the cycling of As within the sediment, with As found to be predominantly within the reducible phases, associated with Fe(oxy)hydroxide minerals in the sediments from both sites.

Determination of the partitioning of As within the sediment before and after incubation has allowed for the description of mobilisation mechanisms occurring within the sediment. Experimental results provide evidence that riverbed sediments from the Allier-Apremont and Loire-Imphy sites contain a reservoir of As able to be released under seasonal changes in environmental conditions, being capable of both dissolution and desorption of As. Release of exchangeable and OM-associated As was seen under alkaline pH conditions, at pH values commonly experienced in both rivers during summer months. The lack of exchangeable As found within the summer sediments supports the removal of As from bed sediments by desorption. During the pH experiments, the rapid release of As indicates that sediments are able to respond to short term pH fluctuations, whilst the ongoing release of As over the 14-day incubation for all the sediments suggests that sediments can act as a source of As over an extended time period in the river.

Under anaerobic conditions, release of As was found to be occurring via both desorption processes and dissolution from the reducible Fe(oxy)hydroxide mineral fractions. While release of Fe(II) was noted in three of the anaerobic experiments, the Fe content of the sediment alone was not the only contributing factor to anaerobic release of As, with lower As release seen from the Loire-Imphy summer sediment despite similar Fe content to the corresponding winter sediment. Increased As(III) found in the river water during summer months provides evidence of anaerobic release of As occurring within the rivers. Under aerobic conditions As release was found to be primarily by desorption. However, the release of OM-associated As was found to vary under changing redox and pH conditions, with lower release seen in low pH aerobic conditions. From these results it is clear that the composition of the sediments, as well as the environmental conditions, will affect the release of As. Such information on the behaviour of river sediments as a source of As illustrates the dynamic processes affecting both the storage and mobilisation of As within fluvial systems. Although the current study was carried out within a silicate dominated fluvial system, the observed geochemical behaviour provides insight into the ongoing seasonal trends of sediment As within other river systems.

3.6 References

Aggett J, O'Brien G. Detailed Model for the Mobility of Arsenic in Lacustrine Sediments Based on Measurements in Lake Ohakuri. Environmental Science & Technology 1985; 19: 231-238.

Ahmann D, Krumholz LR, Hemond HF, Lovley DR, Morel FMM. Microbial mobilization of arsenic from sediments of the Aberjona Watershed. Environmental Science & Technology 1997; 31: 2923-2930.

Akai J, Izumi K, Fukuhara H, Masuda H, Nakano S, Yoshimura T, et al. Mineralogical and geomicrobiological investigations on groundwater arsenic enrichment in Bangladesh. Applied Geochemistry 2004; 19: 215-230.

Anawar H, Mihaljevic M, Garcia-Sanchez A, Akai J, Moyano A. Investigation of Sequential Chemical Extraction of Arsenic from Sediments: Variations in Sample Treatment and Extractant. Soil & sediment contamination 2010; 19: 133-141.

Baltpurvins KA, Burns RC, Lawrance GA, Stuart AD. Effect of pH and Anion Type on the Aging of Freshly Precipitated Iron(III) Hydroxide Sludges. Environmental Science & Technology 1996; 30: 939-944.

Barbier J, Chery L. Relationships between natural geochemical background and high heavy metal levels in waters (Sb, As, Ba, Cr, Ni, Pb, Zn). Application to Auvergne and Limousin, and validation. BRGM report R 39544, Orleans, 1997, pp. 1-51.

Barringer JL, Bonin JL, Deluca MJ, Romagna T, Cenno K, Alebus M, et al. Sources and temporal dynamics of arsenic in a New Jersey watershed, USA. Science of the Total Environment 2007; 379: 56-74.

Bhattacharyya P, Welch A, Stollenwerk KG, McLaughlin MJ, Bundschuh J, Panaullah G. Arsenic in the Environment: Biology and Chemistry. Science of the Total Environment 2007; 379: 109-120.

Bird G, Brewer PA, Macklin MG, Balteanu D, Driga B, Serban M, et al. The solid state partitioning of contaminant metals and As in river channel sediments of the mining affected Tisa drainage basin, northwestern Romania and eastern Hungary. Applied Geochemistry 2003; 18: 1583-1595.

Blute NK, Jay JA, Swartz CH, Brabander DJ, Hemond HF. Aqueous and solid phase arsenic speciation in the sediments of a contaminated wetland and riverbed. Applied Geochemistry 2009; 24: 346-358.

Bourg ACM, Kedziorek MAM, Crouzet C. Seasonal cycles of dissolved Cd, Mn and Zn in river water caused by variations in pH induced by biological activity. Aquatic Geochemistry 2000; 6: 461-471.

Cances B, Juillot F, Morin G, Laperche V, Alvarez L, Proux O, et al. XAS evidence of As(V) association with iron oxyhydroxides in a contaminated soil at a former arsenical pesticide processing plant. Environmental Science & Technology 2005; 39: 9398-9405.

Chaillou G, Schafer J, Anschutz P, Lavaux G, Blanc G. The behaviour of arsenic in muddy sediments of The Bay of Biscay (France). Geochimica et Cosmochimica Acta 2003; 67: 2993-3003.

Cornell RM, Schwertmann U. The iron oxides: structure, properties, reactions, occurrence and uses. Weinheim, Germany: Verlag VCH Verlagsgesellschaft, 1996.

Devesa-Rey R, Paradelo R, Diaz-Fierros F, Barral MT. Fractionation and bioavailability of arsenic in the bed sediments of the Anllons River (NW Spain). Water Air and Soil Pollution 2008; 195: 189-199.

Dixit S, Hering JG. Comparison of Arsenic(V) and Arsenic(III) Sorption onto Iron Oxide Minerals: Implications for Arsenic Mobility. Environmental Science & Technology 2003; 37: 4182-4189.

Duan M, Xie Z, Wang Y, Xie X. Microcosm studies on iron and arsenic mobilization from aquifer sediments under different conditions of microbial activity and carbon source. Environmental geology 2009; 57: 997-1003.

Ehrlich HL. Geomicrobiology. New York: Marcel Dekker, 2001.

Einax JW, Nischwitz V. Inert sampling and sample preparation - the influence of oxygen on heavy metal mobility in river sediments. Fresenius Journal of Analytical Chemistry 2001; 371: 643-651.

Espinosa E, Armienta MA, Cruz O, Aguayo A, Ceniceros N. Geochemical distribution of arsenic, cadmium, lead and zinc in river sediments affected by tailings in Zimapan, a historical polymetalic mining zone of Mexico. Environmental Geology 2009; 58: 1467-1477.

Freeman MC, Aggett J, O'Brien G. Microbial Transformations of Arsenic in Lake Ohakuri, New Zealand. Water Research 1986; 20: 283-294.

Fuller CC, Davis JA. Influence of Coupling of Sorption and Photosynthetic Processes on Trace-Element Cycles in Natural Waters Nature 1989; 340: 52-54.

Gault AG, Jana J, Chakraborty S, Mukherjee P, Sarkar M, Nath B, et al. Preservation strategies for inorganic arsenic species in high iron, low-Eh groundwater from West Bengal, India. Analytical and Bioanalytical Chemistry 2005; 381: 347-353.

Gault AG, Polya DA, Charnock JM, Islam FS, Lloyd JR, Chatterjee D. Preliminary EXAFS studies of solid phase speciation of As in a West Bengali sediment. Mineralogical Magazine 2003; 67: 1183-1191.

Gautier E, Piégay H, Bertaina P. A methodological approach of fluvial dynamics oriented towards hydrosystem management: case study of the Loire and Allier rivers. Geodinamica Acta 2000; 13: 29-43.

Gonzalez Z, Krachler M, Cheburkin A, Shotyk W. Spatial distribution of natural enrichments of arsenic, selenium, and uranium in a minerotrophic peatland, Gola di Lago, Canton Ticino, Switzerland. Environmental Science & Technology 2006; 40: 6568-6574.

Grosbois C, Négrel P, Fouillac C, Grimaud D. Dissolved load of the Loire River: chemical and isotopic characterization. Chemical Geology 2000; 170: 179-201.

Grosbois C, Schäfer J, Bril H, Blanc G, Bossy A. Deconvolution of trace element (As, Cr, Mo, Th, U) sources and pathways to surface waters of a gold mining-influenced watershed. Science of the Total Environment 2009; 407: 2063-2076.

Grybos M, Davranche M, Gruau G, Petitjean P, Pedrot M. Increasing pH drives organic matter solubilization from wetland soils under reducing conditions. Geoderma 2009; 154: 13-19.

Haque S, Ji JF, Johannesson KH. Evaluating mobilization and transport of arsenic in sediments and groundwaters of Aquia aquifer, Maryland, USA. Journal of Contaminant Hydrology 2008; 99: 68-84.

Harrington JM, LaForce MJ, Rember WC, Fendorf SE, Rosenzweig RF. Phase associations and mobilization of iron and trace elements in Coeur d'Alene Lake, Idaho. Environmental Science & Technology 1998; 32: 650-656.

Howard AG, Arbabzavar MH, Apte S. The Behaviour of Dissolved Arsenic in the Estuary of the River Beaulieu Estuarine Coastal and Shelf Science 1984; 19: 493-504.

Hudson-Edwards KA, Houghton SL, Osborn A. Extraction and analysis of arsenic in soils and sediments. TrAC Trends in Analytical Chemistry 2004; 23: 745-752.

Islam FS, Gault AG, Boothman C, Polya DA, Charnock JM, Chatterjee D, et al. Role of metal-reducing bacteria in arsenic release from Bengal delta sediments. Nature 2004; 430: 68-71.

Jones CA, Langner HW, Anderson K, McDermott TR, Inskeep WP. Rates of Microbially Mediated Arsenate Reduction and Solubilization. Soil Science Society of America Journal 2000; 64: 600-608.

Jones CA, Nimick DA, McCleskey RB. Relative effect of temperature and pH on diel cycling of dissolved trace elements in Prickly Pear Creek, Montana. Water Air and Soil Pollution 2004; 153: 95-113.

Jung HB, Charette MA, Zheng Y. Field, Laboratory, and Modeling Study of Reactive Transport of Groundwater Arsenic in a Coastal Aquifer. Environmental Science & Technology 2009; 43: 5333-5338.

Kalnejais L, Martin W, Signall R, Bothner M. Role of sediment resuspension in the remobilization of particulate-phase metals from coastal sediments. Environmental Science & Technology 2007; 41: 2282-2288.

Klarup DG. The influence of oxalic acid on release rates of metals from contaminated river sediment. Science of the Total Environment 1997; 204: 223-231.

La Force MJ, Hansel CM, Fendorf S. Arsenic speciation, seasonal transformations, and co-distribution with iron in a mine waste-influenced palustrine emergent wetland. Environmental Science & Technology 2000; 34: 3937-3943.

Linge K, Oldham C. Arsenic remobilization in a shallow lake: The role of sediment resuspension. Journal of Environmental Quality 2002; 31: 822-828.

Lloyd JR, Oremland R. Microbial transformations of arsenic in the environment: from soda lakes to aquifers. Elements 2006; 2: 85-90.

Lovley DR, Phillips EJP. Availability of Ferric Iron for Microbial Reduction in Bottom Sediments of the Fresh-Water Tidal Potomac River Applied and Environmental Microbiology 1986; 52: 751-757.

Lyman W. Transport and transformation processes In: Rand G, editor. Fundamentals of Aquatic Toxicology: Effects, environmental fate, and risk assessment. Taylor and Francis, USA, 1995.

Manning BA, Goldberg S. Adsorption and stability of arsenic(III) at the clay mineral-water interface. Environmental Science & Technology 1997; 31: 2005-2011.

Masscheleyn PH, Delaune RD, Patrick WH. Effect of redox potential and pH on arsenic speciation and solubility in a contaminated soil. Environmental Science & Technology 1991; 25: 1414-1419.

Masson M, Schafer J, Blanc G, Pierre A. Seasonal variations and annual fluxes of arsenic in the Garonne, Dordogne and Isle Rivers, France. Science of the Total Environment 2007; 373: 196-207.

McArthur JM, Banerjee DM, Hudson-Edwards KA, Mishra R, Purohit R, Ravenscroft P, et al. Natural organic matter in sedimentary basins and its relation to arsenic in anoxic ground water: the example of West Bengal and its worldwide implications. Applied Geochemistry 2004; 19: 1255-1293.

McLaren S, Kim N. Evidence for a seasonal fluctuation of arsenic in New Zealands longest river and the effect of treatment on concentrations in drinking water. Environmental Pollution 1995; 90: 67-73.

Michel P, Boutier B, Chiffoleau JF. Net fluxes of dissolved arsenic, cadmium, copper, zinc, nitrogen and phosphorus from the Gironde Estuary (France): Seasonal variations and trends. Estuarine Coastal and Shelf Science 2000; 51: 451-462.

Miller JN, Miller JC. Statistic and Chemometrics for Analytical Chemistry. Harlow, England: Pearson Education Limited, 2005.

Mok WM, Wai CM. Distribution and Mobilization of Arsenic Species in the Creeks Around the Blackbird Mining District, Idaho. Water Research 1989; 23: 7-13.

Morin G, Lecocq D, Juillot F, Calas G, Ildefonse P, Belin S, et al. EXAFS evidence for sorbed arsenic-(V) and pharmacosiderite in a soil overlying the Echassieres geochemical anomaly, Allier, France. Bulletin de la Societe Geologique de France 2002; 173: 281-291.

Mucci A, Richard LF, Lucotte M, Guignard C. The differential geochemical behavior of arsenic and phosphorus in the water column and sediments of the Saguenay Fjord estuary, Canada. Aquatic Geochemistry 2000; 6: 293-324.

Nagorski SA, Moore JN. Arsenic mobilization in the hyporheic zone of a contaminated stream. Water Resources Research 1999; 35: 3441-3450.

Négrel P. Multi-element chemistry of Loire estuary sediments: Anthropogenic vs. natural sources. Estuarine Coastal and Shelf Science 1997; 44: 395-410.

Négrel P, Grosbois C. Changes in chemical and 87Sr/86Sr signature distribution patterns of suspended matter and bed sediments in the upper Loire river basin (France). Chemical Geology 1999; 156: 231-249.

Négrel P, Grosbois C, Kloppmann W. The labile fraction of suspended matter in the Loire River (France): multi-element chemistry and isotopic (Rb-Sr and C-O) systematics. Chemical Geology 2000; 166: 271-285.

Négrel P, Roy S. Investigating the sources of the labile fraction in sediments from silicate-drained rocks using trace elements, and strontium and lead isotopes. Science of the Total Environment 2002; 298: 163-181.

Pearcy CA, Chevis DA, Haug TJ, Jeffries HA, Yang N, Tang J, et al. Evidence of microbially mediated arsenic mobilization from sediments of the Aquia aquifer, Maryland, USA. Applied Geochemistry 2011; 26: 575-586.

Pedersen HD, Postma D, Jakobsen R. Release of arsenic associated with the reduction and transformation of iron oxides. Geochimica et Cosmochimica Acta 2006; 70: 4116-4129.

Polya D. TRPEAK, Unpublished Turbo Pascal Programme. Department of Earth Sciences (now SEAES). University of Manchester, UK, 1998.

Polya D. DBSCORR, Unpublished Turbo Pascal Programme. Department of Earth Sciences (now SEAES). University of Manchester, UK, 1999.

Raven KP, Jain A, Loeppert RH. Arsenite and Arsenate Adsorption on Ferrihydrite: Kinetics, Equilibrium, and Adsorption Envelopes. Environmental Science & Technology 1998; 32: 344-349.

Roussel C, Neel C, Bril H. Minerals controlling arsenic and lead solubility in an abandoned gold mine tailings. Science of the Total Environment 2000; 263: 209-219.

Rowland HAL, Pederick RL, Polya DA, Pancost RD, Van Dongen BE, Gault AG, et al. The control of organic matter on microbially mediated iron reduction and arsenic release in shallow alluvial aquifers, Cambodia. Geobiology 2007; 5: 281-292.

Seyler P, Martin JM. Distribution of arsenite and total dissolved arsenic in major French estuaries - dependence on biogeochemical processes and anthropogenic inputs. Marine Chemistry 1990; 29: 277-294.

Sherman DM, Randall R. Surface complexation of arsenic(V) to iron(III) (hydr)oxides: Structural mechanism from ab initio molecular geometries and EXAFS spectroscopy. Geochimica et Cosmochimica Acta 2003; 67: 4223-4230.

Smedley PL, Kinniburgh DG. A review of the source, behaviour and distribution of arsenic in natural waters. Applied Geochemistry 2002; 17: 517-568.

Swedlund PJ, Webster JG. Adsorption and polymerisation of silicic acid on ferrihydrite, and its effect on arsenic adsorption. Water Research 1999; 33: 3413-3422.

Taylor G, Owens PN, Batalla RJ, Celso G. Sediment and contaminant sources and transfers in river basins. Sustainable Management of Sediment Resources. Volume 4. Elsevier, 2008, pp. 83-135.

Tessier A, Campbell PGC, Bisson M. Sequential Extraction Procedure for the Speciation of Particulate Trace-Metals. Analytical Chemistry 1979; 51: 844-851.

Turner JN, Brewer PA, Macklin MG. Fluvial-controlled metal and As mobilisation, dispersal and storage in the Río Guadiamar, SW Spain and its implications for long-term contaminant fluxes to the Doñana wetlands. Science of the Total Environment 2008; 394: 144-161.

van Geen A, Rose J, Thoral S, Garner JM, Zheng Y, Bottero JY. Decoupling of As and Fe release to Bangladesh groundwater under reducing conditions. Part II: Evidence from sediment incubations. Geochimica et Cosmochimica Acta 2004; 68: 3475-3486.

Vasile G, Tanase I, Dinu C. The Influence of the Air-drying Pretreatment of Sediment Samples for Metallic Element Mobilities. Analytical letters 2010; 43: 1199-1206.

Webster-Brown JG, Lane V. Modeling Seasonal Arsenic Behavior in the Waikato River, New Zealand. In: O'Day P, Vlassopoulos D, Meng X, Benning L, editors. Advances in Arsenic Research: Integration of Experimental and Observational Studies and Implications for Mitigation. 915. American Chemical Society, Washington, 2005, pp. 253-266.

Wenzel WW, Kirchbaumer N, Prohaska T, Stingeder G, Lombi E, Adriano DC. Arsenic fractionation in soils using an improved sequential extraction procedure. Analytica Chimica Acta 2001; 436: 309-323.

Zobrist J, Dowdle PR, Davis JA, Oremland RS. Mobilization of arsenite by dissimilatory reduction of adsorbed arsenate. Environmental Science & Technology 2000; 34: 4747-4753.

CHAPTER 4

Occurrence of Arsenic in River Sediments: The use of Pb and Sr isotopic analysis in the Loire River Basin (France)

4.1 Introduction

Arsenic (As) has been identified as a priority contaminant in aquatic systems by the European Community (2000/60/EC). Elevated levels of As in water is both a human health and environmental hazard. Due to ever increasing demands for water resources putting pressure on both ground- and surface waters as potential drinking water reserves, the occurrence and subsequent mobilisation of As from sediments is a problem of worldwide concern (Casiot et al., 2007; Charlet and Polya, 2006; Linge and Oldham, 2002; Masson et al., 2009; 2007; Polizzotto et al., 2008; Ravenscroft et al., 2009; Smedley and Kinniburgh, 2002; Winkel et al., 2008).

In river basins, sediments have a key role to play in the removal and mobilisation of As in the aqueous environment. Sediments have the ability to act as both a source and a sink of As under certain environmental conditions (Ahmann et al., 1997; Chaillou et al., 2003), due to the release of As from the underlying sediments, or from suspended particulate matter that has settled to the bottom sediments (Mucci et al., 2000). River sediments typically contain higher concentrations of As (along with other trace elements) than the overlying waters: this has been attributed to the coprecipitation and adsorption of arsenate (As(V)) with iron(Fe) (oxy)hydroxides in the sediment (Ahmann et al., 1997; Négrel and Roy, 2002).

Although an extensive amount of work has recently been carried out involving sediments and aquifers, there is still debate over the mineral source (McArthur et al., 2004; Ravenscroft et al., 2009; Rowland et al., 2005). In addition to the questions over the source of As, mechanisms of As release are also not understood comprehensively, with a range of possible triggers including the role of carbon sources, microbially mediated pathways and redox triggers all being investigated (Bauer and Blodau, 2006; Buschmann et al., 2006; Chatain et al., 2005; Islam et al., 2004; Miao et al., 2006; Signes-Pastor et al., 2007; Solaiman et al., 2009). Despite an increased understanding of the behaviour of As in freshwater (Aggett and O'Brien, 1985; Chow and Taillefert, 2009; Linge and Oldham, 2004; Masson et al., 2007; McLaren and Kim, 1995; Nicholas et al., 2003), there is also a lack of understanding in the source and processes controlling mobilisation in freshwater sediments (Masson et al., 2007).

A common tool to investigate the partitioning of trace elements including As within a soil or sediment is to utilise a sequential extraction technique to provide useful insights into the associations of As within different phases of the sediment. Typically, schemes seek to investigate the associations of As with minerals containing Fe, aluminium (Al) or manganese (Mn), as well as organic/sulphide associated As within the sediment, with exact steps varying depending on the study. In sediments, As is frequently found to be strongly associated with Fe-oxides (or (oxy)hydroxides) and other mineral phases including Mn-oxides and Fe-sulphides, although contributions from adsorbed or organic associated As are not uncommon (Blute et al., 2009; Devesa-Rey et al., 2008; Gonzalez et al., 2006; Haque et al., 2008).

Whilst sequential extraction procedures (SEPs) are relatively easy to perform, there are a number of recognised limitations to their use (Wenzel et al., 2001), mainly relating to the use of a wide range of extractants in the literature, making intercomparisons between studies very difficult (Bacon and Davidson, 2008; Bacon et al., 2006; Gonzalez et al., 2006). Because As is an anion, there have been a number of As-specific SEPs developed, based on the original work of Tessier (1979) dealing with the extraction of metals (Gonzalez et al., 2006; Wenzel et al., 2001). Despite the ongoing development of SEPs, issues relating to the specificity of an individual extractant for the chosen sediment phase still exist, as well as other problems including incomplete dissolution of phases, re-adsorption of released As, or alteration of the sample during the extraction. The lack of a standard extraction scheme for As, such as the BCR scheme established for metals (Marin et al., 1997), means that extreme care must be taken in the interpretation and comparison of data, and as such, sequential extraction results should only ever be considered as extraction specific fractions. The chemical processes removing As during the SEP are likely to be similar to the environmental processes occurring within the sediments, and as such description of the SEP in terms of the operational processes used allows for some comment to be made. Despite the advances in SEP development, information on the specific mineral source of the As within a fraction of the SEP, as well as the release mechanism of As within freshwater and groundwater sediments (Dowling et al., 2002; Nicholas et al., 2003; Nickson et al., 2000; Seddique et al., 2008; van Geen et al., 2004) requires further work.

Because of the lack of a direct tool for linking either the occurrence or release of As with the mineral source there is a need for development of a means to further understand the mineral sources of As within river sediments. Sequential extractions can be performed on sediments

both before and after different leaching or incubation experiments to provide information on the changes in partitioning occurring after release of As. However, limitations with the analytical limits of detection mean that differences in the fractions can often be within error, or below detection (Linge and Oldham, 2002). If observed, any changes in the operationally defined fractions cannot be directly linked to a specific mineral source.

Use of isotopic analysis is a very well established tool to provide information on the origin of elements such as lead (Pb), and strontium (Sr) in the characterisation of both sediment and water samples (Aberg, 1995; Bacon and Hewitt, 2005; Dawson et al., 2010; Grosbois et al., 2000; Millot et al., 2004; Négrel and Grosbois, 1999). Strontium and Pb ratios are commonly used in characterisation studies as the physical, chemical and biological processes occurring in both sediment and aqueous environments are not thought to fractionate the isotopic values obtained. Of the four naturally occurring Sr isotopes, only one is radiogenic (^{87}Sr), so the ratio of ^{87}Sr to the stable ^{86}Sr is a function of the age of the material and the initial ratio present. Lead has four isotopes, ^{204}Pb, ^{206}Pb, ^{207}Pb and ^{208}Pb, of which three are formed by the radioactive decay of ^{238}U, ^{235}U and ^{232}Th respectively. Each of these ratios is dependent on the initial concentration of Pb, Th, U, half lives of decay processed and time. It has been shown that both Sr and Pb isotope ratios act as signatures of the rocks and minerals present in the sample (Négrel and Grosbois, 1999; Négrel et al., 2004), with Sr also able to provide information on water movement through the redistribution of Sr from minerals during formation and dissolution of particulates (Andersson et al., 1994), allowing for interpretation of origins of the obtained signatures.

Generally application of these isotopes with sediments is coupled with single step extractions, more commonly total digests, where the sample is analysed as a whole, and typically investigate the origin of metals along vertical profiles in sediments (Backstrom et al., 2006; Bacon and Hewitt, 2005; Munksgaard and Parry, 2002; Prohaska et al., 2005; Steinmann and Stille, 1997). Single step digestions are unable to distinguish the different minerals held within the sample providing only an overall signature, and so cannot provide signatures for the different phases held within. Previous work combining isotopic analysis with digests obtaining the labile part of the sediment; known as acid extractable material (AEM); has highlighted the potential for investigating different phases within a sediment sample (Négrel and Roy, 2002). The combination of leaching of the AEM of both sediment and suspended particulate matter (SPM) from the Loire River and both Sr and Pb isotopes have shown that the trace elements in

the AEM have originated from crustal weathering (Négrel et al., 2004). Another study by Négrel & Grosbois (1999) using Sr isotopes on Loire River SPM found unique signatures that helped identify two different reservoirs of SPM that contributed under different flow conditions (Négrel and Grosbois, 1999).

The combination of sequential extractions with isotopic analysis has been identified as a potentially powerful technique that can provide information of the origin of the metals within a sediment (Bacon and Davidson, 2008). Combination of SEPs with Pb isotopic analysis has been undertaken to trace the geological and anthropogenic sources of Pb in sediment samples (Bacon et al., 2006; Bacon and Hewitt, 2005; Cicchella et al., 2008; Teutsch et al., 2001). The Sr isotopic composition of SEPs have been investigated as a provenance tracer of dusts, soils and sediments (Xu and Marcantonio, 2004; Yokoo et al., 2004). Xu and Marcantonio (2004) utilised a 6-step SEP to understand the carrier phases of mobile Sr in river sediments, finding that although Mn and Fe (oxy)hydroxides are potential carrier phases of Sr, the carbonate and organic phases of the sediment exerted more control on the Sr isotopic composition than the sediments Fe-Mn component. In addition to provenancing, the combination of SEPs and the isotopes have been studied to understand the fractionation processes occurring to Fe during biological (Guelke et al., 2010) and weathering processes (Wiederhold et al., 2007).

4.1.1 Study Aim

To date, studies employing both SEPs and isotopic characterisation have focussed solely on understanding the origin of the element with multiple isotopes (Bacon et al., 2006; Hindshaw et al., 2011; Wiederhold et al., 2007; Xu and Marcantonio, 2004). Use of Pb isotopes is well established in the determination of anthropogenic contamination within a sample (Ayuso and Foley, 2008; Bacon and Hewitt, 2005). While the combination of Pb and Sr isotopes, providing information on material origins and water movements respectively, are being increasingly applied to environmental studies (Erel and Torrent, 2010; Luck and Ben Othman, 1998; Steinmann and Stille, 1997), there has been a lack of investigation as to the relationship of obtained isotopic signatures from either Sr or Pb and the correlation of other trace elements present in the samples. In fluvial systems, the labile fraction of SPM and sediment is known to be significant in the storage and transport of a range of trace elements, including Fe, Sr, Mn and Pb (Négrel et al., 2002). In natural fluvial systems, the origin of trace elements is ultimately from the bedrock material and minerals found in the catchment. Although the weathering

processes occurring in the system may be affecting trace elements differently, correlations between trace elements are possible as the same physical and chemical processes are affecting the material during its transportation. It follows that the isotopic signatures of one element could provide information on mineral processes occurring within the sediment. Instead of a chemical extraction approach, work undertaken on obtained mineral separates by Ayuso and Foley (2008), found a positive correlation between As and Pb in the aquifer sediments of an As enriched watershed in Coastal Maine, USA. Using a range of digestions specific for sulphide and secondary mineral separates, they investigated the role of anthropogenic and mineral sources of Pb in the transport pathways of As. While a strong link was found between the obtained ratios and natural Pb sources, contributions from anthropogenic sources of Pb were also identified, likely due to the selection of a study area in a region of industrial activity with anomalously high levels of Pb and As.

This paper builds upon the previous work conducted on AEM in sediments of the Loire and Allier Rivers (Grosbois et al., 2000; Négrel et al., 1997; Négrel et al., 2000; Négrel et al., 2002; Négrel et al., 2004; Négrel et al., 2003; Négrel and Roy, 2002) by examining the potential for the use of Sr and Pb isotopes in an As-specific sequential extraction. The relationship between the partitioning of As, Sr and Pb in sediments is explored in the present work to evaluate the suitability of each as a tracer for the source of As in river sediments. To provide insight into the mineralogical source of trace elements including As within the sediment, the controls on the Sr and Pb isotopic composition of each sediment fraction are determined. As mineral-water interaction during laboratory incubations could also provide signature isotopic information on mineral phases undergoing mobilisation processes, the role of isotopic analysis in incubation studies is also evaluated. One objective of this work was to isotopically characterise both solutions and sediments after changes in physicochemical conditions during incubation studies. Results from this study provide a framework for better understanding the behaviour of Sr and Pb isotopes in sediments, and help determine their utility in tracing the links of As occurrence and mobilisation.

4.2 Study Area

Both the Loire and Allier Rivers investigated in this study flow from the French Massif Central, forming part of the Loire River Catchment. The Massif Central is known to contain As concentrations higher than average world background values due to a variety of hydrothermal and mining-related sources (Cances et al., 2005; Roussel et al., 2000; Smedley and Kinniburgh, 2002). While both the Loire and Allier Rivers share an origin within the Massif Central, the contrasting geologies along the river paths provides an opportunity to evaluate the geogenic origins of As. The older volcanic and plutonic rocks drained by the Loire River are not known to be high in As, while the Allier River passes through the areas of Margeride, Auvergne and Echassieres, which are known to contain anomalously high As levels in the sediment (Barbier and Chery, 1997; Morin et al., 2002).

The Loire in central France is approximately 1010 km long and drains an area of 117,800 km^2, while the Allier is a tributary of the Loire, and is approximately 400km long, draining an area of 14,320km^2. Initially, the Loire and Allier both flow in a south to north direction originating in the Massif Central, they join near the town Nevers (Figure 4.1) and continue as the Loire up to the city of Orléans, 650 km from the source. The Loire River then follows a general east to west direction to the Atlantic Ocean, entering the Bay of Biscay at St Nazaire. The Loire River is one of the main European riverine inputs to the Atlantic ocean (Négrel, 1997).The oceanic receiving environment, the Bay of Biscay, is enriched in As due to the presence and exploitation of As-bearing ores in the drainage catchments (Chaillou et al., 2003).

The bedrock composition of the rivers has been well characterized with both rivers sharing the silicate dominated basement of the Loire River Catchment. The upstream section of the Loire includes older plutonic rocks, granite, gneiss and mica schist; and a large volcanic area which represent 46 % of the total basin surface (Négrel et al., 2000). The intermediate section of the Loire features the sedimentary series of the Paris Basin, consisting primarily of carbonate deposits (Négrel 1999). The geology of the Allier differs slightly to the Loire (Figure 4.1), with the main gravel and sand components being of granitic–gneissic and basaltic origin from the Massif Central; carbonates from the Limagne d'Allier can also be a source of material (Négrel and Roy, 2002).

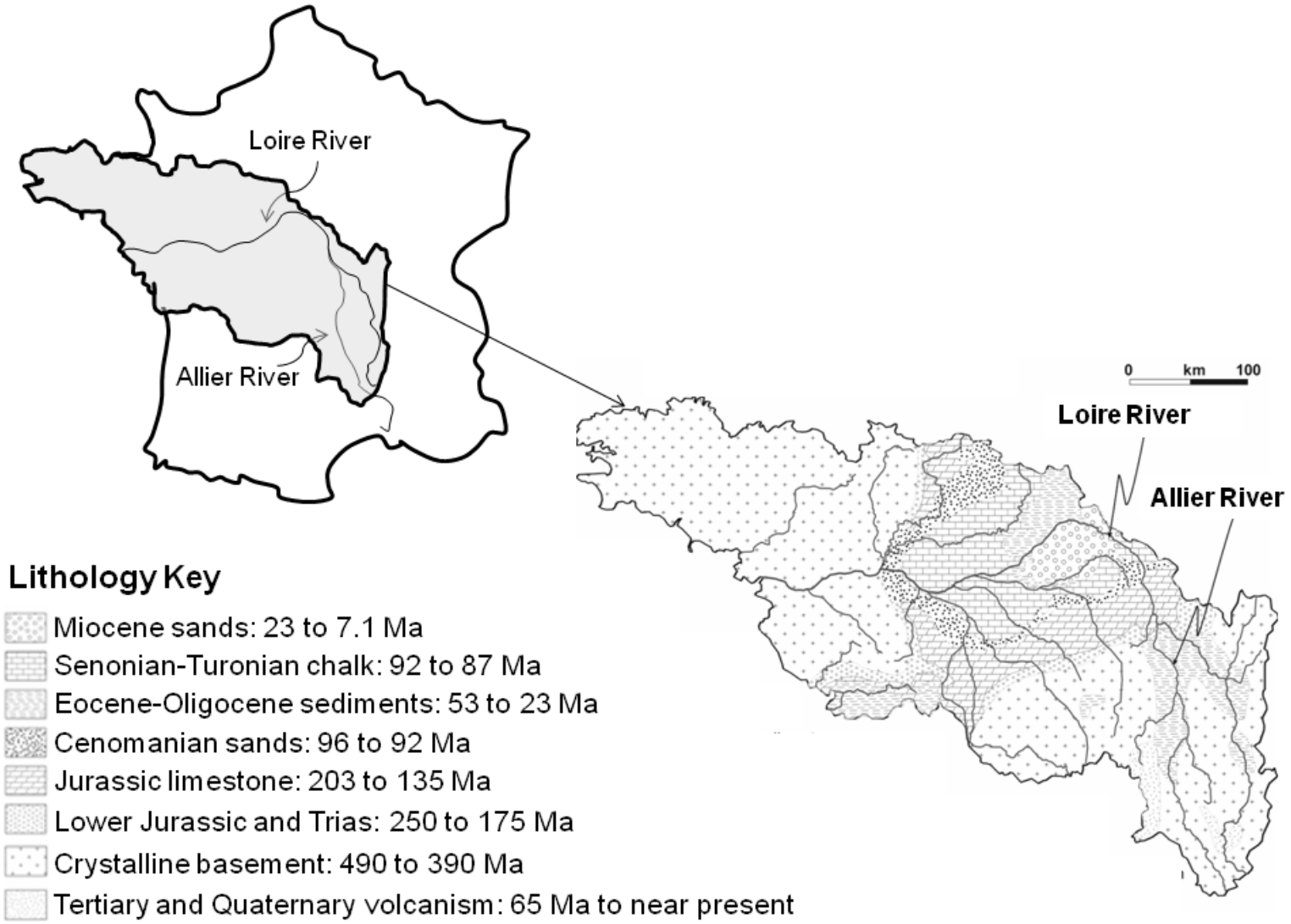

Figure 4.1 **Simplified geological map of the Loire and Allier River catchment(s). Lithology map and information provided by R. Millot (brgm)**

4.3 Materials and Methods

4.3.1 Sediment sample collection and processing

Surface sediment and water samples were taken during November 2008 from three sites within the Bec d'Allier region near Nevers, France. In order to contrast the differing geologies along the Loire and Allier Rivers, two sites were located on the Loire River, at Imphy and Marzy, located respectively before and after the confluence with the Allier River, with the third site located on the Allier River, at Apremont (Figure 4.2).

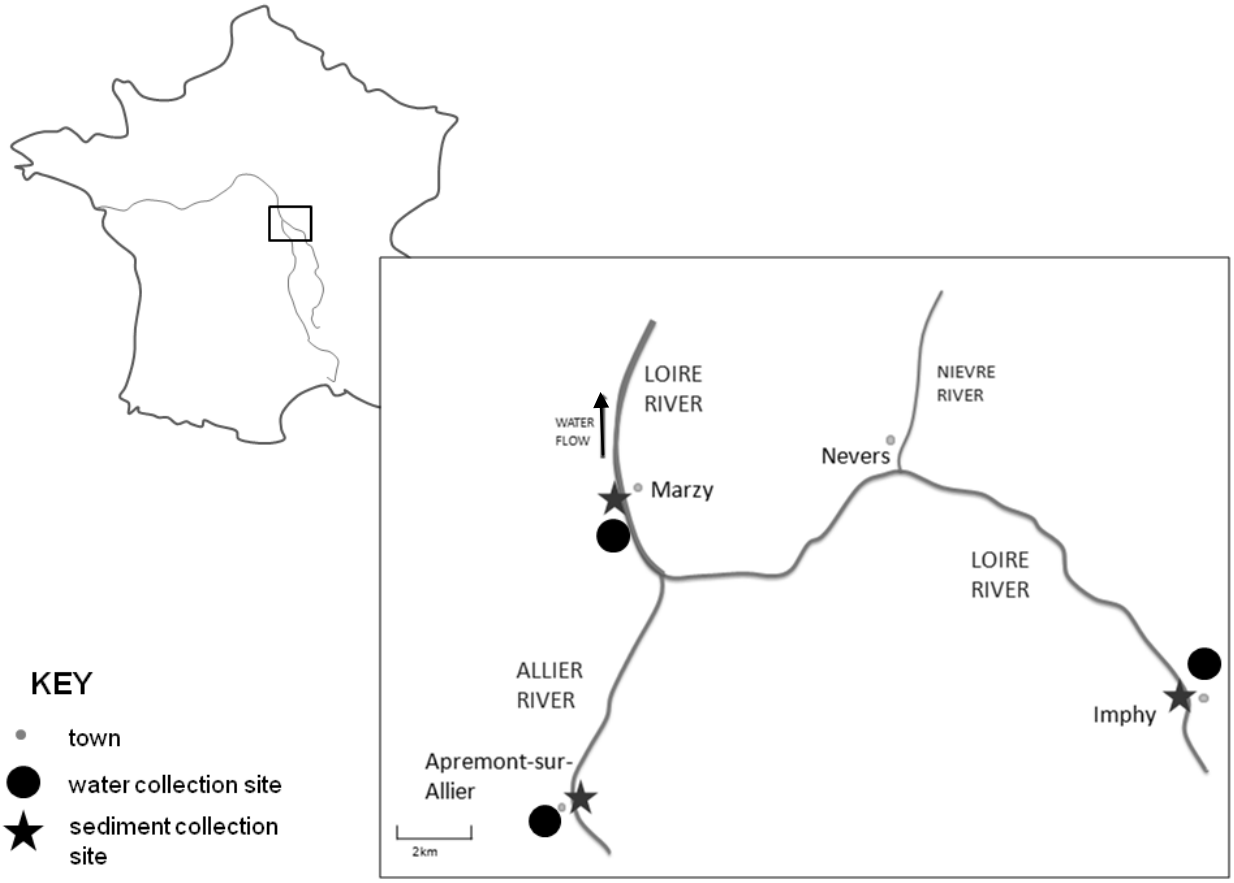

Figure 4.2 **Location map of sampling sites. Sediment (indicated by stars) and water samples (indicated by circular marks) were collected from Allier-Apremont, Loire-Imphy and Loire-Marzy in November 2008.**

River water samples were collected in 100 ml polypropylene containers, filtered through precleaned 0.45 μm Whatman cellulose nitrate filters using a precleaned Nalgene filter apparatus. Each sample was acidified with HNO_3 to pH< 2 on site. Prior to collection, all plastic-ware was cleaned by soaking in 10 % (v/v) HNO_3 for >24hr followed by rinsing with Milli-Q water ($18M\Omega$). Sediments from the top 50 cm were initially collected using a sediment corer, however use of a spade was also required due to the loose nature of the sediment at both the Loire-Imphy and Loire-Marzy sites. After transportation back to the laboratory, the samples were sieved through a 2 mm sieve to remove large stones and plant debris from the samples. In order to minimise disturbance to the samples, each sample was stored in a sealed glass jar, under a N_2 atmosphere, in the dark at 10^{o}C. As typical sediment preparation techniques such as drying and grinding are known to affect the partitioning of trace elements including As (Anawar et al., 2010; Einax and Nischwitz, 2001; Vasile et al., 2010), all sequential extraction work was undertaken using sediment that had not been processed in any way. Prior to analysis a subsample of sediment was weighed and oven-dried at 70^{o}C to obtain the dry-weight. Prior to total digests, samples were oven-dried at 70^{o}C, ground in a ball-mill, homogenized, quartered and dry-sieved through a 165-μm nylon mesh. Mineral identification was undertaken on a portion of each sediment using a combination of density, magnetic character and microscopy.

4.3.2 Sequential Extraction Procedure

There are currently a range of SEPs being utilised to investigate the partitioning of both trace elements and As in sediment samples (Hudson-Edwards et al., 2004; Wenzel et al., 2001). As an anion, the behaviour of the adsorbed As species differs from metallic cations and so recent work by Wenzel (2001) has altered the standard SEP used in metals analysis (Tessier et al., 1979) to allow for the targeting of As in the first two steps. However, as the newly developed As protocols are not standard protocols (c.f. the BCR protocol for metals), use of a commonly employed procedure is required to ensure suitability of the application of isotopic analysis and comparability between studies. For this study, a SEP based on the Wenzel (2001) and Tessier (1979) extractions was selected. Table 4.1 outlines the experimental procedure, and notes the operational processes and likely environmental processes causing removal of As from each fraction. Portions of sediment (1 g dry weight, unprocessed/dried), were carefully weighed into screwcap polypropylene centrifuge tubes (Fisher Scientific, Loughborough, UK) and subjected to the sequential extraction procedure detailed in Table 4.1.

Table 4.1 Summary of sequential extraction procedure

Code	Extractant	Notes / Reaction time	Wash steps	Target phase	Operational/ Environmental process
F1	0.05 M $(NH_4)_2SO_4$ (25mls)	4hr		Nonspecifically sorbed	Removal by desorption through changes in ionic strength
F2	0.05M $NH_4H_2PO_4$ (25mls)	16hr		Specifically sorbed	Removal by competitive sorption / desorption e.g.PO_4^{3-}
F3	0.2 M NH_4 – oxalate buffer (pH 3.0) (25mls)	4hr (dark)	12.5mls 0.2 M NH_4 –oxalate 10 min	Poorly crystalline hydrous oxides of Fe/Al	Dissolution triggered by reduction
F4	0.2 M NH_4 - oxalate buffer (pH 3.0) and 0.1 M ascorbic acid (25mls)	30min waterbath (light)	12.5mls 0.2 M NH_4 –oxalate 10min	Well crystallised hydrous oxides of Fe/Al	Reduction/ dissolution from more resistant minerals
F5	$KClO_4$ (1g) /HCl (20mls) DIW (15mls)	45min, Addition of DIW prior to centrifugation	DIW	Organics and sulphides	Oxidation
F6	HF-H_3BO_3-HNO_3	Microwave (sample dried)		Residual	Not removed by environmental processes / Long term sink

All reagents were of analytical reagent grade (Fisher Scientific, 99+% Certified AR grade). End-over-end mixing was utilised in steps 1-3, with occasional shaking employed for steps 4 and 5. The supernatants from wash steps 3 and 4 were combined with that withdrawn from their respective main extraction step. After each stage, the sediment–extractant mixture was centrifuged (1700 x g for 20 min) and the supernatant decanted, filtered at 0.45 µm and refrigerated until analysis. The sediment was then subjected to the next step. The reproducibility of our sequential extraction method was examined with duplicate analyses. Procedural blanks were also run in duplicate over the SEP simultaneously and found to contain negligible levels of As (<2.3 %), Sr (<0.58 %) and Pb (0.15 %) in all extraction steps.

4.3.3 Alteration of SEP

Previous work developing an As-specific SEP (Wenzel et al., 2001) discounted the inclusion of a SEP step targeting carbonates due to the lack of an association between As and carbonates. However, because of the known association of Sr for carbonates (Xu and Marcantonio, 2004), the use of 1M CH_3COONa (pH 5) step specifically targeting carbonates was included in the SEP as the 3rd step, (F2b) for the Allier-Apremont sediment in order to evaluate the role of both Sr and carbonates in the partitioning of As. Inclusion of this step will also be used to help determine the specificity of the extraction steps for their operationally defined phases.

4.3.4 Total digests & XRF

The total metal concentrations in the sediment were determined by a total digestion procedure, using a microwave digestion. A mixture of HF- HNO_3 was left with 0.3 g sediment (measured) in a Teflon microwave vessel overnight to allow dissolution of silicate material. The sediment was then digested in a Milestone Ethos 1 microwave over two hours. After cooling, H_3BO_3 was then added to complex the HF, as removal of HF by volatilisation is also thought to also remove the volatile AsF_5 species, giving low concentrations (Gault et al., 2003).

The total solid phase elemental concentrations were also determined for each sediment by X-ray fluorescence (XRF). Ground, homogenised sediment samples (12 g) are mixed with a wax binder (3 g) and pressed into sediment pellets. The pellets were analyzed using a wavelength separation XRF Spectrometer (Axios) for a range of elements including As, Sr and Pb.

4.3.5 Sediment Incubations

The effect of changing physicochemical conditions on the Allier-Apremont sediment was investigated through two different incubation studies. Firstly, a pH_{stat} leaching test was conducted on the sediment to determine how alterations in pH affected the release of As, Sr and Pb from the sediment. To maintain an ionic strength similar to river water, 20 g sediment (unprocessed) was mixed with a solution of 0.01M $NaNO_3$ to obtain a slurry water/sediment ratio of 3:1(weight: weight). Each slurry was adjusted with NaOH or HNO_3 to obtain a pH of 3, 8.5 and 10, and were mixed end-over-end aerobically, over a period of two weeks. The pH of each slurry was monitored daily, and adjustments made to maintain desired pH. At the end of two weeks, a sample of the aqueous phase was taken, filtered at 0.45 µm and acidified with HNO_3 prior to analysis.

The second test involved a microcosm study on the sediment to determine the effect of anaerobic conditions on the release of trace elements. Wet sediment (3 ± 0.1 g) was mixed with filtered (0.45 µm) river water from the Loire-Marzy sample site that had been degassed with N_2, at a water/sediment ratio of 3:1. In an anaerobic cabinet (under N_2 atmosphere), each anaerobic slurry was placed in a 20 ml serum bottle, fitted with butyl rubber stoppers, sealed with an aluminium clamp, and incubated at 20^{o}C. The aerobic samples, were prepared using river water that had not been degassed, and the manipulations were carried out on a lab bench in normal aerobic conditions. For each sampled timepoint, a separate sacrificial slurry was created in order to avoid the possible contamination associated with sampling the same vessel multiple times. Aerobic conditions were maintained by piercing the butyl stoppers with a hypodermic syringe to allow the free passage of oxygen into the microcosm. All experiments were performed in triplicate using sterile, acid-washed equipment.

4.3.6 Metal concentration analysis

Arsenic, Fe, Sr and Pb were measured in the non-residual SEP solutions and incubation studies using inductively coupled plasma – mass spectrometry (ICP-MS) with a detection limit of < 1 µg l^{-1}. Because of high total dissolved solids (TDS) in solutions from the HF-H_3BO_3-HNO_3 total digestion analysis using the ICP-MS was not possible. Instead, the trace element contents were determined by inductively coupled plasma – atomic emission spectroscopy (ICP-AES, Horizon, Fisons) using matrix matched standards. Quality control standards were used

throughout the course of analysis for both instruments to monitor analytical performance. Commercial multi-element standards were used to prepare standard calibration curves which were used to correct measured concentrations using weighted ordinary least squares linear regression, with analytical errors calculated using the methods of Miller and Miller (2005).

4.3.7 Isotope Analysis

Because of resource limitations, isotope analysis was performed on a single sample from each sediments SEP fractions. The reproducibility of the isotopic analysis was examined through the triplicate analysis of F3 and F4 of the Allier-Apremont sediment.

a) Strontium isotope analysis

Chemical purification of Sr from each SEP fraction was performed using an ion-exchange column (Sr-Spec) (described in Chapter 2) before mass analysis according to a method adapted from a procedure used on silicate samples (Deniel and Pin, 2001). Total blanks were <1 ng for the entire chemical purification. After chemical separation, approximately 150 ng of Sr was loaded onto a tungsten filament with tantalum activator and analyzed with a Finnigan MAT 262 multi-collector mass spectrometer. The $^{87}Sr/^{86}Sr$ ratios were normalized to an $^{86}Sr/^{88}Sr$ ratio of 0.1194. An average internal precision of about ±10 ppm (2 σ_m) was obtained. Reproducibility of the $^{87}Sr/^{86}Sr$ ratio measurements was tested through repeated analyses of the NBS987 standard (accepted value 0.710248), for which we obtained a mean value of 0.710230 ± 20×10^{-6} (2σ, n=17) during the period of analysis.

b) Lead isotope analysis

Lead isotopic ratios were determined on the solutions from the SEP and total digests of sediment by using a Neptune Multi Collector(MC)-ICP-MS with Faraday Cups (Thermo Fischer Scientific) in operation at the BRGM Isotopic Geochemistry Laboratory. According to the recent protocol developed in BRGM and presented by Cocherie and Robert (2007), the key parameter for the analysis of solutions by the mean of the MC-ICP-MS is the Pb concentration and the cation matrix of the water sample. The high sensitivity of the MC-ICP-MS allows direct measurements at Pb concentration levels as low as 10 ng ml^{-1}, with no matrix effects where the ion charge is lower than 400 mg l^{-1} (Cocherie and Robert, 2007). Volumes of sample were prepared to a final concentration of 10 ppb Pb with a mix of HNO_3, H_2O and thallium (Tl) standard (used for mass discrimination correction) and analysed by direct measurement by

MC-ICP-MS. The dead time of the detector is optimised prior to the analyses by measuring the $^{208}Pb/^{204}Pb$ ratio of the NIST SRM 981 standard at various concentrations (10, 20, 50 and 100 ppb). Solutions F1 and F5 were unable to be used for MC-ICP-MS Pb isotope measurement due to a low Pb concentration, and an elevated ion charge respectively. When using this method, a Tl correction technique is used for mass discrimination calculation following an exponential correction to $^{205}Tl/^{203}Tl = 2.3871$. In such conditions, 2σ standard errors of 0.10 % and 0.01 % are achieved for $^{206}Pb/^{204}Pb$, $^{207}Pb/^{204}Pb$, $^{208}Pb/^{204}Pb$ ratios and $^{207}Pb/^{206}Pb$ and $^{208}Pb/^{206}Pb$ ratios respectively. Long term measurement of SRM981 standard material gave mean values of 16.932 ± 0.015, 15.486 ± 0.014 and 36.679 ± 0.030 respectively for $^{206}Pb/^{204}Pb$, $^{207}Pb/^{204}Pb$ and $^{208}Pb/^{204}Pb$ ratios (2σ, n = 38).

For the aqueous samples resulting from sediment incubations and for the river waters, the concentration of Pb was too low to enable the dilution required for detection by Faraday Cups. Therefore for these samples, the use of multi-ion-counters system (MIC)-ICP-MS was employed (Négrel et al., 2010). This detection method achieved 2σ standard errors of between 0.5-1.3% for $^{206}Pb/^{204}Pb$, $^{207}Pb/^{204}Pb$, $^{208}Pb/^{204}Pb$ ratios and 0.08-0.15% for $^{207}Pb/^{206}Pb$ and $^{208}Pb/^{206}Pb$ ratios. Measurements were carried out for solutions having 0.1 µg l^{-1} of Pb. In that case, the method of sample-standard bracketing was used for the mass discrimination effect correction (normalization to the SRM-981 standard solution). For Pb isotope analysis, we performed the direct measurement of a solution containing 0.1 µg l^{-1} of lead without any sample preparation beforehand (i.e., without chemical separation of the matrix). Only dilution or pre-concentration by evaporation (on a hot plate) of the sample were used to adjust the concentration of the solution to 0.1 µg l^{-1} of lead in 3% v/v sub-boiling HNO_3. The major advantage of this method is that all Pb isotopes (including the minor isotope ^{204}Pb) are measured in a static mode, hence it reduces significantly the uncertainty of measurement. For mass discrimination correction, the method of sample-standard bracketing was used and the reference standard (SRM981) adjusted to the same concentration as the samples (0.1 µg l^{-1}).

All the sample dilutions or preconcentrations were carried out in a clean room, with the instrument itself housed in a clean laboratory. Reproducibility and accuracy of the method was tested by repeated measurement of the NBS SRM981 standard with a concentration adjusted to 0.1 µg l^{-1} of lead, for which we obtained mean values of 16.941 ± 0.060, 15.494 ± 0.038 and 36.694 ± 0.100 for $^{206}Pb/^{204}Pb$, $^{207}Pb/^{204}Pb$ and $^{208}Pb/^{204}Pb$ ratios respectively (2σ, n = 20) over the period of the duration of the analyses.

4.4 Results

4.4.1 Sediment mineralogy

The two Loire River sediments sampled at Imphy (upstream) and Marzy (downstream) have very similar mineralogy, with quartz, feldspars and micas making up 95% of the sediment. Rock debris made up a component of both sediments, with the other minerals present including Fe(oxy)hydroxides, zircon, apatite, pyrite and clays. The Allier-Apremont sediment was similar in make-up to the Loire River sediments, with clays making up a larger proportion of the sample and rutile and pyroxene also present.

4.4.2 Elemental results

The concentrations of As, Sr and Pb from each fraction of the SEP are listed in Table 4.2. There is generally good agreement between the sum of the fractions and the total digest of the bulk sediment indicating there was little loss of sample throughout the SEP. High TDS precluded the use of ICP-MS, and due to issues relating to the matrix and the higher limit of detection (LOD) of the ICP-AES, As was not detected in the total, or residual (F6) samples. Therefore XRF concentrations are used for the total concentration of As. The agreement between the XRF and the SEP sum of the steps suggests that F6 (residual material) is not a significant store of As within the sediment.

The acid extractable material (AEM) percentage of the sediment was determined by the difference in weight after steps F1-F5 (the 'labile' fractions). Results are presented in Table 4.2, and demonstrate the prominence of the residual phase in the sediment of both the Loire and Allier rivers. Levels of AEM are low at all three sites, with the Loire-Marzy site AEM% at 1.6 % and the Loire-Imphy and Allier-Apremont sediments at 6.3 % and 6.5 % respectively. Whilst the Loire-Marzy site has lower AEM %, all three sites are lower than reported AEM% for SPM within the Loire River (at Orléans) (8-47 %) (Négrel et al., 2000).

In contrast to As, the residual phase (F6) contains the majority of Sr (85-98 %) for all three sites (Table 4.2). The residual phase is also important for Pb, with the majority of Pb in the Loire River sediments found within F6 (76-87 %), however, there is more non residual (labile) Pb in the Allier-Apremont sample, with less than half (41 %) the total Pb found within F6. The total concentration of Sr is reasonably consistent between the three sites (104-112 μg g^{-1}), while Pb

is higher in the Allier-Apremont sample (43 μg g^{-1}) than at either the Imphy or Marzy Loire River sites (22 & 28 μg g^{-1} respectively).

Considering the labile fractions, concentrations of As, Sr and Pb are higher in the Allier River sediment than in the Loire River samples (Figure 4.3). From Figure 4.2, it can be seen that As is generally found within F3 and F4 in all three samples, highlighting the importance of the association of As with the mineral component of the sediment. Specifically sorbed As (F2) also plays a minor role in As storage within the sediment (F2) at all three sites, however the contribution is greatest in the Allier-Apremont sample (Figure 4.3). While the role of F5 (organic matter and sulphides) is minor at both Loire River sites, there is a small pool of As present within this fraction at the Allier-Apremont site.

For both Loire River sites, over 50 % of the labile Sr is found within F1 (Figure 4.3), indicating that the majority of labile Sr is adsorbed to the sediment rather than incorporated within. The Allier-Apremont sediment shows a different pattern of partitioning, with a slightly increased role for F3 and F4 within the sediment. There is also a significant pool of Sr within the F5 fraction of the Allier-Apremont sediment.

The labile partitioning of Pb matches As more closely than Sr, with an increased role for both F3 and F4. Pb is not present in either of the adsorbed phases (F1 & F2). Once again, there is a significant pool of Pb present within F5, suggesting a different behaviour of the organic-sulphidic component in the Allier-Apremont sediment.

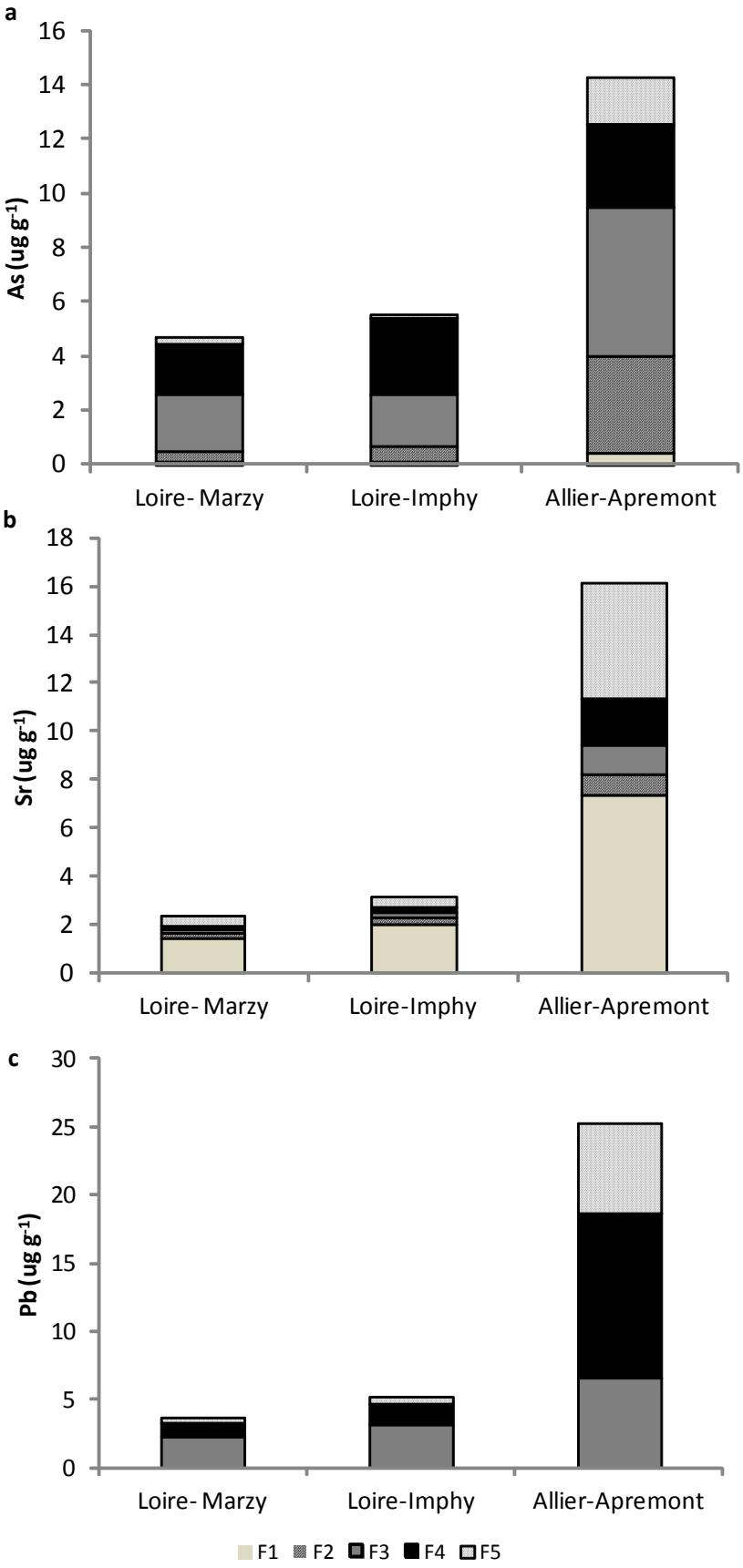

Figure 4.3 **Non residual (labile) partitioning of a) As, b) Sr and c) Pb within each sediment (µg g^{-1}).** (F1, F2= exchangeable fractions, F3, F4= reducible fractions, F5=organic fraction)

4.4.3 Sr Isotopic Results

Distinctly different $^{87}Sr/^{86}Sr$ isotope ratios are obtained for each fraction of the SEP in all three sediments, despite the dominance of the residual fraction in Sr storage (Table 4.2). All three sediments present a similar pattern of $^{87}Sr/^{86}Sr$ isotope ratio for each of the steps (Figure 4.4). The ratios obtained for F1 and F2 (Allier-Apremont; 0.71207-0.71187, Loire-Imphy; 0.71214, 0.71212, Loire-Marzy; 0.71139, 0.71149) closely align with those obtained in the river water (Allier-Apremont 0.71210, Loire-Imphy 0.71219 and Loire-Marzy 0.71150), indicating that the adsorbed Sr was in isotopic equilibrium with the river water when it was adsorbed. The ratios obtained for F3 and F5 are lower than those obtained for F1, F2 and F4, however all the labile ratios are significantly lower when compared to each sediments residual $^{87}Sr/^{86}Sr$ ratio (F6- 0.71633, 0.72516, 0.72619 for Allier-Apremont, Loire-Imphy and Loire-Marzy respectively). The $^{87}Sr/^{86}Sr$ isotope ratio for F6 in the Allier-Apremont sediment differs from the two Loire sediments, with a significantly lower value obtained.

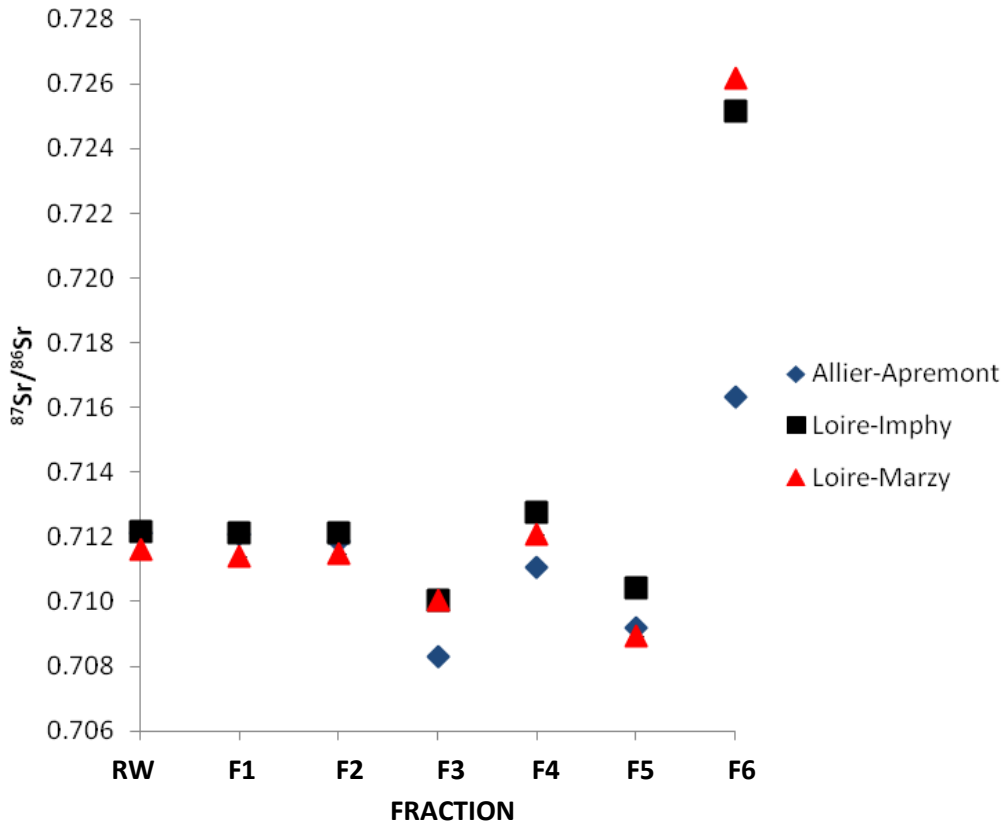

Figure 4.4 **Sr isotope ratios obtained from the SEP of each sediment. Note RW is the value obtained from the river water at the time of sampling. (F1, F2= exchangeable fractions, F3,F4= reducible fractions, F5=organic fraction, F6= residual fraction).**

Table 4.2 As, Sr and Pb concentrations and Pb and Sr isotope ratios of bulk sediments and SEP fractions

Sample	[As] µg g^{-1}	[Sr] µg g^{-1}	[Pb] µg g^{-1}	AEM %	$^{87}Sr/^{86}Sr$	$2\sigma_{(m)}$	$^{206}Pb/^{204}Pb$	2σ	$^{207}Pb/^{204}Pb$	2σ	$^{208}Pb/^{204}Pb$	2σ	$^{207}Pb/^{206}Pb$	2σ	$^{208}Pb/^{206}Pb$	2σ
Allier-Apremont				6.5												
river water (µg l^{-1})	4.6	163	0.2		0.71210	0.000009	N/M		N/M		N/M		N/M		N/M	
F1	0.4	7.3	BDL		0.71207	0.000008	N/M		N/M		N/M		N/M		N/M	
F2	3.6	0.9	0.02		0.71187	0.000009	18.519	0.101	15.797	0.090	38.820	0.216	0.853	0.002	2.096	0.005
F3	5.5	1.2	6.5		0.70829	0.000010	18.381	0.002	15.642	0.002	38.405	0.004	0.851	0.00001	2.089	0.00005
F4	3.1	1.9	12.1		0.71105	0.000010	18.370	0.002	15.633	0.002	38.379	0.005	0.851	0.00001	2.089	0.00005
F5	1.7	4.8	6.6		0.70918	0.000008	N/M		N/M		N/M		N/M		N/M	
F6	N/M	96.1	17.9		0.71633	0.000007	18.151	0.018	15.591	0.016	38.074	0.038	0.859	0.00009	2.098	0.0002
SUM	14.2 ± 0.29	112.2 ± 11.1	43.2 ± 4.5													
TOTAL	N/M	108.7 ± 31.5	39.9 ± 4.9		0.71574	0.000008	18.498	0.018	15.647	0.016	38.499	0.038	0.846	0.00008	2.081	0.0002
XRF	15.8 ± 1.3	117.1 ± 0.2	43.3 ± 0.5													
Loire-Imphy				6.3												
river water (µg l^{-1})	2.0	112	0.3		0.71219	0.000008	N/M		N/M		N/M		N/M		N/M	
F1	0.03	1.9	BDL		0.71214	0.000009	N/M		N/M		N/M		N/M		N/M	
F2	0.6	0.3	0.01		0.71212	0.000009	19.901	0.108	15.775	0.080	40.011	0.199	0.793	0.002	2.012	0.004
F3	2.0	0.2	3.2		0.71003	0.000008	18.553	0.002	15.642	0.002	38.484	0.005	0.843	0.00002	2.074	0.00006
F4	2.8	0.2	1.5		0.71274	0.000008	18.754	0.002	15.656	0.002	38.642	0.005	0.835	0.00001	2.060	0.00004
F5	0.1	0.4	0.5		0.71042	0.000011	N/M		N/M		N/M		N/M		N/M	
F6	N/M	105.9	16.6		0.72516	0.000007	18.406	0.018	15.632	0.016	38.427	0.0384	0.849	0.00008	2.088	0.0002
SUM	5.5 ± 0.3	109.0 ± 24.7	21.799 ± 3.1													
TOTAL	N/M	113.0 ± 10.3	24.2 ± 1.5		0.72506	0.000007	18.358	0.018	15.647	0.016	38.391	0.0384	0.852	0.00009	2.091	0.0002
XRF	6.4 ± 1.2	143.6 ± 0.2	28.8 ± 0.5													
Loire-Marzy				1.6												
river water (µg l^{-1})	3.7	115	BDL		0.71160	0.000008	N/M		N/M		N/M		N/M		N/M	
F1	0.02	1.4	BDL		0.71139	0.000009	N/M		N/M		N/M		N/M		N/M	
F2	0.4	0.2	0.007		0.71149	0.000010	18.531	0.095	15.668	0.078	38.456	0.196	0.846	0.00181	2.076	0.00430
F3	2.1	0.1	2.3		0.71003	0.000017	18.572	0.002	15.643	0.002	38.523	0.004	0.842	0.00002	2.074	0.00007
F4	1.9	0.2	1.0		0.71209	0.000011	18.788	0.002	15.664	0.002	38.719	0.005	0.834	0.00002	2.061	0.00005
F5	0.3	0.4	0.4		0.70893	0.000012	N/M		N/M		N/M		N/M		N/M	
F6	N/M	96.1	24.5		0.72619	0.000010	18.359	0.024	15.630	0.022	38.383	0.054	0.851	0.00009	2.091	0.00021
SUM	4.6 ± 0.1	98.4 ± 19.7	28.2 ± 6.5													
TOTAL	N/M	104.2 ± 5.9	26.6 ± 1.2		0.72432	0.000008	18.333	0.018	15.642	0.016	38.366	0.038	0.853	0.00009	2.093	0.00021
XRF	5.4 ± 1.2	137.5 ± 0.2	27.8 ± 0.5													

Trace element concentrations expressed as µg g^{-1}. Acid-extractable matter (AEM), representing the labile fractions, determined by weight and expressed as a percentage of the total matter content. N/M not measured due to insufficient Pb concentration, non-collection of Pb contamination-free field samples (river water & F1) and analytical difficulties with matrices (F5), BDL below detection limit. (F1, F2= exchangeable fractions, F3, F4= reducible fractions, F5=organic fraction, F6= residual). Errors (where given) represent ±2σ

The completion of a total digest on the sediment, run in parallel to the SEP, allows the opportunity to establish an isotope mass balance between the sum of the six fractions and the total digestion. A mass balance can be calculated according to the following formula, where $[Sr]_n$ is the Sr in fraction n, and IR is the isotopic ratio of $^{87}Sr/^{86}Sr$.

$$^{IR}Sr_{total,calc} = \Sigma_n(^{IR}Sr_n \times [Sr]_n) \qquad \text{equation 1}$$

Good agreement, between 0.03 and 0.08 % was found for all three sediments between the obtained and calculated total sediment $^{87}Sr/^{86}Sr$ isotopic ratio indicating that loss of Sr throughout the procedure was minimal (Table 4.3).

Table 4.3 Sr Isotope Mass Balance

Site	Measured Ratio	Predicted Ratio	combined error ‰	‰ difference
Loire-Marzy	0.72432	0.72472	0.069	0.06
Loire-Imphy	0.72506	0.72567	0.069	0.08
Allier-Apremont	0.71574	0.71550	0.070	0.03

As isotopic ratio measurements are routinely performed on single samples, the reproducibility of the obtained $^{87}Sr/^{86}Sr$ isotopic ratios was tested using triplicate extractions of the Allier-Apremont sediment for both F3 and F4, and on duplicate total digests (Table 4.4) of all three sediments. There is good agreement between the $^{87}Sr/^{86}Sr$ isotopic ratios obtained for duplicate total digests, with 0.71574 - 0.71575 for Allier-Apremont sediment, 0.72506 - 0.72509 for Loire-Imphy and 0.72432 - 0.72432 for Loire-Marzy (Table 4.4). Reasonable agreement between the triplicate extractions is obtained for leachates in both F3 and F4 for the Allier-Apremont sediment (Table 4.4). While the ratios for each step are not within the analytical error limits, there is a consistent, significant difference between F3 and F4 indicating that the extraction is attacking a different pool of Sr in each step. Observed differences are likely due to a combination of sample homogeneity issues related to the use of sediment that has not been dried and ground and slight procedural variations between samples. However it should be noted that use of moist, unground samples is common practice for SEPs, due to the chemical and physical alteration of the sample during drying and grinding processes. The use of single samples for isotopic analysis is common in isotopic studies (Smith et al., 2009; Wu et

al., 2009; Yokoo et al., 2004), and the agreement seen in Table 4.4 gives confidence that the ratios obtained are reflecting real differences in the SEP fractions.

Table 4.4 Replicate total digestions and SEP (F3 & F4)

Sample		$^{87}Sr/^{86}Sr$	$2\sigma_{(m)}$	$^{206}Pb/^{204}Pb$	$2\sigma_{(m)}$	$^{207}Pb/^{206}Pb$	$2\sigma_{(m)}$
Total digest	Imphy - 1	0.72506	0.000020				
	Imphy - 2	0.72509	0.000020				
	Marzy - 1	0.72432	0.000008				
	Marzy - 2	0.72432	0.000008				
	Allier - 1	0.71574	0.000008				
	Allier - 2	0.71575	0.000011				
Triplicate F3 (Allier-Apremont)	1	0.709824	0.000012	18.352	0.018	0.85181	0.0001
	2	0.709702	0.000011	18.350	0.018	0.85167	0.0001
	3	0.709800	0.000016	18.356	0.018	0.85170	0.0001
Triplicate F4 (Allier-Apremont)	1	0.711516	0.000008	18.367	0.018	0.85087	0.0001
	2	0.711442	0.000008	18.368	0.018	0.85083	0.0001
	3	0.711525	0.000010	18.373	0.018	0.85086	0.0001

4.4.4 Pb Isotopic Results

The five Pb isotope ratios considered in this study ($^{206}Pb/^{204}Pb$, $^{207}Pb/^{204}Pb$, $^{208}Pb/^{204}Pb$, $^{207}Pb/^{206}Pb$ and $^{208}Pb/^{206}Pb$) all vary significantly with each successive step for all three sediments (Table 4.2). For both the $^{207}Pb/^{206}Pb$ and $^{208}Pb/^{206}Pb$ isotope ratios, the Allier-Apremont sediment has higher ratios than the two Loire sediments for all the analysed fractions (Figure 4.5). The $^{207}Pb/^{206}Pb$ (0.793) and $^{208}Pb/^{206}Pb$ (2.012) isotope ratios for F2 of the Loire-Imphy sample are significantly lower than the Loire-Marzy (0.846 and 2.076) and Allier-Apremont (0.853 and 2.096) sediments. While the same general pattern of isotopic ratios is observed for Loire-Marzy and Loire-Imphy for F3, 4 and 6, the Allier-Apremont sediment does not show the same sharp decrease in F4 as seen in the other two sediments.

The $^{206}Pb/^{204}Pb$, $^{207}Pb/^{204}Pb$ and $^{208}Pb/^{204}Pb$ isotopic ratios for F3, F4 and F6 display a similar pattern for all the two Loire River sediments, with an increase from F3 to F4, and a decrease to F6 (Table 4.2). The Allier-Apremont sediment displays a similar pattern, but the F3 and F4

isotope ratios are closer (but outside error range), with a slight decrease from F3 to F4. The behaviour of F2 varies in each of the three isotope ratios; with the $^{206}Pb/^{204}Pb$ and $^{208}Pb/^{204}Pb$ isotope ratios being distinctly higher for Loire-Imphy, while both the Loire-Imphy and Allier-Apremont sediments have higher $^{207}Pb/^{204}Pb$ isotope ratios.

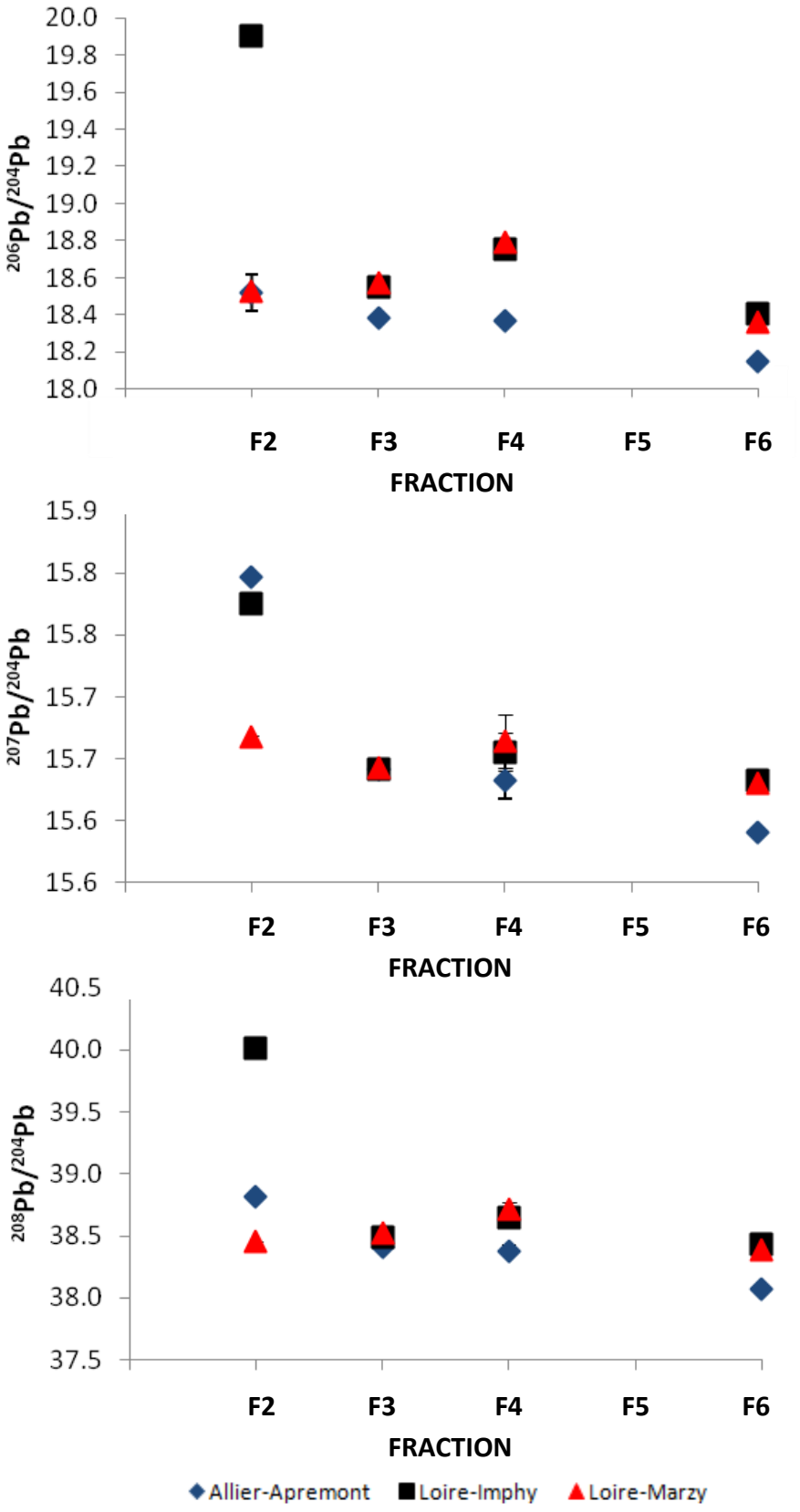

Figure 4.5 **Pb isotope ratios obtained from the SEP of each sediment.** (F1, F2= exchangeable fractions; F3, F4= reducible fractions; F5=organic fraction; F6=residual fraction). Error bars represent errors represent ±2σ, where not visible error is within icon.

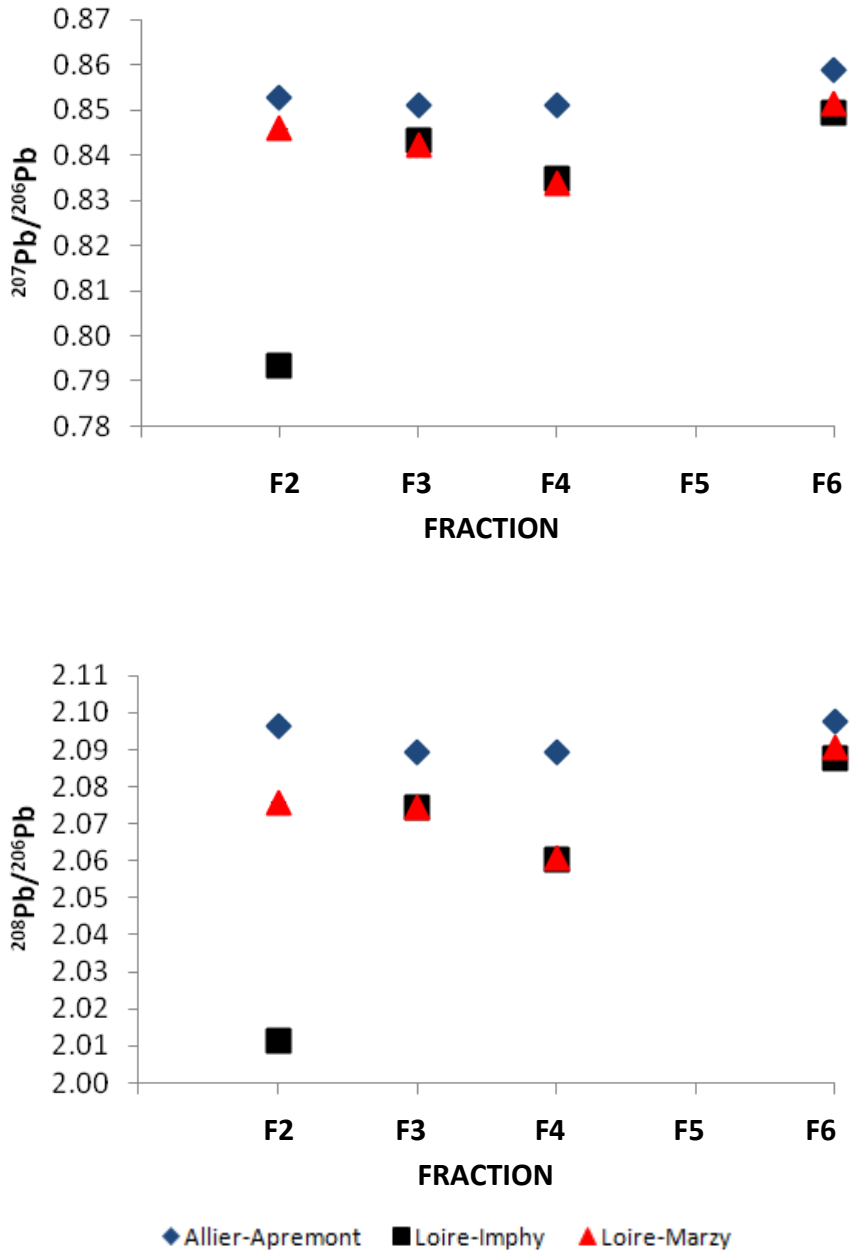

Figure 4.5 (cont.) Pb isotope ratios obtained from the SEP of each sediment. (F1, F2= exchangeable fractions; F3, F4= reducible fractions; F5=organic fraction; F6=residual fraction). Error bars represent errors represent ±2σ, where not visible error is within icon.

Reproducibility of Pb isotope ratios was evaluated by analysis of triplicate extractions of F3 and F4 from the Allier-Apremont sediment. However the analytical error from the MIC-ICP-MS on the triplicate SEP analysis was 10X higher than obtained for the original analysis (0.01% vs. 0.1%, due to the fact that using MIC-ICPMS measurement are performed at very low signals using ion counters) therefore, combined with the small differences between F3 and F4 for the Allier-Apremont sediment in the original analysis, comparison of F3 and F4 was not appropriate for all isotope ratios. The $^{208}Pb/^{206}Pb$ isotope ratio gave similar (0.01%) errors in both sets of analyses, and so was used as a comparison. Reasonable agreement was achieved between the replicates for each fraction (Table 4.4). It is clear that distinctly different ratios are obtained for the two fractions (2.0897- 2.0900±0.01% for F3 and 2.0880 - 2.0883±0.01% for F4), and that there is confidence in the replication of the obtained ratios from separate sediment samples. However, a mass balance of Pb isotope ratios was not possible due to the lack of a measured isotope ratio for F5.

4.4.5 Addition of Carbonate Step to SEP

Strontium concentrations obtained using the carbonate step altered SEP are presented in Table 4.5. In the Allier-Apremont sediment, 14% of the labile Sr is associated with carbonates, which is lower than reported elsewhere for river sediments (37 % of labile Sr, Xu & Marcantonio (2007)). As the overall proportion of labile Sr in the Loire River sediments are considerably lower (at 2-3 %) than the Allier-Apremont sediment (15 %), and other reported sediments (Grosbois et al., 2000; Négrel and Roy, 2002; Xu and Marcantonio, 2004), the relative role of carbonates in the Allier and Loire watersheds is assumed to be relatively low.

Changes in partitioning of Sr can be evaluated by comparison with the original Allier-Apremont SEP (Table 4.5). It is apparent that while F3, F4 and F5 all decrease their Sr concentration after the addition of the new step targeting carbonates, F4 and F5 experience larger decreases than F3. Clearly the addition of a new step affects the obtained results of more than one of the following steps, highlighting the importance of protocol ordering. Results of the Sr and Pb isotope ratios from the Allier-Apremont sediment for the steps following the additional carbonate step are presented in Table 4.6. Loss of both Sr and Pb from the sediment during the carbonate step does not have a drastic effect on the Sr and Pb isotopic ratios obtained for F3 ($^{87}Sr/^{86}Sr$ 0.70829 – 0.70839 and $^{206}Pb/^{204}Pb$ 18.381 - 18.379, Table 4.6), giving confidence to the specificity of the phase targeted by the NH_4 -oxalate buffer. It can be seen that the ratios

obtained for the other fractions do undergo minor changes suggesting that the carbonate associated Sr and Pb was previously being removed from across the other fractions.

Table 4.5 Sr partitioning during altered SEP with carbonate step

FRACTION	Sr $\mu g\ g^{-1}$	sd	Sr $\mu g\ g^{-1}$	Sd
F1	7.289	0.059	7.82557	0.41926
F2	0.894	0.011	0.82201	0.01313
F2b			2.29001	0.31518
F3	1.181	0.083	0.76127	0.00856
F4	1.914	0.069	1.15227	0.02724
F5	4.817	0.280	3.22095	0.03797

4.4.6 Sediment Incubations

Results of As, Sr and Pb release are presented in Table 4.7 along with the changes in aqueous phase isotopic ratios and post incubation sediment digests. It is striking to note that the behaviours of As, Sr and Pb do not follow the same patterns during both the pH and anaerobic microcosms. Whilst anaerobic conditions see a relatively high increase in dissolved As, Sr concentrations only increase slightly from day 2 to day 14, but dissolved Pb levels decrease. During aerobic incubation, dissolved As and Pb both experience decreases in the aqueous phase, whilst Sr increases, but not to the same extent as seen during the anaerobic incubation. The pH_{stat} leaching test increasing aqueous concentrations of As from the pH 3 to pH 6.5 to the highest dissolved concentrations in the pH 10 experiments, while concentrations of Pb are highest after the pH 10 experiment.

Changes in the $^{87}Sr/^{86}Sr$ isotopic ratio are observed in the aqueous phase of all incubations. An increase is seen in both anaerobic and aerobic conditions over the 14-day incubation, with a greater increase seen in the anaerobic conditions (Figure 4.6). Isotopes of Pb ($^{206}Pb/^{204}Pb$, $^{207}Pb/^{204}Pb$ and $^{208}Pb/^{204}Pb$) in the aqueous phase show a marked decrease from day 2 to day 14, but the change is the same in both the aerobic and anaerobic conditions (Table 4.7). A different relationship is evident for $^{207}Pb/^{206}Pb$, where aerobic conditions lead to an increase, and anaerobic conditions to a decrease in $^{207}Pb/^{206}Pb$ ratio (Table 4.7). During the pH_{stat} incubations, the $^{87}Sr/^{86}Sr$ isotope ratio of the aqueous phase increases with increasing pH, with

the different ratios obtained in relation to the microcosm reflecting the different matrix utilized in the experiment ($NaNO_3$ vs. river water). As pH increases from 3 to 10, $^{206}Pb/^{204}Pb$, $^{207}Pb/^{204}Pb$ and $^{208}Pb/^{204}Pb$ isotope ratios increase, while the $^{207}Pb/^{206}Pb$ isotope ratio decreases. It should be noted that the Pb isotope ratios obtained for the microcosm incubations are significantly higher than those obtained during the pH_{stat} incubations. The obtained Pb ratios for the microcosm (Table 4.7) are consistently well below those obtained for the SEP fractions for the Allier-Apremont sediment (Table 4.2), and for aquifer water from the Allier (18.183 $^{206}Pb/^{204}Pb$, 15.654 $^{207}Pb/^{204}Pb$ and 38.046 $^{208}Pb/^{204}Pb$, Millot & Négrel, unpublished), suggesting that the use of river water in the incubation has altered the obtained Pb isotopes.

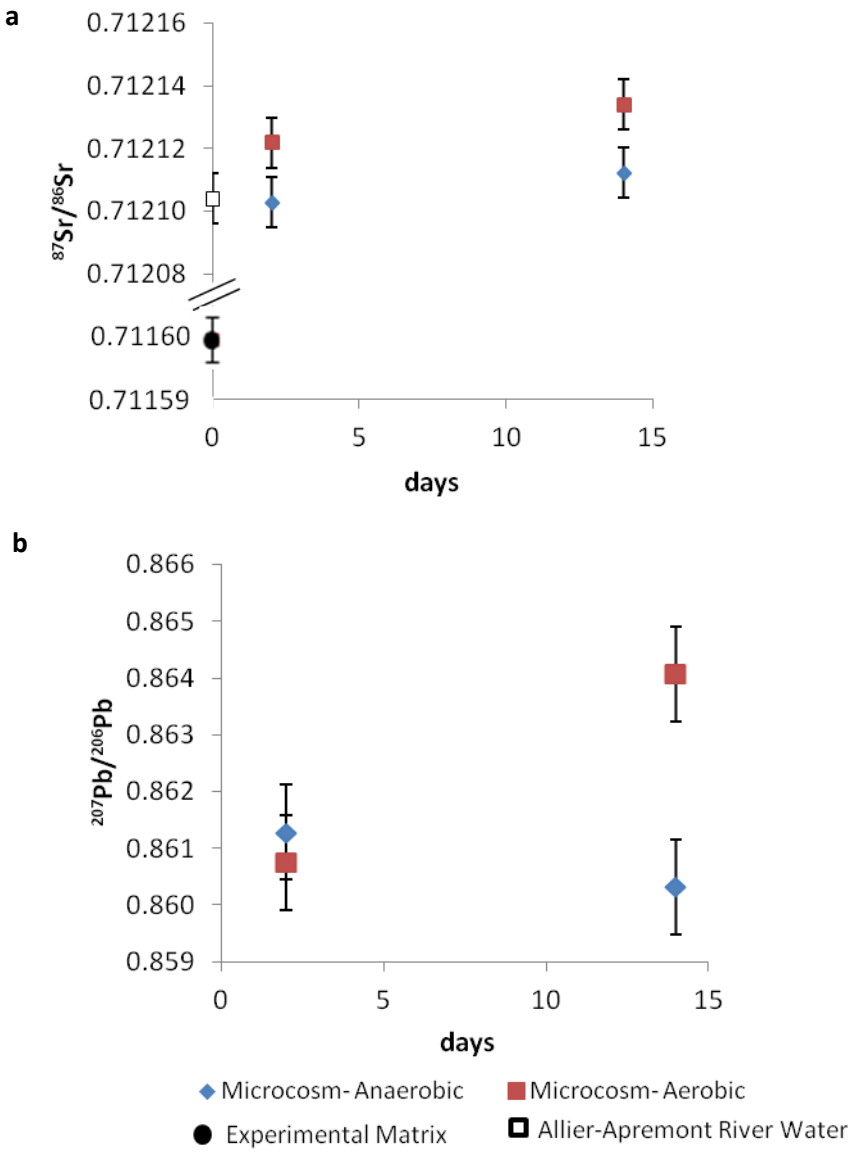

Figure 4.6 **Changes in a) $^{87}Sr/^{86}Sr$ and b) $^{207}Pb/^{206}Pb$ in the aqueous phase of microcosm incubations (Allier-Apremont sediment).** Note that the $^{87}Sr/^{86}Sr$ data point (0.712110) on day 0 represents the river water for the Allier-Apremont sample.

In the sediment digestions the $^{87}Sr/^{86}Sr$ isotope ratio increases from 0.71574 to 0.71585 in the pH 10 incubation, while falling to 0.71571 at pH 3. During the microcosms, the ratio decreases in both aerobic (0.71554) and anaerobic (0.71564) conditions, with a larger decrease seen in the aerobic sediment. $^{206}Pb/^{204}Pb$ isotopic ratios increase in all sediment incubations, from 18.151 in the original bulk sediment to 18.490 at pH 3, and 18.601 at pH 10. While the microcosm experiments (conducted at a slurry pH 6.5) also gave distinct ratios, falling between these extremes at 18.493 (aerobic) 18.530 (anaerobic). Isotope ratios for the other Pb isotopes are presented in Table 4.7.

Table 4.6 Sr and Pb isotope ratios during altered SEP with carbonate step

	$^{87}Sr/^{86}Sr$		$^{206}Pb/^{204}Pb$		$^{207}Pb/^{204}Pb$		$^{208}Pb/^{204}Pb$		$^{207}Pb/^{206}Pb$		$^{208}Pb/^{206}Pb$	
SAMPLE ID	original	altered	original	altered	original	altered	original	altered	original	altered	original	altered
CARBONATE		0.71197 ±0.00002		18.408 ±0.304		15.684 ±0.231		38.467 ±0.692		0.852 ±0.003		2.090 ±0.011
F3	0.70829 ±0.00002	0.70838 ±0.00002	18.381 ±0.018	18.379 ±0.018	15.642 ±0.016	15.656 ±0.016	38.405 ±0.038	38.407 ±0.038	0.851 ±0.0009	0.852 ±0.00009	2.089 ±0.0002	2.090 ±0.0002
F4	0.71104 ±0.00002	0.71189 ±0.00002	18.370 ±0.018	18.535 ±0.019	15.633 ±0.016	15.721 ±0.016	38.379 ±0.038	38.624 ±0.039	0.851 ±0.0009	0.848 ±0.00008	2.089 ±0.0002	2.084 ±0.0002
F5	0.70918 ±0.00002	0.70816 ±0.00002	N/M	18.957 ±0.019	N/M	16.115 ±0.016	N/M	39.540 ±0.039	N/M	0.850 ±0.00009	N/M	2.085 ±0.002
F6	0.71633 ±0.00002	0.71564 ±0.00002	18.151 ±0.018	18.607 ±0.019	15.591 ±0.016	15.804 ±0.016	38.074 ±0.038	38.832 ±0.039	0.859 ±0.0009	0.849 ±0.00008	2.098 ±0.0002	2.087 ±0.002

N/M refers to not measured values, errors represent ±2σ

Table 4.7 Summary table of concentration and Sr and Pb isotopic ratios obtained during laboratory incubations

Sample description	Matrix	pH	Incubation time	As µg l^{-1}	Sr µg l^{-1}	Pb µg l^{-1}	$^{87}Sr/^{86}Sr$	$2\sigma_{(m)}$	$^{206}Pb/^{204}$ Pb	$2\sigma_{(m)}$	$^{207}Pb/^{204}$ Pb	$2\sigma_{(m)}$	$^{208}Pb/^{204}$ Pb	$2\sigma_{(m)}$	$^{207}Pb/^{206}Pb$
Aqueous Phase															
Marzy river water	N/A	8.5	0	3.71	115	>0.01	0.71160	0.000008	N/M	N/M	N/M	N/M	N/M	N/M	N/M
Microcosm- Anaerobic	Marzy River Water	6.5	2	1.61	96.4	1.12	0.71210	0.000008	14.171	0.112	12.204	0.092	29.855	0.380	0.861
Microcosm- Anaerobic	Marzy River Water	6.5	14	8.53	99.5	0.739	0.71211	0.000008	12.807	0.101	11.013	0.083	26.920	0.342	0.860
Microcosm- Aerobic	Marzy River Water	6.5	2	1.46	93.7	0.751	0.71212	0.000008	14.183	0.112	12.209	0.092	29.786	0.379	0.861
Microcosm- Aerobic	Marzy River Water	6.5	14	0.82	97.6	0.303	0.71213	0.000010	12.786	0.101	11.052	0.083	26.911	0.342	0.864
pH_{stat} leaching	$NaNO_3$	3	14	3.35	32.0	32.9	0.71178	0.000009	18.314	0.018	15.614	0.016	38.289	0.038	0.853
pH_{stat} leaching	$NaNO_3$	6.5	14	2.34	727	23.6	0.71222	0.000008	18.442	0.018	15.719	0.016	38.548	0.039	0.852
pH_{stat} leaching	$NaNO_3$	10	14	152	64.4	16.4	0.71217	0.000008	18.668	0.019	15.896	0.016	39.004	0.039	0.852
Sediment Digest															
Allier Bulk Sediment	none		0	nd	117	43.3	0.71574	0.000008	18.151	0.018	15.591	0.016	38.074	0.038	0.859
Post pH_{stat} leaching	$NaNO_3$	3	14	nd	98	25.0	0.71571	0.000008	18.490	0.018	15.663	0.016	38.608	0.039	0.847
Post pH_{stat} leaching	$NaNO_3$	10	14	nd	98	6.0	0.71585	0.000008	18.601	0.019	15.714	0.016	38.916	0.039	0.845
Anaerobic	Marzy River Water	6.5	14	nd	162	19.7	0.71564	0.000010	18.530	0.019	15.675	0.016	38.718	0.039	0.846
Aerobic	Marzy River Water	6.5	14	nd	151	25.0	0.71554	0.000009	18.493	0.018	15.653	0.016	38.623	0.039	0.846

nd refers to not determined (due to matrix interferences), N/A : not applicable, N/M :not measured ('Pb-contamination free' field sample unable to be collected)

4.5 Discussion

4.5.1 Sr and Pb partitioning and the relationship with As

Labile As has been found to occur largely within the reducible fractions (F3 and F4) in all three sample areas (60-87 %), reflecting the importance of Fe-Mn oxides in the storage and control of As in river sediments. The overall partitioning of As at both Loire River sites is very similar, with a limited contribution of F1, suggesting non-specifically sorbed As is not an important storage component within Loire River sediment. While the oxidisable As (organic matter and sulphides as given in F5) is negligible within Loire River sediments (2-6 %), there is a minor role (12 %) within the Allier-Apremont sediment. Despite the analytical uncertainties relating to the measurement of As in the residual fraction (F6), the agreement between the sum of fractions F1-F5 and the XRF of the sediment clearly indicate that a minor proportion of As is held within the residual fraction, which is in agreement with other studies on As in sediments (Blute et al., 2009; Linge and Oldham, 2002).

The measured trace element sediment concentrations reflect the differing geologies of each river course. While both Loire River sediments show close agreement in their As, Sr and Pb contents, the Allier-Apremont sediment shows considerably higher concentrations of As, Sr and Pb, suggesting that contributions from the Massif Central basin may be more pronounced, or increased volcanic rock contributions over the course of the Allier River may be causing elevated trace element levels in the sediment. In addition to the variation in total concentrations between the samples, differences observed in the partitioning of As, Sr and Pb within each of the sediments reflects differences in each sediments geochemical behaviour. Understanding these differences is important in determining the utility of Sr and Pb as isotopic tracers in the occurrence of As.

The most striking difference relates to the importance of the residual phase in the storage of Sr and Pb within the sediment. The partitioning of Sr in all three sediments appears very different to that of As, with 85-98 % of Sr found within the residual fraction. This is in general agreement with work by Xu & Marcantonio (2004), where 70-87 % of Sr was held within the residual fraction of sediment from within the Mississippi River mixing zone. The residual phase is also important in the storage of Pb, but as the proportion of Pb within the Allier-Apremont sediment (41 %) is significantly lower than the Loire River sediments (Loire-Imphy 76 %, Loire-Marzy 87 %), the differences suggest varying mineralogy and weathering processes between rivers. Previously, sediment from tributaries of the Allier River was found to contain lower

levels of Pb within the residual fraction of the sediment than the AEM fraction (Négrel and Roy, 2002). The lower amount of residual Pb, yet higher overall concentration within the Allier-Apremont sediment suggests either there is a different, more labile source of Pb within the sediment in the Allier River, or that mobilisation processes between the two rivers differ. The proportion of residual Pb observed in this study are in a similar range to those observed by a number of SEP sediment studies, including rivers in Spain (Gismera et al., 2004; Morillo et al., 2008) and Chile (Segura et al., 2006). However variability in Pb partitioning in sediments, has been found to depend on the Pb sources within a catchment. The proximity of roads was thought to contribute labile Pb to nearby sediments (Gismera et al., 2004), while in areas of high industrial activity, elevated Pb concentrations were found in the residual fraction of sediments with higher Pb content (Morillo et al., 2008; Pagnanelli et al., 2004). The residual fraction appears to be more important in the storage of Pb in sediments than soils (Bacon et al., 2006; Emmanuel and Erel, 2002; Teutsch et al., 2001), illustrating the different processes affecting trace elements within sediments. Xu & Marcantonio (2004) noted that the increased concentrations of trace elements (Sr, Mn and Fe) within the residual phases of sediment relative to particulates, related to the increased physical and chemical processes occurring within sediments e.g. compaction and mineralisation.

When considering only the labile fractions (Figure 4.2), there is a considerable difference in the partitioning of As and Sr. Labile Sr appears to be largely non-specifically sorbed in all three sediments, with only minor roles for the remaining fractions. Strontium associated within the reducible fraction of the sediment (Fe-Al oxides within F3 & F4) comprise 14-19 % of the labile Sr within the sediments, which is similar to the observations of Xu & Marcantonio (2004), who found ~18 % of nonresidual Sr on average associated with Fe-Mn (oxy)hydroxides. Alteration of the SEP, with the addition of a step specifically targeting carbonates showed that 18% of labile Sr was associated with carbonates in the Allier-Apremont sediment, lower than previously observed for sediments (Xu and Marcantonio, 2004). Samples for the present study were obtained during winter, and so may lack the biogenic carbonate thought to be more prominent in summer seasons downstream in the Loire river (Négrel et al., 2000). Arsenic was not found within the Allier-Apremont sediment carbonate phase (<2 %, data not shown), supporting the findings of Wenzel et al., (2001) where the non-association of As and carbonate was used to eliminate a carbonate specific step from their As-SEP. It appears that different reservoirs within the sediment are important in understanding the partitioning of these two trace elements.

Lead follows a similar pattern of occurrence to As within the sediment, with exchangeable Pb not found within the sediment (in F1 or F2), but instead 74-91 % of labile Pb is found within reducible fractions F3 and F4, suggesting that the role of Fe (oxy)hydroxides is key in Pb storage within the sediments. The association of Pb with the reducible fraction of sediments and soils is also found by a range of studies, indicating the prevalence and scavenging nature of Fe minerals in the non residual part of sediments (Bacon et al., 2006; Négrel and Roy, 2002). The addition of a step targeting carbonates in the Allier-Apremont sediment showed that like As, Pb is not associated with carbonates (<1 %, data not shown) within the sediment. Such an association also indicates the Pb to be geogenic in origin, with anthropogenic Pb found to bind preferentially with carbonate in soils (Teutsch et al., 2001). The role of the organics and sulphides (F5) is once again more predominant in the Allier-Apremont sediment for storage of both Sr and Pb, reflecting the different biogeochemical behaviour of the individual river sediments.

Evaluation of the SEP concentration data for As and Sr as a whole reveals the lack of a clear relationship between the two trace elements. However, considering the steps of the SEP separately, it is evident that there is a general positive trend between As and Sr within each labile fraction (Figure 4.7). This implies that while the differences in partitioning between the fractions of sediment may mean that larger amounts of Sr are present in fractions where As occurrence is limited, there is still a broad relationship between the occurrence of As and Sr within each of the different (operationally defined) fractions of each sediment. The relationship between As and Pb is more clear, with a general positive trend observed for all labile SEP data, and this relationship is also evident when looking within each SEP fraction (Figure 4.7), suggesting that there is similarity between the occurrence of Pb and As within the sediments.

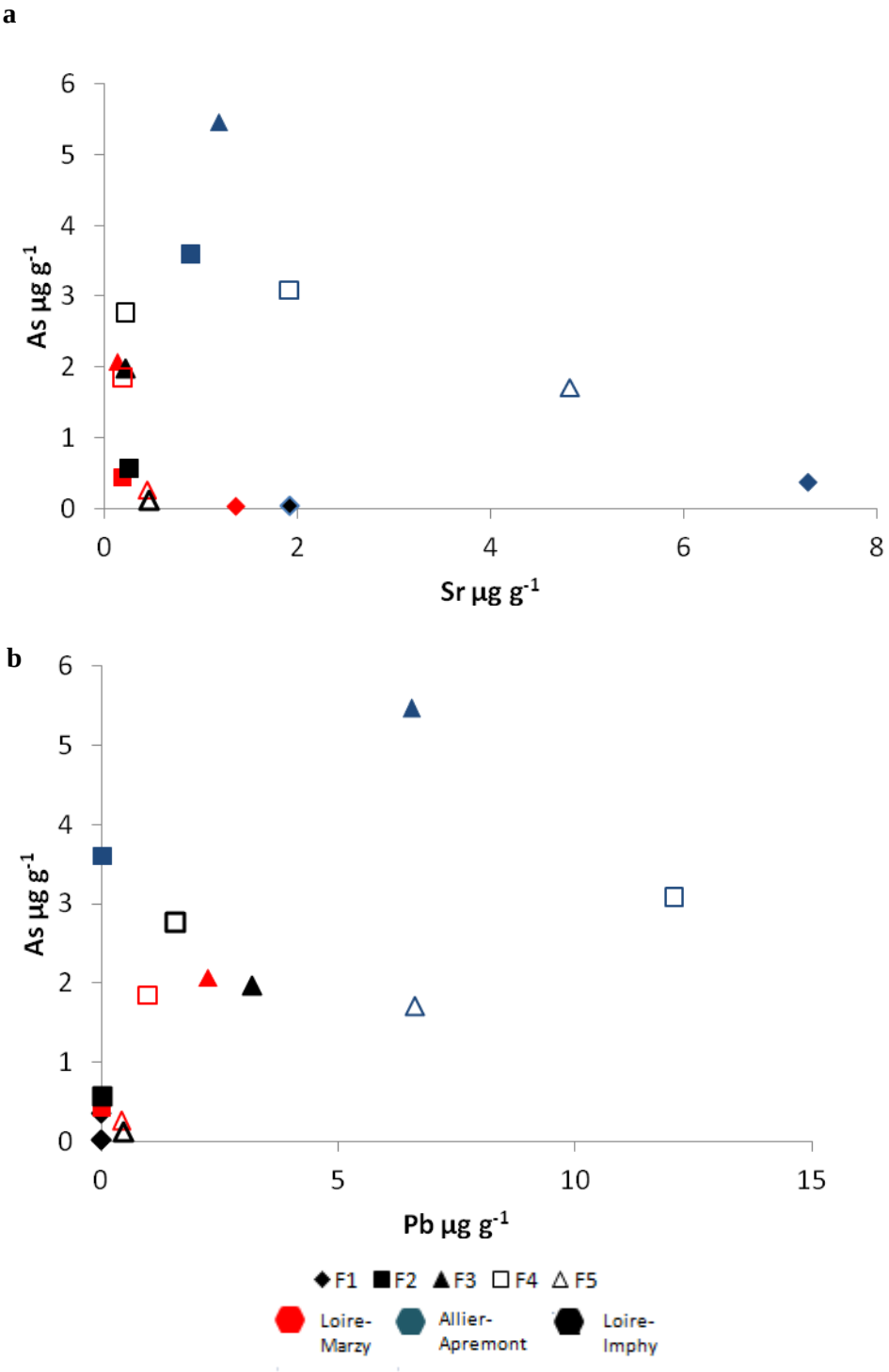

Figure 4.7 **Relationship between concentration of As and concentrations of both a) Sr and b) Pb in sediment SEP fractions.**
Red colour represents Loire-Marzy, black Loire-Imphy and blue Allier-Apremont samples.

The presence of both Sr and Pb along with As within the fractions of the As-specific SEP suggests similar processes are acting on these trace elements (to different extents) within the river sediment. The correlation of As and Pb from all three sediments can be used to describe the likely phases present within each SEP fraction. Evaluation of the data for F3 shows a As/Pb slope close to 1, with zero origin suggesting that all three sediments are acquiring As and Pb within the amorphous Fe oxides at a 1:1 ratio. The relationship observed for F4 is different however, with a slope closer to 0.1, and an intercept of 2. This could be due to two distinct phases present in F4 in differing proportions between the Loire and Allier sediments, one containing only As, and the second with both As and Pb at a ratio of 0.1. A similar pattern is observed for Sr, with F3 showing possibility of two distinct phases, one with only As, and the other with both As and Sr at a ratio of 3.The broad positive relationship observed for Pb suggests that similar sources and/or mobilisation mechanisms may be acting on both elements, giving confidence in the application of Pb as a tracer of the mineral origin within the river sediment. Whilst Sr is partitioned quite differently, the existence of a weak positive relationship within each fraction suggests the processes occurring within each fraction are affecting the two elements in similar ways.

4.5.2 Controls on Sr and Pb isotopic composition of labile fractions

i) Strontium

As natural processes do not fractionate $^{87}Sr/^{86}Sr$ isotope ratios, the variation of the obtained Sr isotope ratios directly reflects the mixing of different sources of Sr within the sediment, including Sr associated with Fe or Mn minerals, or Sr bound with carbonates or clays. The difference in $^{87}Sr/^{86}Sr$ isotope ratio obtained for the labile phases within the sediments indicates that separate sources of Sr are contributing to the different fractions. However, the similar patterns observed between the three sediments suggest similar processes controlling the isotopic composition within the two river basins. The $^{87}Sr/^{86}Sr$ isotope ratios for F1 and F2 for the Loire-Imphy and Allier-Apremont River sediments match to the $^{87}Sr/^{86}Sr$ isotope ratios obtained for the river water (Table 4.2), while the Loire-Marzy F1 and F2 $^{87}Sr/^{86}Sr$ isotope ratios are slightly lower. The similarity of the adsorbed phases with the dissolved phase, indicates that these sediments are in equilibrium with the water at the point of sampling, while the difference observed at the Loire-Marzy site suggests that the sediments are not in equilibrium. The lower $^{87}Sr/^{86}Sr$ ratios observed for the water at Loire-Marzy could be

attributable to the influence of discharge from the town of Nevers, just prior to the confluence, or from the Nievre River, just prior to Nevers. A range of anthropogenic influences may originate from the city of Nevers, including urban heating (0.708-0.712) and stormwater runoff from roads (0.7080-0.7085) (Négrel et al., 2007). The lower $^{87}Sr/^{86}Sr$ ratios seen in F1 for the Loire-Marzy sediment could be related to the effect of the Bec d'Allier confluence of the two rivers (Bouchez et al., 2010), it is possible that the Marzy site is within the mixing zone of the Bec d'Allier, causing the sediment sample to be inhomogeneous at the point of sampling.

Although the use of mixing diagrams for Sr has been questioned due to the multiple removal processes for dissolved Sr (Faure, 1986; Négrel et al., 2000; Négrel et al., 2002) application to SEP data has been used by Xu & Marcantonio (2004) to evaluate the isotopic data of labile vs. residual fractions of a SEP. It can be observed that the relationship between $^{87}Sr/^{86}Sr$ isotope ratios obtained for the labile fractions (Figure 4.8) and the inverse of their Sr content is not linear, indicating that there are more than two endmembers contributing to the source of Sr within the sediment. Despite the lack of a clear or simple mixing array for the labile fractions, the obtained $^{87}Sr/^{86}Sr$ isotope ratios for the residual fractions of all three sediments lie far off those of the labile fractions. This observation indicates two points: 1) that there is preferential removal of lower $^{87}Sr/^{86}Sr$ isotope ratios during weathering, as seen for Fe in soils (Wiederhold et al., 2007) and 2) factors other than the attack of the residual phase are influencing the composition of labile phases (Xu and Marcantonio, 2004). Comparison of the obtained ratios with known Sr isotopic ratios for sediments from both the Loire and Allier Rivers (Figure 4.8) illustrate the differences in geology of the two rivers. While both the total digest and residual fraction of the two Loire River sediments are close to the ratios obtained from the residuals of granite derived sediment (0.72432-0.72619 vs. 0.72663-0.73736 respectively (Négrel and Roy, 2002)), the Allier-Apremont total and residual digests have much lower $^{87}Sr/^{86}Sr$ isotope ratios (0.71574- 0.71633), which suggests a contribution of basalt, as observed for the Allanche region along the Allier River (0.70382-0.70414), by Negrel et al., (2002).

The range of $^{87}Sr/^{86}Sr$ isotope ratios obtained for the labile fractions of the Loire and Allier River sediments agree with ratios previously obtained for the AEM component of SPM and sediment from both rivers (Figure 4.8a) (Négrel and Grosbois, 1999; Négrel et al., 2000; Négrel and Roy, 2002). Grouping of the F3 and F4 fractions (Figure 4.8) illustrates a separation between the two Loire River sediments and the Allier-Apremont sediment. In both fractions, the Allier-Apremont $^{87}Sr/^{86}Sr$ isotope ratio is lower, and the Sr concentration higher than those obtained for the Loire River sediments, in agreement with the lower ratios previously observed

for the AEM of Allier River sediment (Négrel and Roy, 2002), and suggesting an increased basaltic contribution to these fractions (AEM basalt 0.70381-0.70409 (Négrel and Roy, 2002)). Despite the known association of Sr and carbonates (Négrel et al., 2000; Smith et al., 2009; Yokoo et al., 2004), with the exception of F3 from the Allier-Apremont sediment the SEP solutions all lie outside of the range for calcium carbonates and barites from the Jurassic to the Neogene, indicating that carbonates play a minor role within the sediments. The high flows during the sampling period combined with the lack of Sr found within the carbonate (CH_3COONa) extraction of the Allier-Apremont indicate that the formation of authogenic calcite, as observed during summer months can be excluded, and the carbonate present is likely to be from a detrital calcite reservoir, as found by Negrel & Grosbois (1999).

There is a clear distinction between the reducible fractions F3 and F4 in Figure 4.8 for all three sediments, indicating a distinct Sr source is targeted by the NH_4 -oxalate buffer and NH_4 -oxalate buffer/ ascorbic acid fractions targeting poorly crystalline and well crystallised Fe/Al hydrous oxide minerals respectively. Previous work has suggested that the difference in dissolved and particulate Sr ratios is due to the conservative behaviour of oxides in the water column. As oxides are not equilibrated with the water as they are transported, the $^{87}Sr/^{86}Sr$ isotope signature of hydroxides should reflect that of the water from which they formed (Négrel et al., 2000; Négrel et al., 2002). If the Fe-Al hydrous oxides originate from the Massif Central, the associated Sr should be from the weathering of the different bedrock formations contained within this area. Previous work with the AEM of SPM from the Loire River also showed that the $^{87}Sr/^{86}Sr$ isotope ratios of hydroxides were lower than those observed in the dissolved phase, indicating that the hydroxides within the SPM had been transported from upstream. Waters with low $^{87}Sr/^{86}Sr$ isotope ratios have been reported for waters draining the Massif Central, with Négrel et al., (1997) reporting 0.70951 - 0.71266 during low and high flow conditions respectively in the Allier River. The lower $^{87}Sr/^{86}Sr$ isotope ratios observed for F3 and indicates the movement of sediment or particulate matter (and subsequent settling) containing Fe-Al hydrous oxides from upstream.

Comparison of the Sr isotopic ratios obtained from the SEP fractions and those of the river water illustrates key differences between the sediments (Table 4.2). While the ratios observed for F3 are lower than those measured in the dissolved phase at each respective sample site, the ratios of F4 for both Loire River sites are only slightly higher than those seen in F1 and F2, whilst the $^{87}Sr/^{86}Sr$ ratio obtained for Allier-Apremont F4 sample is lower, but within the range reported previously for Allier River water (Négrel et al., 1997). The similarity of the ratios of

F1/F2 and F4 for the sediments implies that F4 is in closer equilibrium with the river water than F3. This observation suggests that while formation of amorphous Fe minerals such as ferrihydrite are occurring upstream of the studied sites, the Fe mineral transformation from amorphous to crystalline minerals is actively taking place within the river sediments, close to the point of sampling. This observation provides evidence that the presence of Fe(II) and cyclic redox conditions required for ferrihydrite crystallisation at ambient temperatures (Pedersen et al., 2005); exist within the river sediments, leading to the formation of more stable crystalline Fe minerals (Warren and Haack, 2001). While the transformation of ferrihydrite to more stable, crystalline minerals such as goethite requires the release of initially surface bound As, it has been noted to occur incongruently from Fe, with almost all (>99 %) As incorporated within the resulting crystal lattice (Pedersen et al., 2006). The degree to which this mineral transformation is taking place could have important implications for the transport of As, as both F3 and F4 are important stores of As within the sediment. Once within the more stable crystal lattice of crystalline Fe minerals, significant changes in environmental conditions such as the onset of reductive dissolution (possibly microbially assisted) are required for the mobilisation of As (Blute et al., 2009; Postma et al., 2010).

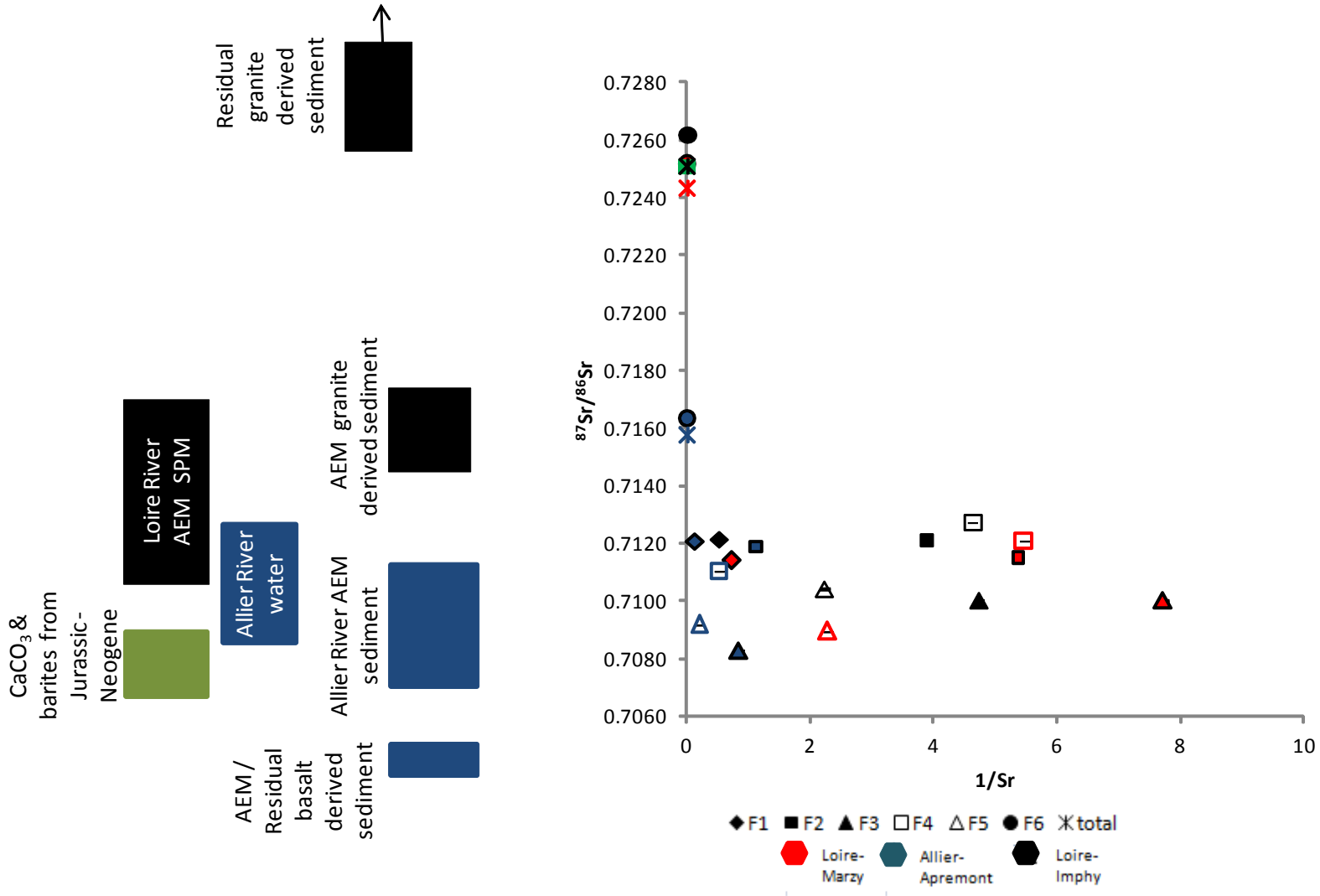

Figure 4.8 **Sediment $^{87}Sr/^{86}Sr$ ratios represented as a function of 1/Sr ratios.** Red colour represents Loire-Marzy, black Loire-Imphy and blue Allier-Apremont samples. Fields for previously reported water and sediment digests from the Loire and Allier Rivers are included (Négrel et al., 2000; Négrel et al., 2007; Négrel et al., 2002)

ii) Lead

The variability in Pb isotopic ratio obtained for each of the three sediments SEPs is significant, indicating that different reservoirs of Pb are contained within each of the sediments. Clearly the weathering processes within the sediment, including oxide dissolution and reprecipitation are ineffective at homogenising the labile Pb reservoir (Emmanuel and Erel, 2002). From this observation, it is evident that while bulk soil digests can only provide an average picture of both chemical and isotopic compositions, the use of SEPs allows different soil reservoirs to be identified.

The removal of dissolved Pb by oxides allows the comparison of Pb isotope ratios with Pb content in Pb mixing diagrams. Figure 4.9 presents the relationship between both the Pb isotope ratios $^{206}Pb/^{204}Pb$ and $^{208}Pb/^{206}Pb$ and the inverse of Pb content. From this graph, it is clear that F3 and F4 contain distinct reservoirs of Pb. The mixing line evident between F3 and F4 in both graphs suggests that two endmembers at least are required for the mixing model. Determining the source of Pb in the fractions requires the knowledge of different possible Pb reservoirs within the catchments. The two potential crustal endmembers are Massif Central granite and basalts. The $^{206}Pb/^{204}Pb$ isotope ratios for the Allier-Apremont sediment fall within the range previously reported for the AEM of basalt derived sediments and the AEM of Allier River sediments, while the Loire sediments fall within previously reported $^{206}Pb/^{204}Pb$ isotope ratios of the AEM of granite derived sediments, and the $^{208}Pb/^{206}Pb$ isotope ratios of Loire River sediments (Négrel et al., 2004; Négrel and Roy, 2002), again reflecting the altered geology between the Loire and Allier Rivers. Despite overlapping with other published data on Pb isotopes from AEM of sediments, both F3 and F4 from the Allier-Apremont sediment fall in the range given by Negel & Roy (2002) as being from Fe-oxides, suggesting this as a possible third endmember for Pb within the sediment. The influence of Fe in the Allier-Apremont sediment is likely to be large due to the increased Fe concentrations at this site (20.1 vs. 5.1 $\mu g\ g^{-1}$ for the Loire-Imphy and Allier-Apremont sediments respectively, data in Chapter 3).

Unlike Sr, the Pb isotopic ratios of the residual fractions do not lie far off the mixing array of the labile fractions (Figure 4.9), but are isotopically distinct from the labile fractions. The presence of a distinct residual isotopic signature is indicative of weathering processes occurring within the sediment, and has been observed in other soils and sediments (Emmanuel and Erel, 2002; Teutsch et al., 2001). As the sediment is transported, a range of mechanical and chemical weathering processes can act upon the sediment to incorporate the original Pb-

mineral material into various phases of the sediment (Emmanuel and Erel, 2002). Depending on the resistance of each Pb-mineral present in the material, weathering processes will remove the more labile Pb-minerals, creating a reservoir of more weathering resistant Pb-minerals within the residual phase. Although it is important to note that as the residual fraction is effectively what is 'left over' in the sediment following the SEP, the removal of Pb in previous steps in the SEP will influence the composition of the remaining material. The residual F6 fraction of the Allier-Apremont sediment has a significantly lower $^{206}Pb/^{204}Pb$ isotopic ratio, indicating the Pb-minerals within the Allier-Apremont sediment have different weathering properties than the two Loire River sediments.

In the plots of $^{208}Pb/^{204}Pb$ vs. $^{206}Pb/^{204}Pb$ and $^{208}Pb/^{206}Pb$ vs. $^{207}Pb/^{206}Pb$ (Fig 4.10a,b), the position of Pb-isotopic compositions of AEM with respect to the various endmembers is shown. It is clear that the SEP fractions from all three sediments fall in a linear mixing line between the basalts and granites (Négrel et al., 2004; Négrel and Roy, 2002). From the combination of these graphs, the Pb contained within the sediment can therefore be described as being of geogenic origin, as already mentioned. The total digests of the Loire River sediments fall within the range reported for whole rock granites for $^{208}Pb/^{204}Pb$ vs. $^{206}Pb/^{204}Pb$ (Downes et al., 1997; Michard-Vitrac et al., 1981), while the Allier-Apremont sediment total digest has a higher Pb isotopic ratio, towards the range expected for whole rock basalts. Natural inputs of Pb such as the weathering of granites and basalt are likely responsible for the Pb content within the different fractions of the sediments. While the Loire River sediments fall within the range seen for the AEM of granite derived sediment in the $^{208}Pb/^{204}Pb$ vs. $^{206}Pb/^{204}Pb$ graph (Figure 4.10a), the Allier-Apremont sediment plots lower, along with the previously reported sediment AEM range for Allier-Apremont sediment, reflecting the basaltic composition of the sediment. In addition, there is no evidence of contribution of anthropogenic sources of Pb in these samples, as the gasoline domain does not lie within the binary mixing of the samples (Figure 4.10a). While the previously reported ratios for Pb industrial components fall closer to the mixing line- the large area representing the multiple sources of Pb in industrial contamination indicates the source is erratic, and as the SEP fractions fall within previously reported ratios for AEM of naturally derived Pb in sediments, the role of anthropogenic Pb can be discounted.

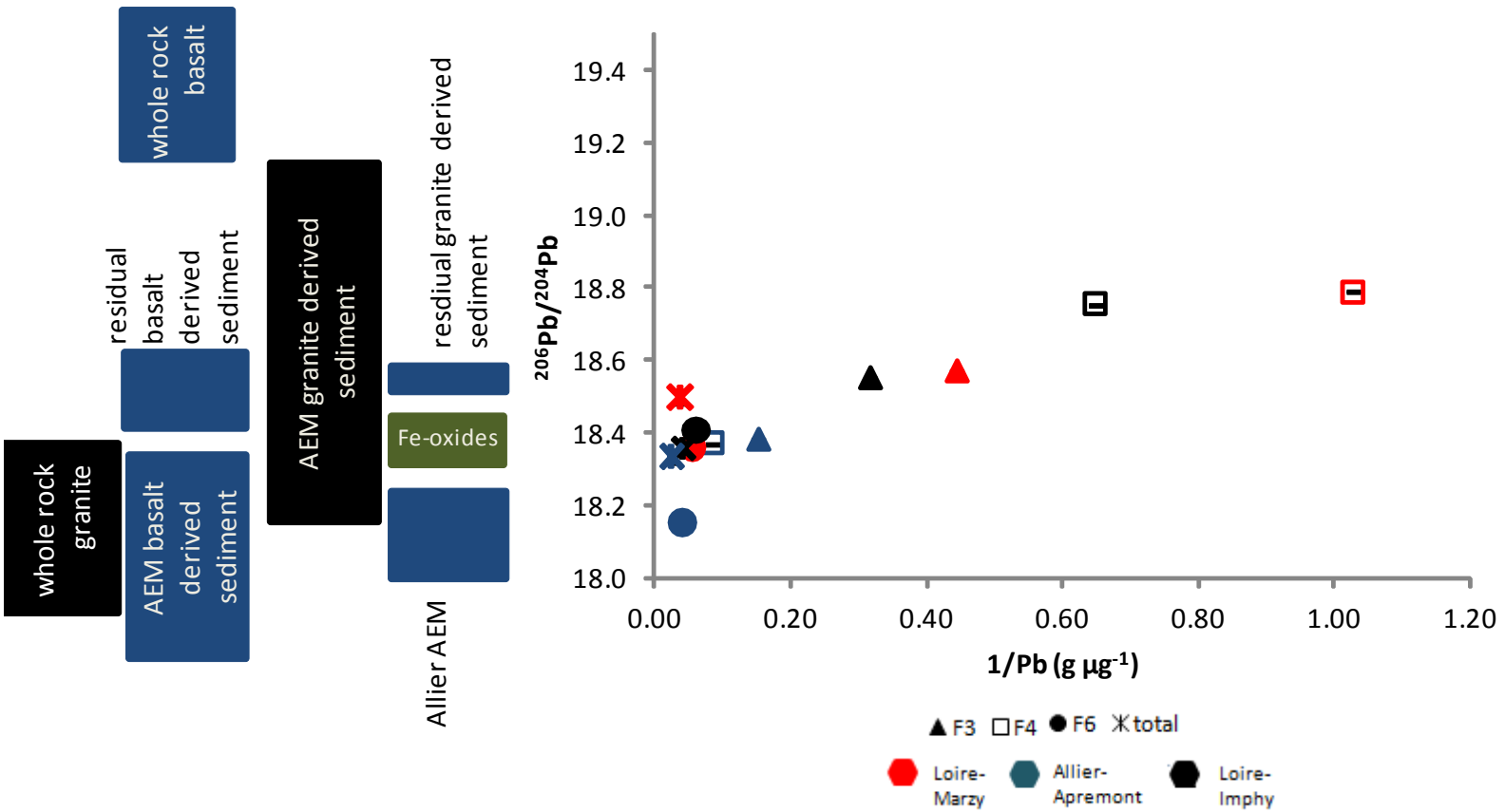

Figure 4.9 **a) Sediment $^{206}Pb/^{204}Pb$ ratios represented as a function of 1/Pb ratios.** Red colour represents Loire-Marzy, black Loire-Imphy and blue Allier-Apremont samples. Fields for previously reported sediment and rock digests from the Loire and Allier Rivers have also been added (Négrel et al., 2004; Négrel and Roy, 2002).

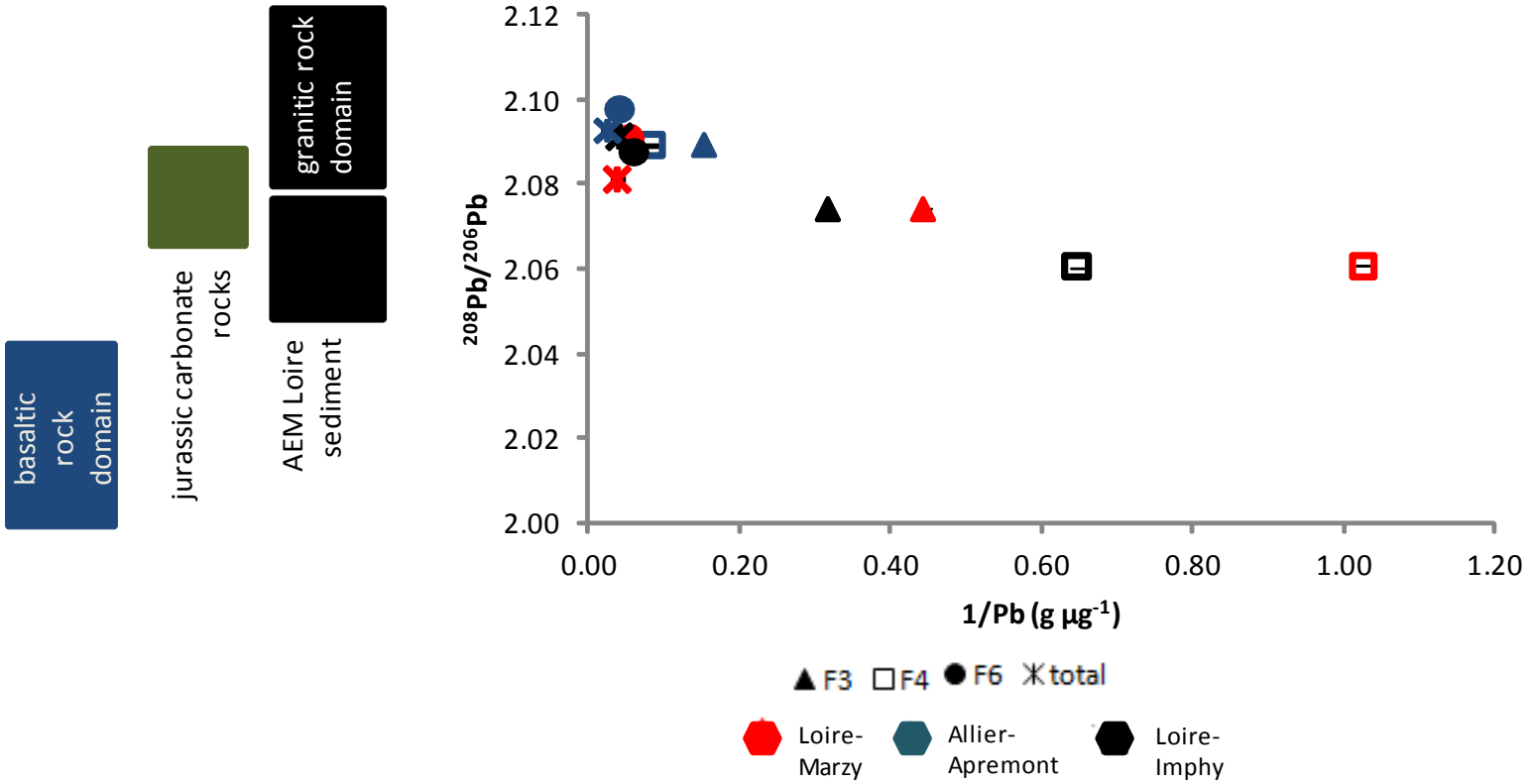

Figure 4.9 (cont) b) Sediment $^{208}Pb/^{206}Pb$ ratios represented as a function of 1/Pb ratios. Red colour represents Loire-Marzy, black Loire-Imphy and blue Allier-Apremont samples. Fields for previously reported sediment and rock digests from the Loire and Allier Rivers have also been added (Négrel et al., 2004; Négrel and Roy, 2002).

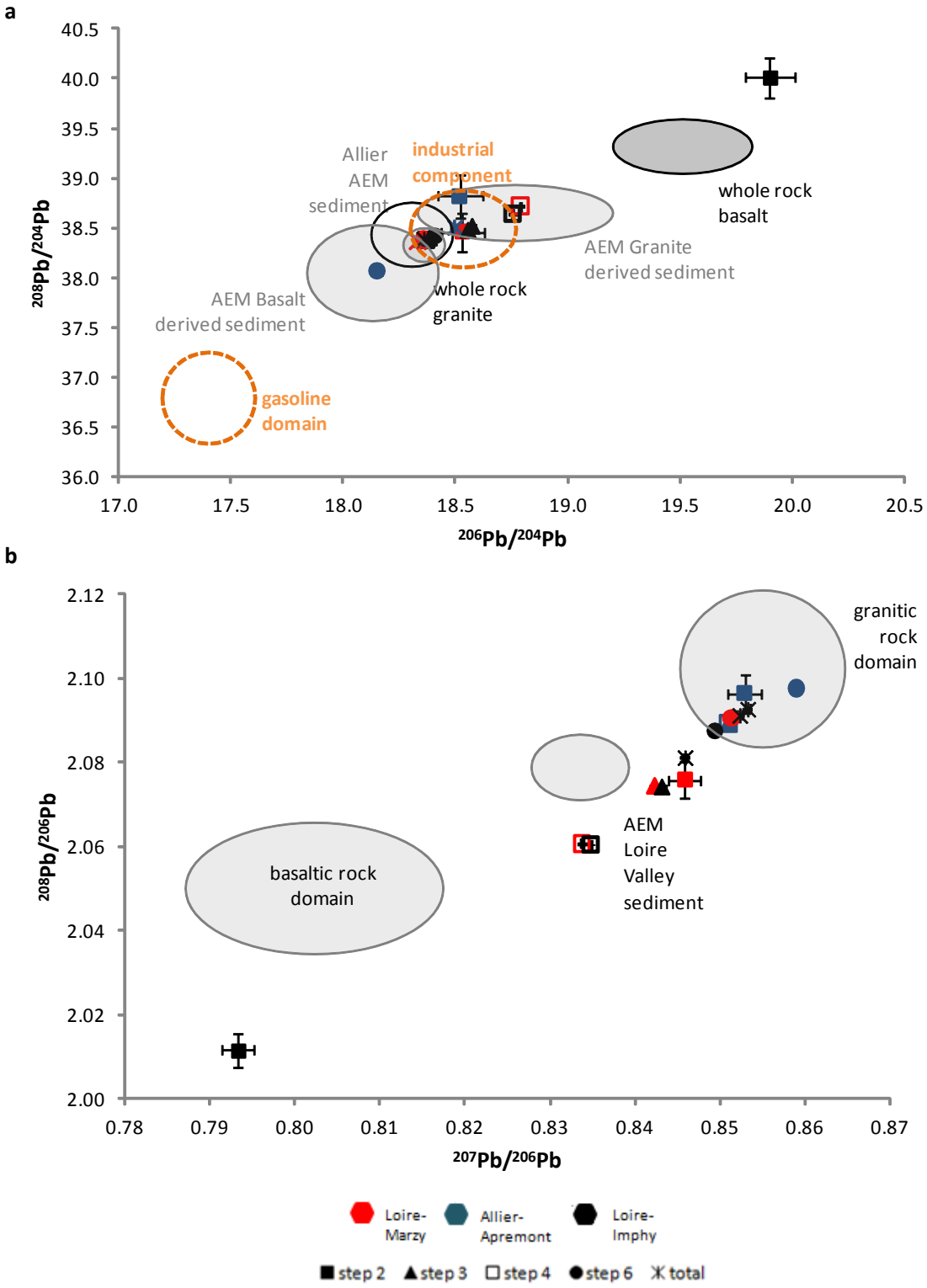

Figure 4.10 **Relationship between $^{208}Pb/^{204}Pb$ and $^{206}Pb/^{204}Pb$ (a) and $^{208}Pb/^{206}Pb$ and $^{207}Pb/^{206}Pb$ (b) in Loire and Allier River sediment SEP fractions.** Red colour represents Loire-Marzy, black Loire-Imphy and blue Allier-Apremont samples. The shaded fields represent the various basement rocks from the Loire catchment. The dashed fields represents Pb isotope data in common anthropogenic sources (Monna et al., 1997; Négrel and Roy, 2002)

4.5.3 Implications for source of As

The presence of distinct Pb and Sr isotopic signals for fractions within the SEP of each sediment suggests there is potential to identify specific trace element reservoirs within each sediment. Adaption of the existing mixing models (Figure 4.8 & 4.9) with the content of As relative to either Sr or Pb allows for interpretation of the relationship between Pb and Sr isotopic ratios and As content. Figure 4.12a&b illustrates the relationship between $^{86}Sr/^{87}Sr$ and As/Sr and $^{206}Pb/^{204}Pb$ and As/Pb respectively. As observed for the Sr mixing model using the inverse of Sr content, there is a spread of data from left to right in Figure 4.11a, reaffirming that more than two endmembers are required to explain variation. Because of the different environmental processes affecting the SEP fractions, analysis of the data within each fraction rather than as a whole may be a useful tool to evaluate the As/Sr relationship. Review of the three sediments for each SEP fraction shows that for the reducible fractions F3 and F4, there is a generally positive relationship between As content and Sr isotopic ratio, with the sediment fractions containing higher As concentrations also found to contain Sr of higher isotopic ratio. While the ratios for F3 and F4 remain within the expected range for the AEM of sediment and SPM from the Loire and Allier Rivers (Figure 4.11a), it can be seen that higher Sr isotopic ratios are generally expected from the AEM of granitic derived sediment (Négrel and Roy, 2002).

Within the SEP, the reducible fractions consist of both poorly crystalline and well crystallised hydrous oxides of Fe and Al in F3 and F4 respectively. Because the labile fractions of Sr are considered to be in isotopic equilibrium with the water phase in which they were formed, the differing $^{87}Sr/^{86}Sr$ isotopic ratios found for these two fractions can provide information on the formation of the oxides (Andersson et al., 1994). The lower $^{87}Sr/^{86}Sr$ isotopic ratios found for F3 in all three sediments suggest that formation of this fraction either did not occur within the sediment (or settled SPM) at the point of sampling, or were formed *in situ* when dissolved $^{87}Sr/^{86}Sr$ isotopic ratios in each river were significantly lower. Cyclical variations in $^{87}Sr/^{86}Sr$ isotopic ratios of the AEM of SPM have been found for the Loire River, with the lower $^{87}Sr/^{86}Sr$ isotopic ratios (0.71058) thought to be the result of erosion of hydrous Mn-Fe oxides. Despite the high flows during the sample period, dissolved $^{87}Sr/^{86}Sr$ isotopic ratios were not observed to be as low as found in F3, suggesting that their formation has taken place upstream e.g. in waters immediately draining the Massif Central (Négrel et al., 1997). The higher ratios obtained for F4, in closer agreement with the dissolved phase at the point of sampling, suggest that the process of formation has occurred downstream from F3. Given the importance of

both F3 and F4 in the storage of As, the location of the formation and alteration of these phases has important implications for the mobility of As.

While Sr isotopes can provide information on mineral formation through the state of equilibrium with water at the time of precipitation, Pb isotopes are able to determine the importance of weathering processes of the original bedrock material in the distribution of trace elements within the river sediment. The clear relationship between Pb isotope and the inverse of Pb content indicated a two member system existing, at least for the reducible fractions. This relationship, along with the presence of isotopically distinct residual fraction highlights the role of the residual fraction redistributing Pb and other trace elements between labile fractions. Evaluation of the data with an isotope-isotope diagram (Figure 4.10) demonstrated that the Pb isotopes within the SEP of all three sediments represented a mix between the two endmembers: granites and basalts. This result combined with the exclusion of anthropogenic sources of Pb, suggests As within the sediment is likely of geogenic origin. Despite only having data for both Pb isotope and As content available for F3, F4 and F6, a good relationship between $^{206}Pb/^{204}Pb$ and As/Pb is apparent, with a clear mixing line evident (Figure 4.11b). Considering the As content of each sample, for both Loire River sediments there is a linear relationship evident between Pb isotopic ratio and the As content of the sample. However F3 for the Allier-Apremont sediment the $^{206}Pb/^{204}Pb$ isotopic ratio lies off the expected mixing line, indicating a contribution other than expected from the mixing of basalts and granites. The observed As/Pb ratio may be the result of the high labile Pb concentration found within the Allier-Apremont sediment (Table 4.2) being largely contained within the As-rich F3 and F4. The obtained $^{206}Pb/^{204}Pb$ isotopic ratios for the Allier-Apremont sediment indicate this endmember is likely to be Fe-oxide (Figure 4.11). Observation of this shift in relationship from the basalt-granite mix is more pronounced due to the increased Fe content of the Allier-Apremont sediment (Refer Chapter 3).

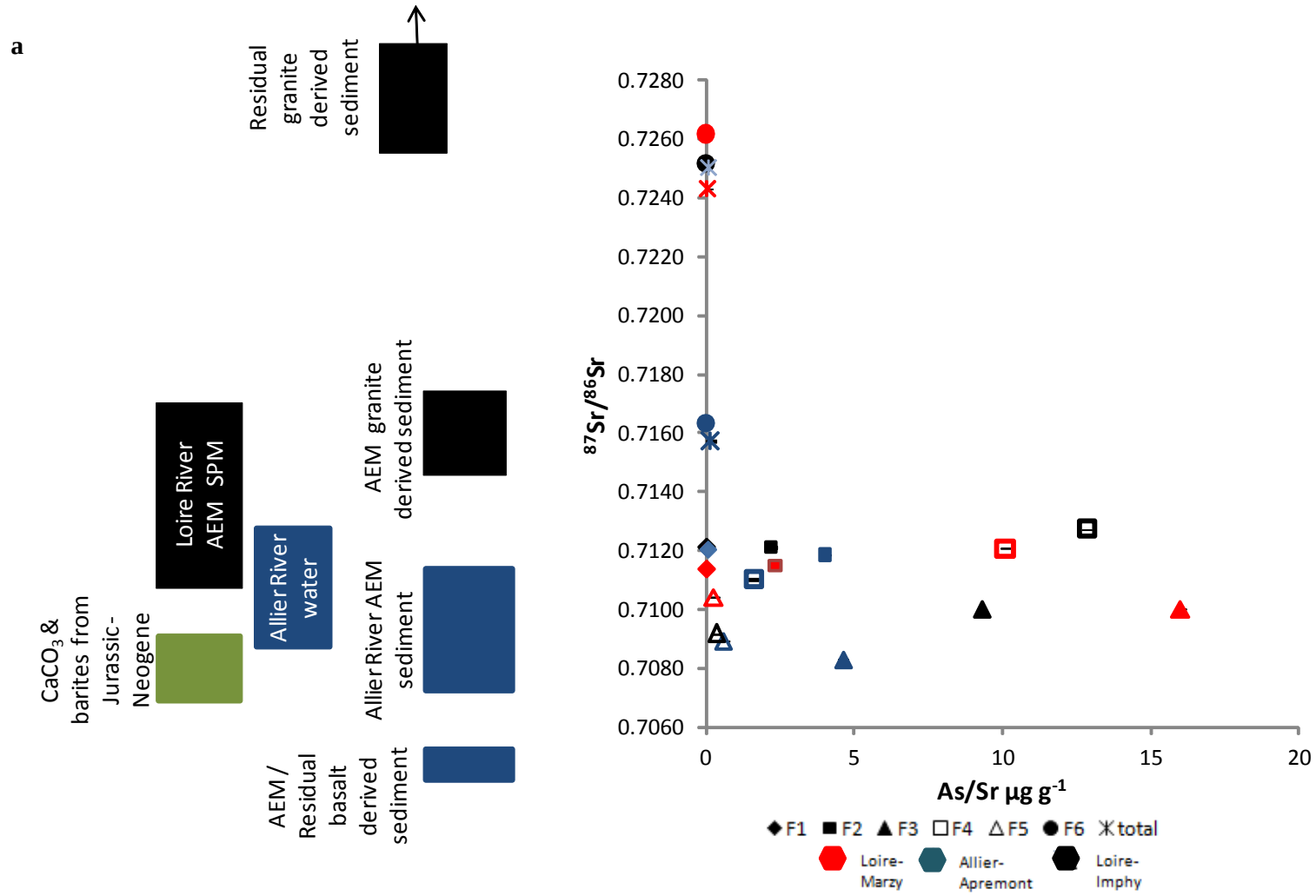

Figure 4.11 **Sediment $^{87}Sr/^{86}Sr$ (a) and $^{206}Pb/^{204}Pb$ (b) ratios represented as a function of As/Sr and As/Pb ratios respectively.**
Red colour represents Loire-Marzy, black Loire-Imphy and blue Allier-Apremont samples. Fields for previously reported sediment and rock digests from the Loire and Allier Rivers have also been added (Négrel et al., 2004; Négrel and Roy, 2002).

b

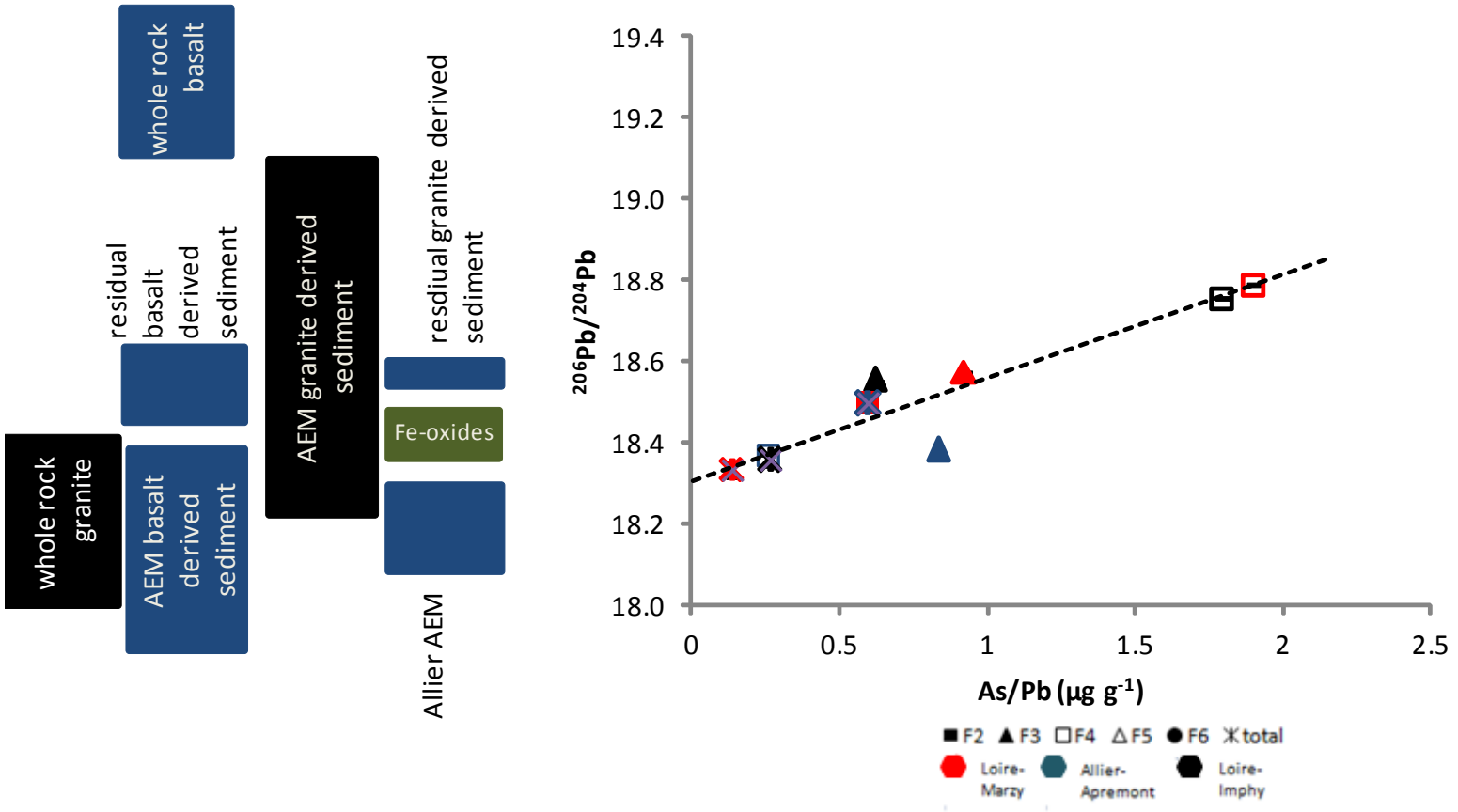

Figure 4.11(cont) **b) Sediment $^{206}Pb/^{204}Pb$ (b) ratios represented as a function of As/Pb ratios.**

Red colour represents Loire-Marzy, black Loire-Imphy and blue Allier-Apremont samples. The dashed line in b) represents the mixing line. Fields for previously reported sediment and rock digests from the Loire and Allier Rivers have also been added (Négrel et al., 2004; Négrel and Roy, 2002)

4.5.4 Post-Incubation changes in isotopic composition in aqueous and solid phases

The lack of any significant changes in both Sr and Pb concentration during the aerobic/anaerobic incubations of the Allier-Apremont sediment (Table 4.7) would suggest that little activity was taking place within the sediment. Although isotopic ratios for both Sr and Pb were only measured at two time intervals (day 2 and day 14), the resulting isotopic ratios make it clear that varied levels of isotopic transformations/exchange are occurring within the sediment.

4.5.5 Anaerobic Incubations

Over time the $^{87}Sr/^{86}Sr$ isotopic ratio increases in both incubations of the Allier-Apremont sediment, with the resulting ratio higher in aerobic incubation (Figure 4.6). Clearly the processes occurring within the sediment under both these conditions are producing varied, yet significant changes in the $^{87}Sr/^{86}Sr$ isotopic ratio of the dissolved phase. Review of concentration data for both the aqueous and solid phase indicates that Sr has been removed from the experimental matrix. An increase in the dissolved phase $^{87}Sr/^{86}Sr$ isotopic ratio suggests there is a dynamic exchange of Sr between the aqueous and solid phase during the incubation, where the loss of lower ratio $^{87}Sr/^{86}Sr$ from solution, or release of Sr from a relatively higher $^{87}Sr/^{86}Sr$ phase is occurring. Release of sediment-held porewater, and easily exchangeable Sr, assumed to have a $^{87}Sr/^{86}Sr$ close to that of the river-water at Allier-Apremont (0.71210) could also account for the increase in dissolved $^{87}Sr/^{86}Sr$ ratio, however the observed ratios do increase beyond that expected from porewater release alone. Despite the differences in behaviour resulting from the environmental conditions, the increased Sr ratios observed from both conditions does not identify the likely phase reacting under the varying the redox environments. Therefore there appears to be limited application of such analysis to the further understanding of processes occurring during incubations.

Post incubation total digests of the sediment observe an increase in Sr content of the sediment, suggesting incorporation of Sr from within the experimental matrix. The corresponding decrease in $^{87}Sr/^{86}Sr$ isotopic ratio suggests that Sr with a lower ratio has been added to the solid phase (Table 4.7). As isotopic analysis gives an average measurement of the ratios present in the dissolved phase, it is possible that Sr has been released in minor

quantities, either into the aqueous phase or to be later readsorbed by the labile fractions. Isotopic exchange within the labile phases may have also occurred within the sediment, where lower ratio Sr may be released and then sorbed by a different fraction. Because we have only measured the dissolved phase, and the bulk sediment, we are unable to note any changes in the partitioning that may confirm this movement.

Lead isotopes showed varied relationship with incubation. While the $^{206}Pb/^{204}Pb$ isotopic ratio decreased in both anaerobic and aerobic incubations, the decrease was the same under both conditions (Table 4.7). The $^{207}Pb/^{206}Pb$ isotopic ratio does show altered behaviour, with an increase observed during the aerobic incubation, and a slight decrease during anaerobic incubation (Figure 4.6). While it appears that the anaerobic release of As is not matched by a characteristic change in either $^{206}Pb/^{204}Pb$ or $^{207}Pb/^{206}Pb$ isotopic ratio of the aqueous phase, the altered ratio observed in the $^{207}Pb/^{206}Pb$ aerobic incubation is indication that the processes of Pb release/sorption are subject to environmental conditions. There are a number of possible mechanisms by which changes in isotopic composition of the sediment may be changing, including anaerobic processes equilibrating the Pb isotopic exchange within the sediment, resulting in the stable ratio observed in the aqueous phase.

While the aqueous phase showed similar behaviours for Pb isotopic ratios, the total digests reveal differences in behaviour. As concentration data (Table 4.7) shows there has been a loss of Pb from both sediments, the obtained ratios for the total digest are difficult to interpret with the available information. The anaerobic sediment $^{206}Pb/^{204}Pb$ isotopic ratio has increased, reflecting the loss of lower ratio Pb from the sediment. However this information cannot identify an independent fraction as releasing Pb, as all F3, F4 and F6 have lower ratios, and a mix of any of them could result in the observed ratios. Because the aerobic sediment digest was within the range of the original sediment digest despite the lower Pb concentration, the loss of Pb must be from across all fractions, suggesting one single phase is not responsible for the release of Pb during incubation.

4.5.6 pH_{stat} Incubations

While the anaerobic incubations were conducted using river water, the pH_{stat} leaches were conducted using $NaNO_3$, removing the complication of observing Sr and Pb already in solution. An increase in pH from 7.5 to 10 results in a decrease in $^{87}Sr/^{86}Sr$ isotopic ratio in the aqueous

phase (Figure 4.12a), suggesting that release of Sr from the labile fractions has occurred. This is confirmed by the digest of the bulk sediment following the incubation, with a corresponding increase in the $^{87}Sr/^{86}Sr$ isotopic ratio. The significant variation observed in the total digest of the bulk sediment indicates that exposure to different pH conditions can affect the $^{87}Sr/^{86}Sr$ isotopic ratio of sediment.

An increase in pH was seen to increase the $^{206}Pb/^{204}Pb$, $^{207}Pb/^{204}Pb$ and $^{208}Pb/^{204}Pb$ isotopic ratios and decrease the concentration of Pb within the dissolved phase (Figure 4.12b, Table 4.7), suggesting that alteration of pH releases Pb from relatively high $^{206}Pb/^{204}Pb$, $^{207}Pb/^{204}Pb$ and $^{208}Pb/^{204}Pb$ ratio sources respectively. As pH changes are known to affect adsorption and desorption processes, it is the more labile fractions that are likely to be affected by the changing conditions. Possible contributing mineral phases are not able to be identified, as the mineral fractions of the SEP all gave lower ratios than the dissolved phases (Table 4.7). The increase in observed Pb isotope ratio suggests a release of Pb with a higher Pb isotope ratio. Evaluation of the SEP fractions obtained indicates that the likely phase release under alteration of pH is the surface adsorbed fractions (F2). This indicates the importance of the exchangeable Pb present in sediments undergoing pH induced desorption. However, the increase in ratio observed for pH 10 relative to pH 3 suggests that at lower pH, in addition to removal of adsorbed Pb, a contribution from the mineral phases is also possible.

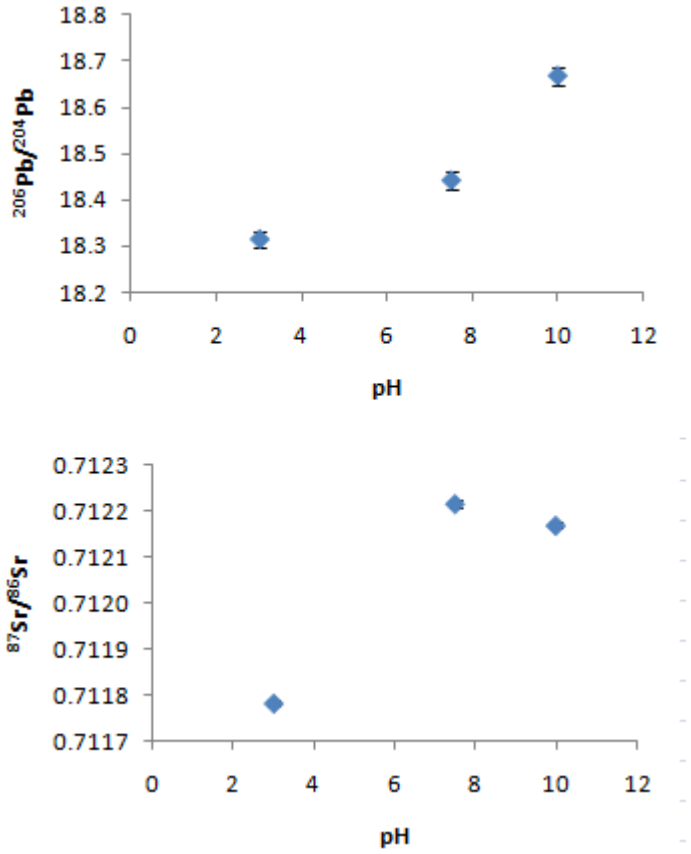

Figure 4.12 **Relationship between $^{206}Pb/^{204}Pb$ (a) and $^{87}Sr/^{86}Sr$ (b) and pH in the aqueous phase of pH incubations.** Error lines represent analytical error on isotopic measurements, and where not visible are within the icon.

4.6 Conclusions

The object of this study was to investigate the combination sequential extraction and isotopic analysis as a tool to trace the origin of As within sediments. The principal findings are briefly summarized below:

- The application of a SEP to sediments from the Loire and Allier Rivers (France) indicates that there is considerable difference in the partitioning of As within the sediments compared to both Sr and Pb. Despite this, correlations between both As/Sr and As/Pb within each fraction were found, allowing the determination of isotopic composition.

- Variation of the obtained Sr isotope ratios reflects the mixing of different sources of Sr within the sediment. Exchangeable Sr was in equilibrium with the river water at two of the sampling sites, however mixing zone dynamics and possible other river inputs prevented equilibration between exchangeable Sr and river water at the Loire-Marzy site.

- A Sr mixing diagram indicating more than two endmembers were required to describe the source of Sr. The obtained $^{87}Sr/^{86}Sr$ isotope ratios for the residual fractions of the sediments suggest both that there is preferential removal of lower $^{87}Sr/^{86}Sr$ isotope ratios during weathering, and that factors other than the attack of the residual phase are influencing the composition of labile phases.

- $^{87}Sr/^{86}Sr$ isotope ratios were able to show that the amorphous Fe minerals targeted in the F3 fraction of the SEP were formed upstream, likely in waters immediately draining the Massif Central. The higher $^{87}Sr/^{86}Sr$ ratios obtained for F4, in closer agreement with the dissolved phase at the point of sampling, suggest that the process of formation has occurred downstream from that of F3.

- Variable Pb isotopic ratios obtained for the SEP indicate the presence of different reservoirs of Pb within the sediment, likely to be granites and basalts, with the composition affected by weathering processes.

- Anthropogenic Pb was not found to be significant within the sediments by comparison of $^{208}Pb/^{204}Pb$ vs. $^{206}Pb/^{204}Pb$ to known anthropogenic Pb domains, and by the lack of Pb associated with carbonates in the Allier-Apremont sediment.

- While $^{87}Sr/^{86}Sr$ isotopic ratios were unable to indicate the sediment phase contributing to release during anaerobic incubations, exposure to different pH conditions was capable of affecting both the $^{87}Sr/^{86}Sr$ and Pb isotopic ratios, indicating the role of the exchangeable fractions in the adsorption/desorption processes. However the role of individual fractions was unable to be determined.

The presence of multiple sources of both Pb and Sr in sediments resulted in difficulty in resolving all the information obtained. However, this study provides a first order basis on which to better understand the application of isotopic analysis in order to determine the mineralogical origins of sediments. The combination of isotopic analysis and SEP was able to provide information on the nature of both Pb and Sr within the sediments, with important

implications for understanding the mobility of As within the studied systems. Comparison of labile $^{87}Sr/^{86}Sr$ ratios to the reducible fractions showed that the formation of the more crystalline minerals was occurring downstream than the more amorphous minerals, indicating the occurrence of the cyclic redox conditions required for ferrihydrite crystallisation and the likely release of surface bound As during the transformation. The degree to which this mineral transformation is taking place could have important implications for the transport of As, given the importance of reducible As within the sediments. Use of Pb isotopes was also able to provide information on the likely anthropogenic origin of Pb within the rivers and therefore other contaminants including As. Future research should continue to identify the Sr and Pb isotopic ratios of sediments and waters in a wider range of aquatic environments, over a longer seasonal period, in order to advance understanding of the interchange occurring between phases, and the role of physicochemical changes on Sr and Pb isotopic composition.

4.7 References

Aberg G. The use of natural strontium isotopes as tracers in environmental studies. Water, Air, & Soil Pollution 1995; 79: 309-322.

Aggett J, O'Brien G. Detailed Model for the Mobility of Arsenic in Lacustrine Sediments Based on Measurements in Lake Ohakuri. Environmental Science & Technology 1985; 19: 231-238.

Ahmann D, Krumholz LR, Hemond HF, Lovley DR, Morel FMM. Microbial mobilization of arsenic from sediments of the Aberjona Watershed. Environmental Science & Technology 1997; 31: 2923-2930.

Anawar H, Mihaljevic M, Garcia-Sanchez A, Akai J, Moyano A. Investigation of Sequential Chemical Extraction of Arsenic from Sediments: Variations in Sample Treatment and Extractant. Soil & sediment contamination 2010; 19: 133-141.

Andersson PS, Wasserburg GJ, Ingri J, Stordal MC. Strontium, dissolved and particulate loads in fresh and brackish waters: The Baltic Sea and Mississippi Delta. Earth and Planetary Science Letters 1994; 124: 195-210.

Ayuso RA, Foley NK. Anthropogenic and natural lead isotopes in Fe-hydroxides and Fe-sulphates in a watershed associated with arsenic-enriched groundwater, Maine, USA. Geochemistry-Exploration Environment Analysis 2008; 8: 77-89.

Backstrom M, Bohlin H, Karlsson S, Holm NG. Element (Ag, Cd, Cu, Pb, Sb, Tl and Zn), element ratio and lead isotope profiles in a sediment affected by a mining operation episode during the late 19th century. Water Air and Soil Pollution 2006; 177: 285-311.

Bacon J, Davidson CM. Is there a future for sequential chemical extraction? The Analyst 2008; 133: 25-46.

Bacon JR, Farmer JG, Dunn SM, Graham MC, Vinogradoff SI. Sequential extraction combined with isotope analysis as a tool for the investigation of lead mobilisation in soils: Application to organic-rich soils in an upland catchment in Scotland. Environmental Pollution 2006; 141: 469-481.

Bacon JR, Hewitt IJ. Heavy metals deposited from the atmosphere on upland Scottish soils: Chemical and lead isotope studies of the association of metals with soil components. Geochimica et Cosmochimica Acta 2005; 69: 19-33.

Barbier J, Chery L. Relationships between natural geochemical background and high heavy metal levels in waters (Sb, As, Ba, Cr, Ni, Pb, Zn). Application to Auvergne and Limousin, and validation. BRGM report R 39544, Orleans, 1997, pp. 1-51.

Bauer M, Blodau C. Mobilization of arsenic by dissolved organic matter from iron oxides, soils and sediments. Science of the Total Environment 2006; 354: 179-190.

Blute NK, Jay JA, Swartz CH, Brabander DJ, Hemond HF. Aqueous and solid phase arsenic speciation in the sediments of a contaminated wetland and riverbed. Applied Geochemistry 2009; 24: 346-358.

Bouchez J, Lajeunesse E, Gaillardet J, France-Lanord C, Dutra-Maia P, Maurice L. Turbulent mixing in the Amazon River: The isotopic memory of confluences. Earth and Planetary Science Letters 2010; 290: 37-43.

Buschmann J, Kappeler A, Lindauer U, Kistler D, Berg M, Sigg L. Arsenite and arsenate binding to dissolved humic acids: Influence of pH, type of humic acid, and aluminum. Environmental Science & Technology 2006; 40: 6015-6020.

Cances B, Juillot F, Morin G, Laperche V, Alvarez L, Proux O, et al. XAS evidence of As(V) association with iron oxyhydroxides in a contaminated soil at a former arsenical pesticide processing plant. Environmental Science & Technology 2005; 39: 9398-9405.

Casiot C, Ujevic M, Munoz M, Seidel JL, Elbaz-Poulichet F. Antimony and arsenic mobility in a creek draining an antimony mine abandoned 85 years ago (upper Orb basin, France). Applied Geochemistry 2007; 22: 788-798.

Chaillou G, Schafer J, Anschutz P, Lavaux G, Blanc G. The behaviour of arsenic in muddy sediments of The Bay of Biscay (France). Geochimica et Cosmochimica Acta 2003; 67: 2993-3003.

Charlet L, Polya DA. Arsenic in Shallow, Reducing Groundwaters in Southern Asia: An Environmental Health Disaster. Elements 2006; 2: 91-96.

Chatain V, Bayard R, Sanchez F, Moszkowicz P, Gourdon R. Effect of indigenous bacterial activity on arsenic mobilization under anaerobic conditions. Environment International 2005; 31: 221-226.

Chow SS, Taillefert M. Effect of arsenic concentration on microbial iron reduction and arsenic speciation in an iron-rich freshwater sediment. Geochimica et Cosmochimica Acta 2009; 73: 6008-6021.

Cicchella D, De Vivo B, Lima A, Albanese S, R.A.R M, R.R P. Heavy metal pollution and Pb isotopes in urban soils of Napoli, Italy. Geochemistry: Exploration, Environment, Analysis 2008; 8: 102-112.

Cocherie A, Robert M. Direct measurement of lead isotope ratios in low concentration environmental samples by MC-ICP-MS and multi-ion counting. Chemical Geology 2007; 243: 90-104.

Dawson JJC, Tetzlaff D, Carey A-M, Raab A, Soulsby C, Killham K, et al. Characterizing Pb Mobilization from Upland Soils to Streams Using 206Pb/207Pb Isotopic Ratios. Environmental Science & Technology 2010; 44: 243-249.

Deniel C, Pin C. Single-stage method for the simultaneous isolation of lead and strontium from silicate samples for isotopic measurements. Analytica Chimica Acta 2001; 426: 95-103.

Devesa-Rey R, Paradelo R, Diaz-Fierros F, Barral MT. Fractionation and bioavailability of arsenic in the bed sediments of the Anllons River (NW Spain). Water Air and Soil Pollution 2008; 195: 189-199.

Dowling CB, Poreda RJ, Basu AR, Peters SL, Aggarwal PK. Geochemical study of arsenic release mechanisms in the Bengal Basin groundwater. Water Resources Research 2002; 38: 18.

Downes H, Shaw A, Williamson BJ, Thirlwall MF. Sr, Nd, Pb in Hercynian granodiorites and monzogranites, Massif Central, France. Chemical Geology 1997; 136: 99-122.

Einax JW, Nischwitz V. Inert sampling and sample preparation - the influence of oxygen on heavy metal mobility in river sediments. Fresenius Journal of Analytical Chemistry 2001; 371: 643-651.

Emmanuel S, Erel Y. Implications from concentrations and isotopic data for Pb partitioning processes in soils. Geochimica et Cosmochimica Acta 2002; 66: 2517-2527.

Erel Y, Torrent J. Contribution of Saharan dust to Mediterranean soils assessed by sequential extraction and Pb and Sr isotopes. Chemical Geology 2010; 275: 19-25.

Faure G. Principles of Isotope Geology. Chichester, UK: Wiley, 1986.

Gault AG, Polya DA, Charnock JM, Islam FS, Lloyd JR, Chatterjee D. Preliminary EXAFS studies of solid phase speciation of As in a West Bengali sediment. Mineralogical Magazine 2003; 67: 1183-1191.

Gismera MJ, Lacal J, da Silva P, García R, Teresa Sevilla M, Procopio JR. Study of metal fractionation in river sediments. A comparison between kinetic and sequential extraction procedures. Environmental Pollution 2004; 127: 175-182.

Gonzalez Z, Krachler M, Cheburkin A, Shotyk W. Spatial distribution of natural enrichments of arsenic, selenium, and uranium in a minerotrophic peatland, Gola di Lago, Canton Ticino, Switzerland. Environmental Science & Technology 2006; 40: 6568-6574.

Grosbois C, Négrel P, Fouillac C, Grimaud D. Dissolved load of the Loire River: chemical and isotopic characterization. Chemical Geology 2000; 170: 179-201.

Guelke M, von Blanckenburg F, Schoenberg R, Staubwasser M, Stuetzel H. Determining the stable Fe isotope signature of plant-available iron in soils. Chemical Geology 2010; 277: 269-280.

Haque S, Ji JF, Johannesson KH. Evaluating mobilization and transport of arsenic in sediments and groundwaters of Aquia aquifer, Maryland, USA. Journal of Contaminant Hydrology 2008; 99: 68-84.

Hindshaw RS, Reynolds BC, Wiederhold JG, Kretzschmar R, Bourdon B. Calcium isotopes in a proglacial weathering environment: Damma glacier, Switzerland. Geochimica et Cosmochimica Acta 2011; 75: 106-118.

Hudson-Edwards KA, Houghton SL, Osborn A. Extraction and analysis of arsenic in soils and sediments. TrAC Trends in Analytical Chemistry 2004; 23: 745-752.

Islam FS, Gault AG, Boothman C, Polya DA, Charnock JM, Chatterjee D, et al. Role of metal-reducing bacteria in arsenic release from Bengal delta sediments. Nature 2004; 430: 68-71.

Linge K, Oldham C. Arsenic remobilization in a shallow lake: The role of sediment resuspension. Journal of Environmental Quality 2002; 31: 822-828.

Linge K, Oldham C. Control mechanisms for dissolved phosphorus and arsenic in a shallow lake. Applied Geochemistry 2004; 19: 1377-1389.

Luck J-M, Ben Othman D. Geochemistry and water dynamics: II. Trace metals and Pb-Sr isotopes as tracers of water movements and erosion processes. Chemical Geology 1998; 150: 263-282.

Marin B, Valladon M, Polve M, Monaco A. Reproducibility testing of a sequential extraction scheme for the determination of trace metal speciation in a marine reference sediment by inductively coupled plasma-mass spectrometry. Analytica Chimica Acta 1997; 342: 91-112.

Masson M, Schäfer J, Blanc G, Dabrin A, Castelle S, Lavaux G. Behavior of arsenic and antimony in the surface freshwater reaches of a highly turbid estuary, the Gironde Estuary, France. Applied Geochemistry 2009; 24: 1747-1756.

Masson M, Schafer J, Blanc G, Pierre A. Seasonal variations and annual fluxes of arsenic in the Garonne, Dordogne and Isle Rivers, France. Science of the Total Environment 2007; 373: 196-207.

McArthur JM, Banerjee DM, Hudson-Edwards KA, Mishra R, Purohit R, Ravenscroft P, et al. Natural organic matter in sedimentary basins and its relation to arsenic in anoxic ground water: the example of West Bengal and its worldwide implications. Applied Geochemistry 2004; 19: 1255-1293.

McLaren S, Kim N. Evidence for a seasonal fluctuation of arsenic in New Zealands longest river and the effect of treatment on concentrations in drinking water. Environmental Pollution 1995; 90: 67-73.

Miao S, DeLaune R, Jugsujinda A. Influence of sediment redox conditions on release/solubility of metals and nutrients in a Louisiana Mississippi River deltaic plain freshwater lake. The Science of The Total Environment 2006; 371: 334-343.

Michard-Vitrac A, Albarede F, Allegre CJ. Lead isotopic composition of Hercynian granitic K-feldspars constrains continental genesis. Nature 1981; 291: 460-464.

Miller JN, Miller JC. Statistic and Chemometrics for Analytical Chemistry. Harlow, England: Pearson Education Limited, 2005.

Millot R, Allegre CJ, Gaillardet J, Roy S. Lead isotopic systematics of major river sediments: a new estimate of the Pb isotopic composition of the Upper Continental Crust. Chemical Geology 2004; 203: 75-90.

Monna F, Lancelot J, Croudace I, Cundy A, Lewis J. Pb isotopic composition of airborne particulate material from France and the Southern United Kingdom: Implications for Pb pollution sources in urban areas. Environmental Science & Technology 1997; 31: 2277 –2286.

Morillo J, Usero J, Rojas R. Fractionation of metals and As in sediments from a biosphere reserve (Odiel salt marshes) affected by acidic mine drainage. Environmental Monitoring and Assessment 2008; 139: 329-337.

Morin G, Lecocq D, Juillot F, Calas G, Ildefonse P, Belin S, et al. EXAFS evidence for sorbed arsenic-(V) and pharmacosiderite in a soil overlying the Echassieres geochemical anomaly, Allier, France. Bulletin de la Societe Geologique de France 2002; 173: 281-291.

Mucci A, Richard LF, Lucotte M, Guignard C. The differential geochemical behavior of arsenic and phosphorus in the water column and sediments of the Saguenay Fjord estuary, Canada. Aquatic Geochemistry 2000; 6: 293-324.

Munksgaard NC, Parry DL. Metals, arsenic and lead isotopes in near-pristine estuarine and marine coastal sediments from northern Australia. Marine and Freshwater Research 2002; 53: 719-729.

Négrel P. Multi-element chemistry of Loire estuary sediments: Anthropogenic vs. natural sources. Estuarine Coastal and Shelf Science 1997; 44: 395-410.

Négrel P, Fouillac C, Brach M. Occurrence of mineral water springs in the stream channel of the Allier River (Massif Central, France): chemical and Sr isotope constraints. Journal of Hydrology 1997; 203: 143-153.

Négrel P, Grosbois C. Changes in chemical and 87Sr/86Sr signature distribution patterns of suspended matter and bed sediments in the upper Loire river basin (France). Chemical Geology 1999; 156: 231-249.

Négrel P, Grosbois C, Kloppmann W. The labile fraction of suspended matter in the Loire River (France): multi-element chemistry and isotopic (Rb-Sr and C-O) systematics. Chemical Geology 2000; 166: 271-285.

Négrel P, Guerrot C, Millot R. Chemical and strontium isotope characterization of rainwater in France: influence of sources and hydrogeochemical implications. Isotopes in Environmental and Health Studies 2007; 43: 179-196.

Négrel P, Kloppman W, Garcin M, Giot D. Strontium isotopic record of signatures of Holocene fluvial sediments in the Loire valley, France. Hydrology and Earth System Sciences 2002; 6: 849-858.

Négrel P, Kloppmann W, Garcin M, Giot D. Lead isotope signatures of Holocene fluvial sediments from the Loire River valley. Applied Geochemistry 2004; 19: 957-972.

Négrel P, Millot R, Roy S, Guerrot C, Pauwels H. Lead isotopes in groundwater as an indicator of water-rock interaction (Masheshwaram catchment, Andhra Pradesh, India). Chemical Geology 2010; 274: 136-148.

Négrel P, Petelet-Giraud E, Barbier J, Gautier E. Surface water-groundwater interactions in an alluvial plain: Chemical and isotopic systematics. Journal of Hydrology 2003; 277: 248-267.

Négrel P, Roy S. Investigating the sources of the labile fraction in sediments from silicate-drained rocks using trace elements, and strontium and lead isotopes. Science of the Total Environment 2002; 298: 163-181.

Nicholas DR, Ramamoorthy S, Palace V, Spring S, Moore JN, Rosenzweig RF. Biogeochemical transformations of arsenic in circumneutral freshwater sediments. Biodegradation 2003; 14: 123-137.

Nickson RT, McArthur JM, Ravenscroft P, Burgess WGA, K.M. Mechanism of arsenic release to groundwater, Bangladesh and West Bengal. Applied Geochemistry 2000; 15: 403-413.

Pagnanelli F, Moscardini E, Giuliano V, Toro L. Sequential extraction of heavy metals in river sediments of an abandoned pyrite mining area: pollution detection and affinity series. Environmental Pollution 2004; 132: 189-201.

Pedersen HD, Postma D, Jakobsen R. Release of arsenic associated with the reduction and transformation of iron oxides. Geochimica et Cosmochimica Acta 2006; 70: 4116-4129.

Pedersen HD, Postma D, Jakobsen R, Larsen O. Fast transformation of iron oxyhydroxides by the catalytic action of aqueous Fe(II). Geochimica et Cosmochimica Acta 2005; 69: 3967-3977.

Polizzotto ML, Kocar BD, Benner SG, Sampson M, Fendorf S. Near-surface wetland sediments as a source of arsenic release to ground water in Asia. Nature 2008; 454: 505-8.

Postma D, Jessen S, Hue NTM, Duc MT, Koch CB, Viet PH, et al. Mobilization of arsenic and iron from Red River floodplain sediments, Vietnam. Geochimica et Cosmochimica Acta 2010; 74: 3367-3381.

Prohaska T, Wenzel WW, Stingeder G. ICP-MS-based tracing of metal sources and mobility in a soil depth profile via the isotopic variation of Sr and Pb. International Journal of Mass Spectrometry 2005; 242: 243-250.

Ravenscroft P, Richards K, Brammer H. Arsenic Pollution: A Global Synthesis. Chichester, UK: Wiley-Blackwell, 2009.

Roussel C, Neel C, Bril H. Minerals controlling arsenic and lead solubility in an abandoned gold mine tailings. Science of the Total Environment 2000; 263: 209-219.

Rowland HAL, Gault AG, Charnock JM, Polya DA. Preservation and XANES determination of the oxidation state of solid-phase arsenic in shallow sedimentary aquifers in Bengal and Cambodia. Mineralogical Magazine 2005; 69: 825-839.

Seddique AA, Masuda H, Mitamura M, Shinoda K, Yamanaka T, Itai T, et al. Arsenic Release from Biotite into a Holocene Groundwater Aquifer in Bangladesh. Applied Geochemistry 2008; 23: 2236-2248.

Segura R, Arancibia V, Zúñiga MC, Pastén P. Distribution of copper, zinc, lead and cadmium concentrations in stream sediments from the Mapocho River in Santiago, Chile. Journal of Geochemical Exploration 2006; 91: 71-80.

Signes-Pastor A, Burlo F, Mitra K, Carbonell-Barrachina AA. Arsenic biogeochemistry as affected by phosphorus fertilizer addition, redox potential and pH in a west Bengal (India) soil. Geoderma 2007; 137: 504-510.

Smedley PL, Kinniburgh DG. A review of the source, behaviour and distribution of arsenic in natural waters. Applied Geochemistry 2002; 17: 517-568.

Smith JP, Bullen TD, Brabander DJ, Olsen CR. Strontium isotope record of seasonal scale variations in sediment sources and accumulation in low-energy, subtidal areas of the lower Hudson River estuary. Chemical Geology 2009; 264: 375-384.

Solaiman ARM, Meharg AA, Gault AG, Charnock JM. Arsenic mobilization from iron oxyhydroxides is regulated by organic matter carbon to nitrogen (C:N) ratio. Environment International 2009; 35: 480-484.

Steinmann M, Stille P. Rare earth element behavior and Pb, Sr, Nd isotope systematics in a heavy metal contaminated soil. Applied Geochemistry 1997; 12: 607-623.

Tessier A, Campbell PGC, Bisson M. Sequential Extraction Procedure for the Speciation of Particulate Trace-Metals. Analytical Chemistry 1979; 51: 844-851.

Teutsch N, Erel Y, Halicz L, Banin A. Distribution of natural and anthropogenic lead in Mediterranean soils. Geochimica et Cosmochimica Acta 2001; 65: 2853-2864.

van Geen A, Rose J, Thoral S, Garner JM, Zheng Y, Bottero JY. Decoupling of As and Fe release to Bangladesh groundwater under reducing conditions. Part II: Evidence from sediment incubations. Geochimica et Cosmochimica Acta 2004; 68: 3475-3486.

Vasile G, Tanase I, Dinu C. The Influence of the Air-drying Pretreatment of Sediment Samples for Metallic Element Mobilities. Analytical letters 2010; 43: 1199-1206.

Warren LA, Haack EA. Biogeochemical controls on metal behaviour in freshwater environments. Earth-Science Reviews 2001; 54: 261-320.

Wenzel WW, Kirchbaumer N, Prohaska T, Stingeder G, Lombi E, Adriano DC. Arsenic fractionation in soils using an improved sequential extraction procedure. Analytica Chimica Acta 2001; 436: 309-323.

Wiederhold J, Teutsch N, Kraemer S, Halliday A, Kretzschmar R. Iron isotope fractionation in oxic soils by mineral weathering and podzolization. Geochimica et Cosmochimica Acta 2007; 71: 5821-5833.

Winkel L, Berg M, Amini M, Hug SJ, Annette Johnson C. Predicting groundwater arsenic contamination in Southeast Asia from surface parameters. Nature Geosci 2008; 1: 536-542.

Wu W, Xu S, Yang J, Yin H, Tao X. Sr fluxes and isotopic compositions in the headwaters of the Yangtze River, Tongtian River and Jinsha River originating from the Qinghai-Tibet Plateau. Chemical Geology 2009; 260: 63-72.

Xu Y, Marcantonio F. Speciation of strontium in particulates and sediments from the Mississippi River mixing zone. Geochimica et Cosmochimica Acta 2004; 68: 2649-2657.

Yokoo Y, Nakano T, Nishikawa M, Quan H. Mineralogical variation of Sr-Nd isotopic and elemental compositions in loess and desert sand from the central Loess Plateau in China as a provenance tracer of wet and dry deposition in the northwestern Pacific. Chemical geology 2004; 204: 45-62.

Chapter 5

Solid-phase arsenic distribution in ombrotrophic peat: Evidence for the variability of post-depositional mobility

5.1 Introduction

Elevated concentrations of arsenic (As) in water, sediments and soils pose both a human health risk and an environmental hazard on a global scale (Mandal and Suzuki, 2002; Smedley and Kinniburgh, 2002). Increased global pressure on drinking water reservoirs has highlighted the problem of elevated As concentrations in streams and rivers arising from both geogenic and anthropogenic sources, and consequently the lack of understanding of its biogeochemical cycling in a range of environments. In aqueous environments, As can exist as a range of species, largely dependent on redox state and pH (Bissen and Frimmel, 2003). Under oxic conditions, the inorganic arsenate ion ($H_2AsO_4^-$ and $HAsO_4^{2-}$) dominates, changing to the reduced species arsenite ($H_3AsO_3^0$ and $H_2AsO_3^-$) under oxygen depleted reducing conditions through the action of either chemical or microbial reduction (Smedley and Kinniburgh, 2002). A range of other species have also been recorded including thiols and methylated species (Andreae, 1979; Huang and Matzner, 2007) with their presence largely dictated by the localised environmental and biological conditions. The complexation and adsorptive behaviour of different species once mobilised has been the focus of a significant body of laboratory based studies, with the mobility and toxicity of As dependent on the speciation (Cullen and Reimer, 1989; De Vitre et al., 1991; Korte and Fernando, 1991). Inorganic As is generally thought to be more toxic and less mobile than the organic species (Blodau et al., 2008; Mandal and Suzuki, 2002), with the adsorptive preferences of inorganic As(III) and As(V) variable due to factors including pH, Eh, nature of binding surface and competition for binding sites with other ions (Dixit and Hering, 2003; Korte and Fernando, 1991). Because of its toxicity, there is a need to understand the distribution and cycling of As in the natural environment.

As an organic rich material that experiences a range of redox conditions due to its close relationship to the water table, peats can play an important role in the storage and cycling and trace elements in the natural environment (Steinmann and Shotyk, 1997; Tipping et al., 2003). Ombrotrophic peats are distinct from other peats as they receive their inputs exclusively from the atmosphere (rainwater fed). Release of industrial plumes containing large quantities of metals and metalloids into the atmosphere has resulted in widespread contamination of the peats of Northern England. Arsenic found in upland ombrotrophic peat environments has been linked to historic industrial activity, including mining and smelting (Cloy et al., 2009). Use of isotopic dating on the immobile metal lead (Pb) found within the peat has enabled the construction of records of historic contamination and distinguish between the sources of contamination (Rothwell et al., 2010).

Once in the environment, both naturally occurring and anthropogenically sourced As are affected by the same biogeochemical processes. However, despite an increasing awareness of organic-rich soils as an important store of As, there has been little investigation of the biogeochemical processes affecting its storage and mobilisation in organic-rich systems (Gonzalez et al., 2006). Within sediments of low organic composition, As has a strong affinity for iron (Fe)- (oxy) hydroxide minerals, as well as aluminium (Al) and manganese (Mn) hydroxides (Dixit and Hering, 2003; La Force et al., 2000). Mobilisation of As has therefore been closely linked to the redox cycles of Fe (Ahmann et al., 1997; Masscheleyn et al., 1991; Smedley and Kinniburgh, 2002), although minor roles for surface bound and organic matter (OM)-bound As have also been established (Jay et al., 2005; Linge and Oldham, 2002). The partitioning of As within the solid phase is of significance as it ultimately affects both the processes which will mobilise As and therefore its long term storage. Despite a paucity of studies on the partitioning of As in ombrotrophic peat, recent partitioning work on minerotrophic peats found a strong role for OM-bound As in the accumulation of As within the solid phase (Gonzalez et al., 2006). This finding indicates that assumptions of partitioning of As need to consider the environmental matrix, and that extrapolation across different sediments may not be appropriate.

Given the ability for As to accumulate in organic-rich systems, there is a requirement to understand both the storage and mobilisation mechanisms of As within peat systems. Mobilisation of As from the solid phase to the aqueous phase is linked to its partitioning within the solid phase. Sequential extractions are one commonly used tool to describe the distribution of an element within the solid phase (Bacon and Davidson, 2008; Hudson-Edwards et al., 2004; Tessier et al., 1979). These procedures utilise a range of chemical extractions that make use of different chemical processes to remove As from the solid phase (Hudson-Edwards et al., 2004; Wenzel et al., 2001). Typically the results of sequential extractions are interpreted in terms of the process that has extracted the As, e.g. reducible, or adsorbed. Surface bound As is considered labile, as simple pH changes can mobilise it through desorption. Other pools of As within the solid phase are less labile, requiring changes in redox state, possibly microbially mediated (Campbell et al., 2006; Islam et al., 2004), before mobilisation can occur. An understanding of the partitioning is therefore required in order to assess the potential As threat to a receiving environment. In addition to the mobilisation of aqueous As, physical processes may also introduce As into stream systems through the action of erosion. Erosion, where the surface of peat is disrupted, vegetation lost and the underlying peat dried and

subsequently introduced to stream systems as particles is a significant problem in UK peatlands (Daniels et al., 2008; Rothwell et al., 2005). The causes of erosion are widespread, relating to both climatic changes and anthropogenic action. Degraded peats may experience creation of new gullies, altering the underlying water tables, and creating a local drawdown effect that can affect redox conditions within the neighbouring peat (Daniels et al., 2008; Rothwell et al., 2009). Erosion therefore has the ability to both introduce As into the aqueous system as particulates, and to also influence the ongoing mobilisation processes occurring within the intact peat.

In addition to the well-known accumulation of As within minerotrophic peat bogs, where organic-rich peat is connected to mineralised groundwaters (Gonzalez et al., 2006; Shotyk et al., 1996; Steinmann and Shotyk, 1997), there is increasing awareness of the dynamic role of OM in the mobilisation of As. Organic matter can play two roles with regards to adsorption processes, acting to both remove As from; and keep As within solution. Organic matter can provide an available surface for As binding, or OM, in form of dissolved organic carbon (DOC) can compete with As for binding sites (Grafe et al., 2002). In solution, OM can form complexes with aqueous As, and influence the stability of As bearing colloids (Buschmann et al., 2006; Redman et al., 2002). As both OM and As are negatively charged within the normal pH and redox (Eh) conditions of natural waters, binding has been observed to occur with assistance of a bridging cation, such as Fe (Redman et al., 2002; Ritter et al., 2006). While the solid phase partitioning of As in organic-rich soils and sediments is not well understood, there is a general agreement in metal distribution work conducted in peat that Pb is associated OM. Lead cations (Pb^{2+}) are thought to strongly bind to OM (Vile et al., 1999), and the profiles of Pb have been used to date contamination in organic-rich sediments (Bacon and Hewitt, 2005; Cloy et al., 2009). Within organic-rich sediments, the storage of As has been linked to both Pb and OM (Cloy et al., 2009; Rothwell et al., 2009). Although the close association of As with Pb, and therefore implied immobility has been found at some sites (Cloy et al., 2009; Rothwell et al., 2010), recent research has observed the release of As from peat, and is thought to be related to the changes in redox brought about by the physical drying and rewetting of peat, linked to the redox cycling of Fe (Blodau et al., 2008; Rothwell et al., 2009; Rothwell et al., 2010). The association of As within the peat therefore has clear implications for the mobility of the stored As.

Calculation of fluvial flux is a useful tool to give an estimate of the amount of As exported from a catchment, but also as a means of gaining insight into the mobilization process occurring

within the solid phase. Recent work by Rothwell et al., (2011) has highlighted that As leaving ombrotrophic peat is to be mainly found in the aqueous phase, rather than transported in particulate form. Although questions still remain over the long term associations of As within the peat, the post-depositional diagenetic remobilisation of As in association with the redox cycle of Fe is well established in lake and wetland sediments (Farmer and Lovell, 1986; Huang and Matzner, 2006; Olivie-Lauquet et al., 2001). In the absence of oxygen, As is found to be released when Fe(oxy)hydroxides are reduced. Mobilised Fe is transported vertically up the profile, where Fe minerals are typically precipitated in the oxic surface layers, resulting in the natural enrichment of As in near surface layers due to the binding affinity of As for Fe (La Force et al., 2000). Recently evidence for the post-depositional mobilisation (PDM) of As has been observed in total concentration profiles of As in ombrotrophic peat (Rothwell et al., 2009; Rothwell et al., 2010). Contrast of single cores obtained at topographically and hydrologically varying sites indicated that PDM was associated with changes in water table caused by erosion and gullying, with the association of As with Pb linked to waterlogged conditions (Rothwell et al., 2010). The link between water table fluctuations and the release of As illustrates the potential for mobilisation in changing environmental conditions. The variability of water table within ombrotrophic catchments is thought to be large- and so release may not be linked to sites with apparent topographical anomalies. As peat covers large areas of the Peak District, the large pool of potentially available As means there is a need to understand whether PDM is an environmental process operating on a large scale in the environment.

The purpose of this study was to determine retention and binding mechanisms of As within ombrotrophic peat, and to identify the environmental processes contributing to the mobilisation of As from ombrotrophic peats.

Given the limitations of extrapolating single core analyses across whole catchments (Rothwell et al., 2007), a specific objective of this work was to determine the solid phase profile of As and other trace elements within multiple cores of peat from upland peat environments. The obtained profiles from within each of the studied subcatchments (Site 30 and site 50, Figure 5.1) were utilised to assess the spatial variability of As contamination within apparently homogeneous microtopography.

Although in the same catchment of Crowden Great Brook, Peak District, UK, Site 30 and Site 50 experience divergent surface conditions, with site 50 surface peat extremely degraded and lacking in vegetation. Because erosion may have a marked effect on the release of material

into receiving environments (Rothwell et al., 2005), the total concentration profiles from both sites will enable the determination of the effect of erosion on As storage within the peat.

Calculation of the total store of As within each catchment was made in order to understand the total potential for As release from upland peat catchments, and to estimate the loss of contaminated material from the eroded site.

To assess the transportation of As from both the eroded and vegetated catchment, both the unfiltered and soluble flux of As was determined using a combination of long term in-situ data, and point-sample collected streamwater As concentrations.

Whilst the localised effect of water table variability/erosion on changes in As association have been previously addressed through total concentration analysis (Rothwell et al., 2010), currently no work has been conducted on the partitioning of As within ombrotrophic peat. The partitioning of As within peat provides information not only on associations with other elements, but also on likely environmental processes able to mobilise the As. To further the understanding of the retention of As within organic rich soils, the solid phase partitioning of As within the peat was determined using a sequential extraction.

5.2 Methods

5.2.1 Site description

The study area, Crowden Great Brook, is located within the Peak District National Park which is part of the southern Pennine uplands, situated between Manchester and Sheffield in the UK (Figure 5.1). The position of the Peak District has resulted in years of atmospheric contamination from historic mining, smelting and industrial activity in neighbouring areas. Concentrations of contaminants such as As, Pb and other trace elements are known to be elevated in the surface peat (Lee and Tallis, 1973; Rothwell et al., 2010). The total catchment area (7 km^2) is drained by a stream flowing from black hill (530 m above ordnance datum (AOD)) into Torside reservoir; part of the Longdendale reservoir series (220 m AOD) (Todman, 2005). At higher altitudes the area is overlain by ombrotrophic peat which covers approximately 70 % of the catchment (Todman, 2005). The dominance of the ombrotrophic peat within the surface soils has resulted in a relatively uniform mean carbon content within the area, ranging from 45 % - 50 % (Rothwell et al., 2009). However, the condition of the ombrotrophic peat is not uniform. While close to the headwaters of the main stream the peat is largely vegetated (Figure 5.1d), further downstream to the west of the river substantial

sections of the peat are in a degraded state, without vegetation, and subject to erosion of surface layers (Figure 5.1d).

Two sampling areas were selected within the Crowden Great Brook catchment to allow for determination of the effect of peat condition in the storage of As within the peat. Site 30 (Ordnance survey (OS) grid 06162 02936) is the sampling location to which the vegetated peat sub-catchment (3 km^2), site 50 (OS grid 05849 00912) the eroded peat sub-catchment (0.5 km^2)(Figure 5.1c). While the underlying geology of the area is dominated by Upper Carboniferous sandstone, shale and mudstone, with kinder grit the dominant series (Gaffney, 2008), a band of marine shale is also present in the vicinity of Site 30.

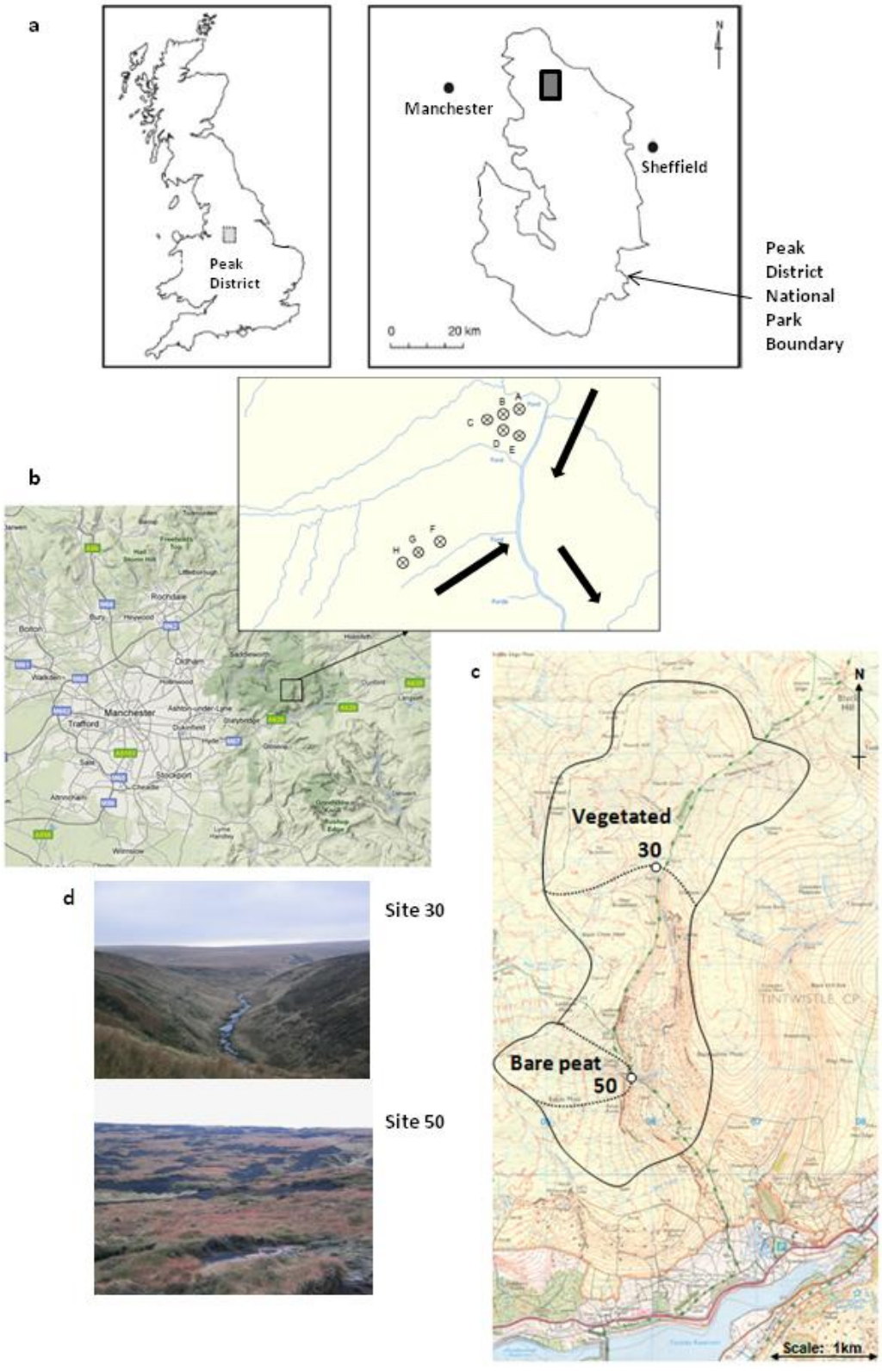

Figure 5.1 **Location map and Crowden Great Brook study area. a) denotes the location of the Peak District relative to major cities, b) marks locations of cores at both sites, with outline and direction of stream flows , c) the black outline illustrates the total catchment and site 30 and 50 subcatchments, d) illustrates the vegetated peat at site 30 and degraded peat at site 50 respectively.** ***Adapted from Rothwell et al., (2009)***

5.2.2 Collection, preparation and analyses of peat samples

In November 2010, a total of eight peat cores (A-H) were collected from the upland peat at Crowden Great Brook, with five cores (A- E) collected from the vegetated peat at Site 30, and three peat cores (F-H) from Site 50. The peat core locations were chosen on a basis of covering a representative surface area of the peat area adjacent to the stream draining each subcatchment (Figure 5.1c). Cores A-E at site 30 were all within a flat vegetated area immediately adjacent to the main stream. The area is elevated from the main stream, and contained by a small contributing stream to the north. All cores were collected within apparently homogeneous microtopography, with no cores taken in close proximity to gullies relating to either stream. At site 50 the three cores represent a cross-section of the surface peat present within the subcatchment. Core F represents the vegetated area within the subcatchment, while core H is from an area that had been assessed visually to have undergone a significant amount of erosion.

At each location cores were taken with a stainless steel peat corer (5 cm diameter, 50 cm length). Due to the consistency of the peat, cores of varied length were obtained from each site, with a standard length of 33 cm obtainable from each core location. In order to obtain enough material for analytical determinations, a number of cores had to be obtained from multiple adjacent cores within one core location. Surface vegetation was carefully removed and each core was sectioned in the field every 3 cm by use of a plastic ruler, resulting in a total of 88 individual samples. Samples were transported in paper sediment bags, each contained within a plastic bag to ensure samples were sealed. Upon returning to the laboratory the peat was stored at 10^{o}C prior to sample handling, which was undertaken within 24 hrs of collection. The peat was carefully divided into two subsamples, one was maintained in its original condition and stored in at 10^{o}C in sealed polypropylene containers. The second subsample was weighed, dried and weighed again to determine the moisture content of each sample. The dried peat was subsequently milled to a fine powder using an agate planetary ball mill (Pulverizette 5, Fritsch, Idar-Oberstein, Germany).

5.2.3 Total concentration determination

The total metal concentrations in the peat were determined by two methods including a total digestion procedure, and by X-Ray Fluorescence (XRF). Total digestions typically incorporate dissolution of residual material using hydrofluoric acid (HF). Use of HF was avoided in this

study due to both the logistical constraints of such a large sample group, and because of difficulties experienced with the determination of concentrations of solutions with high total dissolved solids (Refer Chapter 3 & 4). Because of the high organic content of the peats, an HF digest was also not considered to be essential, with minimal residual silicate material expected.

The total digest method selected used a common microwave digestion protocol for organic-rich soils. A mixture of ultrapure nitric acid (HNO_3) and hydrogen peroxide (H_2O_2) (SpeciFied, Fisher Scientific) was left with 0.3 g peat in a Teflon microwave vessel for 10 minutes to allow for subsidence of any vigorous reactions between the peat and the H_2O_2. The peat was then digested in a MARS Xpress microwave (CEM, Germany) using a closed vessel system under US EPA method 3051A. After cooling, additional H_2O_2 was then added and the solution made up to a known volume. Prior to analysis each solution was diluted to 1% v/v (0.16 M) HNO_3 and filtered at 0.2 µm to remove any residual material, although this was primarily done as a precaution to inductively coupled plasma – mass spectrometry (ICP-MS) analysis, with the digest able to produce essentially clear solutions.

All vessels were washed and soaked overnight in 10 % HNO_3 then rinsed in de-ionised water. Solutions were analysed for As, Pb and sulfur (S) by ICP-MS (VG Elemental) with a detection limit of < 1 µg l^{-1}. Iron was determined by inductively coupled plasma – atomic emission spectrometry (ICP-AES, VG Elemental Horizon). Instrumental drift was corrected through use of linear interpolation of standards run every 10 samples. Reagent blanks were run and found to be below the limit of detection on the ICP-MS.

Due to the high number of samples, duplicate analysis was not possible for all samples. In order to determine the experimental error associated with the analysis a range of samples encompassing both high and low concentrations were selected for triplicate analysis, along with the use of an organic-rich ombrotrophic peat (low ash) reference material NIMT/UOE/FM/001 (Yafa et al., 2004). For the data presented here, good agreement was found between replicate measurements, with measured values found to be within 5 % of the mean value for As, Pb and Fe and within 10 % for S. Good recovery was obtained from the reference material, with As, Pb and Fe all falling within the acceptable limits of the reference material. The error between the measured value and the reference material value was similar to that obtained from the samples, between 3 % - 5 % for As, Fe, Pb and S (Table S5-2, Appendix 3).

Trace element total solid phase concentrations were also determined for each sample by non-destructive XRF. Ground, homogenised peat samples (12 g) were mixed with a wax binder (MERCK Hoechst wax C micropowder, 3 g) and pressed into sediment pellets. The pellets were analyzed using a wavelength separation XRF Spectrometer (Axios) for a range of elements including As, Fe and Pb. The performance of the XRF on the low ash content peat material was checked using the ombrotrophic peat (low ash) reference material NIMT/UOE/FM/001 (Yafa et al., 2004). Results were mixed, with only the result for Pb falling in the acceptable range suggesting there was an issue in determination of total concentrations using XRF. Results for As and Fe were 145 % and 30 % over the certified reference material values (Table S5-2, Appendix 3).

5.2.4 Sequential extraction

A sequential extraction procedure (SEP) was employed in order to determine the distribution of As within the solid phase. As typical sediment preparation techniques such as drying and grinding are known to affect the partitioning of trace elements including As (Anawar et al., 2010; Einax and Nischwitz, 2001; Vasile et al., 2010), all sequential extraction work was undertaken using peat that had not been dried or processed in any way. Prior to analysis a subsample of peat was weighed and oven-dried at 70^{o}C to obtain the dry-weight.

There are currently a range of SEPs being utilised to investigate the partitioning of both trace elements and As in sediment samples (Hudson-Edwards et al., 2004; Wenzel et al., 2001). As an anion, the behaviour of the adsorbed As species differs from metallic cations and so recent work by Wenzel et al., (2001) has altered the standard SEP used in metals analysis (Tessier et al., 1979) to allow for the targeting of surface-bound As. However, as the newly developed As protocols are not standard protocols (e.g. the Community Bureau of Reference (BCR) protocol for metals), use of a commonly employed procedure is required to ensure comparability between studies. While there are a number of recognised limitations to the use of SEPs (Wenzel et al., 2001), an understanding of the chemical processes removing As during the SEP and the likely similarity to the environmental processes occurring within the sediments allows for description of the SEP in terms of the operational processes used. For this reason the results are described not in terms of the targeted species, but by the environmental process that operates using a similar mobilisation process (described below).

For this study, a SEP based on a modification of those proposed by Keon et al., (2001) and Tessier et al., (1979) was selected due to its applicability to organic-rich soils (Gonzalez., 2006). Portions of sediment (1 g dry weight, not processed or dried), were carefully weighed into screwcap polypropylene centrifuge tubes (Fisher Scientific, Loughborough, UK) and subjected to a four step sequential extraction procedure detailed below.

- Initially, adsorbed As was extracted in the first step by end over end shaking with 25 ml of 1M NaH_2PO_4 (pH 5) (Fisher Scientific, 99+% Certified AR grade) for 24 hrs at 25 °C [one repetition]. A water wash (25 ml, 24hrs) was followed to ensure all surface bound As was removed. This step targets strongly adsorbed As through anion exchange; throughout this study this fraction is referred to as 'exchangeable'.

- Arsenic coprecipitated with carbonates, Mn oxides, and amorphous Fe (oxy)hydroxides was then targeted by end over end shaking with 25 ml 1N HCl (SpeciFied, Fisher Scientific) for 1 h at 25 °C [one repetition]. A water wash (25 ml, 1hr) was followed to ensure any readsorbed As was removed. This step used reducing conditions to mobilise As, and is therefore referred to as 'reducible'.

- Arsenic bound to OM was then removed through a process of oxidation. Initially, addition of 3 ml of 0.02M HNO_3 (SpeciFied, Fisher Scientific)and 5 ml of 30 % H_2O_2 (SpeciFied, Fisher Scientific)with adjusted pH of 2 with HNO_3 is made. The mixture was heated to 85± 2 °C for 2 hrs with occasional agitation. A second 3 ml aliquot of 30 % H_2O_2 was added (pH 2 with HNO_3), and heated again at 85± 2 °C for 3 hr with intermittent agitation. After cooling, 5 ml of 3.2 M NH_4OAc (99+% certiFied AR, Fisher Scientific) in 20 % (v/v) HNO_3 was added. The sample was diluted to 20 ml with deionised water and agitated again for 30 min. Throughout this study, this fraction is referred to as 'oxidisable'.

- Residual As was determined through a closed vessel digest with 16 N HNO_3 (trace element grade)+ 30 % H_2O_2 (SpeciFied, Fisher Scientific) (microwave digestion). Throughout this study, this fraction is referred to as 'residual'.

After the agitation time, each solution was centrifuged at 1700 x g for 20 minutes. The supernatant was decanted and filtered at 0.45 µm, and acidified with HNO_3 prior to analysis. Because of high total dissolved solids in some of the extractions, the supernatants were

measured for As and Pb with either ICP-MS (detection limit 1 µg l^{-1}) for water washes, reducible and residual solutions, or ICP-AES (detection limit 10 µg l^{-1}) for exchangeable and oxidisable As/Pb solutions.

5.2.5 Collection, preparation and analyses of water samples

A combination of intensive storm water sampling and general interval water sampling was conducted in the streams at both sites. Over a period of ten months from October 2009 through to July 2010, over 90 samples were collected at each site. Sampling was distributed throughout this period, and achieved by both spot sampling, and by the use of two automatic sampling systems (SIGMA 900), triggered by manual sample programming. Each sampler inlet was located as close as practicable to the centre of the stream channel and above the channel bed. The water sampler was programmed to extract 500 ml samples with an inlet rinse between each sample.

Upon returning to the laboratory each water sample was divided into two subsamples: an unfiltered (UF) sample was kept, and a portion was filtered through pre-rinsed 0.2 µm cellulose nitrate membranes to produce a soluble (<0.2 µm) fraction. Although previous studies typically use a cut-off of 0.45 µm to represent the dissolved phase, the ongoing work in this catchment had used 0.2 µm, and so to enable continuity, 0.2 µm was used in this study also. Both 0.2 µm and 0.45 µm exclude particulate material, but include dissolved species and some degree of colloidal material (Benoit, 1995), and as such represent an important size fraction in the transportation of contaminants.

A portion of each sample was acidified using concentrated HNO_3 (Analar grade, Fisher chemicals, UK) to pH< 2. Sample handling was achieved within 12 hrs of return from field. Prior to collection, all plastic-ware was cleaned by soaking in 10 % (v/v) HNO_3 for >24hr followed by rinsing with Milli-Q water (18MΩ). Samples were subsequently analysed for As, Fe, Pb and other trace elements using a combination of ICP-MS and ICP-AES. A combination of blanks and replicate standards and samples were used in the analysis to correct for drift and measure error.

Continuous *in situ* data from each site was collected as part of an ongoing catchment study. Data was collected using Sentry II loggers (Intelisys, UK). At each site, attached to each logger

is a pressure transducer (Intelisys, UK), pH probe (Russell, Fife, Scotland) and turbidity cell (Partech, St Austell, UK). At site 50 a barometer (Intelisys, UK) was additionally positioned to adjust for atmospheric pressure when considering stage and discharge (Q). The sampling interval on each logger was set to 15 minutes. Prior to placing the equipment in the field all probes were calibrated using known standards and Sentry II software (Intelisys, UK). Data was periodically downloaded, with spot samples of pH taken using calibrated field probes and measurements of Q taken to check and correct for drift in the probes. Discharge was determined by dilution gauging according to the protocol detailed in Gaffney (2008) (Outlined in Chapter 2) on each site visit. Subsequently, stage measurements were converted into a continuous Q record using a discharge relationship developed for each site with ongoing data collected from 2003 (Gaffney 2008).

5.2.6 Calculation of total As store

The obtained total concentration profiles from each of the cores (A-E and F-H) were used for a total As and Pb inventory calculation for each site. Rather than focussing on a specific period of contamination associated with an activity (e.g. industrial contamination), the whole store of available As within the catchment was determined. Firstly an estimation of the depth of affected peat had to be made. In order to do this, separately obtained samples of grit and shale from the bedrock were also digested using the total digest protocol outlined for the peat samples (Table S5-2, Appendix 3). The decrease in As concentration measured over the bottom half of each core was extrapolated using a regression line to determine the distance required to achieve the bedrock concentration. The weight of affected peat was then estimated using this determined depth, the moisture content of the peat and the weight of water. A mean concentration of both Pb and As was then determined for each core, and a mean for each site then applied to the calculated weight of affected peat to calculate the total inventory per unit area of the peat surface (g m^{-2}). For site 50, the percentage of vegetated peat was taken as 30 %, and at site 30 as 100 %. The sensitivity of the calculation was tested through variation of the depth of affected peat, and by application of altered mean concentrations (as determined by range of mean values measured for cores) to a proportion of the peat.

5.2.7 Calculation of As flux

Two methods of flux determination were utilised in this study. The first, used a simple interpolation to estimate the amount of both UF and soluble (< 0.2 µm) As (or Pb) leaving each catchment. Each of the UF and <0.2 µm concentrations (µg l^{-1}) obtained from the collected

water samples was multiplied by the calculated Q (l s^{-1}), and sample interval to give the total amount of unfiltered and soluble As and Pb transported during the sample period. This number was then applied to the period of time until the next measurement was collected. The total amount of each element was then summed, and divided by the total time period and the area of each subcatchment to give a flux (kg km^{-2} yr^{-1}). Error was determined by the extrapolation of analytical uncertainty in the interpolation calculation.

The second method utilised a ratings curve approach, using the relationship between pH and As concentration. Previous work in contaminated organic-rich catchments (Rothwell et al., 2008) has identified a relationship between the pH and trace element content of streamwater. It is thought that the flushing of porewaters containing high levels of humic acids also transport quantities of other dissolved elements (Rothwell et al., 2008; Tipping et al., 2003). Continuous pH data was only available at site 50, and as such this method could only be used for site 50. Using a continuous record of pH (15 min intervals) at site 50 for the seven months between October 2009 and July 2010, dissolved As concentrations (µg l^{-1}) were estimated for each 15 min period using a regression model. The continuous Q record and the area of each subcatchment were then used to determine a 15 min flux for each continuous data point (26170 points). These fluxes were then summed to give the total flux for the data period, which was then converted to an annual flux. The standard error for the regression line was used to calculate the error on each of the annual fluxes.

5.3 Results and Discussion

5.3.1 Evaluation of total concentration determination method

Due to the combination of a large volume of samples to be analysed and difficulties in ongoing total digest method development (refer Chapter 2), two methods of total concentration determination (XRF and total digest) were performed in order to get complete analysis of the samples (Table S5-1, Appendix 3). Both methods were evaluated using a high organic matrix reference material (Yafa et al., 2004) (Table 5.1). The HNO_3/H_2O_2 digest method produced results within the acceptable error of the reference material for total As, Fe and Pb indicating it was a suitable method of total concentration determination. However, the XRF was found to be high for the determination of both As and Fe (Table S5-2, Appendix 3).

Further to the comparison of the reference material between the two methods, the obtained core profiles from the total digest were compared with the XRF (Figure 5.2). Figure 5.2 illustrates the agreement achieved between the two methods for As in cores A, C, F & G, with the correlation between results for all cores presented in Table 5.1 (full dataset provided in Table S5-1, Appendix 3).

Table 5.1 **Correlation coefficients[a] between XRF and Total Digest for As, Fe and Pb within peat**

	As	Fe	Pb
Core			
A	0.94	0.98	1.00
B	0.89	-	0.83
C	0.86	0.99	0.98
D	0.87	1.00	0.99
E	0.94	0.98	0.85
F	-	-	-
G	-	-	-
H	n/a	n/a	n/a

[a]significant at 0.0001
- not a significant correlation
n/a: correlation not applicable as no TD performed on core H

It is evident that whilst overall, a good correlation was found in the site 30 cores (Table 5.1), varying agreement in concentration was found between the two methods. Whilst good agreement is seen in core A (Figure 5.2), core C illustrates the overestimation in concentration also seen in the XRF of the reference material. Despite these issues, because of the good correlation seen for the two methods, and due to the small number of samples needed, cores A (15 cm), C (9, 24 cm), D (6, 24 cm) and E (3 cm) included the bracketed XRF values to achieve complete total concentration profiles.

A lack of correlation in the two cores analysed by both methods at site 50 (Table 5.1) suggests that the XRF was not able to obtain a correct reading. This could be due to the samples not having enough mineral material to gain a stable reading (Givelet et al., 2004), possibly due to loss of the upper layers of peat due to erosion. However, the difference in concentration obtained by both methods is most marked for core F, where a completely different profile is

obtained from the total digest method (Figure 5.2). This suggests that it is not simply loss of material through erosion causing the XRF to not work, but possibly some other property of the peat at site 50. Because of this, the gap in the total digest profile for core F at depth 24cm was left. However, regardless of the performance of the XRF, the general low concentrations obtained for core G by digest and XRF (<5 μg g^{-1}) (Figure 5.2) do suggest that both core G and H show no significant contamination, and as such the XRF profile obtained for core H (where no total digest was performed) was included in the dataset.

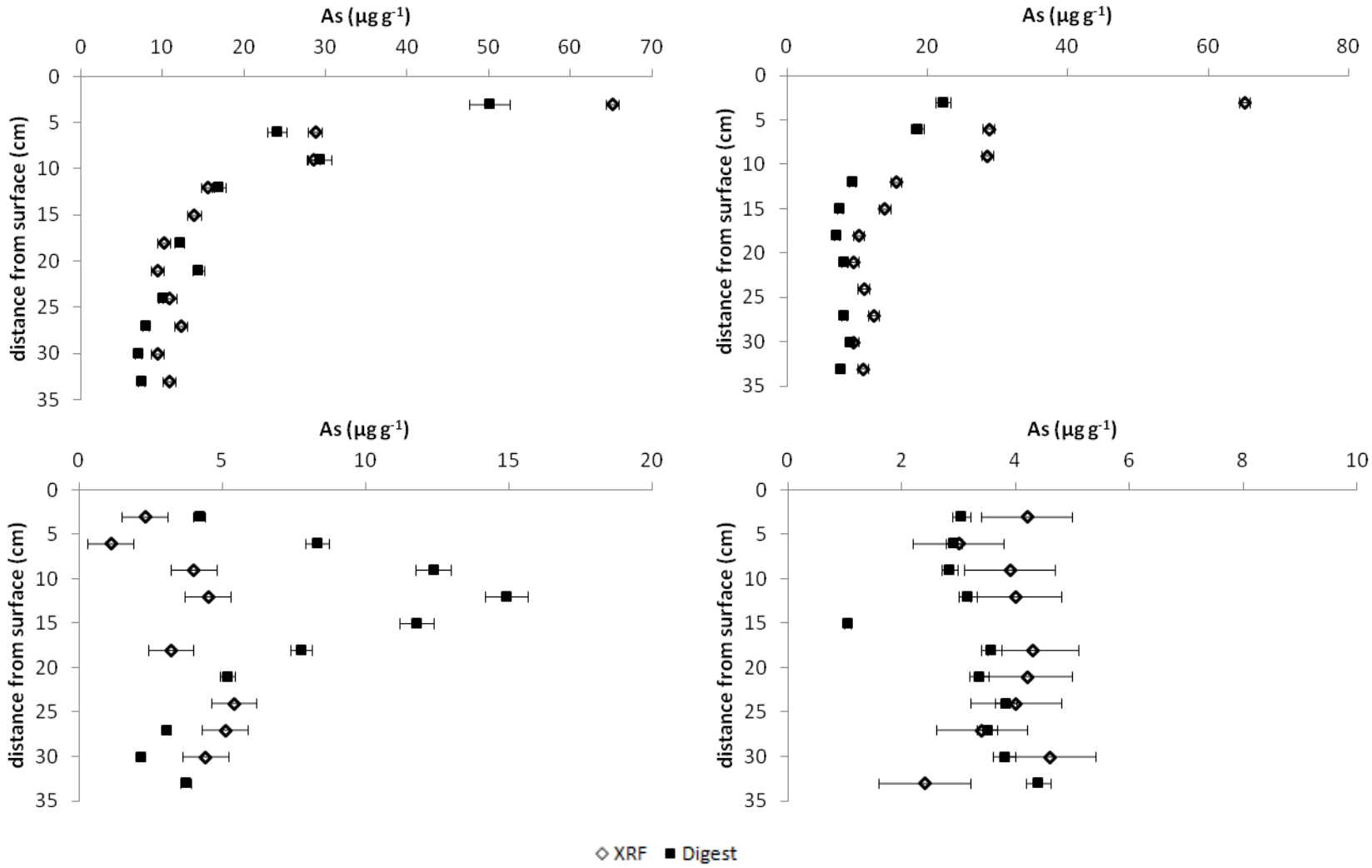

Figure 5.2 **Profiles of total As obtained by XRF and Total Digest for selected cores**

5.3.2 Variability of As profiles

The total concentration profiles of As, Pb, Fe and S at both site 30 and site 50 in Crowden Great Brook are shown along with % moisture in Figure 5.3 (refer Table S5-2 Appendix 3 for error determination). The elevated concentrations of As, Pb and Fe within the upper layers of peat (Figure 5.3); consistent with studies conducted in similar areas (Cloy et al., 2009; Nieminen et al., 2002; Rothwell et al., 2010); are evidence of historical atmospheric contamination of both catchments.

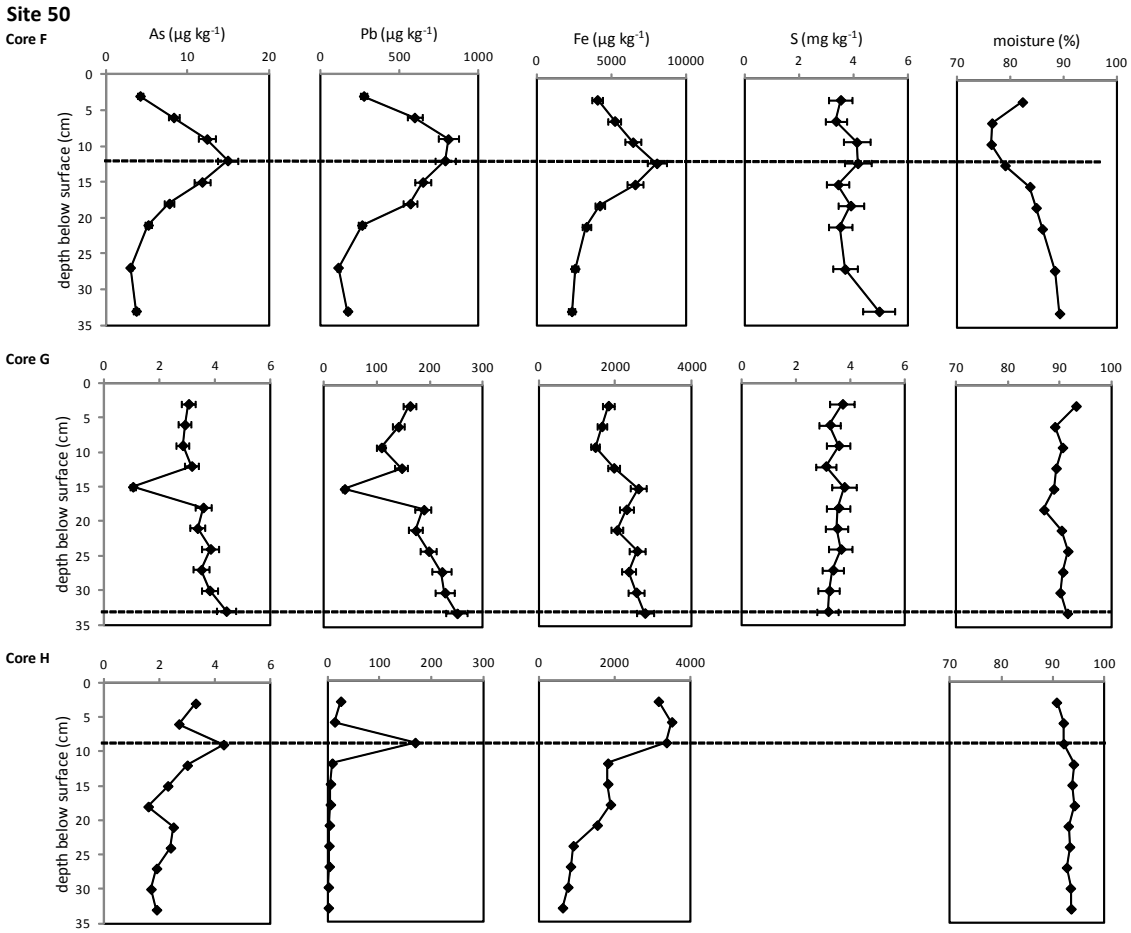

Figure 5.3 **Profiles of elemental concentration (As, Fe, Pb µg g^{-1}, S in mg g^{-1}) and moisture (%) versus depth in cores F-H - Site 50. Dotted line is position of As concentration maximum.**

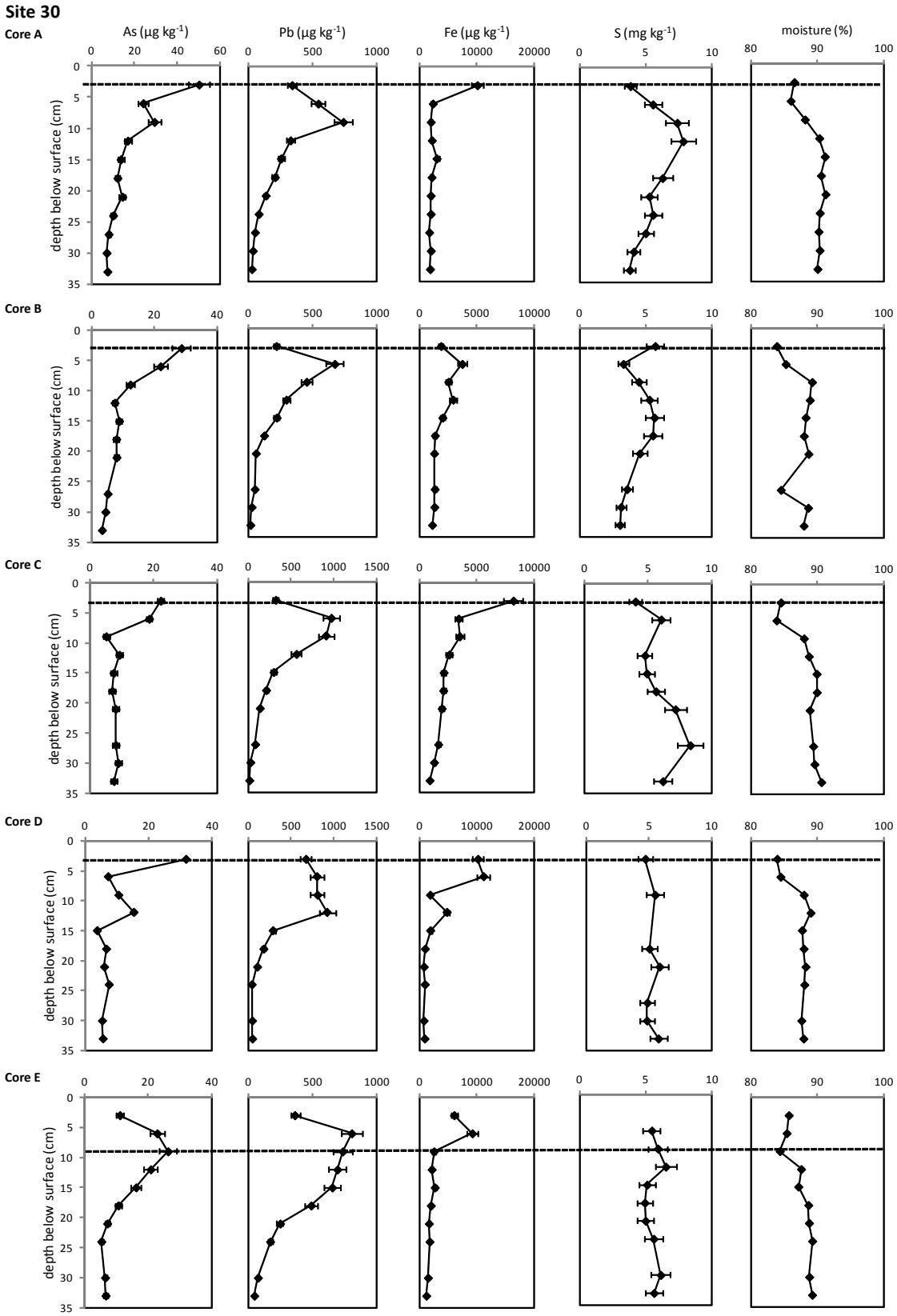

Figure 5.3(cont.) Profiles of elemental concentration (As, Fe, Pb µg g^{-1}, S in mg g^{-1}) and moisture (%) versus depth in cores A-E - Site 30. Dotted line is position of As concentration maximum.

However, despite the likelihood that the atmospheric contamination was originally deposited homogenously over the upland area, there is clear variation in both concentration and obtained vertical profile of As, both between the two catchments and, strikingly, within the cores collected from a single catchment (Figure 5.3a&b). Peak As (50 μg g^{-1}) concentrations in core A are elevated in relation to the other site 30 cores (Table 5.2), however, peak As concentrations in all site 30 cores fall above the UK's current guideline value for non-commercial/non-industrial land, currently set at 20 μg g^{-1} (Figure 5.3b) (DEFRA, 2002).

Table 5.2 Summary of Catchment Core Profiles

	Site 30	Site 50
catchment area (km^2)	3	0.5
number cores	5	3
estimated vegetation (%)	100	30
mean depth to bedrock (cm)	153	129
Max	163	195
Min	130	40
st dev	13	80
Average core As concentration (μg g^{-1})	12.1	4.3
Range of core averages	9.5 - 17.6	2.5 - 7.2
st dev of core averages	3.3	2.5

Mean concentrations of As also show variation within site 30, with core A having the highest at 17.6 μg g^{-1}, with cores B-E falling within 9.5 – 12.7 μg g^{-1}. All cores within Site 30 are considered to be within a homogeneous microenvironment, and as such, would be expected to show similar concentrations and profiles. Below 21 cm depth, within site 30, concentrations fluctuate around 6 μg g^{-1} in all cores, with significant variation in concentration in the upper layers (Figure 5.3). In addition to variation in peak concentration, review of the shape of each As profile (Figure 5.3) reveals that Core E is the only core to present a clear As peak (29 μg g^{-1} at depth 9 cm), with the remaining cores (A-D) having their highest concentrations in the surface sample (3 cm). A similar observation was made in a neighbouring Peak District catchment, with Rothwell et al., (2009) finding distinct As profiles in the three cores sampled across a dome/gully environment. However, this was attributed to contrasting water table

conditions relating to the positioning of the gully edge causing a changing redox environment and subsequent mobilisation of As.

Profiles of Pb, Fe and S within site 30 also show variation in peak concentration and profile shape over their 33 cm core lengths. In addition to the observed variation of each element between cores, it can be noted that the position of peak concentration for As (Figure 5.3a&b) does not coincide for all elements, or in fact consistently between the cores. Lead concentrations were higher in cores C and D, having peak concentrations of 966 μg g^{-1} and 926 μg g^{-1} respectively, whereas the peak concentrations in cores A, B and E ranged from 672 - 803 μg g^{-1}. Despite all cores showing a 'complete peak' profile for Pb concentrations, there is variation amongst the cores in the peak depth and shape. Both cores A and B show a sharp peak at depth 9 cm (738 μg g^{-1}) and 6 cm (671 μg g^{-1}) respectively, cores D and E show much broader peaks, with elevated concentrations over 9 cm of their profiles. Iron profiles all show a similar profile, with highest concentrations observed in the top cm's of the core. Such behaviour is typical of post depositional mobility of Fe, brought about by Fe's response to changes in redox conditions within the peat- possibly related to variations in water table (Rothwell et al., 2010). Concentrations of S did not vary greatly in any of the cores (Figure 5.3a&b), with no consistent pattern observed in the site 30 cores, suggesting that there is minimal accumulation of sulfide minerals within the peat. Lower moisture content (84-86 %) was found within the top 9 cm of each site 30 core, with minimal fluctuation (87-91 %) below this (Figure 5.3). Clearly the cores are experiencing fluctuations in moisture and are not under continually waterlogged conditions. Drying and re-wetting of peat has been shown to affect the redox conditions, and subsequently mobilisation of Fe within the peat (Blodau et al., 2008). The concentration profiles of Fe combined with the variation in moisture content suggests that these varying redox conditions are occurring within the top sections of all cores at site 30.

A different picture is evident at site 50, with significantly different concentrations and profiles of As apparent within cores G and H compared with core F. Core F is significantly enriched in both As (14.9 μg g^{-1}), Pb (807 μg g^{-1}) and Fe (8 mg g^{-1}) compared with cores G (mean As: 3.2 μg g^{-1}, mean Fe: 2.2 mg g^{-1}, mean Pb: 169 μg g^{-1}) and H (mean As: 2.4 μg g^{-1}, mean Fe: 1.7 mg g^{-1}, mean Pb: 22 μg g^{-1}) (Figure 5.3). Within core F, elevated levels of As are evident down to 21 cm depth, with concentrations <5 μg g^{-1} below 21 cm depth. Visual assessment of the catchment indicates that a significant percentage is degraded, suggesting that upper layers of peat may have been lost from the catchment. Within each subcatchment, the measured depth to bedrock (Table 5.2) can be used as a measure of peat movement, either by erosion or

accumulation. Areas that have experienced significant erosion would be expected to have lost the surface layers of peat, and consequently have a shorter depth to bedrock. Field observations of level of erosion at each site were supported by measured depths, with similar depths to bedrock measured within site 30 (130 – 163 cm), indicating that the physical movement of peat is limited within this catchment. Within site 50, core H was the most affected by erosion, with only 40 cm of peat cover, while cores G and H have 152 cm and 195 cm peat cover respectively. The lack of a distinct accumulation of either As or Pb within core G, despite the relatively large depth to bedrock is of interest, and suggests that the process of erosion is complex, and may occur in a fragmented pattern, over an extended period of time rather than during high Q events. It could also indicate that erosion/movement of peat can affect not only the surface layers of enriched peat, but possibly the translocation of previously depleted peat from adjacent areas.

Observed moisture content also reveals that core F is more similar to site 30 cores in its behaviour than the more degraded peat at core G and H, with lower moisture observed in the top section of the core. The generally high % moisture (mean G: 90 %, mean H: 93 %) combined with the lack of any significant change in moisture content in cores G and H, suggests that the exposed surface created by the erosion occurring within the catchment is allowing water to enter the peat unimpeded, creating water logged conditions. The observation that peak concentrations in core F are similar in magnitude to those seen in site 30, suggests that erosion has not affected all peat present in the site 50 catchment, and elevated concentrations are still present. Review of total concentration profiles has presented two clear results: 1) Erosion has resulted in the loss of the contaminated upper layers of peat at site 50, and 2) variation exists within apparently homogenous microtopography within site 30, and is not attributable to a physical process such as erosion.

5.3.3 Retention of As and Pb in contrasting upland peat environments

The variation in both concentration and profile of As and Pb both between and within each site indicates the spatial variability in the occurrence of both As and Pb within the upland peat environments of the Peak District, UK. In order to determine the total inventory of As and Pb within anthropogenically contaminated peat systems, studies have typically employed application of a single core to represent a site. The observation of profile variability within a site as seen for sites 30 and 50, suggests that care should be taken when applying single core

profiles to an entire catchment. The total amount of stored As within the peat is a factor of both the initial application (if aerially deposited) and any geological contributions, and the removal by both physical and geochemical means. Therefore, estimation of the total store of As in each catchment requires determination of both the vertical profile within the peat as well as evaluation of the variability occurring across the area. The concentration profiles of As and Pb obtained at both site 30 and site 50 are shown in Figure 5.4. It is apparent that the bulk of the contamination of both Pb and As is contained within the top 15 cm at site 30, but is much more varied within site 50, with one core (F) showing elevated levels down to 20 cm, while the remaining two cores show no evidence of accumulation.

Calculation of the total store of an element is highly dependent on the depth of peat affected by the contamination (Rothwell et al., 2010). Although measured concentrations were found not to fluctuate greatly below 15 cm (site 30) or 21 cm (site 50), evidence of elevation in concentrations in respect to the background levels can be made by comparison with the main contributors to the bedrock. Concentrations of As were found to be in the order of 2 – 3 $\mu g\ g^{-1}$ in the marine shale and grit material that comprise the bulk of the bedrock, clearly lower than the bottom peat core samples obtained at depth 33 cm in cores A (7.4 $\mu g\ g^{-1}$), C (7.6 $\mu g\ g^{-1}$), D (5.6 $\mu g\ g^{-1}$) and E (6.7 $\mu g\ g^{-1}$). This indicates that the 33 cm profiles obtained do not completely encompass the contaminated layers of peat within the catchment. Mean concentrations in cores G and H were similar in magnitude to the shale and grit samples, indicating these cores contain background levels of As only. To ensure the complete As profile is included in the solid phase As store calculation- an estimate of the depth to achieve the bedrock concentrations was made based on the proportional decrease observed in the bottom section of each core (Table 5.3). Concentrations of Pb were all below the bedrock values at the bottom of cores at site 30, with only core F at site 50 requiring an adjusted depth.

At site 30, use of the mean concentration of As gives an inventory of 0.72 $g\ m^{-2}$, while increasing the depth to 80 cm increases the inventory to 1.2 $g\ m^{-2}$ (Table 5.3). The calculation at site 50 assumes a 30 % vegetation cover, which was supported by visual assessment. The calculated inventory at site 50 is lower, at 0.23 $g\ m^{-2}$ using 33 cm depth, and 0.28 $g\ m^{-2}$ using 40 cm depth, suggesting that As is not conservative between the two sites. However, evaluation of the conservative element Pb, also shows a similar decrease between sites 30 (50 cm: 19 $g\ m^{-2}$) and 50 (33 cm: 11 $g\ m^{-2}$). This observation indicates that it is the loss of contaminated layers of peat due to the physical action of erosion that is responsible for the decreased inventory at site 50, rather than mobilization of As and Pb within the peat being

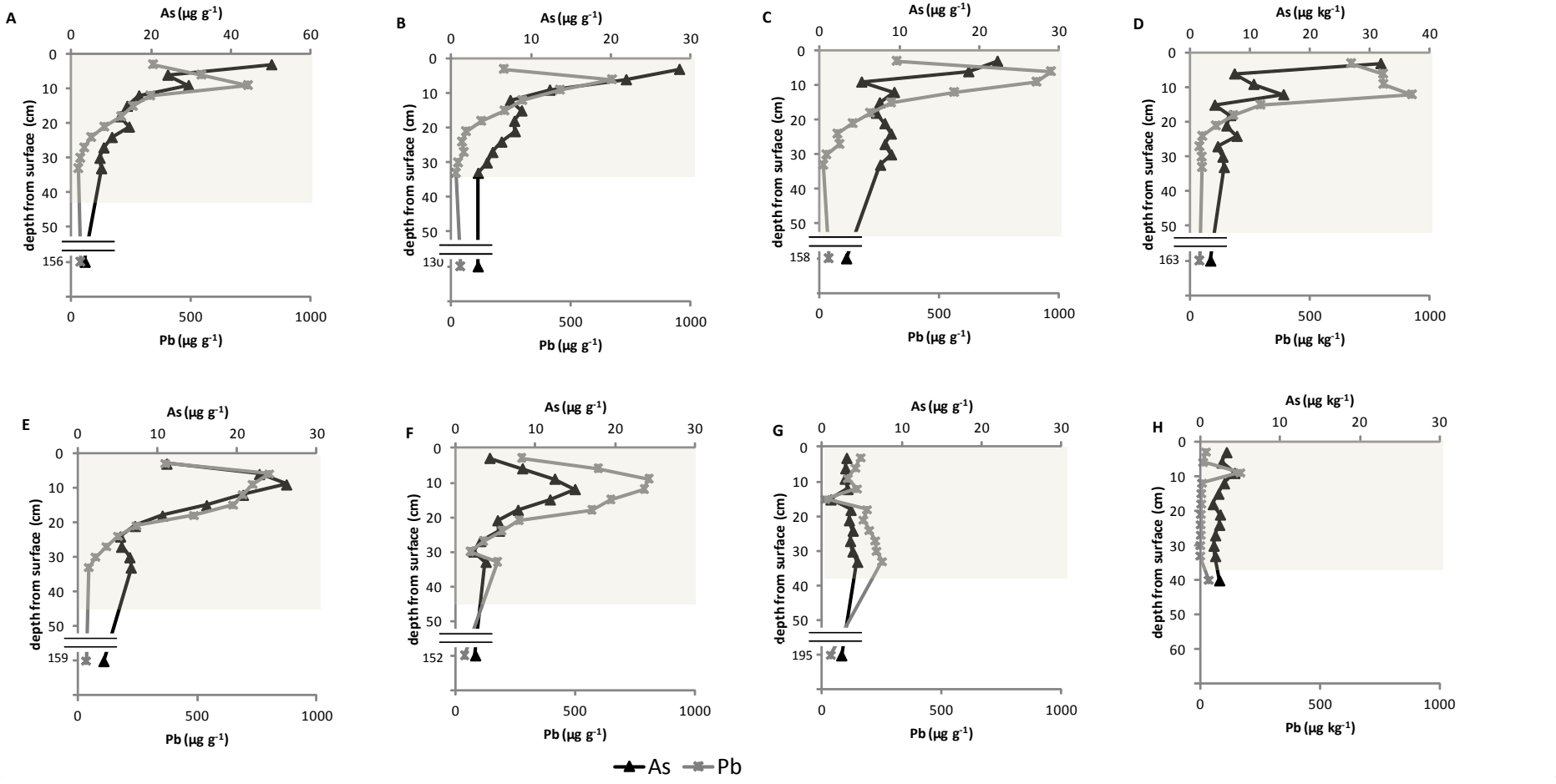

Figure 5.4 **Core depth profiles of As, Pb-contaminated peat used in inventory calculations. Shaded area indicates approximate depth of contaminated peat.**

measured. The calculated inventories for site 50 are within the range of reported values for peat in neighbouring (Rothwell et al., 2010) and similar (Cloy et al., 2009) ombrotrophic peat environments. The calculated inventory for site 30 is slightly above those reported by Rothwell et al., (2010) and Cloy et al., (2009). Both these studies have focused on dating the anthropogenic contamination within the peat, utilising Pb isotopic dating to calculate the age of contamination for different depths of peat. Inventories have been reported on a basis of age, reflecting the timing of anthropogenic contamination, rather than calculating the total store of As potentially available for mobilization in the peat. This is especially critical when the variation between As and Pb profiles observed within our sites is taken into account. Review of the published profiles with respect to the calculated age of the contamination reveals that the full profile of As has not been included in their calculations, and as such, this study's inventory calculation provides a more complete picture of the total As inventory.

Table 5.3 Calculation of total store of As and Pb within Site 30 and 50

	Site 30			**Site 50**	
Average depth to background level (cm)	51			36	
Range (cm)	33 - 83			33 – 43	
	As $g\ m^{-2}$	**Pb** $g\ m^{-2}$		**As** $g\ m^{-2}$	**Pb** $g\ m^{-2}$
Depth 50cm	0.72	19	**Depth 33cm**	0.23	11
Depth 80cm	1.2	30	**Depth 40cm**	0.28	13
Depth 50cm, (50% peat at core A concentration)	0.85	22	**Depth 33cm, (50% vegetation cover)**	0.27	13

The calculation of each inventory was adjusted to determine the influence of potentially having under-sampled the higher concentrations found in core A and F within each respective site. Assuming the sampling had missed the most contaminated areas of peat within each catchment, at site 30, use of core A as 50 % of the total peat in the area, at the minimal depth of 50 cm gave 0.85 g m^{-2} for As and 22 g m^{-2} for Pb. The assumption of depth of affected peat has more influence on the inventory estimate at site 30 than the adjustment of the mean concentration. At site 50, assuming vegetation cover was at 50 % (core F), the calculated inventory for As and Pb are now comparable to the increased depth (40 cm) calculation (Table 5.3). It is evident that confidence in the depth profiles of both elements from multiple core locations is required in order to gauge the appropriate depth to extend over the catchment. The number of cores will also determine the confidence in the overall picture of the contamination experienced at a given site. It is important to consider the number of cores that will be representative of the site, as use of a single core for site 50 would have greatly affected the calculated inventory.

5.3.4 Transportation of As in streamwaters

Mean concentrations of As measured for unfiltered and <0.2 µm samples from October 2009-July 2010 are presented in Table 5.4 for both sites. Calculations of As flux in both size fractions for each catchment are shown in Table 5.4. A number of recognised methods to calculate the flux of metal(loids) exist for streams and rivers (Grosbois et al., 2009; Masson et al., 2007; Michel et al., 2000; Rothwell et al., 2011; Walling and Webb, 1985), typically interpolation or use of a rating relationship. The latter, involving the use of the relationship of concentration for both UF and <0.2 µm datasets for each catchment and Q was not suitable due to the lack of a significant relationship (Figure 5.5).

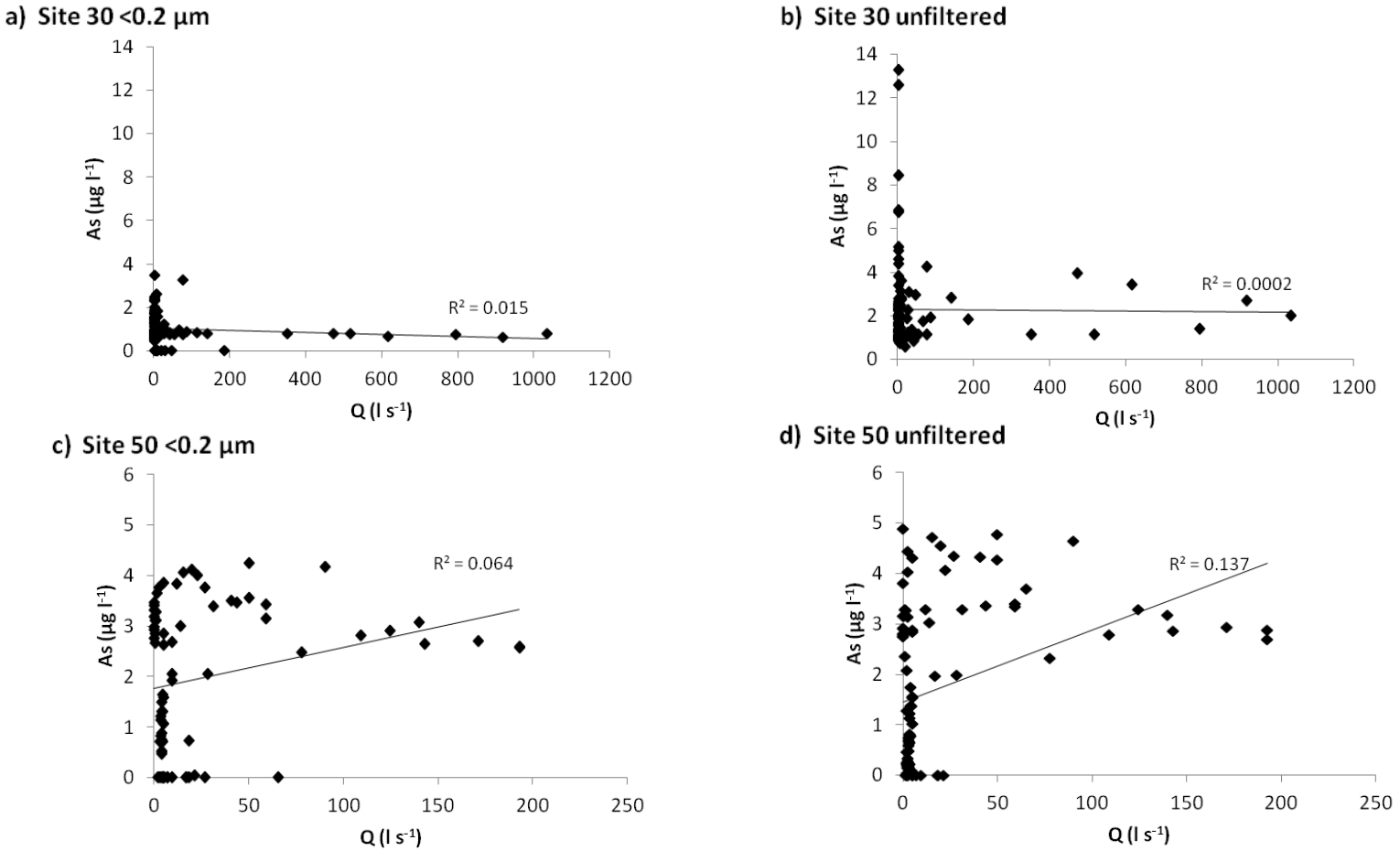

Figure 5.5 **Comparison of As concentration with discharge (Q). a) site 30, <0.2 µm, b) site 30 UF, c) site 50, <0.2 µm, d) site 50 UF. Drawn line represents linear relationship, with calculated R^2 displayed within each graph.**

Table 5.4 Summary of aqueous water chemistry and determination of annual and event flux of As and Pb

			Aqueous concentration			
			< 0.2 µm		UF	
			Mean	range	mean	Range
Site 30	As	µg l^{-1}	2	0 - 3.3	2.6	0.6 - 33.8
	Pb	µg l^{-1}	0.1	0 - 6.7	0.7	0 - 80.7
Site 50	As	µg l^{-1}	2	0 - 4.2	1.7	0 - 3.3
	Pb	µg l^{-1}	0.1	0 - 11.0	2.1	0 - 49.5

		Interpolation		pH ratings curve	
		< 0.2 µm	UF	< 0.2 µm	UF
Site 30	As kg km^{-2} yr^{-1}	0.16 ± 0.02	0.30 ± 0.02	-	-
	Pb kg km^{-2} yr^{-1}	0.13 ± 0.03	0.70 ± 0.1	-	-
Site 50	As kg km^{-2} yr^{-1}	0.23 ± 0.03	0.35 ± 0.03	1.14 ± 0.21	1.74 ± 0.33
	Pb kg km^{-2} yr^{-1}	0.09 ± 0.02	2.10 ± 0.20	-	-

	% of calculated annual As mass transported in events			
Winter 'first flush' event				
Site 30	2	3	-	-
Site 50	11	8	2	3
Summer 'post first flush' event				
Site 30	0.1	0.1	-	-
Site 50	2	1	-	-

Interpolation between daily concentration measurements was used to calculate fluvial fluxes for the UF and <0.2 µm fractions of 0.16 ± 0.02 kg km^{-2} yr^{-1} and 0.30 ± 0.02 kg km^{-2} yr^{-1} respectively for site 30 and 0.23 ± 0.03 kg km^{-2} yr^{-1} and 0.35 ± 0.03 kg km^{-2} yr^{-1} for site 50 (Table 5.4). However, these fluxes are low in comparison to those determined by Rothwell (2011) for a neighbouring catchment (at 6.5 kg km^{-2} yr^{-1}). Variation in calculated flux is not uncommon, and inherent due to the different methods utilised (Walling and Webb, 1985). Comparison of the values obtained for each site shows that the flux of As is higher for the more degraded site 50 than the vegetated site 30. This observation would suggest that erosion, significant at Site 50, played an important role in introducing metal(loid)s to the stream. However, review of the fluxes obtained for the two size fractions show that it is not simply the aqueous phase as a whole that is implicated in the transport of As (Rothwell et al.,

2011), but that there is a clear division in the transportation of As between the UF and soluble (<0.2 µm) fraction. This division does not appear to be linked to the visual degradation of a catchment, as the proportion of As transported in the <0.2 µm fraction at the vegetated site 30, is lower than at the degraded site 50. Had erosion been the sole source of As into the stream, the proportion of soluble As would be expected to be minor, and/or there should be a difference observed between the two contrasting sites. The significant contribution (>50 %) of the soluble fraction at both sites indicates that the effect of erosion on the transport of As at site 50 appears to be secondary to other mobilisation processes occurring within the peat.

The similarity of the calculated As fluxes for each catchment, where there is in fact a higher proportional release of As from within the degraded site 50 catchment is of interest. This suggests that while the total amount of As held within the site 50 catchment is significantly lower than at site 30, the proportion of peat within the degraded catchment that is As-contaminated and remains intact is able to release mobilised aqueous As over time. Movement of As in both catchments appears to involve dissolved and colloidal forms of As as key transport species. The movement of As in the soluble fraction is in contrast to the calculated fluxes for Pb, (Table 5.4) which show that Pb is primarily moved in the >0.2 µm fraction, indicating particulate movement, possibly through erosion, of Pb is key to transport of Pb. This is further supported by the increased UF Pb flux calculated for Site 50 relative to site 30. The difference in transport of As and Pb suggests that either different mobilisation processes are acting on these elements within the peat, or that if peat is being physically mobilised, As undergoes rapid transfer to dissolved species. Consequently, the role of biogeochemical mobilisation appears to be greater for As than for Pb (Rothwell et al., 2011).

Based on the interpolation calculated fluxes (Table 5.4), at Site 30 approximately 0.9 kg of As is mobilised in the unfiltered fraction of streamwater over a year, at Site 50 the amount of UF As transported is 0.17 kg yr^{-1}. Based on these removal rates, the mobilization of the total store of As at each catchment (2169 kg at Site 30, 193 kg at Site 50) is likely to continue on a timescale of >thousand years for both sites, representing a significant source of As to the downstream water collection areas. However, interpolation at this resolution is likely to be uncertain because the method only uses point samples obtained for each site, regardless of available in situ data. Despite the extensive sample collection (>87 samples), it cannot incorporate the large variation in conditions likely occurring over non-sampled times. The importance of high Q events in the transportation of As was evaluated through two events incorporated into the point sample collection. The percentage of total As transported during the two events are

displayed in Table 5.4. It is apparent that the first flush event, lasting 10 hours, represents a significant proportion of the total As transported during a year, as calculated by the interpolation method for both sites. However, the sampling of the second event, in July 2010, missed the initial flush, and consequently, despite the elevated Q at both sites experienced during the sampled part of the event (data not shown), the amount of As transported is minimal (Table 5.4). Clearly, flux determined by interpolation relies on not only a representative range of Q values, but also consideration of the temporal weather conditions that will affect the transportation of metal(loids) during an event.

Comparison of a method incorporating the available continuous data allows for an assessment of the variability relating to the changes in Q at the site to be made. A second method of flux calculation was possible due to the availability of pH data for site 50. The relationship between As and pH at site 50 is presented in Figure 5.6. As pH decreases, for example when humic acids are flushed from the porewaters of the peat, the amount of released As increases. The calculated fluvial flux for site 50 using the relationship with pH and utilising the continuous Q data was found to be higher than those calculated by interpolation at 1.14 ± 0.21 kg km^{-2} yr^{-1} and 1.74 ± 0.33 kg km^{-2} yr^{-1} for >0.2 µm and UF respectively (Table 5.4). It is apparent that inclusion of the continuous dataset (of both pH and Q) has increased the calculated flux. Once again, the importance of As transport in the <0.2 µm fraction is highlighted, and an implicit role in the porewaters of the peat being released into the streamwater is identified through the relationship in pH, giving confidence to the importance of dissolved and colloidal transport of As within both catchments.

a) Site 50 <0.2 µm

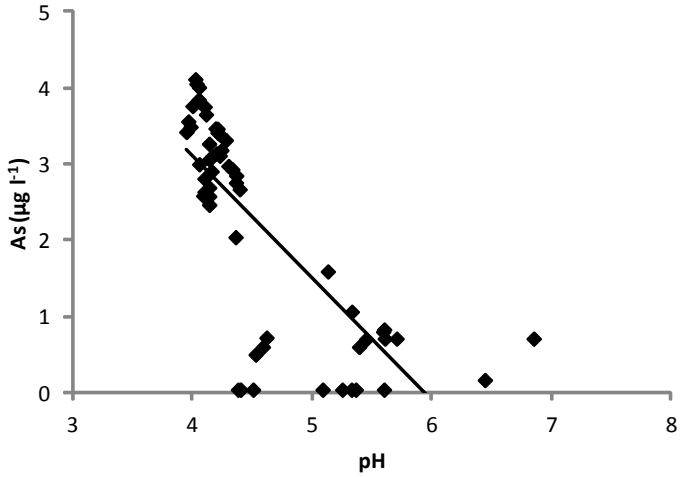

b) Site 50 unfiltered

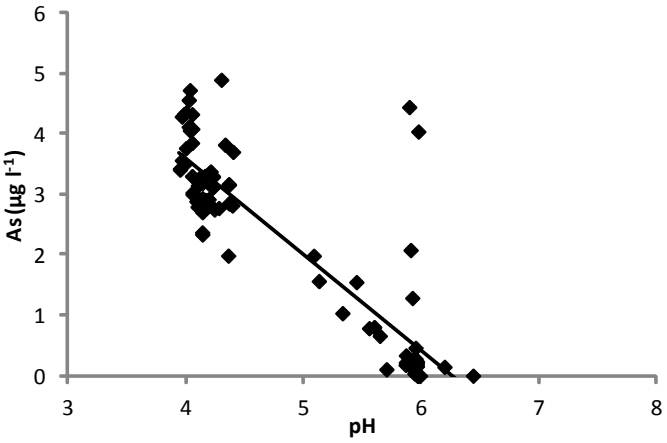

Figure 5.6 **Relationship between As and pH in site 50 streamwater. a)< 0.2 µm, and b) UF streamwater**

Understanding how As enters the streamwater is central to understanding the processes ultimately controlling its fate. Whilst the calculated fluxes can provide information on how the As is transported in the stream, the possibility of peat particles being effectively dissolved within the streamwaters upon entering cannot be excluded. In addition to the comparison of calculated fluxes in the <0.2 µm and UF fractions, use of the ratio of the metal(loids) existing within the peat can be used to gauge whether simple physical movement of peat and subsequent dissolution is the primary method of mobilisation. Three ratios are utilised in this investigation, outlined in Table 5.5. It can be seen that the ratios of As:Fe, Fe:OC and As:OC within the peat are similar for the cores within site 30. At site 50, there is some variation between the cores, with core F showing higher ratios than the other cores at the site, due to the increased level of contamination seen in this core.

Table 5.5 Ratios (As, Fe, OC) calculated within peat and streamwater

	Site 30				Site 50		
Peat core	**As:Fe ratio**	**As:OC ratio[a]**	**Fe:OC ratio**	**Peat core**	**As:Fe ratio**	**As:OC ratio**	**Fe:OC ratio**
A	0.0067	0.032	5.1	**F**	0.0016	0.013	7.8
B	0.0054	0.019	3.5	**G**	0.0015	0.006	4.0
C	0.0046	0.018	4.7	**H**	0.0024	0.005	2.4
D	0.0055	0.017	5.0				
E	0.0052	0.023	5.1				
core average	0.0055	0.022	4.7	**core average**	0.0018	0.008	4.7
Streamwater							
All data points (UF)	0.00045	0.00010	0.26	**All data points (UF)**	0.0071	0.00012	0.018
Winter event (whole)	0.00045	0.00008	0.20	**Winter event (whole)**	0.0050	0.00007	0.015
Winter event (rise limb)	0.00041	0.00011	0.28	Winter event (rise limb)	0.0033	0.00006	0.018
Winter event (fall limb)	0.00051	0.00005	0.10	Winter event (fall limb)	0.0067	0.00008	0.012

[a] assuming peat C content = 55% (pers comm Dr. S. Boult)

Comparison of the ratios measured in the unfiltered streamwater between the sites shows that there is a striking dissimilarity between the behaviour of Fe and As. At site 30, the presence of an Fe shale band has resulted in the streamwaters being enriched in Fe in relation to the peat, consequently the streamwaters As:Fe are lower. At site 50, either As is being mobilized at a higher ratio than Fe from the peat, or the in-stream processes are acting to remove Fe more effectively than As. Comparison of the mean obtained ratios from the peat shows that there is no similarity to the ratios obtained in the unfiltered streamwater, suggesting that simple dissolution has not occurred within the stream waters. Because adsorption processes could be occurring within the streamwater, acting to remove Fe, OC, or As, evaluation of data collected during an event was also made (Table 5.5). At both sites the ratios are altered with the rise/fall in Q, however, neither site shows ratios close to those expected from the dissolution of peat. These ratios, combined with the information from the calculated <0.2 μm and UF fraction fluxes indicate that erosion is not a primary mobilisation process for As. Understanding of the biogeochemical processes resulting in the mobilisation of As within the peat will provide insight into the ongoing transport of As within these catchments.

5.3.5 Post-depositional mobility

The post depositional movement of Fe in response to cycling redox conditions is well-established (Harrington et al., 1998). This is primarily caused by the reductive dissolution of Fe from the solid phase, and subsequent diffusion of Fe through the porewaters towards the oxic surface sediment layers where formation of Fe minerals then removes Fe from solution. This behaviour has been previously linked to the accumulation of As in the surface sediments in lakes (Aggett and O'Brien, 1985; Chaillou et al., 2003; Farmer and Lovell, 1986; Jay et al., 2005), due to the high affinity of As for Fe (in form of ferric (oxy)hydroxides) within the oxic surface sediments. The post depositional movement of As has been observed in ombrotrophic peat, related to either the release of associated As during the mobilisation of Fe minerals, or to the breakdown of As-OM bonds due to increased acidity related to sulfide mineral weathering. Although there is still uncertainty about the mechanism of As release, there has been a clear role identified relating to fluctuations in water table and redox conditions (Rothwell et al., 2010).

In addition to uncertainty relating to mobilisation mechanisms, the movement of As within organic rich sediments is also disputed, with the relative immobility of As also being described within ombrotrophic peat (Cloy et al., 2009). Such varied observations indicate that uncertainty about the behaviour of As in organic-rich materials still exists. It is clear from the observed variability amongst total concentration core profiles at both Crowden Great Brook sites (Figure 5.3), that As is experiencing some degree of PDM. However, the degree to which PDM has affected solid phase As within each site appears to vary without apparent change in surface conditions or peat moisture levels. As previous studies have looked at small numbers of cores covering extremes in physicochemical conditions, they have been unable to describe the natural variability occurring within similar environments. As a consequence of this, the conditions required for mobilisation of As from peat may be not be fully understood.

Whilst the occurrence of Fe PDM is evident in a number of the sampled cores, it is interesting to note that three cores (B, E and F) do not show a total concentration profile typical of PDM (Figure 5.3). This is most striking at site 50 core F, where a clear peak profile is seen, with maximum Fe concentration observed at 12 cm depth (Figure 5.3). This observation suggests that the cyclic water table movement associated with fluctuating redox conditions, and expected to be similar within sites based on surface conditions, is not occurring consistently within the peat at each site. Whilst fluctuations in water table of peatlands are known to vary considerably with time (Daniels et al., 2008), the lack of any distinguishing topography changes within the proximity of cores taken from site 30 (Figure 5.1) would suggest that water table variations would be minimal.

Lead, an element whose immobility has been used to date historic deposition of contamination in a number of studies across the globe (Cloy et al., 2009; Farmer et al., 2005; Shotyk et al., 1996), also displays core profiles characteristic of the Peak Districts historic contamination within all cores sampled within Crowden Great Brook (Figure 5.3). Atmospheric contamination of Pb is consistent with historic mining and industrial activities occurring between the cities of Sheffield and Manchester. Core D provides the only exception to the peak shape seen amongst the sampled cores, where the elevated concentrations are seen at the top depth sample (3 cm), possibly relating to removal of surface vegetation/peat during sampling, or by the existence of very narrow band of non-contaminated peat at the top not picked up by the 3 cm sample resolution.

Comparison of the position of As, Fe and Pb concentration maxima reveals that maximum total As concentrations are generally occurring alongside Fe at its peak (Table 5.6). However, cores B and E show peak positions of both Fe and Pb are coupled with peak As concentrations. Only two of the eight sampled cores display a profile of As that displays a clear peak (E, F). The occurrence of these two profiles (E, F) where the PDM of As has not occurred amongst the other cores clearly experiencing some degree of PDM is of note. Although the conditions required for As PDM are not fully understood, this observation suggests that the processes must not be occurring uniformly within the peat. From the obtained profiles, it is apparent that the PDM of As is occurring alongside the mobilisation of Fe. With the exception of core B, the occurrence of the As-enriched surface layers of peat is coupled with a similar enrichment of Fe. While core B displays a similar Fe trend, an elevated concentration of Fe was not observed in the top 3 cm. This observation suggests that these two elements are linked in their behaviour. This is not unexpected, given that Fe(oxy)hydroxides are well-known adsorptive materials for As in oxic conditions, with a number of possible binding mechanisms documented for the different Fe minerals (Coker et al., 2006; Dixit and Hering, 2003; Pedersen et al., 2006; Sherman and Randall, 2003; van Geen et al., 2004).

Table 5.6 Comparison of the position of the concentration maximum of As relative to those of other selected

core	position of max. As concn (cm) relative to that of max concn of:		
	Pb	**Fe**	**S**
A	6	0	9
B	3	3	0
C	3	0	24
D	9	0	21
E	-3	-3	3
F	3	0	21
G	0	0	18
H	0	3	-

Minus (-) represents lesser depth

Because peak position does not take the whole shape of each profile into account, the correlation between profiles was used to gain understanding of the relationship between the total concentration of elements within each profile (Table 5.7). The correlations once again highlight the relationship between Pb and Fe, unexpected based on the mobility of Fe under

cycling redox conditions (Harrington et al., 1998), observed at a number of cores. In cores B and F, significant correlations $R^2 > 0.9$ are observed, with less strong, but significant correlations seen between Fe and Pb in cores D, E and H. The presence of cores where clear peaks in both As and Pb are observed (cores E, F), supports the idea of codeposition of these elements in the peat (Rothwell et al., 2010), and suggests that they are being held within the peat by the same associations. The association of Pb within peat has been proposed to be with OM, with Pb^{2+} cations found to be scavenged by OM (Vile et al., 1999). Lead has also been found to be within the reducible fraction of peat (Bacon et al., 2006; Jones, 1987; Syrovetnik et al., 2007), suggesting a possible role for the reductive dissolution of Fe minerals in the mobilisation of Pb. As an anion, the behaviour of As under variations in environmental conditions differs to that of cationic metals. Arsenic can occur as range of anionic species ($[H_2AsO_4]^-$, $[H_3AsO_3]^0$), with differing binding and complex formation preferences (Dixit and Hering, 2003; Manning and Goldberg, 1997; Pierce and Moore, 1982). The association of As within the solid phase will therefore differ to that of the cation Pb^{2+}, resulting in different mobilisation processes.

Table 5.7 **Correlation coefficients between As, Pb, Fe & S within peat cores**

	Correlation coefficients[a] within cores							
	Site 30					Site 50		
	A	**B**	**C**	**D**	**E**	**F**	**G**	**H**
As + Pb	0.41	0.87	-	-	0.88	0.92	0.90	0.66
As + Fe	0.73	0.72	0.71	0.60	-	0.95	-	0.55
Pb + Fe	-	0.90	-	0.45	0.35	0.90	-	0.33
As + S	-	-	-	-	-	-	-	-

[a] $p<0.05$

Despite the role of FeS as a sorption surface identified in anoxic layers of minerotrophic peats (Blodau et al., 2008; Gonzalez et al., 2006), the observed difference in peak concentration position (Table 5.6) and the lack of any correlation between either Fe, As and S (Table 5.7) indicates that sulfide minerals are not playing a key role in binding of As, suggesting that OM may have a large part to play in anoxic conditions (Dawson et al., 2010; Gonzalez et al., 2006; Rothwell et al., 2009). The correlation of As within the cores is clearly divided between Fe and

Pb (Table 5.7). While As is often correlated with both Fe and Pb (cores A, B, F H), in two cores it is only correlated significantly with Fe (C, D) and in two cores it is only correlated significantly with Pb (E, G). Of the eight cores sampled, only two display a peak profile where peak As is coupled with the maximum Pb concentration (cores E and F. From these observations, a range of As behaviours are observed within the peat at Crowden Great Brook. Arsenic can be seen both associated with Pb, present in a clear profile within the peat, or it has undergone PDM, and been transferred (via diffusion) with Fe, vertically up the profile to the surface layers, where it is re-oxidised and consequently re-adsorbed to Fe within the solid phase. Additionally, core E provides an example of peat where Fe appears to have undergone PDM, with Fe-enriched layers of surface peat, but with no corresponding As PDM evident (Figure 5.3). This observation implies that the environmental conditions acting on solid phase Fe and As are different, and the inference of As behaviour based on Fe movement may be misleading. Furthermore, the association of As within the peat may be divided between OM and Fe, with the relative roles varying dependent on water table/redox conditions. Prediction of the occurrence of PDM is not possible based on site location and surface conditions alone, adding uncertainty to the application of expected profiles across visually equivalent areas.

5.3.6 Potential sorbents of As

The results of the sequential extraction completed at depth 9 – 12 cm across all cores (Table 5.8) show the clear differences in the partitioning of As and Pb within the peat. All sampled cores show ~100 % extractable Pb in the first three SEP steps, indicating that Pb is relatively extractable within the peat. The distribution of As varied by core, with higher proportion of extractable As (~100 %) seen in cores A, E and F, with much lower proportions seen in cores B, C, H and G. This variability in extractability could be a result of the 9-12 cm sample positioning in relation to the total core profile. For most of the cores, the 9-12 cm sample is falling on the downward slope of the typical PDM profile, while for samples E and F, this sample is occurring at a total concentration peak (Figure 5.3). The lower extractability for the cores where the sample is not located on an As peak suggest that labile As has already been mobilised from this depth. Core A presents a different pattern, as the 9-12 cm sample is not occurring on a peak, but the extraction is showing the As present to be labile. This could be due to the elevated levels of As present in this core relative to the others, as well as the shape of the enrichment curve being above the level found in the deeper peat layers at the 9-12 cm sample point.

Table 5.8 Partitioning of As & Pb across all cores at 9-12cm depth (%)

Site 30

	core A		core B		core C		core E	
	As	**Pb**	**As**	**Pb**	**As**	**Pb**	**As**	**Pb**
Exchangeable	31 ± 8	2 ± 0.5	6 ± 0.9	2 ± 0.02	21 ± 2	1 ± 0.1	32 ± 0.9	2 ± 0.4
Reducible	6 ± 0.7	98 ± 4	4 ± 0.4	88 ± 1	5 ± 0.6	41 ± 0.8	3 ± 0.6	80 ± 5
Oxidisable	71 ± 5	12 ± 6	38 ± 0.3	4 ± 0.3	28 ± 1	2 ± 0.04	52 ± 10	10 ± 1
Residual *	*0*	*0*	*52*	*7*	*47*	*56*	*13*	*8*
TOTAL	108	113	48	93	46	44	87	92

Site 50

	core F		core G		core H	
	As	**Pb**	**As**	**Pb**	**As**	**Pb**
Exchangeable	28 ± 6	5 ± 1	33 ± 0.2	5 ± 3	42 ± 0.2	1 ± 0.1
Reducible	4 ± 0.5	83 ± 1	5 ± 0.7	85 ± 4	2 ± 0.2	123 ± 2
Oxidisable	79 ± 7	10 ± 0.3	32 ± 8	5 ± 0.4	10 ± 4	18 ± 3
Residual *	*0*	*2*	*30*	*4*	*47*	*0*
TOTAL	110	98	70	96	53	141

* due to sample loss, determined by difference in sum of previous steps and total concentration

Distribution of As between the three sampled fractions reveals that As is held within the oxidisable fraction, implying a role for OM, over Fe-minerals in the storage of As. There is some variability in the partitioning of As in the remaining fractions between the cores, with cores A, E and F having a minor role for exchangeable As, and cores B and C having a larger proportion of residual As. As exchangeable As is the more labile pool of As present in the peat, its mobilisation and subsequent transport to either other regions of peat, or into the near-by stream could account for the observed variability in this fraction. Contrast of the two sites reveals that the distribution of As is reasonably similar, with the oxidisable fraction containing the largest pool of labile As within the peat. Core H presents an exception to this observation, with a larger proportion of exchangeable As present. This core represents the most eroded site within the studied area, and has a correspondingly low total As concentration (Figure 5.3). The occurrence of exchangeable As in addition to residual As, could be an indicator of the movement of previously mobilised As within the peat.

The distribution of Pb is in contrast to that of As, with the reducible fraction containing the majority of the Pb. This observation suggests that while there is documented evidence of the affinity of Pb for OM (Vile et al., 1999), Fe minerals have a role to play in the storage of Pb in

organic-rich materials. Similar distributions have been found in other organic rich systems, where the waterlogged nature of the soil has been suggested as a reason for the easier extractability of the Pb (Bacon et al., 2006). Studies into the distribution of anthropogenic Pb have found that the distribution may be independent of soil type, with roles for reducible Pb found in a range of other studies (Emmanuel and Erel, 2002; Jones, 1987; Syrovetnik et al., 2007; Teutsch et al., 2001). The coupling of SEP and isotopic ratio studies have determined that the different origins of Pb (anthropogenic vs. lithogenic) do not show any evidence of different binding affinities (Bacon et al., 2006). The dissimilarity in distribution of As and Pb within the peat suggests that different binding affinities are responsible for their occurrence within the solid phase, and indicates that differing environmental conditions responsible for mobilisation of each element.

Variation in distribution with depth of both As and Pb was explored with the SEP of core A. Total concentrations of As in core A showed a typical PDM profile, with elevated concentrations of As evident in the surface layers of peat. A strong correlation with Fe ($R^2 >$ 0.7) was evident within the total concentrations, with a smaller but significant correlation with Pb. Results from the SEP indicate that unlike Pb, the role of reducible As is minor throughout all sampled depths in the core (Figure 5.7a). There is clear variation in the proportion of exchangeable and oxidisable As within the peat, with the relative role of oxidisable As increasing towards the surface layers of peat. The proportion of exchangeable As is higher in the bottom samples of the core, but is also elevated in the top 3cm. This finding is in contrast to previous work with minerotrophic peat, where the oxidisable fraction was found to be the most important pool of As. Although the moisture content of the peat was also noted to affect the partitioning, with drier conditions resulting in higher levels of exchangeable As (Gonzalez et al., 2006). Moisture content seems to play a part in the observed distributions in core A, with the highest level of exchangeable As observed in the top 3 cm, where the peat was driest (Figure 5.7a). The elevated concentration, and increased role of exchangeable As could also be due to the transportation of previously mobilised As either from lower down in the profile, or from adjacent areas.

The extractant used in the SEP for exchangeable As is a higher ionic strength (1 M NaH_2PO_4 vs. 0.05 M $(NH_4)H_2PO_4$) than other SEPs (Gonzalez et al., 2006; Wenzel et al., 2001), and as such may be targeting a larger range of adsorbed As species. Use of higher ionic strength phosphate solutions has been found to release both non-specifically sorbed and specifically sorbed As, as well as breaking the bonds between inner sphere complexes of As and Fe-minerals (Wenzel et

al., 2001). Consequently, the exchangeable fraction of As may represent As associated with Fe as well as other surface sorbed species, in agreement with work conducted on peat soils (Blodau et al., 2008; Huang and Matzner, 2006). The presence of OM has been found to alter the structure of Fe minerals present (Dixit and Hering, 2003; Pierce and Moore, 1982), with a more amorphous structure found in high-OM sediments. Because of the non crystalline structure of amorphous Fe minerals, in addition to surface sites, cavities within the structure are available leading to increased opportunity for binding of As. The formation of chelations between Fe and OM within the structure have also been observed (Pfeifer et al., 2004). Because of the varied extraction schemes utilised by different studies, explicit comparison of obtained concentrations cannot be made. However, regardless of the extraction procedure used, it can be noted that As is typically associated with the reducible fraction of soils and sediments, due to its affinity for Fe (oxy)hydroxides (Smedley and Kinniburgh, 2002). Work with higher organic sediments by Blute et al., (2009) using wetland sediments found that higher levels of As were found within the exchangeable fraction of the sediment than in related river sediments. It is evident from this that the origin and composition of the sediment plays a role in the storage of As.

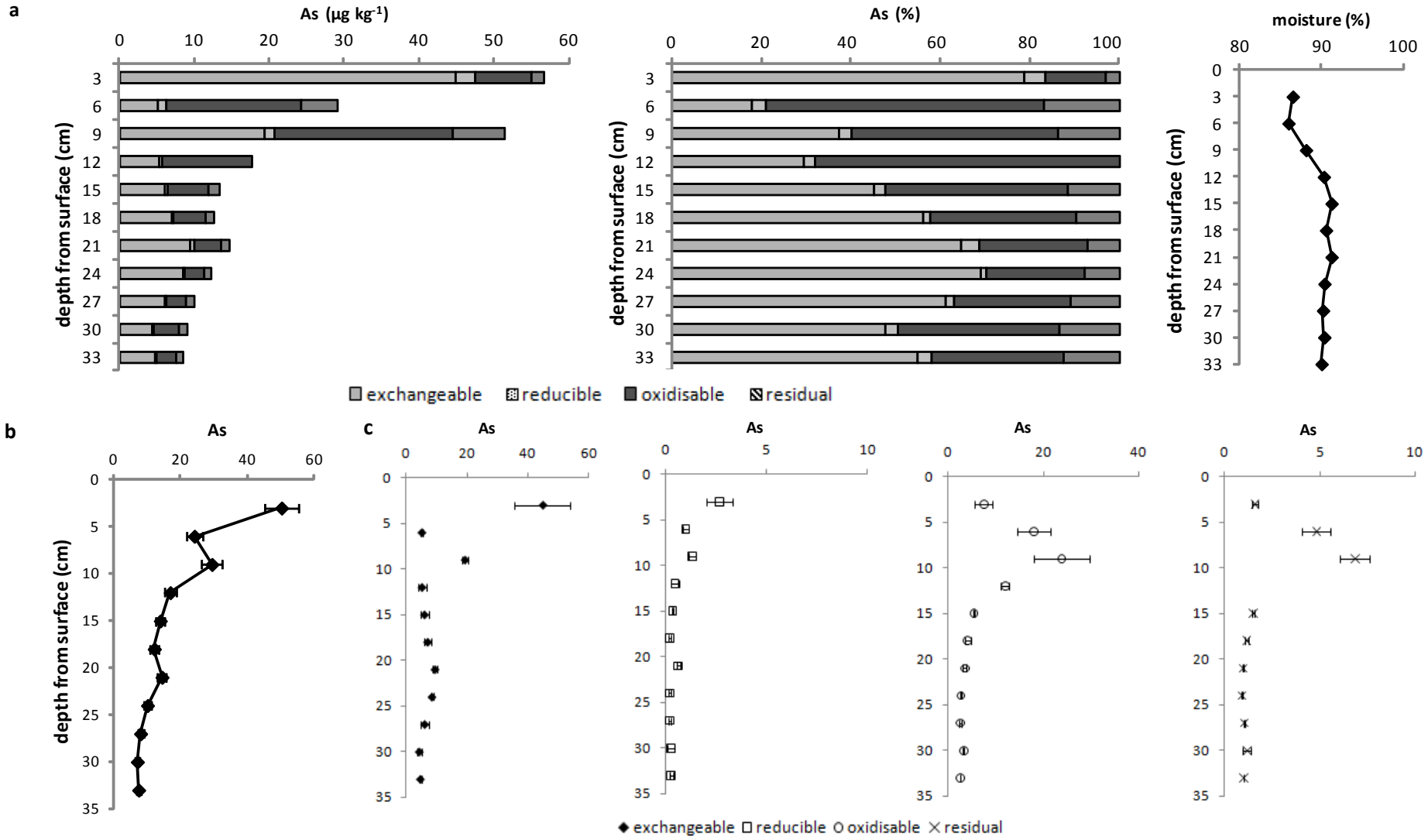

Figure 5.7 **Partitioning of As within core A (Site 30). a) Illustrates both the absolute concentration (µg g^{-1}) and proportion of total As at each depth, b) displays the core depth profile for the total As concentration (µg g^{-1}), c) the core depth profile for As (µg g^{-1}) within each SEP fraction.**

Although Pb is stored mainly within the reducible fraction of the peat at all depths, there is some variation evident in its distribution with depth in core A (Figure 5.8). As seen for As, the proportion of exchangeable Pb increases with depth, with oxidisable Pb higher in the surface layers. As the extractant used in exchangeable SEP step is specific to the anionic As species, the proportion of exchangeable Pb may be underestimated by this SEP. As a consequence of this, the reducible step may contain a proportion of the exchangeable Pb. Despite this, the overwhelming proportion of Pb within the reducible fraction, and minimal occurrence of Pb within the oxidisable phase is indicative of the minor role played by OM. The higher proportion of oxidisable Pb in the surface layers appears to be coupled to the lower moisture content of the surface peat. Waterlogged conditions experienced in the lower core profile appear to be supporting the observation of increased mobility made by Bacon et al., (2006).

The dominance of the reducible fraction in the partitioning of solid phase Pb supports the observations made in similar organic rich systems, where the origin of Pb was not found to alter the binding affinity (Bacon et al., 2006). As the historical contamination of Pb was atmospherically deposited, the upper part of the profile should have a different origin to that at the bottom (Rothwell et al., 2010). The dominance of the reducible phase for Pb at all depths suggests that whilst the environmental conditions responsible for the reductive dissolution and subsequent mobilisation of Fe are occurring within the peat, the same processes do not appear to be affecting the storage of Pb. Or it could indicate the released Pb is readily readsorbed by Fe remaining throughout the profile. The total concentration profile of Fe (Figure 5.3) indicates that elevated levels of Fe are present at all depths.

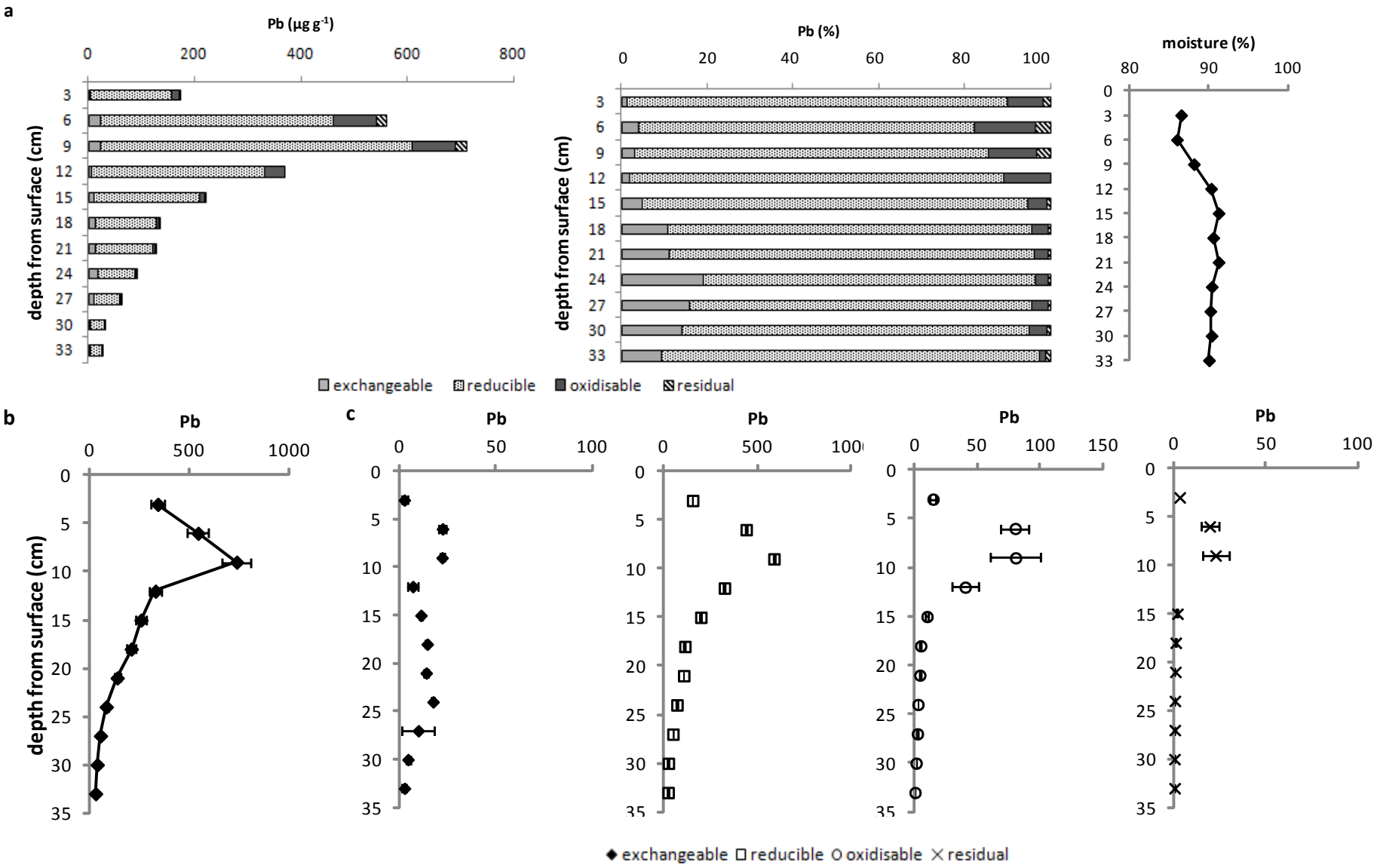

Figure 5.8 **Partitioning of Pb within core A (Site 30). a) Illustrates both the absolute concentration (µg g^{-1}) and proportion of total Pb at each depth, b) displays the core depth profile for the total Pb concentration (µg g^{-1}), c) the core depth profile for Pb within (µg g^{-1}) each SEP fraction.**

By looking at the profiles in concentration of both As and Pb within each SEP fraction, an interesting observation can be made. The distribution of As within each fraction can be divided into two groups: 1) displaying the PDM enriched surface layer profile and 2) displaying the full peak profile (Figure 5.7b). The exchangeable and reducible fractions of As both display the PDM profile, indicating that adsorbed As is likely to be bound to Fe(oxy)hydroxides. Arsenic released due to the reductive dissolution of Fe is subsequently adsorbed by the newly formed Fe(oxy)hydroxides at the surface of the peat. In contrast to the more labile fractions, the oxidisable and residual fractions of As show a clear peak in concentration at 9 cm depth (Figure 5.7b). This peak coincides with that of Pb within the oxidisable phase (Figure 5.8b) and suggests that a proportion of both As and Pb are being held by OM at the original deposition depth of peat. In contrast to As, the reducible, oxidisable and residual fractions of Pb display a clear peak profile (Figure 5.8b) with a consistent depth of maximum concentration within each fraction, indicating that whilst a significant proportion of Pb is held within the reducible fraction, unlike As, it has not undergone any vertical mobilisation. The observed profiles of the different solid phase As pools indicates that potential stores of As, although apparently more stable, exist at depths not noted through total concentration determinations.

5.3.7 Implications for Mobilisation of As

Information on the storage of both As and Pb has shown different binding mechanisms are responsible for the storage of As. Whilst previous studies have linked the occurrence of Pb and As within ombrotrophic peat, it is evident that different retention mechanisms exist for these elements. Evidence from mesocosm experiments conducted with peat has previously shown that aqueous concentrations of As are elevated under anoxic and reducing conditions (Blodau et al., 2008). Information gained from the sequential extractions has illustrated that As is relatively labile and subsequently subject to mobilisation under the environmental conditions experienced at both sites. Evidence of the accumulation of labile As in the surface peat, combined with the variability in concentrations observed within each site indicates that both horizontal and vertical transport of As is occurring within the peat. Such mobilisation would expect to increase porewater concentrations of As. Elevated concentration of As have been observed in the porewaters of Crowden Great Brook (Up to 20 µg l^{-1}, data not shown). Increased rainfall may act to wash out porewaters into neighbouring streams, or subsequent changes in pH and competition from competing ions, such as DOC, may remove As from the labile fractions of peat and result in an increase of soluble As leaving the catchment. With

exchangeable As forming an important pool of As at all depths of the sampled core, the effect of competing ligands for sorption sites could significantly influence the mobilisation of As. Previous studies have shown that humic substances, including DOC, can compete with As for sorption sites, or form aqueous complexes (Bauer and Blodau, 2006; Grafe et al., 2002; Lin et al., 2008; Redman et al., 2002; Ritter et al., 2006). The availability of solid phase As to environmental processes is of concern considering the large pool of As stored with the upland peat.

5.4 Conclusions

The results of this study demonstrate that the distribution of As within ombrotrophic peat soils in the Peak District National Park are variable both within the vertical profile and across apparently homogenous microtopography. Profiles of total As concentration generally showed enrichment in surface layers, suggestive of PDM linked to the redox cycling of Fe. However, within a subcatchment, evidence of clear subsurface peaks, suggestive of the retention of As within the peat, was also found, with the observed As profiles following either the profiles of Fe and Pb, two elements known for their divergent mobility behaviour. These observations suggest that the processes controlling the PDM of Fe and As are subject to local conditions not apparent from surface topography. Prediction of the occurrence of PDM is not possible based on site location and surface conditions alone. The partitioning of As was found to be in contrast to Pb, with reducible Pb dominating, whereas As was found within the oxidisable fraction of the peat across both vegetated and degraded catchments, suggesting that OM is an important adsorbent of As with the ombrotrophic peat. The partitioning of As was found to vary with depth, with the exchangeable and reducible As present showing signs of PDM, whilst oxidisable and reducible As remained in a profile similar to that of Pb. This suggests that a proportion of both As and Pb are being held by Fe/OM at the original deposition depth of peat.

Long term erosion of a subcatchment resulted in lower As stores than a comparable vegetated site, illustrating the effect of site degradation on remaining contamination levels within the peat. Measured depth of peat at the degraded site varied significantly, indicating the movement of peat resulting from a lack of covering vegetation. However, evidence for the physical movement of particulate As in waters draining either of the monitored subcatchments was not found. High resolution monitoring showed that As leaving the subcatchments was largely in the soluble form; the proportion of particulates, which are most likely the product of physical erosion, appearing to be secondary. The predominance of soluble As within the

streamwaters at both sites suggests that biogeochemical processes are key in releasing As from the solid phase. However, evidence that the ongoing movement of particulate material through the process of erosion is ongoing was found through the monitoring of Pb. The transport of Pb contrasted with that of As, with the majority of Pb transported within the particulate fraction. The calculated fluxes of particulate Pb leaving each subcatchment demonstrated the removal of particulate material at both subcatchments, with degraded site 50 showing significantly higher particulate transport of Pb than the vegetated site 30. Given that a similar pattern was not observed for As, despite the close association found by correlation of total concentrations of As and Pb within the solid phase, this indicates that particulate As introduced to the streams must undergo in stream processing, altering its size and affecting subsequent mobility.

Further understanding of the transport of As within the aqueous phase of organic-rich waters is required in order to better assess the level of risk posed by the stored As within the Peak District on downstream water supplies. Given the mobilisation of As evident from within the peat under current conditions, future work should also focus on understanding the effect of changing climatic conditions on the rate of mobilisation.

5.5 References

Aggett J, O'Brien G. Detailed Model for the Mobility of Arsenic in Lacustrine Sediments Based on Measurements in Lake Ohakuri. Environmental Science & Technology 1985; 19: 231-238.

Ahmann D, Krumholz LR, Hemond HF, Lovley DR, Morel FMM. Microbial mobilization of arsenic from sediments of the Aberjona Watershed. Environmental Science & Technology 1997; 31: 2923-2930.

Anawar H, Mihaljevic M, Garcia-Sanchez A, Akai J, Moyano A. Investigation of Sequential Chemical Extraction of Arsenic from Sediments: Variations in Sample Treatment and Extractant. Soil & sediment contamination 2010; 19: 133-141.

Andreae M. Arsenic speciation in seawater and interstitial waters: The influence of biological-chemical interactions on the chemistry of a trace element. Limnology and Oceanography 1979; 24: 440-452.

Bacon J, Davidson CM. Is there a future for sequential chemical extraction? The Analyst 2008; 133: 25-46.

Bacon JR, Farmer JG, Dunn SM, Graham MC, Vinogradoff SI. Sequential extraction combined with isotope analysis as a tool for the investigation of lead mobilisation in soils: Application to organic-rich soils in an upland catchment in Scotland. Environmental Pollution 2006; 141: 469-481.

Bacon JR, Hewitt IJ. Heavy metals deposited from the atmosphere on upland Scottish soils: Chemical and lead isotope studies of the association of metals with soil components. Geochimica et Cosmochimica Acta 2005; 69: 19-33.

Bauer M, Blodau C. Mobilization of arsenic by dissolved organic matter from iron oxides, soils and sediments. Science of the Total Environment 2006; 354: 179-190.

Benoit G. Evidence of the particle concentration effect for lead and other elements in fresh water based on ultraclean technique analyse. Geochimica et Cosmochimica Acta 1995; 59: 2677-2687.

Bissen M, Frimmel FH. Arsenic- a Review. Part 1: Occurrence, Toxicity, Speciation, Mobility. Acta Hydrochimica et Hydrobiologica 2003; 31: 9-18.

Blodau C, Fulda B, Bauer M, Knorr K-H. Arsenic speciation and turnover in intact organic soil mesocosms during experimental drought and rewetting. Geochimica et Cosmochimica Acta 2008; 72: 3991-4007.

Blute NK, Jay JA, Swartz CH, Brabander DJ, Hemond HF. Aqueous and solid phase arsenic speciation in the sediments of a contaminated wetland and riverbed. Applied Geochemistry 2009; 24: 346-358.

Buschmann J, Kappeler A, Lindauer U, Kistler D, Berg M, Sigg L. Arsenite and arsenate binding to dissolved humic acids: Influence of pH, type of humic acid, and aluminum. Environmental Science & Technology 2006; 40: 6015-6020.

Campbell K, Malasarn D, Saltikov CW, Newman DK, Hering JG. Simultaneous Microbial Reduction of Iron(III) and Arsenic(V) in Suspensions of Hydrous Ferric Oxide. Environmental Science & Technology 2006; 40: 5950-5955.

Chaillou G, Schafer J, Anschutz P, Lavaux G, Blanc G. The behaviour of arsenic in muddy sediments of The Bay of Biscay (France). Geochimica et Cosmochimica Acta 2003; 67: 2993-3003.

Cloy J, Farmer J, Graham M, MacKenzie A. Retention of As and Sb in Ombrotrophic Peat Bogs: Records of As, Sb, and Pb Deposition at Four Scottish Sites. Environmental Science & Technology 2009; 43: 1756-1762.

Coker VS, Gault AG, Pearce CI, Van Der Laan G, Telling ND, Charnock JM, et al. XAS and XMCD Evidence for Species-Dependent Partitioning of Arsenic During Microbial Reduction of Ferrihydrite to Magnetite. Environmental Science & Technology 2006; 40: 7745-7750.

Cullen WR, Reimer KJ. Arsenic speciation in the environment. Chemical Reviews 1989; 89: 713-764.

Daniels SM, Agnew CT, Allott TEH, Evans MG. Water table variability and runoff generation in an eroded peatland, South Pennines, UK. Journal of Hydrology 2008; 361: 214-226.

Dawson JJC, Tetzlaff D, Carey A-M, Raab A, Soulsby C, Killham K, et al. Characterizing Pb Mobilization from Upland Soils to Streams Using 206Pb/207Pb Isotopic Ratios. Environmental Science & Technology 2010; 44: 243-249.

De Vitre R, Belzile N, Tessier A. Speciation and adsorption of arsenic on diagenetic iron oxyhydroxides. Limnology and Oceanography 1991; 36: 1480-1485.

DEFRA. Soil guideline values for lead contamination. Environment Agency, Bristol, 2002.

Dixit S, Hering JG. Comparison of Arsenic(V) and Arsenic(III) Sorption onto Iron Oxide Minerals: Implications for Arsenic Mobility. Environmental Science & Technology 2003; 37: 4182-4189.

Einax JW, Nischwitz V. Inert sampling and sample preparation - the influence of oxygen on heavy metal mobility in river sediments. Fresenius Journal of Analytical Chemistry 2001; 371: 643-651.

Emmanuel S, Erel Y. Implications from concentrations and isotopic data for Pb partitioning processes in soils. Geochimica et Cosmochimica Acta 2002; 66: 2517-2527.

Farmer JG, Graham MC, Bacon JR, Dunn SM, Vinogradoff SI, Mackenzie AB. Isotopic characterization of the historical lead deposition record at Glensaugh, an organic-rich, upland catchment in rural N.E. Scotland. Science of the Total Environment 2005; 346: 121-137.

Farmer JG, Lovell MA. Natural enrichment of arsenic in Loch Lomond sediments. Geochimica et Cosmochimica Acta 1986; 50: 2059-2067.

Gaffney JW. Role of natural organic matter in controlling the behaviour of Fe in natural waters. School of Earth, Atmospheric and Environmental Science. University of Manchester, 2008.

Givelet N, Le Roux G, Cheburkin A, Chen B, Frank J, Goodsite M, et al. Suggested protocol for collecting, handling and preparing peat cores and peat samples for physical, chemical, mineralogical and isotopic analyses. Journal of environmental monitoring 2004; 6: 481-492.

Gonzalez Z, Krachler M, Cheburkin A, Shotyk W. Spatial distribution of natural enrichments of arsenic, selenium, and uranium in a minerotrophic peatland, Gola di Lago, Canton Ticino, Switzerland. Environmental Science & Technology 2006; 40: 6568-6574.

Grafe M, Eick M, Grossl P, Saunders A. Adsorption of arsenate and arsenite on ferrihydrite in the presence and absence of dissolved organic carbon. Journal of Environmental Quality 2002; 31: 1115-1123.

Grosbois C, Schäfer J, Bril H, Blanc G, Bossy A. Deconvolution of trace element (As, Cr, Mo, Th, U) sources and pathways to surface waters of a gold mining-influenced watershed. Science of the Total Environment 2009; 407: 2063-2076.

Harrington JM, LaForce MJ, Rember WC, Fendorf SE, Rosenzweig RF. Phase associations and mobilization of iron and trace elements in Coeur d'Alene Lake, Idaho. Environmental Science & Technology 1998; 32: 650-656.

Huang J-H, Matzner E. Mobile arsenic species in unpolluted and polluted soils. Science of the Total Environment 2007; 377: 308-318.

Huang JH, Matzner E. Dynamics of organic and inorganic arsenic in the solution phase of an acidic fen in Germany. Geochimica et Cosmochimica Acta 2006; 70: 2023-2033.

Hudson-Edwards KA, Houghton SL, Osborn A. Extraction and analysis of arsenic in soils and sediments. TrAC Trends in Analytical Chemistry 2004; 23: 745-752.

Islam FS, Gault AG, Boothman C, Polya DA, Charnock JM, Chatterjee D, et al. Role of metal-reducing bacteria in arsenic release from Bengal delta sediments. Nature 2004; 430: 68-71.

Jay J, Blute N, Lin K, Senn D, Hemond H, Durant J. Controls on arsenic speciation and solid-phase partitioning in the sediments of a two-basin lake. Environmental Science & Technology 2005; 39: 9174-9181.

Jones JM. Chemical fractionation of copper, lead and zinc in ombrotrophic peat. Environmental Pollution 1987; 48: 131-144.

Keon NE, Swartz CH, Brabander DJ, Harvey CF, Hemond HF. Validation of an arsenic sequential extraction method for evaluating mobility in sediments. Environmental Science & Technology 2001; 35: 2778-2784.

Korte NE, Fernando Q. A Review of Arsenic(III) in Groundwater. Reviews in Environmental Control 1991; 21: 1-39.

La Force MJ, Hansel CM, Fendorf S. Arsenic speciation, seasonal transformations, and co-distribution with iron in a mine waste-influenced palustrine emergent wetland. Environmental Science & Technology 2000; 34: 3937-3943.

Lee JA, Tallis JH. Regional and historical aspects of lead pollution in Britain. Nature 1973; 245: 216-218.

Lin HT, Wang MC, Seshaiah K. Mobility of adsorbed arsenic in two calcareous soils as influenced by water extract of compost. Chemosphere 2008; 71: 742-749.

Linge K, Oldham C. Arsenic remobilization in a shallow lake: The role of sediment resuspension. Journal of Environmental Quality 2002; 31: 822-828.

Mandal BK, Suzuki KT. Arsenic round the world: a review. Talanta 2002; 58: 201-235.

Manning BA, Goldberg S. Adsorption and stability of arsenic(III) at the clay mineral-water interface. Environmental Science & Technology 1997; 31: 2005-2011.

Masscheleyn PH, Delaune RD, Patrick WH. Effect of redox potential and pH on arsenic speciation and solubility in a contaminated soil. Environmental Science & Technology 1991; 25: 1414-1419.

Masson M, Schafer J, Blanc G, Pierre A. Seasonal variations and annual fluxes of arsenic in the Garonne, Dordogne and Isle Rivers, France. Science of the Total Environment 2007; 373: 196-207.

Michel P, Boutier B, Chiffoleau JF. Net fluxes of dissolved arsenic, cadmium, copper, zinc, nitrogen and phosphorus from the Gironde Estuary (France): Seasonal variations and trends. Estuarine Coastal and Shelf Science 2000; 51: 451-462.

Nieminen TM, Ukonmaanaho L, Shotyk W. Enrichment of Cu, Ni, Zn, Pb and As in an ombrotrophic peat bog near a Cu–Ni smelter in Southwest Finland. Science of the Total Environment 2002; 292: 81-90.

Olivie-Lauquet G, Gruau G, Dia A, Riou C, Jaffrezic A, Henin O. Release of Trace Elements in Wetlands: Role of Seasonal Variability. Water Research 2001; 35: 943-952.

Pedersen HD, Postma D, Jakobsen R. Release of arsenic associated with the reduction and transformation of iron oxides. Geochimica et Cosmochimica Acta 2006; 70: 4116-4129.

Pfeifer H-R, Gueye-Girardet A, Reymond D, Schlegel C, Temgoua E, Hesterberg DL, et al. Dispersion of natural arsenic in the Malcantone watershed, Southern Switzerland: field evidence for repeated sorption-desorption and oxidation-reduction processes. Geoderma 2004; 122: 205-234.

Pierce M, Moore C. Adsorption of Arsenite and Arsenate on Amorphous Iron hydroxide. Water Research 1982; 16: 1247-1253.

Redman A, Macalady D, Ahmann D. Natural organic matter affects arsenic speciation and sorption onto hematite. Environmental Science & Technology 2002; 36: 2889-2896.

Ritter K, Aiken G, Ranville J, Bauer M, Macalady D. Evidence for the aquatic binding of arsenate by natural organic matter-suspended Fe(III). Environmental Science & Technology 2006; 40: 5380-5387.

Rothwell JJ, Evans MG, Daniels SM, Allott TEH. Peat soils as a source of lead contamination to upland fluvial systems. Environmental Pollution 2008; 153: 582-589.

Rothwell JJ, Evans MG, Lindsay JB, Allott TEH. Scale-dependent spatial variability in peatland lead pollution in the southern Pennines, UK. Environmental Pollution 2007; 145: 111-120.

Rothwell JJ, Robinson SG, Evans MG, Yang J, Allott TEH. Heavy metal release by peat erosion in the Peak District, southern Pennines, UK. Hydrological Processes 2005; 19: 2973-2989.

Rothwell JJ, Taylor KG, Ander EL, Evans MG, Daniels SM, Allott TEH. Arsenic retention and release in ombrotrophic peatlands. Science of the Total Environment 2009; 407: 1405-1417.

Rothwell JJ, Taylor KG, Chenery SRN, Cundy AB, Evans MG, Allott TEH. Storage and Behavior of As, Sb, Pb, and Cu in Ombrotrophic Peat Bogs under Contrasting Water Table Conditions. Environmental Science & Technology 2010; 44: 8497-8502.

Rothwell JJ, Taylor KG, Evans MG, Allott TEH. Contrasting controls on arsenic and lead budgets for a degraded peatland catchment in Northern England. Environmental Pollution 2011; 159: 3129-3133.

Sherman DM, Randall R. Surface complexation of arsenic(V) to iron(III) (hydr)oxides: Structural mechanism from ab initio molecular geometries and EXAFS spectroscopy. Geochimica et Cosmochimica Acta 2003; 67: 4223-4230.

Shotyk W, Cheburkin AK, Appleby PG, Fankhauser A, Kramers JD. Two thousand years of atmospheric arsenic, antimony, and lead deposition recorded in an ombrotrophic peat

bog profile, Jura Mountains, Switzerland. Earth and Planetary Science Letters 1996; 145: E1-E7.

Smedley PL, Kinniburgh DG. A review of the source, behaviour and distribution of arsenic in natural waters. Applied Geochemistry 2002; 17: 517-568.

Steinmann P, Shotyk W. Chemical composition, pH, and redox state of sulfur and iron in complete vertical porewater profiles from two Sphagnum peat bogs, Jura Mountains, Switzerland. Geochimica et Cosmochimica Acta 1997; 61: 1143-1163.

Syrovetnik K, Malmstrom M, Neretnieks I. Accumulation of heavy metals in the Oostriku peat bog, Estonia: Determination of binding processes by means of sequential leaching. Environmental Pollution 2007; 147: 291-300.

Tessier A, Campbell PGC, Bisson M. Sequential Extraction Procedure for the Speciation of Particulate Trace-Metals. Analytical Chemistry 1979; 51: 844-851.

Teutsch N, Erel Y, Halicz L, Banin A. Distribution of natural and anthropogenic lead in Mediterranean soils. Geochimica et Cosmochimica Acta 2001; 65: 2853-2864.

Tipping E, Smith EJ, Lawlor AJ, Hughes S, Stevens PA. Predicting the release of metals from ombrotrophic peat due to drought-induced acidification. Environmental Pollution 2003; 123: 239-253.

Todman M. Controls on water chemistry in an upland catchment. School of Earth, Atmospheric and Enviromental Sciences. PhD. University of Manchester, 2005.

van Geen A, Rose J, Thoral S, Garner JM, Zheng Y, Bottero JY. Decoupling of As and Fe release to Bangladesh groundwater under reducing conditions. Part II: Evidence from sediment incubations. Geochimica et Cosmochimica Acta 2004; 68: 3475-3486.

Vasile G, Tanase I, Dinu C. The Influence of the Air-drying Pretreatment of Sediment Samples for Metallic Element Mobilities. Analytical letters 2010; 43: 1199-1206.

Vile MA, Kelman Wieder R, Novak M. Mobility of Pb in Sphagnum-derived peat. Biogeochemistry 1999; 45: 35-52.

Walling DE, Webb BW. Estimating the discharge of contaminants to coastal waters by rivers: Some cautionary comments. Marine Pollution Bulletin 1985; 16: 488-492.

Wenzel WW, Kirchbaumer N, Prohaska T, Stingeder G, Lombi E, Adriano DC. Arsenic fractionation in soils using an improved sequential extraction procedure. Analytica Chimica Acta 2001; 436: 309-323.

Yafa C, Farmer JG, Graham MC, Bacon JR, Barbante C, Cairns WRL, et al. Development of an ombrotrophic peat bog (low ash) reference material for the determination of elemental concentrations. Journal of environmental monitoring 2004; 6: 493-501.

CHAPTER 6

Controls on the mobility of As in natural waters: The role of the Fe:OC ratio

6.1 Introduction

The occurrence of elevated concentrations of arsenic (As) in water, sediments and soils around the world poses both a human health risk to millions, and an environmental hazard (Smedley and Kinniburgh, 2002). Most notably, concentrations of As within aquifers of South-East Asia (Berg et al., 2007; Charlet and Polya, 2006; Islam et al., 2004; Stanger et al., 2005) exceed the World Health Organisation (WHO) standard of 10 μg l^{-1} (Ravenscroft et al., 2009; WHO, 2004), adversely affecting the health of millions of people. Despite numerous studies into the biogeochemistry of As, there remain significant gaps in the understanding of the mechanisms by which As is mobilised. In addition to the contamination of aquifers, increased global pressure on drinking water reservoirs has highlighted the problem of elevated As concentrations in streams and rivers arising from both geogenic and anthropogenic sources.

In aqueous environments, As can exist as a range of species, largely dependent on redox state and pH (Bissen and Frimmel, 2003). Under oxic conditions, the inorganic arsenate ion (As(V) pK_{a1} =2.2, $H_2AsO_4^-$ and $HAsO_4^{2-}$) dominates, changing to the reduced species arsenite (As(III) pK_{a1} = 9.2, $H_3AsO_3^0$ and $H_2AsO_3^-$) under oxygen depleted reducing conditions through the action of either chemical or microbial reduction (Smedley and Kinniburgh, 2002). A range of other species have also been recorded including thiols and methylated species (Andreae, 1979; Huang and Matzner, 2007) with their presence largely dictated by the localised environmental and biological conditions. The complexation and adsorptive behaviour of different species once mobilised has been the focus of a significant body of laboratory based studies (Bowell, 1994; Ghosh and Yuan, 1987; Manning et al., 1998; Raven et al., 1998), with the toxicity of As dependent on the speciation (Bissen and Frimmel, 2003). Inorganic As is generally thought to be more toxic and less mobile than the organic species (Blodau et al., 2008; Mandal and Suzuki, 2002), with the adsorptive preferences of inorganic As(III) and As(V) variable due to factors including pH, Eh, nature of binding surface and competition for binding sites with other ions (Dixit and Hering, 2003). Because of its toxicity, there is a need to understand the distribution and cycling of As in the natural environment.

Research into the occurrence and mobilisation of As has typically focused on the role of iron (Fe)-(oxy)hydroxides, due to the high affinity of As for these minerals under oxic conditions (Dixit and Hering, 2003). This has led to a large of body of work on the adsorption processes affected As relating to physicochemical conditions (Aguilar and Thibodeaux, 2005; Buschmann et al., 2006; Grafe et al., 2002; Haque et al., 2008; Xu et al., 1988), and on the role of changing

redox conditions related to the reductive dissolution of Fe minerals (Islam et al., 2004; Masscheleyn et al., 1991; Seidel et al., 2001; Signes-Pastor et al., 2007). However, recently the presence of natural organic matter (NOM or OM) has been found to influence the mobility of As within aqueous solutions (Bauer and Blodau, 2006; Buschmann et al., 2006; Redman et al., 2002; Ritter et al., 2006; Rowland et al., 2007). Formed by the decomposition of biomass, NOM is ubiquitous in the aqueous environment. Because of the range of natural processes causing the synthesis and degradation of NOM, the number of possible constituents is described as 'infinite' (Filella, 2009). Natural organic matter is commonly quantified in the aqueous phase by dissolved organic carbon (DOC) or organic carbon (OC), a set of organic molecules including humic acids (HA) and fulvic acids (FA). These molecules are formed from different materials, with FA being lower in molecular weight than HA. Both are capable of forming chemical bonds with trace elements due to the variety of functional groups present within their structure ranging from carboxylic, amino, sulfhydryl, hydroxyl, and phenolic groups (Macalady and Ranville, 1998). Because of the range of nomenclature used to describe OM in the literature (Filella, 2009), and the similarity in intended meaning between OM and OC, for the purposes of this work the term OC shall be used throughout.

A number of interactions between As and OC have been documented including competition of OC with As for binding sites on adsorption surfaces (Redman et al., 2002; Ritter et al., 2006) formation of aqueous complexes (Buschmann et al., 2006; Liu et al., 2011), and the alteration of redox speciation of dissolved As (Masscheleyn et al., 1991). The presence of OC has been found to increase As mobilisation (Williams et al., 2011), however recent work has identified that the form, and condition, of OC is an important factor (Sharma et al., 2011). The formation of aqueous complexes between As oxyanions and humic substances has been observed through both covalent binding mechanisms (Buschmann et al., 2006; Warwick, 2005), and also ternary metal bridging complexes (Liu et al., 2011; Redman et al., 2002). The presence of metals, notably Fe and Al, acting as a cation bridge between As and OC, is necessary given that under the range of pH and redox conditions experienced by natural waters, both OC and As have negative charge (Thanabalasingam and Pickering, 1986). In addition to its role as a bridging cation, Fe also has potentially a more direct control on As mobility. Under changing redox conditions Fe can re-precipitate, forming a mineral surface available for adsorption by As. The structure of the formed mineral may in turn be influenced by the presence of OC, with the occurrence of OC creating a more amorphous structure with larger surface area (Grafe et al., 2002; Pfeifer et al., 2004). These interactions have important implications for the behaviour

of As within aqueous systems given the availability of different organic compounds within the natural environment. There is also increasing awareness of the role of organic-rich soils as an important store of As (Gonzalez et al., 2006), suggesting the role of OC requires further attention. Despite this, to date, there has been little investigation of the biogeochemical processes affecting As storage, mobilisation and transport in organic-rich systems (Tipping et al., 2003).

Ombrotrophic peats are distinct environments as they are organic rich, and receive their inputs exclusively from the atmosphere. Release of industrial plumes containing large quantities of metals and metalloids into the atmosphere has resulted in widespread contamination of the peats of Northern England. Arsenic found in upland ombrotrophic peat environments has been linked to historic industrial activity, including mining and smelting (Rothwell et al., 2009; Rothwell et al., 2010). Within organic-rich surface waters, there has been a growing body of evidence of the association of As and OC within the <1 µm size fraction of the aqueous phase, suggesting colloidal interactions (Barringer et al., 2010; Haque et al., 2007; Rothwell et al., 2009). In addition to these observations, the role of colloids in the transport of As has also been established in a range of both aquifer and surface water systems (Garnier et al., 2011; Guo et al., 2011). The formation of such colloids has implications for the transport of As, as although particulate they are as physically mobile as solutes. However, for their flux to be decoupled from discharge (Q), physicochemical conditions necessary for destabilisation rather than precipitation must occur (Liang and Morgan, 1990).

The occurrence and role of colloids in the transport of As in natural systems is not currently fully understood. Analysis of <1 µm size classes have shown As, Fe and OC concentrations to be correlated (Astrom and Corin, 2000; Davis and Atkins, 2001; Puls and Powell, 1992; Ritter et al., 2006), suggesting the binding of As to colloids rich in OC and Fe (Astrom and Corin, 2000; Bauer and Blodau, 2009). In streamwaters there is a relatively high proportion of total Fe and OC in the colloidal fraction, each component mutually stabilising the other (Gaffney et al., 2008; Pédrot et al., 2011; Pullin and Cabaniss, 2003; Ritter et al., 2006). Therefore, it seems likely that given its affinity for Fe-minerals, As will also be concentrated within this colloidal fraction (Fritzsche et al., 2011; Guo et al., 2011; Sharma et al., 2010). In an effort to understand As mobility within the colloidal size class, recent field based research has concentrated on broadly characterizing the occurrence of colloidal As within field sites (Garnier et al., 2011; Guo et al., 2011).

The interaction of As, Fe and OC in the natural environment is complicated due to a number of factors involving the inherent variability of natural systems. Unlike laboratory systems, the nature and composition of both OC and mineral material is variable, and largely uncharacterised. Recent studies characterising the formation of colloidal material using natural sourced minerals and OC (Fritzsche et al., 2011; Sharma et al., 2011), have found that the type and condition of OC influences the aqueous complexes formed. In addition to the nature of the Fe and OC, stream systems are inherently 'flow through' systems, meaning that there is a dependency on Q to mobilise the stored material within the system, with the possible interactions also dependent on the time available within the system. Discharge within a system is also a complex process, with antecedent conditions impacting the movement of rainwater through the ground (Worrall et al., 2002). Furthermore, the time dependency of the mobilisation and movement of different stores of material within the system may influence the resulting associations, resulting in hysteresis effects (Morel et al., 2009; Taylor et al., 2008; Worrall et al., 2002).

These observations, along with the identified role of colloidal association of As within laboratory systems (Bauer and Blodau, 2009; Redman et al., 2002), clearly illustrates the need to understand the role of both Fe and OC on the partitioning of As within natural systems. Whilst efforts have been made to understand the speciation and size of Fe within natural and laboratory simulations (Gaffney et al., 2008; Ritter et al., 2006), the influence of fluctuating Fe: OC ratios on As partitioning in natural systems is currently unexplored.

In order to understand how As is transported within organic-rich stream environments, the primary aim of this research was to understand the factors controlling the size, and therefore mobility, of As in the aqueous phase. To achieve this, objectives of this research include:

i) Determine the flux of As from an upland peat catchment to ascertain whether transport was primarily occurring in the dissolved phase.

ii) Measurement of the Particle Size Distribution (PSD) of As within the aqueous phase of two streams draining a natural upland catchment (Crowden Great Brook, Peak District, UK) over a range of Q conditions.

iii) Determine how associations between Fe, As, OC change with Q. Use of the correlation between Fe, As, OC and Q in different size classes under different hydrological conditions in order to identify the key factors controlling the distribution and ultimate fate of As.

iv) Given the identified role of both Fe and OC on As distribution in previous studies, the variability of Fe:OC experienced and the size of As present in both streams is determined from both a) long term catchment data, as well as b) intensive event sampling in order to identify their likely role under differing hydrological conditions.

6.2 Methods

6.2.1 Field Area

The study area, Crowden Great Brook, is located within the Peak District National Park which is part of the southern Pennine uplands, situated between Manchester and Sheffield in the UK (Figure 6.1). The position of the Peak District has resulted in years of atmospheric contamination from historic mining, smelting and industrial activity in neighbouring areas. Concentrations of contaminants such as As, Pb and other trace elements are known to be elevated in the surface peat (Lee and Tallis, 1973; Rothwell et al., 2007). The total upland area (7 km^2) is drained by a stream flowing from Black Hill (530 m above ordinance datum (AOD)) into Torside reservoir; part of the Longdendale reservoir series (220 m AOD) (Todman, 2005). At higher altitudes the area is overlain by ombrotrophic (rainwater fed) peat which covers approximately 70 % of the catchment (Todman, 2005).

The dominance of the ombrotrophic peat within the surface soils has resulted in a relatively uniform average carbon content within the area, ranging from 45 % - 50 % (Rothwell et al., 2009). However, the condition of the ombrotrophic peat is not uniform. While close to the headwaters of the main stream the peat is largely vegetated, further downstream to the west of the river substantial sections of the peat are in a degraded state, without vegetation, and subject to erosion of surface layers (Figure 6.1 c,d).

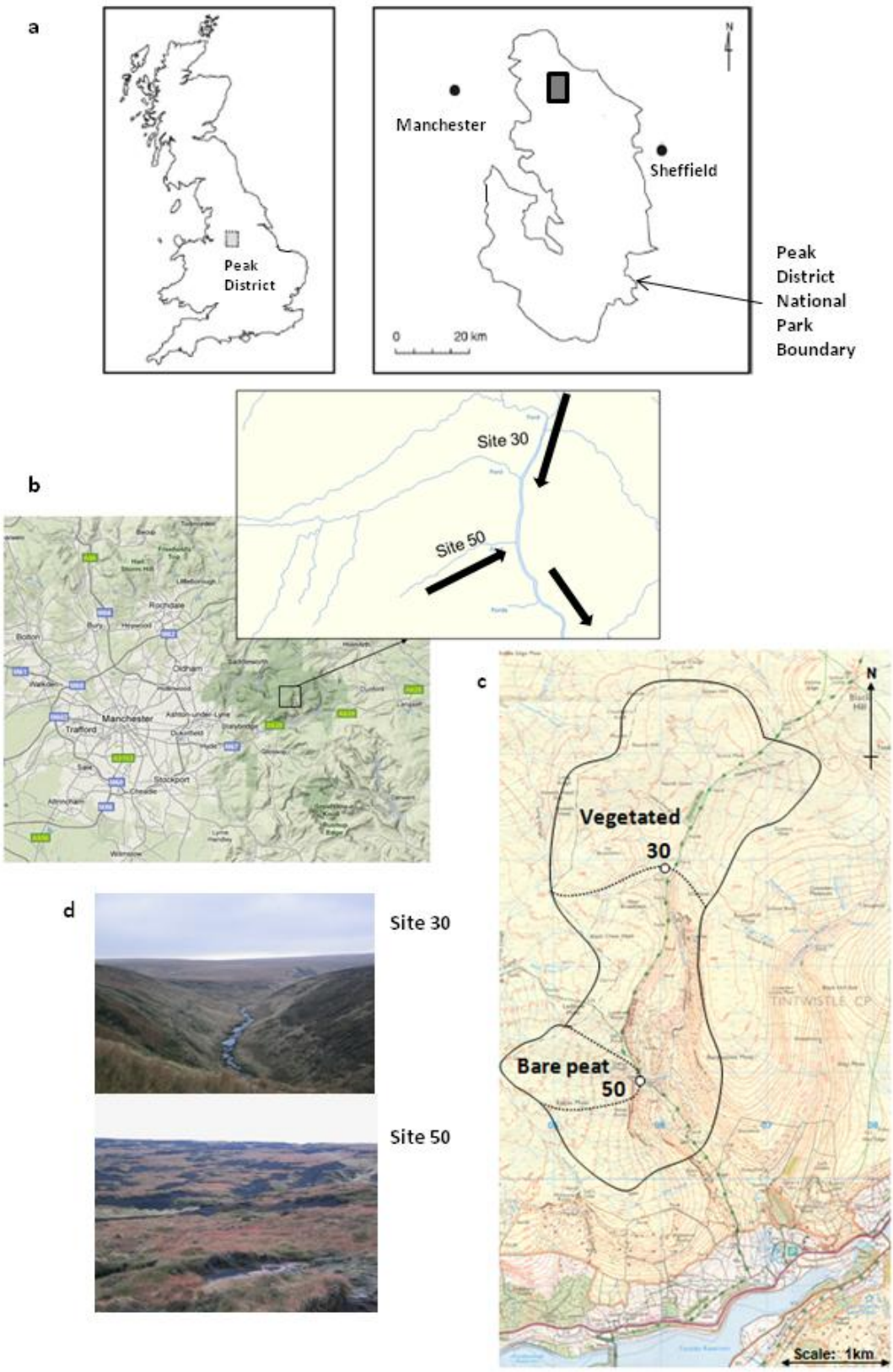

Figure 6.1 **Location map of Crowden Great Brook study area.** **a) denotes the location of the Peak District to major cities, b) illustrates the location of the field area with regard to the Peak District, and stream connectedness within, (arrows indicate direction of stream flow) c) catchment and subcatchment boundaries d)photographs of subcatchments. Adapted from Rothwell et al (2009).**

Two sampling areas were selected within the Crowden Great Brook catchment to allow for determination of the effect of peat condition on the transport of As. Site 30 (OS grid 06162 02936) is the sampling location to which the vegetated peat sub-catchment (3 km^2), site 50 (OS grid 05849 00912) the eroded peat sub-catchment (0.5 km^2)(Figure 6.1b). While the underlying geology of the area is dominated by Upper Carboniferous sandstone, shale and mudstone, with kinder grit, the dominant series (Gaffney et al., 2008), a band of marine shale is also present in the vicinity of Site 30.

6.2.2 Collection, preparation and analyses of water samples

A combination of intensive storm water sampling and general interval water sampling was conducted in the streams at both sites. Over a period of ten months from October 2009 through to July 2010, over 80 samples were collected at each site. Two intensive storm events "discharge events" were also sampled during November 2009 and July 2010. Sampling was distributed throughout the study period, and achieved by both spot sampling, and the use of two automatic sampling systems (SIGMA 900), triggered by manual sample programming. Each sampler inlet was located as close as practicable to the centre of the stream channel and above the channel bed. The water sampler was programmed to extract 500 ml samples with an inlet rinse between each sample. Sampling of the Q event was achieved through manual triggering of the automatic samplers and timing of samples to cover the forecast event.

In addition to collection of streamwaters, collection of porewaters from within the peat at site 30 were undertaken in July 2010 using a variety of methods. Initially, samples were withdrawn from an open borehole located onsite at two depths using a syringe system, samples were placed into acid washed, sealed polypropylene containers for transportation back to the laboratory. In addition to these unfiltered samples, dialysis tubing (<0.2 µm) was also used. Lengths of dialysis tubing were filled with de-ionised water (DIW) and securely tied to a wire handle, each tube was inserted into the ground, and covered with removed peat in order to equilibrate with surrounding porewaters. After several days of equilibration time, the tubing was pulled from the peat and the content carefully placed in sealed polypropylene containers.

At a minimum, upon returning to the laboratory, each water sample was divided into two subsamples: an unfiltered (UF) sample was kept, and a portion was filtered through DIW-rinsed 0.2 µm cellulose nitrate membranes to produce a soluble (<0.2 µm) fraction. Although

previous studies typically use a cut-off of 0.45 µm to represent the dissolved phase, the ongoing work in this catchment had used 0.2 µm, and so to enable continuity, was used in this study also. Both 0.2 µm and 0.45 µm exclude particulate material, but include dissolved species and some degree of colloidal material (Benoit, 1995), and as such represent an important size fraction in the transportation of contaminants. Additional filtration to establish particulate fractionation at a higher resolution was achieved on baseflow and porewater samples from site 30 at pore sizes of 5 µm and 1 µm, and on samples collected from both sites during the November 2009 Q event.

In order to establish the particulate, colloidal and dissolved size fractions of the streamwaters during the Q event, tangential flow ultrafiltration (TFU) (Vivaflow 50 system, VivaScience, UK) was used. While pressure filtration involves forcing sample through a membrane under pressure, the design of TFU allows the sample to pass tangentially over the membrane and molecules of the correct size are pulled through the membrane by gravity, enabling the separation of smaller size classes. Prior to sample analysis, TFU and cellulose filter membranes were always ensured blank by first flushing with 15 MΩ DIW and subsequent filtrates and retentates analysed for OC concentrations. Flushing was repeated until the OC concentration was comparable to that of DIW.

The size classes >0.2 µm as particulate, <0.2 µm, >10 kDa as colloidal and <10 kDa as dissolved were used (Gaffney, 2008). The obtained < 0.2 µm samples were sequentially filtered through paired 1000 kDa, 50 kDa and 10 kDa TFU membranes in order to obtain large (<0.2 µm, >1000 kDa), medium (<1000 kDa, >50 kDa) and small (<50 kDa, >10 kDa) colloids. Once the sample separation was complete, 100 ml of pH 2 DIW and then 100 ml of DIW were recirculated through each membrane in order to recover any remaining material.

A portion of each filtered sample was acidified using concentrated HNO_3 (Analar grade, Fisher chemicals, UK) to pH< 2. Sample handling was completed within 12 hrs of return from field. Prior to collection, all plastic-ware was cleaned by soaking in 10% (v/v) HNO_3 for >24 hr followed by rinsing with Milli-Q water (18MΩ). Samples were subsequently analysed for As, Fe, and other elements including manganese (Mn), magnesium (Mg), calcium (Ca), sodium (Na), lead (Pb) and zinc (Zn) using a combination of inductively coupled plasma- mass spectrometry (ICP-MS, VG Elemental) and inductively coupled plasma- atomic emission spectrometry (ICP-

AES, VG Elemental Horizon). A combination of blanks and replicate standards and samples were used in the analysis to correct for drift and measure error.

Continuous *in situ* data from each site was collected as part of an ongoing catchment study. Data was collected using Sentry II loggers (Intelisys, UK). At each site, attached to each logger are a pressure transducer (Intelisys, UK), pH probe (Russell, Fife, Scotland) and turbidity cell (Partech, St Austell, UK). At site 50 a barometer (Intelisys, UK) is additionally positioned to adjust for atmospheric pressure when considering stage and Q. The sampling interval on each logger was set to 15 minutes. Prior to placing the equipment in the field all probes were calibrated using known standards and Sentry II software (Intelisys, UK). Data was periodically downloaded, with spot samples of pH taken using calibrated field probes and measurements of Q taken to check and correct for drift in the probes. Discharge was determined by dilution gauging according to the protocol detailed in Chapter 2 on each site visit. Subsequently, stage measurements were converted into a continuous Q record using a Q relationship developed for each site with ongoing data collected since 2003 (Gaffney, 2008).

Solutions were analysed for As by inductively coupled plasma – mass spectrometry (ICP-MS, VG Elemental) with a detection limit of < 1 µg l^{-1}. Iron concentrations were determined by ICP-AES. Instrumental drift was corrected through use of linear interpolation of standards run every 10 samples. Reagent blanks were run and found to be below the limit of detection.

Total organic carbon (TOC) analysis was performed on both UF and each filtered water sample using the protocol outlined in Gaffney (2008). Because of the nature of the particle size determinations used in this study, herein OC is used to describe any organic carbon present within a sample, with the appropriate size fraction noted. Briefly, TOC analysis was achieved using a Shimadzu 5050A TOC analyser (Shimadzu, Japan). Total carbon (TC) stock solutions were prepared using 2.125 g potassium hydrogen phthalate (reagent grade, Shimadzu, Japan) in 1 l of 15 MΩ ultra violet (UV) treated DIW (Elga, Option 4, water purifier), and inorganic carbon (IC) stock solutions were prepared using 3.5 g sodium hydrogen carbonate (reagent grade, Shimadzu, Japan) and 4.41 g sodium carbonate (Shimadzu, Japan) in 1 l of UV treated DIW (Elga, Option 4, water purifier).

Standards were prepared daily by diluting the stock solution using 15 MΩ UV treated DIW (Elga, water purifier) and were analysed at the start and end of each period of analysis. TC was calibrated using 0, 1, 5 and 20 mg l^{-1} standards. A 50 mg l^{-1} standard was analysed in the event

of a sample containing >20 mg l^{-1} TC. Samples >50 mg l^{-1} were diluted into the range of the TC standards to avoid sample carryover associated with high TC concentrations. Every 5 samples a standard closest to the concentration of the samples was analysed as a check standard. IC was calibrated using 0, 0.5 and 5 mgl^{-1} standards with a 10 mg l^{-1} standard being analysed in the event of a sample containing >5 mg l^{-1} IC. Every 5 samples a standard closest to the concentration of the samples was analysed as a check standard. Unfiltered samples were manually thoroughly mixed prior to injection to ensure representative sampling of settled material.

Differing instrument performance over the course of a period of analysis was attributed to linear drift of the instrument. This was corrected using a linear drift correction programme (Boult, 2000) which corrects data according to standard concentration and also according to time; assuming that the time and therefore drift between each sample measurement is equal. In effect the programme draws a polygonal surface between standard concentration and between sets of standards (time); assuming that sample values can be corrected to a point somewhere on this surface by linear interpolation between known standard concentrations. Analytical error was considered a result of instrument drift therefore TOC concentrations from hereon are presented with no error as it is assumed to be removed by the linear drift correction process.

6.2.3 Chemical Digestions

In addition to the water samples, ponded Fe(oxy)hydroxide evident at Site 30 was also collected during the winter of 2009 and subjected to a total digest following drying and weighing of the sample. Total metal concentrations were determined by HNO_3-H_2O_2 total digest on dried subsamples using a MARS Xpress microwave (CEM, Germany) utilising a closed vessel system under US EPA method 3051A. The digested sample was analysed for As by ICP-MS (detection limit 1 µg l^{-1}) after dilution to a suitable % HNO_3 to be run on the instrument (Krachler et al., 2002). Iron and other major elements were determined by ICP-AES (VG Elemental Horizon). Matrix matched standards were used in order to allow for the different instrument response. Instrumental drift was corrected through use of linear interpolation of standards run every 10 samples. Reagent blanks were run and found to be below the limit of detection on the ICP-MS.

6.2.4 Calculation of As Flux

Two methods of flux determination were utilised in this study. The first, used a simple interpolation to estimate the rate at which both UF and < 0.2 μm As leave each catchment. Each of the UF and <0.2 μm concentrations (μg l^{-1}) obtained from the collected water samples was multiplied by Q (l s^{-1}), and to give their instantaneous fluxes (μg s^{-1}). These were multiplied by the inter-sample period (s) to give masses (μg) which were summed, and divided by the total time period and the area of each subcatchment to give a flux (kg km^{-2} yr^{-1}). Error was determined by the extrapolation of analytical uncertainty in the interpolation calculation.

To verify the interpolation a second method was used over a period at site 50, during which continuous pH measurement was made. A rating curve approach, using the negative relationship between pH and As concentration allowed an estimation of As flux to be made without temporal interpolation. The pH As relationship had been recognised in previous work wherein it was thought that the flushing of porewaters containing high levels of humic acids also transport quantities of other dissolved elements (Rothwell et al., 2009; Tipping et al., 2003). A continuous record of pH (15 min intervals) at site 50 for the seven months between October 2009 – July 2010, was converted to dissolved As concentrations (μg l^{-1}) using a regression model using 89 data pairs. Multiplication of As concentration by Q, summation and division by the area of the subcatchment gave an annual flux (kg km^{-2} yr^{-1}). The standard error for the regression line was used to calculate the error on each of the annual fluxes.

6.3 Results and Discussion

6.3.1 Streamwater chemistry and As movement

Table 6.1 summarises As, OC and Fe concentrations at sites 30 and 50 over the duration of the study. While soluble (<0.2 μm) mean As concentrations are similar at both sites (1.1 μg l^{-1} at site 30 vs. 2.0 μg l^{-1} at site 50), the range and standard deviation of measured concentrations for both the soluble and UF fractions reveals there is a difference in distribution between the two streams. Within the unfiltered (UF) fraction at site 30, the standard deviation of concentrations is larger (3.8 μg l^{-1}) than within the soluble fraction (1.6 μg l^{-1}). However at site 50 no such difference is observed with the standard deviation of the measured samples similar between both size fractions (soluble 1.4 μg l^{-1}, UF 1.5 μg l^{-1}). This indicates that the size of As

being transported in the streams differs, with the bulk of As within the site 50 stream found in the soluble fraction. The division of As between the two size classes at site 30, and the significant proportion of As found within the UF fraction (Table 6.1) illustrates that particle size, including the role of colloidal material is a factor in the transport of As within this stream.

Table 6.1 Summary of stream water quality and discharge (Q) over study period, including As, Fe and OC concentrations in streamwater and porewater

		streamwater						porewater		
		< 0.2 µm			UF			< 0.2 µm		
		mean	stdev	range	mean	stdev	range	mean	stdev	range
Dates	10/2009 - 08/2010									
Site 30										
No. of points	100							7		
pH range	4.6 - 7.0									
Discharge (Q) (l s^{-1})					61		2 - 1034			
As (µg l^{-1})		1.1	1.6	0 - 15.9	2.6	3.8	0.6 - 33.8	7.6	2.9	4.6 - 11.6
Fe (mg l^{-1})		2.0	1.6	0.3 - 8.1	7.3	16.1	1.12 - 152			
OC (mg l^{-1})		16.2	5.3	0.4 - 34.1	21.4	7.8	6.5 - 67.6	30.6	10.1	16.6 - 38.7
Site 50										
No. of points	81									
pH range	3.9 - 6.9									
Discharge (Q) (l s^{-1})					24		0 - 192			
As (µg l^{-1})		2.0	1.4	0 - 4.2	2.3	1.5	0 - 4.9			
Fe (mg l^{-1})		0.2	0.1	0 - 0.5	0.4	0.2	0 - 1.0			
OC (mg l^{-1})		18.5	8.2	3.1 - 33.7	22.6	13.1	3.6- 67.3			

Concentrations of Fe are significantly elevated in the streamwaters draining the site 30 subcatchment (Figure 6.2) with concentrations as high as 152 mg l^{-1} measured within the UF streamwaters (Table 6.1). The enrichment of Fe reflects the local geology of the catchment, with the peat within site 30 underlain by a marine shale band, containing elevated levels of Fe. In contrast to the behaviour of both As and Fe, concentrations of OC leaving both catchments are similar within both size fractions (Table 6.1, Figure 6.2).

Alongside the comparison of concentration data between sites, the effect of stream flows, and dilution must also be considered. Within site 30 there is a large variation in the Q, ranging from 2 - 1034 l s^{-1}, while at site 50, the flows are considerably lower, ranging from 0 – 192 l s^{-1} (Table 6.1, Figure 6.2). The more consistent concentrations observed at site 50 may be indicative of both the behaviour of the eroded peat, and the Q within the site 30 subcatchment. The lack of vegetation and presence of gullies created by erosion at site 30 may not allow large pools of As to accumulate within the porewaters between flushing events, leading to more consistent

outflows. The lower flows in the stream may also stop any marked dilution effect in measured concentrations.

In addition to the mobilisation processes occurring within the solid phase, the physical movement of released As must also be considered. Hydrological processes involving flow routing are key factors in the transport of contaminants including As. The large variation in concentration seen at site 30, and the difference in the size distribution of As observed between sites within the same catchment, is indicative of the complexity of the environmental processes contributing to the both the mobilisation and transport of As. Previous work (Chapter 5) has shown variation in the concentration profiles of As within both catchments. It was also shown that As undergoes post depositional movement in the peat, leading to release of As from the solid phase. This movement results in porewaters enriched in As and OC, with up to 11.6 µg l^{-1} As and 38.7 mg l^{-1} OC seen in <0.2 µm fraction of porewaters at site 30 (Table 6.1). The channelling of rainwater runoff and the associated 'flushing' of porewaters is dependent on the moisture conditions within the peat, and consequently on the antecedent conditions. Movement of stormflow water through peat catchments has been found to occur through the upper centimetres of the peat (Daniels et al., 2008), while baseflow moves through deeper peat layers. Channelling of flow through different, more As-enriched areas or layers of peat will result in variation in amount of As transferred into the streams.

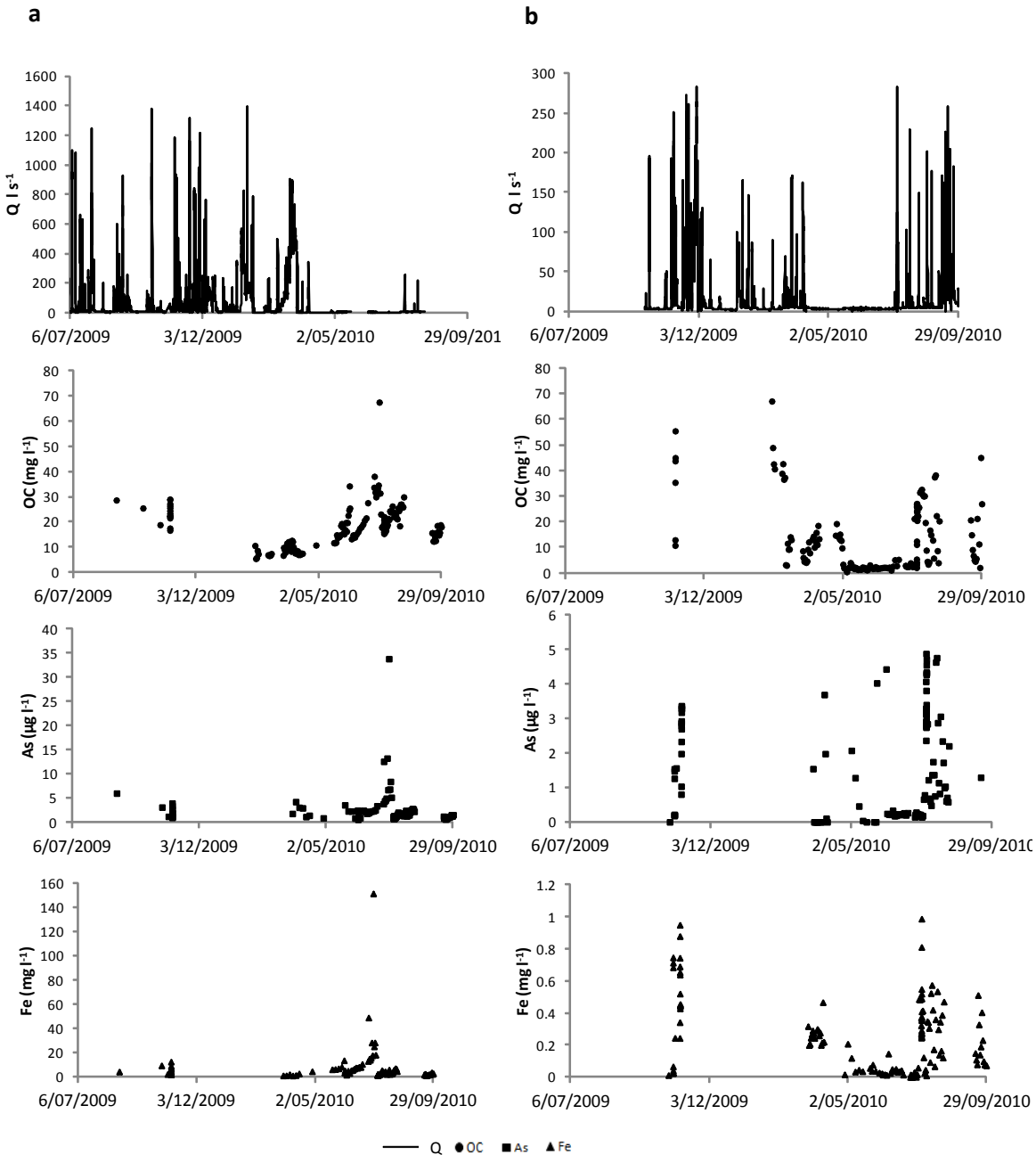

Figure 6.2 **Dissolved As, OC and Fe concentrations and discharge (Q) for a) site 30 and b) site 50 for the period July 2009- November 2010. Data gaps are due to sampling system failures.**

6.3.2 As Flux

Fluvial fluxes for the UF and <0.2 µm fractions were calculated by interpolation to be 0.16 ± 0.02 kg km^{-2} yr^{-1} and 0.30 ± 0.02 kg km^{-2} yr^{-1} respectively for site 30 and 0.23 ± 0.03 kg km^{-2} yr^{-1} and 0.35 ± 0.03 kg km^{-2} yr^{-1} for site 50 (Table 6.2). Comparison of the values obtained for each site shows that the flux (kg km^{-2} yr^{-1}) of As is higher for the more degraded site 50 than the vegetated site 30. This observation would suggest that erosion, significant at Site 50, played an important role in introducing metal(loid)s to the stream. However, the transport of As appears more complex than this, with the interpolated flux for site 30 having a lower proportion of As transported in the <0.2 µm fraction than site 50. Had erosion been the sole source of As into the stream at site 50, the proportion of soluble (<0.2 µm) As would be expected to be minor, and/or there should be a difference observed between the two contrasting sites. The significant contribution (>50 %) of the <0.2 µm fraction at both sites indicates that the effect of erosion on the transport of As at site 50 appears to be secondary to other mobilisation processes occurring within the peat. Transport of As in both catchments appears to involve dissolved and colloidal forms of As as key transport species.

Table 6.2 Flux Calculation Summary

		Interpolation		pH ratings curve	
		< 0.2 µm	**UF**	**< 0.2 µm**	**UF**
Site 30	As kg km^{-2} yr^{-1}	0.16 ± 0.02	0.30 ± 0.02	-	-
Site 50	As kg km^{-2} yr^{-1}	0.23 ± 0.03	0.35 ± 0.03	1.14 ± 0.21	1.74 ± 0.33
		% of calculated annual As mass transported in events			
Winter 'first flush' event					
	Site 30	2	3	-	-
	Site 50	11	8	2	3
Summer 'post first flush' event					
	Site 30	0.1	0.1	-	-
	Site 50	2	1	-	-

Although interpolation uses >87 samples, some taken as frequently as daily, it cannot represent the large variation in conditions evident from the available continuous data (Figure 6.2). The importance of high Q events in the transportation of As was evaluated through two events incorporated into the point sample collection. The percentage of total As transported during the two events are displayed in Table 6.2, illustrating the importance of antecedent conditions. It is apparent that the first flush event, lasting 10 hours, represents a significant proportion of the total As transported during a year, as calculated by the interpolation method for both sites. However, the sampling of the second event, in July 2010, missed the initial flush, and consequently, despite the elevated Q at both sites experienced during the sampled part of the event (data not shown), the amount of As transported is minimal (Table 6.2). This observation is suggestive of the role of flushed porewaters within the peat in the transportation of As from the catchment. As a measure of the transported material within a catchment, flux determined by interpolation relies on not only a representative range of Q values, but also consideration of the temporal weather conditions that will affect the transportation of metal(loids) during an event.

Due to limitations of the low temporal resolution dataset used in calculating an interpolated flux, a second method of flux calculation was used for site 50, with available in-situ continuous pH and Q data. The calculated fluvial flux for site 50 using the relationship with pH and utilising the continuous Q data was found to be higher than those calculated by interpolation at 1.14 ± 0.21 kg km^{-2} yr^{-1} and 1.74 ± 0.33 kg km^{-2} yr^{-1} for >0.2 µm and UF respectively (Table 6.2). It is apparent that inclusion of the continuous dataset (of both pH and Q) has increased the calculated flux. The proportion of As transported in the winter event is correspondingly decreased, however at 2-3 % this still represents a significant movement of As due to the increase in Q. Once again, the importance of As transport in the dissolved and colloidal size range is highlighted, with over 65 % of As transported in the <0.2 µm fraction.

6.3.3 Relationships between As, Fe and OC

The calculated fluxes revealed that the distribution of As between the particulate and <0.2 µm fraction was variable, however dissolved and colloidal transport of As was important at both sites. Given the role of colloidal material in transporting As through each catchment, understanding the associations of As within the streamwater is paramount to understanding the controls on As transport. As a result of the contrasting Fe concentrations between the sites, the ratio of Fe:OC also varies significantly between the two subcatchments (Figure 6.3),

with the ratios at site 30 much higher than those seen at site 50. Within the UF water samples at site 30 there is a positive correlation (R^2 0.79) between the As concentration and the Fe:OC. Although a slight positive correlation is noticeable within the <0.2 µm fraction, it is not significant. Similarly, at Site 50, no relationship is evident between As concentration and Fe:OC when considering the dataset as a whole.

A recent laboratory based study by Bauer and Blodau (2009) found the distribution of As within the aqueous phase to be strongly influenced by the ratio of Fe: OC within the system. Arsenic in colloidal size fractions was found to increase in the presence of OC. At lower initial Fe:OC ratios (<0.02), As was found in the dissolved size fraction, with an increase in ratio causing As to be found in larger size classes due to the binding of As to newly formed Fe(oxy)hydroxides. However, the range of Fe:OC ratios observed in our field systems were much greater than those used in laboratory studies (Bauer and Blodau, 2009; Ritter et al., 2006), suggesting that the application of such results may be inappropriate. Furthermore, their finding that Fe:OC ratios > 0.1 results in all As > 0.2 µm is not supported by our data, where <0.2 µm As is found at ratios up to 0.35. The size distribution of As in the natural environment appears to be controlled by a larger range of factors than those in simple laboratory systems, and use of overall Fe:OC alone is not sufficient to predict particle size within the surface waters.

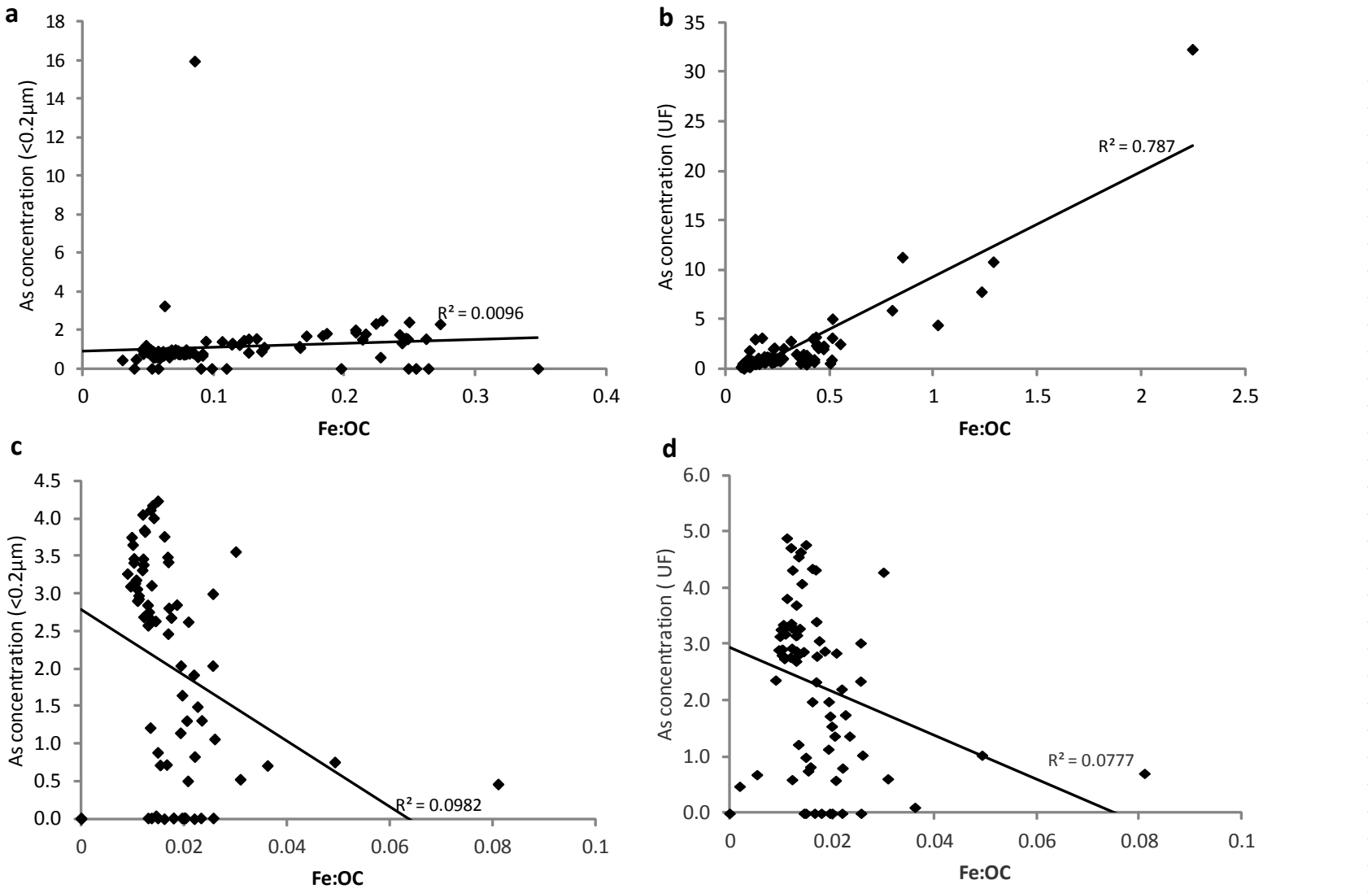

Figure 6.3 **Comparison of As concentration and Fe:OC ratio in <0.2 µm and UF size fractions. a) Site 30 <0.2 µm, b) site 30 UF, c) Site 50 <0.2 µm, d) site 50 UF. Drawn line represents linear relationship, with calculated R^2 displayed within each graph.**

Particle size distribution (PSD) of waters collected during summer baseflow (July 2010) from the stream and porewater at site 30 (Figure 6.4) reveal that processes occurring as As moves though the catchment are causing a shift in its PSD. A slight increase in Q, above the minimum flow of 2 l s^{-1} results in a large spike in (mostly > 0.2 μm) Fe being released into the stream (Figure 6.4a). This is accompanied by increases in both OC and As within the stream. Comparison of the PSD for each element reveals that throughout the sampled period, Fe and As are coupled within the stream waters, with larger particle sizes dominating. Similarity of PSD suggests that there is a chemical or physical association between the two elements (As and Fe) in the water. However, the relative proportion of >5 μm As and Fe material is not constant, visually increasing due to an increase in Q. Relative to Fe and As, the PSD of OC is smaller in size, with a larger proportion of <0.2 μm OC present within the streamwater (Figure 6.4 a,b). This is in contrast to the PSD observed within the porewaters, sampled at two depths (Figure 6.4 c,d), where the PSD of Fe and OC are more closely coupled. Within the porewater, As is mostly found within the <0.2 μm fraction at both depths, indicating that a switch in PSD is occurring during the movement of the porewater to the stream.

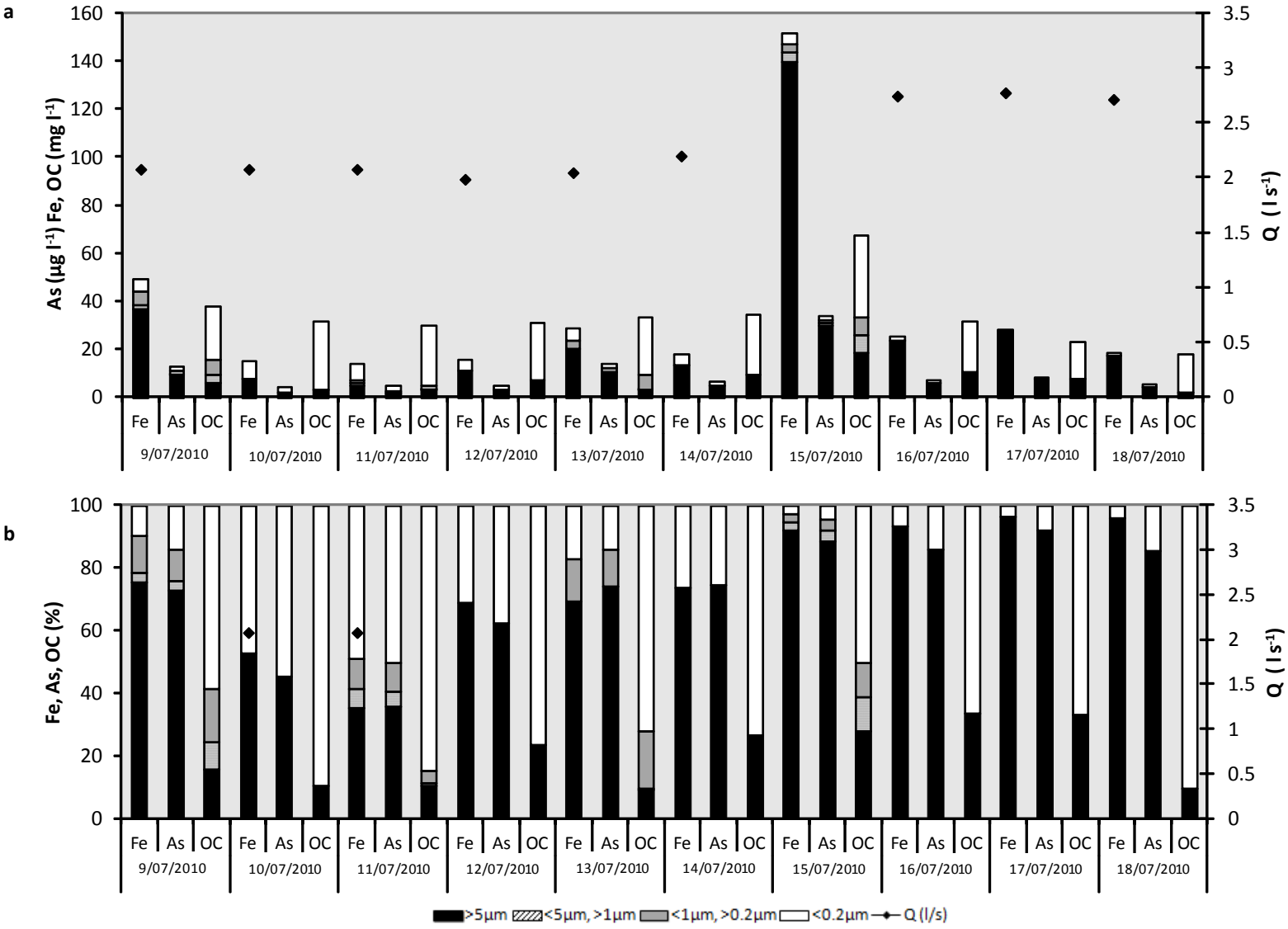

Figure 6.4

Particle Size Distribution (PSD) of As, OC, Fe and Q in baseflow and porewaters of site 30.

a) Absolute concentrations in baseflow streamwater,

b) Proportional PSD in baseflow streamwaters

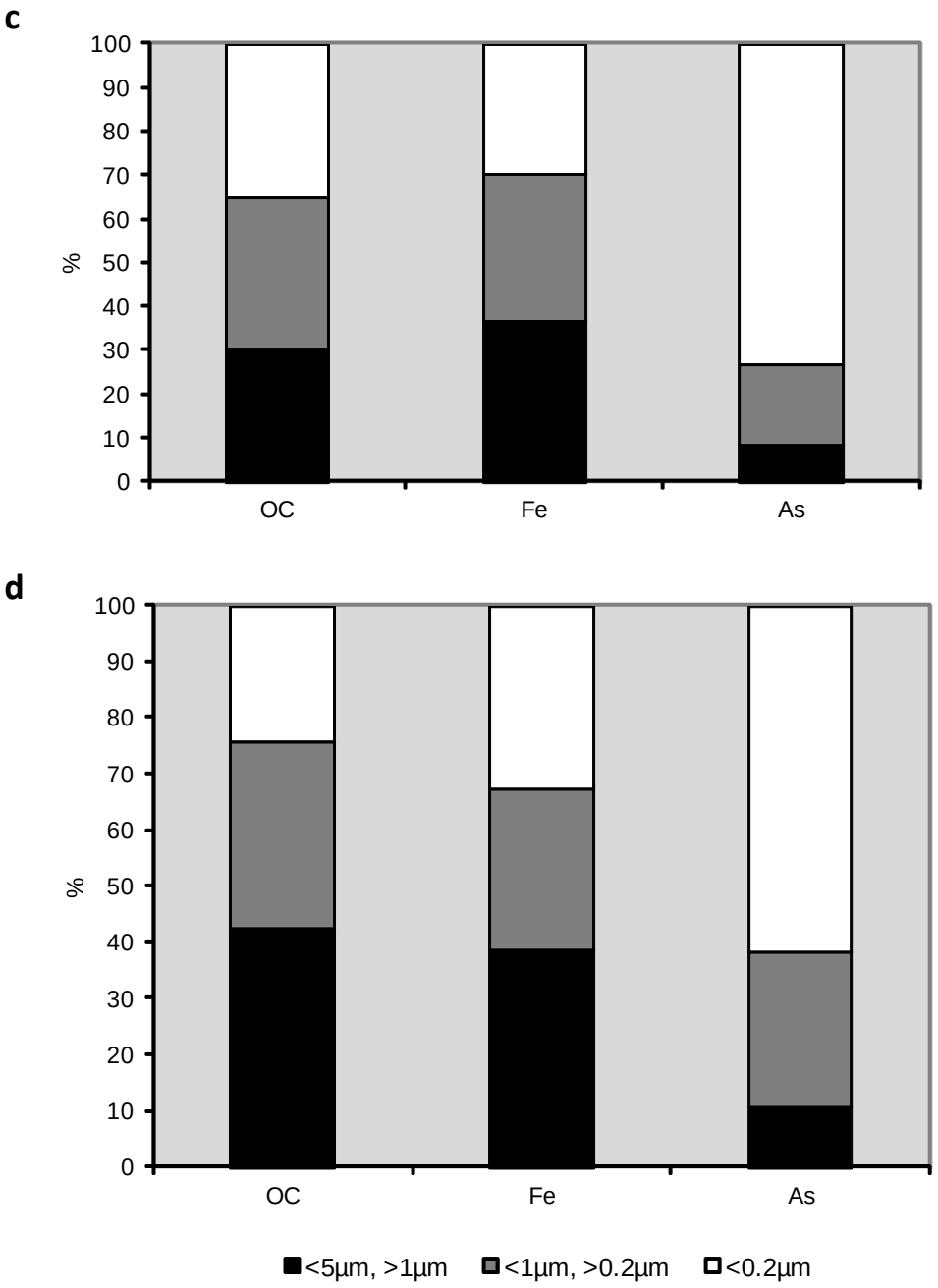

Figure 6.4(cont.) **Particle Size Distribution (PSD) of As, OC, Fe and Q in baseflow and porewaters of site 30. c) PSD in shallow (top 10 cm) porewaters, d) PSD in deeper (50 cm) porewaters**

The variation in concentration observed in the aqueous phase (Figure 6.2), along with the change in PSD of As as it moves from porewater into the stream (Figure 6.4) indicates that an environmental factor, chemical or physical, is affecting the transport of mobilised As. In order to determine the role of different elements within the stream, the correlation coefficients between As, Fe, OC and Q was calculated (Table 6.3). The most notable outcome is the lack of any correlation between As and Q within both UF and <0.2 µm samples at both sites. Similarly, Rothwell et al., (2009) found As concentrations during summer Q events to be uncorrelated with Q. It would appear that simple dilution of a single upstream input is not responsible for variation in As transport from peatlands. Separation of the dataset into high and low flows (10 ls^{-1} and 5 ls^{-1} for site 30 and 50 respectively) shows that while no correlation is seen at site 30 under either flow condition, within the low flows at site 50, a correlation is evident in both size fractions (Table 6.3). The lack of any relationship between As and Q at site 30, and the low relationship evident only at base flows at site 50 points to factors other than flow path and dilution controlling the movement of As from the peat.

Table 6.3 Correlation coefficients of As, Fe, OC and Q

correlation coefficients[a]

	Site 30							Site 50						
	UF			<0.2 µm				UF			<0.2 µm			
	All data							*All data*						
	As	Fe	OC		As	Fe	OC		As	Fe	OC		As	Fe	OC
Fe	0.94	*	*	Fe	0.07	*	*	Fe	0.31	*	*	Fe	0.25	*	*
OC	0.63	0.58	*	OC	0.09	0.40	*	OC	0.54	0.69	*	OC	0.62	0.75	*
Q	-	-	-	Q	-	-	-	Q	-	0.40	0.62	Q	-	0.29	0.45
Stratify data by Q															
	< 10 l s^{-1}							< 5 l s^{-1}						
	As	Fe	OC		As	Fe	OC		As	Fe	OC		As	Fe	OC
Fe	0.95	*	*	Fe	0.56	*	*	Fe	-	*	*	Fe	0.16	*	*
OC	0.75	0.70	*	OC	0.56	0.40	*	OC	0.80	0.23	*	OC	0.73	0.47	*
Q	-	-	-	Q	-	-	-	Q	0.29	-	0.25	Q	0.24	-	-
	> 10 l s^{-1}							> 5 l s^{-1}						
	As	Fe	OC		As	Fe	OC		As	Fe	OC		As	Fe	OC
Fe	0.40	*	*	Fe	-	*	*	Fe	-	*	*	Fe	-	*	*
OC	-	-	*	OC	-	0.34	*	OC	-	0.32	*	OC	0.54	0.61	*
Q	-	-	-	Q	-	-	-	Q	-	-	0.68	Q	-	-	0.40

[a] p <0.01

Within the UF samples from site 30, As is most strongly correlated with Fe (R^2 0.94), while only a weak (but significant) relationship is seen in the <0.2 µm fraction (Table 6.3). This is not unexpected given the observation from both the PSD and calculated fluxes, that showed particulate transport of both Fe and As dominated, especially at low flows (Figure 6.4, Table 6.2). At site 50, similar correlations are seen within the UF and <0.2 µm fractions (R^2 0.31 and R^2 0.25 respectively) (Table 6.3). Separation of the data by Q, reveals that for both size fractions a strong relationship between As and Fe is still evident at site 30 during low flows, with high flows showing a reduced correlation. At site 50, separation of the dataset does not resolve any correlation. Clearly, the role of Fe at site 50 differs to that at site 30, due in part to the geological source of Fe from the marine shale band underlying the peat, and consequent higher aqueous concentrations (Table 6.1). A positive correlation between As and Fe could suggest that the reductive dissolution of Fe occurring within the peat is responsible for releasing As during low flow conditions. Work with peat mesocosms has found the coupled release of As and Fe into porewaters (Blodau et al., 2008), while sequential extractions of peat from the catchment (chapter 5) showed a possible relationship between Fe and adsorbed As. Given that reduced Fe will oxidise in the oxic stream waters to form mineral precipitates, this may in part explain the different relationship observed in the UF and <0.2 µm size fractions, with As preferentially adsorbing to particulates.

Further to the strong relationship evident between As and Fe, the role of OC within the aqueous phase appears strong with correlations also present between both As & OC, and Fe & OC within each whole dataset (Table 6.3). Given the lower Fe & As correlation seen at site 50, the correlation with OC is the most significant (R^2 0.54 and 0.62 for UF and 0.2 µm respectively), and indicates that despite the similarity of OC concentration between the two sites, the higher concentration of Fe at site 30 dominates As behaviour. It is also of note that the correlation of Fe & OC is similar within both size classes at both sites, despite the higher Fe concentrations within site 30 and the association of Fe & As differing (Table 6.1, 6.3). The behaviour of Fe appears more consistent than As in this respect. The behaviour of As within the <0.2 µm size fraction at site 30 appears different to that observed at site 50, and within the UF fraction. The correlation of As & OC is low (R^2 0.09), while OC & Fe remains at a level similar to the UF fraction (Table 6.3). Given that a similar pattern was seen for the relationship between As &Fe, and the correlations within both size fractions are similar for As & OC at site 50, this indicates that not only does the behaviour of Fe vary to As within the <0.2 µm fraction at site 30, but that the size fractions are behaving differently between the sites.

Given the origin of both As and Fe from within the OC-dominated peat, the occurrence of correlations for both Fe and OC with As is not unexpected, being indicative of either colloidal associations between the elements or the adsorption of OC and As onto Fe mineral surfaces. Both these associations within the aqueous phase are suggested by the similarity of the correlations seen in both UF and <0.2 µm size fractions, as adsorption would be expected to make the particulate association of As dominate. These correlations clearly indicate that both Fe and OC have an important role in the transport of As in both systems, suggesting that further exploration of the role of Fe:OC is required.

Although Q was not able to explain the variability of the As dataset as a whole, the flushing of stored porewaters from within the peat is related to a combination of Q and antecedent conditions (Clark et al., 2006; Rothwell et al., 2009; Worrall et al., 2002). Despite a similar relationship at both sites between As & OC when considering the whole dataset, on splitting the data by Q a different pattern is produced (Table 6.3). At site 30, no association between As & OC is seen, while Fe & OC is correlated (R^2 0.34) within the high Q samples. At site 50, As & OC are well correlated at low flows in the UF fraction, while at high flows a correlation is only evident in the <0.2 µm fraction. The effect of sample timing in relation to Q may offer a possible explanation to the lack of any correlation at high flows. Flushed porewaters will dominate the first pulse of water moving from the catchment into each stream, so although Q may stay high, the bulk of mobilised contamination may have passed. Therefore without analysis of detailed hydrographs for each sample, the true effect of a rise in Q may be hidden. Furthermore, at high flows it is interesting to note that no strong correlation was found for As in the <0.2 µm fraction at site 30, while in the UF samples the relationship between As and Fe dominated, indicating that while adsorption onto Fe precipitates is a major factor controlling the transport of As, additional factors must also exist. While further understanding of the relationship between As, Fe and OC can be made by considering Q, the nature of storage within the peat and the movement of water through the catchment relating to antecedent conditions mean that not only Q, but the role of the sequence of variability of Q could be of significance.

6.3.4 As transport during a discharge event

Calculations of flux have identified the importance of Q events in the transport of As within both subcatchments, with evidence from correlations within the aqueous phase revealing a dependence on Q. Given the nature of water storage within peat and the role of antecedent

conditions in controlling the movement of water throughout catchments, evaluation of the transport of As under a temporal change in Q is necessary to further explore the environmental controls on As transport. In order to assess the effect of the sequence variability of Q, analysis of the Q event of November 2009 was undertaken. Occurring on the 01/11/09, this event was a single peak event, with a duration of about 10h (Figure 6.5). There was an initial rise in Q between 06:00 and 06:45, peaking between 10:00 - 10:45, flow then declined to base flow levels at approximately 16:00. The timing of sample collection was such that samples were collected on both rising and falling limbs of the hydrograph, capturing the full event (Figure 6.5). Both sites show a decrease in pH during the initial part of the rising limb, at site 30 pH falls from 6.8 to 4.8 while at site 50 pH drops from 5.6 to 4.2 (Figure 6.6).The pH at both sites remains relatively stable during the event and did not return to pre-flood levels within the time frame of sampling. Because of the stability of pH throughout the event, changes in PSD are unlikely to be due to pH.

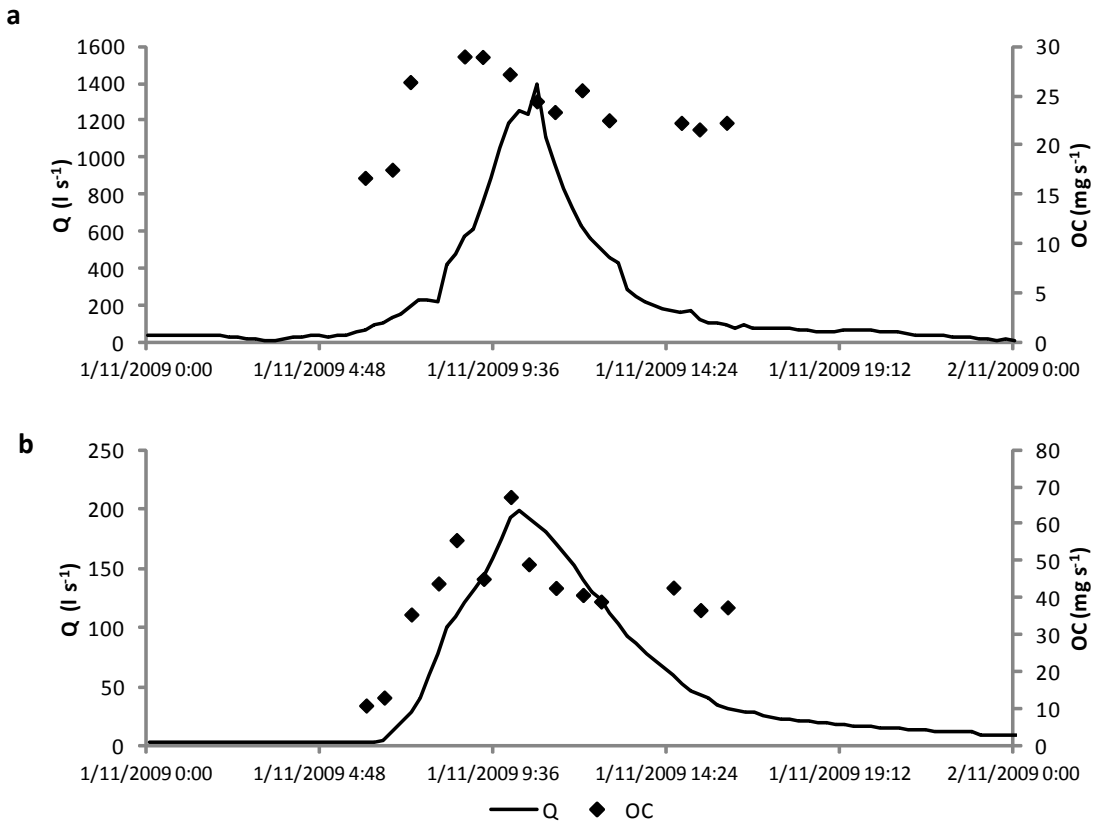

Figure 6.5 **Discharge event sample capture. Continuous discharge (Q) measurements over course of event, with location of samples illustrated by UF OC measurements a) Site 30, b) site 50**

In conjunction with the decrease in pH, the OC concentrations in the streamwaters of both sites show an increase in both UF and <0.2 µm size fractions during the event (Figure 6.6). In site 30, OC increased during the rising limb reaching 29 mg l^{-1} but then fell during peak flow, remaining higher than pre-flood levels at 22 mg l^{-1}. In site 50, the OC concentrations are higher, reaching 67 mg l^{-1} during peak flow, but similarly to site 30 remain high even after flow is fallen back to baseflow levels (Figure 6.6). A decrease in pH and increase in OC concentrations is a common trend observed during stormflow events in rivers draining catchments with NOM rich soils (Rothwell et al., 2007) and is related to the acidic compounds within NOM e.g. HA and FA.

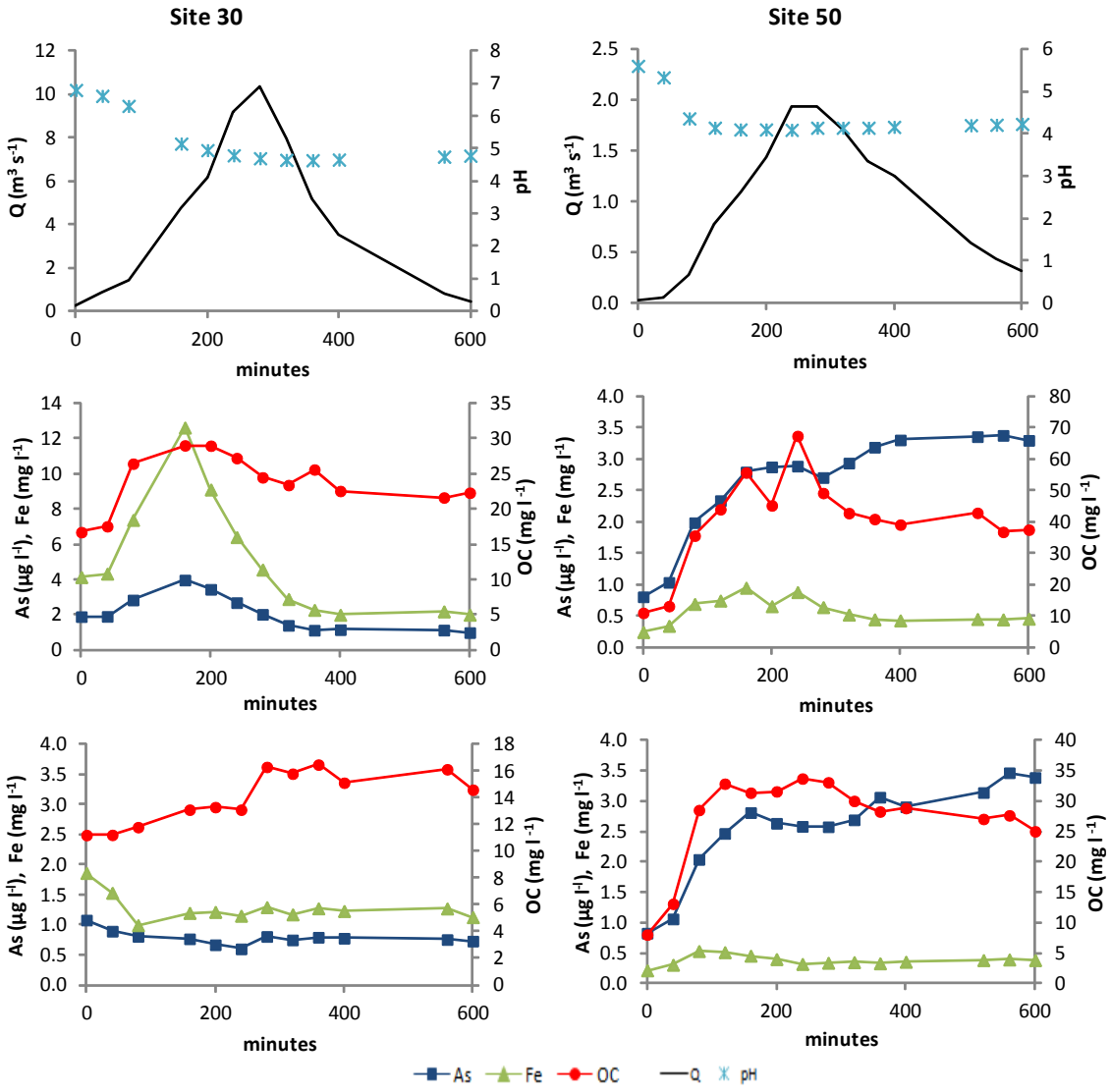

Figure 6.6 **As, Fe and OC concentrations and measured pH and Q over discharge event at site 30 and site 50. a) pH and Q, b) As, Fe and OC concentrations in UF samples, c) As, Fe and OC concentrations in <0.2 µm samples.**

Within both sites, the concentration of OC within the <0.2 µm size fraction is significant (up to 17 mg l^{-1} at site 30 and 34 mg l^{-1} at site 50), suggesting that a large proportion of OC in the streams is present in dissolved and colloidal form.

Unlike pH and OC, concentrations of As and Fe show a clear peak profile in the UF samples from site 30 (Figure 6.6 a,b). The concomitant release of As and Fe supports the role of Fe reduction in the mobilisation of As from the peat within site 30, as seen in rewetting experiments on minerotrophic peat soils (Blodau et al., 2008). Within the site 50 UF samples, while a peak is evident in Fe concentration, As shows no sign of peaking, increasing in concentration (up to 3.3 µg l^{-1}) over the duration of sampling. The difference in profile shape from the two sites is suggestive of different hydrological pathways occurring within the sites. While rapid flushing of both UF Fe and As is seen at site 30 resulting in a peak prior to maximum Q, and subsequent lowering of concentration once the stores of available As/Fe have been exhausted, the release of pooled As/Fe at site 50 is slower. Looking at the the <0.2 µm size fraction (Figure 6.6c), different profiles are observed, with both As and Fe concentrations remaining stable throughout the event at site 30. The profile for the <0.2 µm size fraction at site 50 follows closely the UF profile, reflecting that the bulk of transported As and Fe at site 50 is the <0.2 µm in size.

The complexity of the movement of stored As from within the peat is evident from the relationship with Q (Figure 6.7). It can be seen that low correlations with Q are due to the presence of both rising and falling hydrograph limbs. Discharge alone is not able to predict the concentration of (UF) As within either stream. Furthermore, the sites show differing trajectories with regard to their timeseries data. At site 30, the trajectory shows a clockwise pattern indicating proteresis. Proteresis is known as a 'flush' response, and occurs when concentrations increase more rapidly than the observed Q (Boyer et al., 1997). While at site 50 an anticlockwise trajectory is indicative of hysteresis, and is associated with slow delivery to the channel. This indicates that <0.2 µm As is entering the stream through ground water and/or transfer from deeper soil horizons, in contrast to the large particles that are either remobilised from the sediment or washed off from soil surface. The difference in peak profile and particle size of As and Fe at site 50 could therefore be a function of the hydrology, whereby the more degraded peat at site 50 is already saturated due to the breaks in surface peat condition, resulting in rainwater running off the surface without penetrating the peat. The release of porewaters is therefore restricted to the already saturated deeper layers of peat.

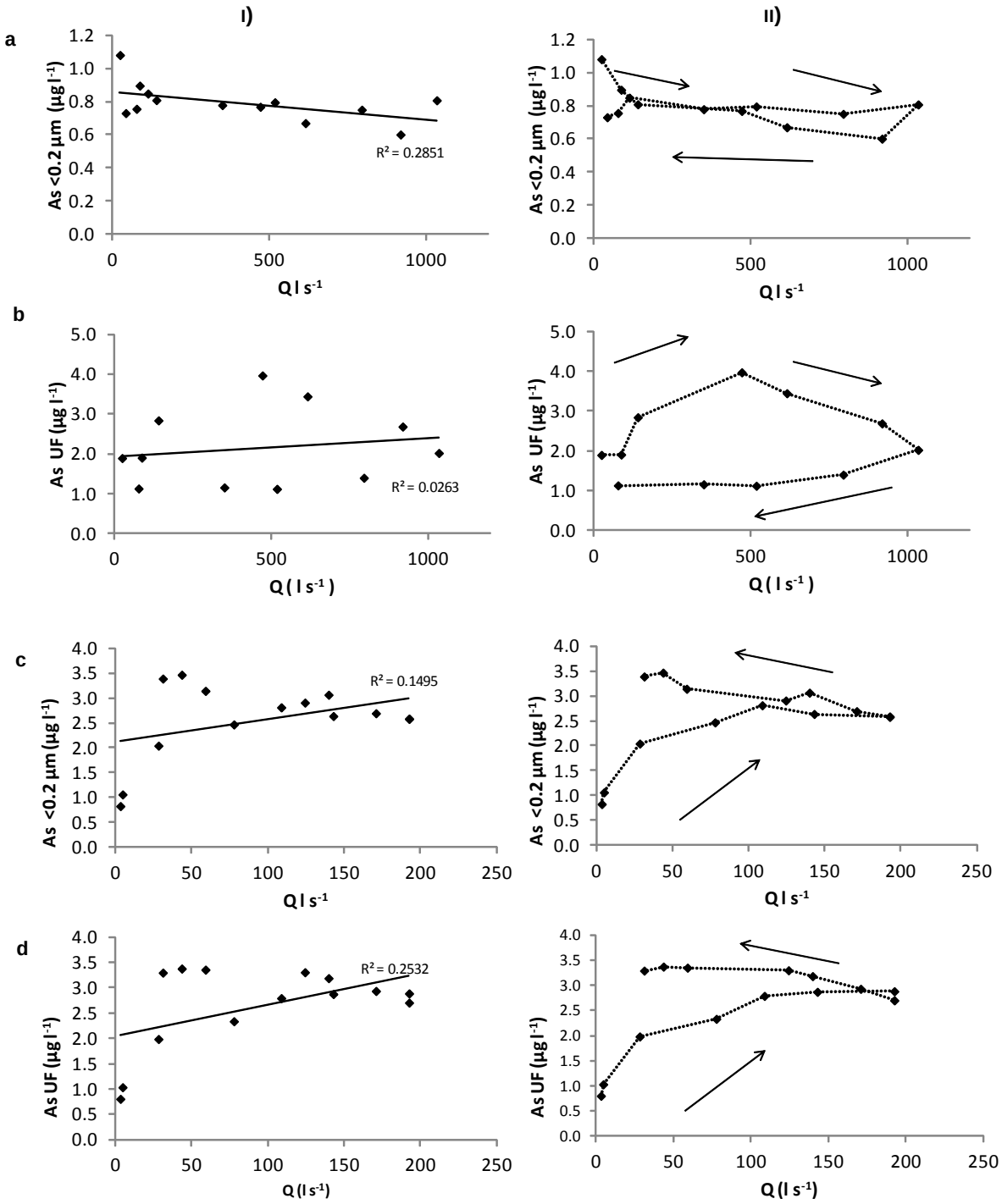

Figure 6.7 **Comparison of As and Q during discharge event. Column i) displays the overall relationship with calculated R^2 displayed, while column ii) illustrates the connectivity of the data time series, showing the time series direction using arrows. a) Site 30 <0.2 µm, b) Site 30 UF, c) Site 50 <0.2 µm, d) site 50 UF.**

While at site 30, stable vegetation has resulted in drier surface layers of peat (refer Chapter 5), allowing for rainwater to penetrate surface layers quickly and flush stores of pooled porewater along with particulate matter.

In addition to the hydrological factors contributing to the dominance of <0.2 μm As at site 50, a second explanation involving the lack of particulate Fe could also be key. Concentrations of Fe at site 30 are significantly higher than at site 50 (Table 6.1), with the proportion of particulate Fe (taken from difference in UF and 0.2 μm) higher at site 30. In addition to the elevated streamwater concentrations, pools of precipitated Fe(oxy)hydroxide were also found within the reaches of the site 30 stream. While, Fe(oxy)hydroxide phases are considered to be one of the most important natural As scavengers (Dixit and Hering, 2003), the precipitate was found to contain less than 0.01 % As, indicating the precipitate had formed in an area with little mobilised As. After accounting for other major ions, the difference in mass was assumed to be organic, resulting in an Fe:OC ratio of 0.43.

As well as the oxidation of released Fe(II)or Fe(III) from the porewaters, mobilisation of this pooled Fe precipitate would result in an increase in particulate Fe in the streamwater. Particulate Fe is then able to act as an adsorption surface for released As, increasing the particle size of As within the stream waters at site 30. Figure 6.8 shows the profile of Fe in the UF fraction along with the ratio of Fe:OC for each of the sites. At site 30, the increase in Fe is matched closely by the change in Fe:OC, peaking at 0.43, consistent with the ratio observed in the ponded Fe precipitate. This indicates that the change in Fe:OC is due to the increase in Fe, rather than from non-Fe containing OC. At Site 50, the Fe:OC is significantly lower ranging from 0.01-0.03 (Figure 6.8b), and does not follow the profile of Fe, indicating the ratio is not controlled by the (minor) Fe content.

a

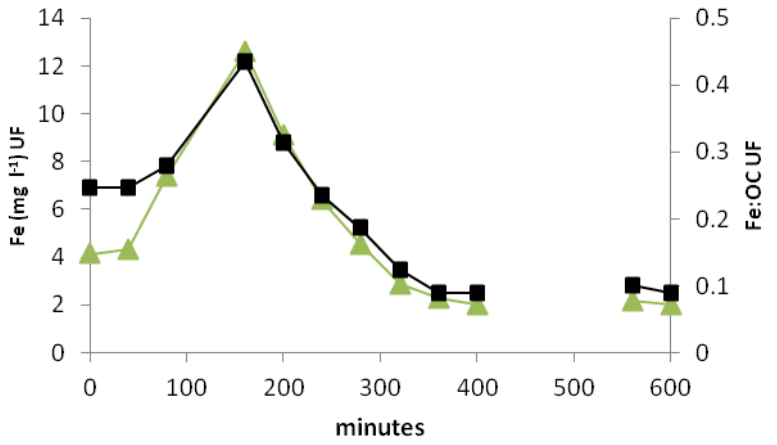

b

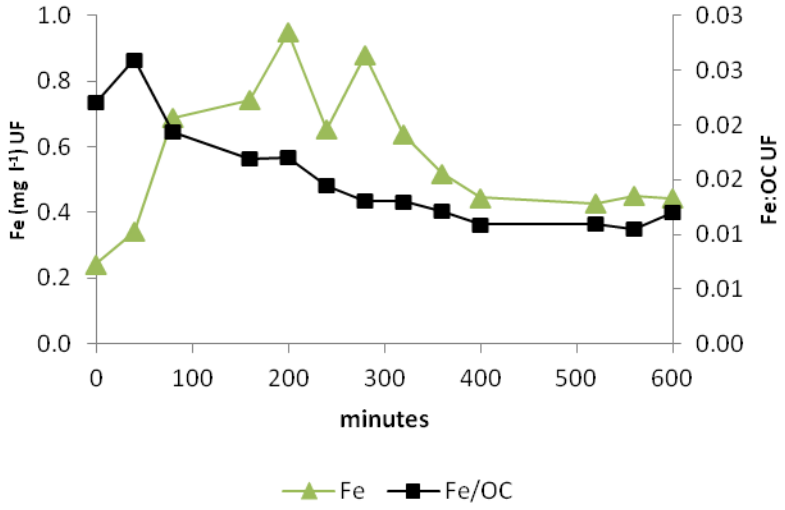

Figure 6.8 **Change in Fe concentration and Fe:OC during discharge event. a) site 30, b) site 50**

6.3.5 Changes in PSD of As, Fe and OC under temporal changes in Q

Central to understanding the factors controlling the size, and therefore mobility of As within aqueous systems is the determination of the PSD of As under a range of hydrological conditions. Review of the PSD at Site 30 during the Q event (Figure 6.9a) reveals that at the beginning of the event; As, Fe and OC distributions are relatively similar. However, As and OC may be more closely coupled with both having a lower proportion of >5 µm particles than Fe, and over 50 % present as >0.2 µm. Review of the colloidal and dissolved size fractions at 0 minutes (Figure 6.10a) reveals that while >1 µm As and Fe may be coupled, the smaller size fractions of OC and As are more similar, with all size classes, including truly dissolved (<10 kDa) represented. During the event, As is closely coupled to Fe within site 30, being found mainly within the >5 µm fraction for the duration of the event (Figure 6.9a). As particulate Fe increases, As also increases, suggesting that the adsorption of As to Fe particulates is a major transport pathway for As within this site. This is also seen in the smaller size fractions, with the proportion of < 1 µm As and Fe negligible at 200 minutes, while the OC composition remains unchanged (Figure 6.10a). At 400 minutes the proportion of >1 µm As and Fe has decreased substantially, with the proportion of >1000 kDa As and OC now similar, and over 10% As present as truly dissolved (Figure 6.10a). During the event at site 30, the PSD of As appears to be controlled by both Fe and OC, with adsorption to particulate Fe the major transport pathway for As at the peak of the event.

At site 50 As is initially found within the <0.2 µm fraction (Figure 6.9b), with a significant portion present in colloidal and truly dissolved species (Figure 6.10b). Over the course of the event, there is an increase in the <1 µm >0.2µm fraction (Figure 6.9b), indicating that the mobilised As is colloidal or dissolved in nature rather than particulate. In contrast to As, both OC and Fe show an increase in the >5 µm fraction, indicating that particulate transport of Fe and OC is important, despite the low Fe concentration (Figure 6.6). In addition to the particulate size fraction, the colloidal size fractions of Fe and OC are also coupled at 0, 200 and 400 minutes (Figure 6.10b), with the relative proportion of colloidal Fe and OC greater at the end of the event.

The size distribution of colloidal/dissolved As does not vary significantly with time, with only a minor proportion of >1 μm As present at 200 mins (Figure 6.10b), and the proportion of truly dissolved As greater than either Fe or OC in all three analysed samples. The coupling of Fe and OC within the particulate size range at site 50 could be a result of the low Fe concentrations allowing OC to dominate adsorption binding sites, preventing As from binding (Grafe et al., 2002; Redman et al., 2002). However, the presence of Fe-OC complexes is also indicated by the occurrence within the colloidal size range.

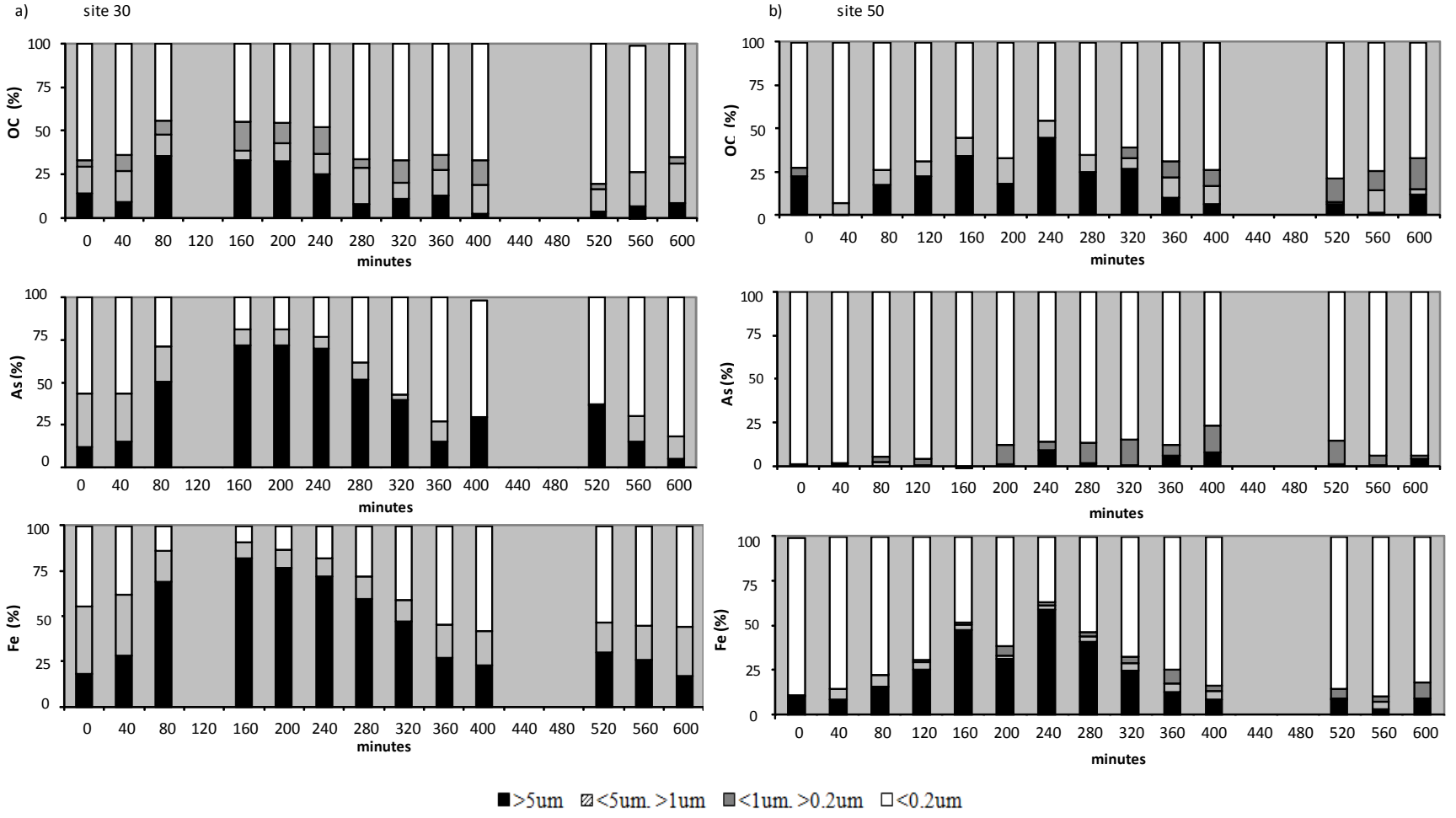

Figure 6.9 **Particle Size Distribution (PSD) of OC, As and Fe during discharge event. a) site 30, b) site 50.**

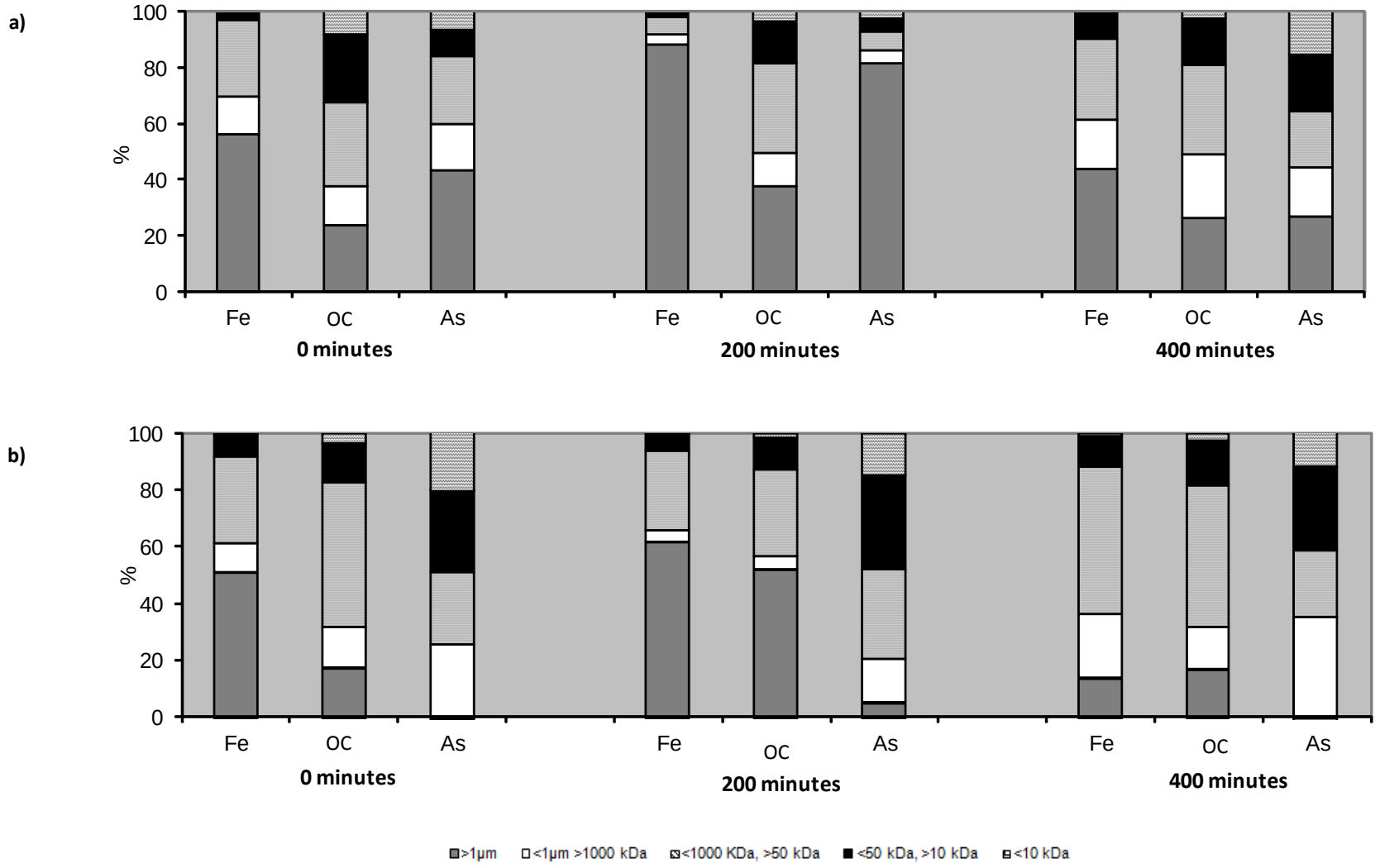

Figure 6.10 **Colloidal and Dissolved Particle Size Distribution (PSD) of Fe, OC and As during discharge event a) site 30, b) site 50.**

6.3.6 Influence of the Fe:OC ratio on the size distribution of As

While concentrations of OC were found to be similar between sites (Figure 6.6), the differing Fe concentrations within the catchment allow an opportunity to determine the effect of changing Fe:OC ratios on the size distribution of As. Previous work has shown the mobility of As to be dependent on the ratio of Fe:OC, with the proportion of As in colloidal and particulate size fractions increasing with increasing ratio (Bauer and Blodau, 2009). Given both similarity in PSD of As, Fe and OC and the determined correlations (Table 6.3) within our studied catchments, the control of the Fe:OC ratio on the size distribution of As was determined for both sites (Figure 6.11).

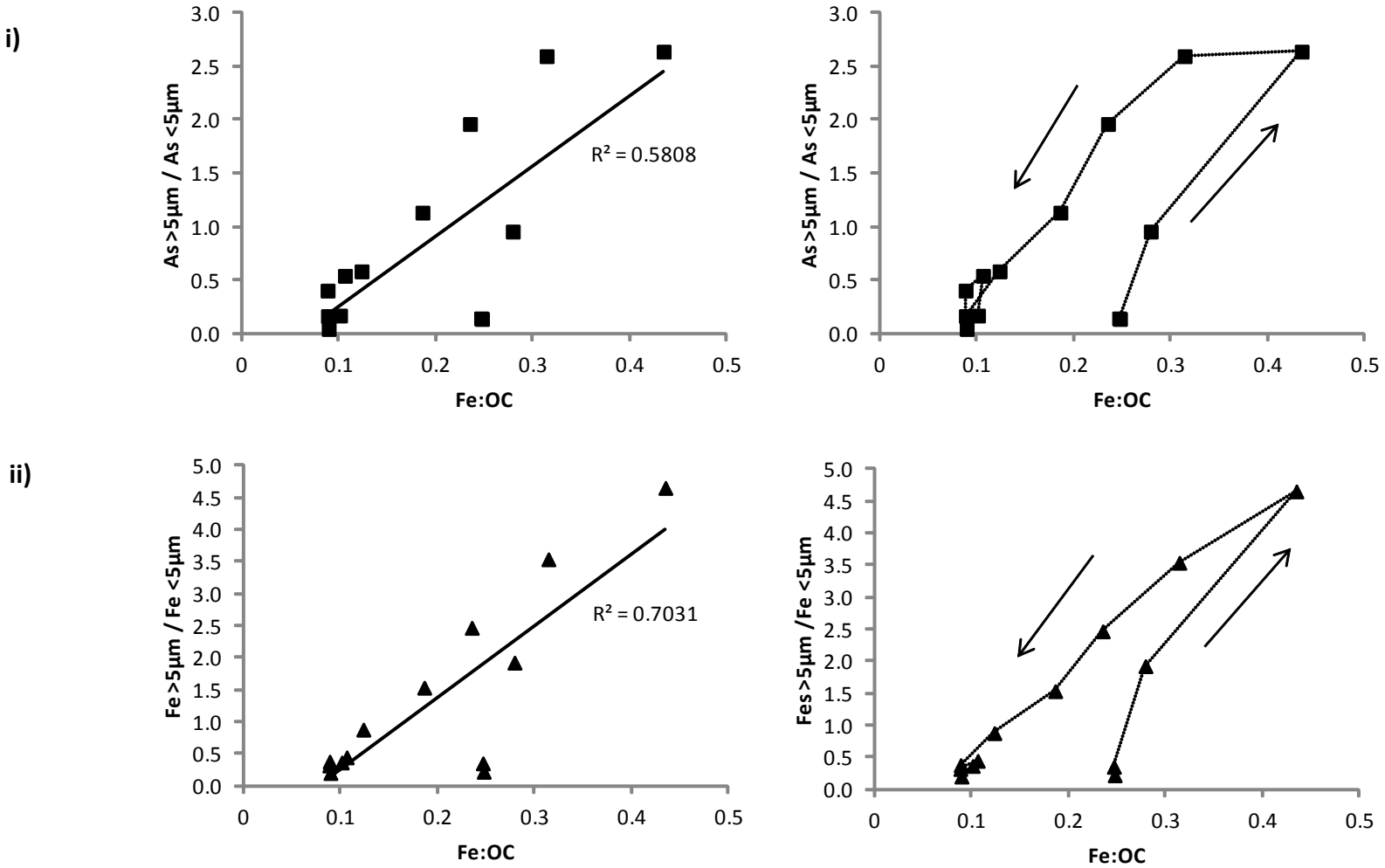

Figure 6.11 **Relationship between As and Fe size and Fe:OC at site 30. Change in size is demonstrated by shift from particle size >5 µm to <5 µm. i) site 30 As, ii) site 30 Fe. Right hand column treats data as a timeseries, arrows indicate direction of timeseries.**

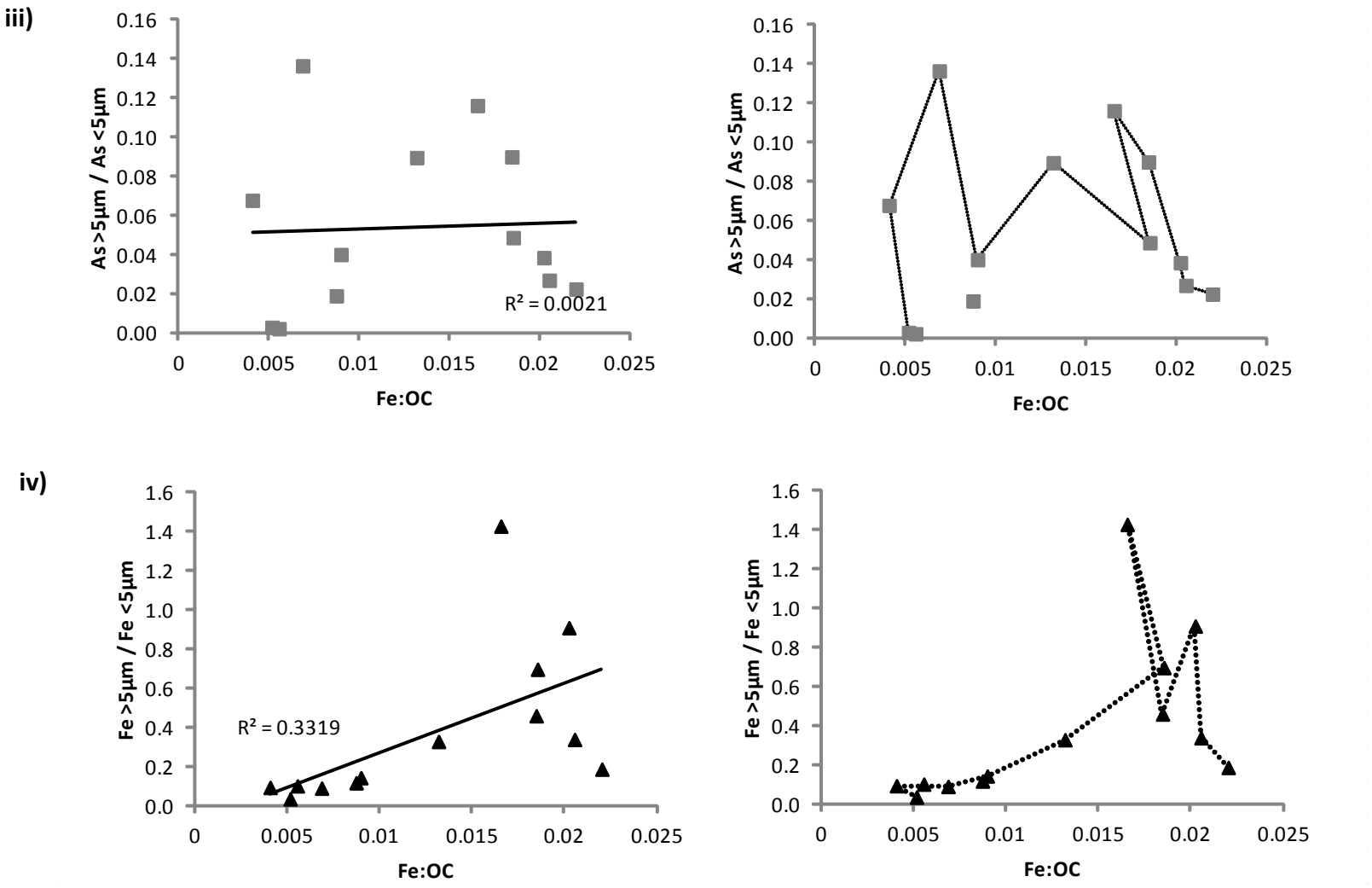

Figure 6.11(cont.) **Relationship between As and Fe size and Fe:OC at site 50. Change in size is demonstrated by shift from particle size >5 µm to <5 µm. iii) site 50 As, iv) site 50 Fe. Right hand column treats data as a timeseries.**

At site 30, considering As >5 µm/ <5 µm (Figure 6.11a, i), despite data scatter, a positive relationship can be seen with Fe:OC (R^2 0.56), indicating that As particle size increases with increasing Fe:OC. Treatment of the data as a timeseries is able to resolve the scatter and reveal the relationship displays hysteresis, with the relationship differing between the rising and falling limb of the hydrograph (Figure 6.11a, i). Such behaviour is suggestive of a temporal change in the Fe or OC present in the streamwater. Given the stability of the OC concentration, and the relationship between Fe and Fe:OC observed in Figure 6.8, a change in the quality of Fe is implicated. Probably, the availability of large (flocculated) Fe(oxy)hydroxides early in the Q event, as indicated by the size of Fe present, changing to smaller and/or even soluble Fe(II) later on.

Data from site 30 indicates the control of Fe:OC on the size of Fe appears to be nearly linear up to 0.43 (R^2 0.70, Figure 6.11a, ii), although this relationship also displays hysteresis. In laboratory based studies, the suspension of Fe in solution was found to decrease with an increasing Fe:OC ratio (Ritter et al., 2006), however the range over which this acted was subsequently noted to be limited to 0.02-0.1 (Bauer and Blodau, 2009). The observed difference between field and lab studies is possibly reflective of the difference in using natural Fe and OC. A positive relationship is initially seen between Fe size and Fe:OC, due to movement of the amorphous ponded Fe(oxy)hydroxides during the initial flush of the event. This particulate material is able to bind larger proportions of OC than the more soluble Fe(II) moved later in the event when the relationship is observed to become negative. Furthermore, despite high (>0.1) Fe:OC ratios in laboratory systems being shown to result in Fe and As > 0.2 µm, at site 30 <0.2µm Fe and As was always present even at Fe:OC = 0.43. In fact, truly dissolved As was present even at Fe:OC = 0.31 (Figure 6.10a). Clearly the stability of colloidal associations of As, Fe and OC in the natural environment differ significantly to laboratory studies.

In contrast to the behaviour of As at site 30, the lack of a relationship between As size and Fe:OC at site 50 (Figure 6.11b, iii) is in line with observations from previous laboratory studies, where the distribution of As was unaffected by changes in Fe:OC when the ratio was <0.02 (Bauer and Blodau, 2009). As seen in the PSD (Figure 6.10b), As present within site 50 is primarily within the dissolved and small colloidal size class, likely due to the dominance of OC saturating the particulate Fe present. The role of Fe:OC within our sites therefore appears to be dominated not only by the concentration of Fe present, but also the form of the Fe. The occurrence of amorphous Fe(oxy)hydroxides at site 30 (>5 µm) dominated the PSD of both As

and Fe, while at site 50 the low Fe:OC resulted in the coupling of Fe and OC, with As remaining in dissolved and colloidal associations.

6.4 Conclusions

Measurements of As concentrations under a range of hydrological conditions downstream of ombrotrophic peatlands in the Peak District, UK, illustrated the variability of the magnitude and composition of As flux within organic-rich stream environments. Measurement of several potential controlling variables allowed mobilisation processes to be identified and the recording of some of these at high temporal resolution allowed the generality of such processes to be recognised.

High temporal resolution monitoring was able to show that As export from these peat catchments is not a function of the physical erodibility of the peat, as similar fluxes were obtained for both vegetated and degraded subcatchments. The predominant occurrence of soluble As within both streams suggested that chemical transformation was the dominant control on mobilisation of As, specific transformations being those associated with the redox cycling of Fe within the peat.

High temporal resolution data also showed there was no direct relationship between As concentration and Q. Particular Q events, however, were responsible for the movement of significant proportions of As into the stream. Consequently, antecedent conditions relating to the storage of As within porewaters were an important factor controlling the transport of As from peatlands during rainfall events. Once mobilised, in-stream processing is a further control on As transportation, indicated by the mismatch of PSD in baseflow and porewaters of the vegetated site 30. Within the porewaters the PSD of Fe and OC were closely correlated, whilst As was present in smaller size fraction. However, in the baseflow streamwater, the PSD of As was correlated with that of Fe.

Within streamwaters the control exerted by the measured variables on the transportation of As changed over time. Arsenic was correlated with both Fe and OC to varying degrees dependent on both particle size and Q conditions. A high resolution time series of Q, concentrations and PSD during a Q event allowed causes to be ascribed to this variability. The concentrations of As, OC and Fe were elevated during the event in November 2010, with the transport of As at site 30 dominated by Fe, while OC dominated 50. Temporal variation in Q revealed that As concentrations displayed both proteresis and hysteresis, with differences in

the moisture conditions within vegetated and degraded peat potentially being responsible for the differing responses to Q events. The flushing of stored As from within site 30 may contribute to the increased As concentration observed within this stream during the initial period of elevated Q. Flushing of both mobilised Fe from within the peat, and pooled Fe(oxy)hydroxides into the oxic streamwaters at site 30 resulted in the dominance of particulate Fe within the stream.

Fe:OC ratios were found to vary within both sites. Ratios of Fe:OC below 0.02, as seen at site 50, did not exert any control over the particle size distribution of either Fe or As. On the other hand, within site 30 there was a linear relationship with increasing Fe size with increasing Fe:OC ratio. The high concentration of Fe present within the Site 30 subcatchment was the main contributing factor resulting in higher Fe:OC ratios. Despite OC-rich waters, the high concentration of OC present was unable to prevent the formation of Fe particulates. Particle size distribution revealed that As was closely coupled with Fe for the duration of the event at site 30, although As was never found solely within the particulate fraction, with the presence of dissolved and colloidal As found even above Fe:OC ratios of 0.2. The occurrence of high concentrations of Fe may dominate control of As within the aqueous phase even in organic-rich environments. Low Fe:OC ratio, as recorded at site 50, results in the PSD of OC more closely matching the PSD of Fe, suggesting the formation of aqueous Fe-OC complexes or the preferential binding of OC to Fe.

In addition to the role of Fe:OC ratio, the form of the Fe was also a key factor in the size of the transported As. The relationship between As and the Fe:OC ratio differed between the rising and falling limbs of the hydrograph. In the former previously pooled particulate Fe became mobilised and Fe(II) became oxidised whilst in the latter more soluble Fe(II) was probably present.

Given the different controls observed within the two subcatchments, relating to both the presence of Fe and OC, and the relative times of their entry to the stream, knowledge of the mixing order and ratio between Fe, OC, and As within natural waters may aid prediction of the mobility and ultimate fate of As.

6.5 References

Aguilar L, Thibodeaux LJ. Kinetics of peat soil dissolved organic carbon release from bed sediment to water. Part 1. Laboratory simulation. Chemosphere 2005; 58: 1309-1318.

Andreae M. Arsenic speciation in seawater and interstitial waters: The influence of biological-chemical interactions on the chemistry of a trace element. Limnology and Oceanography 1979; 24: 440-452.

Astrom M, Corin N. Abundance, Sources and speciation of trace elements in humus-rich streams affected by acid sulphate soils. . Aquatic Geochemistry 2000; 6: 367-383.

Barringer JL, Mumford A, Young LY, Reilly PA, Bonin JL, Rosman R. Pathways for arsenic from sediments to groundwater to streams: Biogeochemical processes in the Inner Coastal Plain, New Jersey, USA. Water Research 2010; 44: 5532-5544.

Bauer M, Blodau C. Mobilization of arsenic by dissolved organic matter from iron oxides, soils and sediments. Science of the Total Environment 2006; 354: 179-190.

Bauer M, Blodau C. Arsenic distribution in the dissolved, colloidal and particulate size fraction of experimental solutions rich in dissolved organic matter and ferric iron. Geochimica et Cosmochimica Acta 2009; 73: 529-542.

Benoit G. Evidence of the particle concentration effect for lead and other elements in fresh water based on ultraclean technique analyse. Geochimica et Cosmochimica Acta 1995; 59: 2677-2687.

Berg M, Stengel C, Trang PTK, Viet PH, Sampson M, Leng M, et al. Magnitude of arsenic pollution in the Mekong and Red River Deltas — Cambodia and Vietnam. Science of the Total Environment 2007; 372: 413-425.

Bissen M, Frimmel FH. Arsenic- a Review. Part 1: Occurrence, Toxicity, Speciation, Mobility. Acta Hydrochimica et Hydrobiologica 2003; 31: 9-18.

Blodau C, Fulda B, Bauer M, Knorr K-H. Arsenic speciation and turnover in intact organic soil mesocosms during experimental drought and rewetting. Geochimica et Cosmochimica Acta 2008; 72: 3991-4007.

Bowell RJ. Sorption of arsenic by iron oxides and oxyhydroxides in soils. Applied Geochemistry 1994; 9: 279-286.

Boyer EW, Hornberger GM, Bencala KE, McKnight DM. Response characteristics of DOC flushing in an alpine catchment. Hydrological Processes 1997; 11: 1635-1647.

Buschmann J, Kappeler A, Lindauer U, Kistler D, Berg M, Sigg L. Arsenite and arsenate binding to dissolved humic acids: Influence of pH, type of humic acid, and aluminum. Environmental Science & Technology 2006; 40: 6015-6020.

Charlet L, Polya DA. Arsenic in Shallow, Reducing Groundwaters in Southern Asia: An Environmental Health Disaster. Elements 2006; 2: 91-96.

Clark JM, Lane SN, Chapman PJ, Adamson JK. Link between DOC in near surface peat and stream water in an upland catchment. 5th International Symposium on Ecosystem Behavior. Elsevier Science Bv, Santa Cruz, CA, 2006, pp. 308-315.

Daniels SM, Agnew CT, Allott TEH, Evans MG. Water table variability and runoff generation in an eroded peatland, South Pennines, UK. Journal of Hydrology 2008; 361: 214-226.

Davis A, Atkins D. Metal distribution in Clark Fork River sediments. Environmental Science & Technology 2001; 35: 3501-3506.

Dixit S, Hering JG. Comparison of Arsenic(V) and Arsenic(III) Sorption onto Iron Oxide Minerals: Implications for Arsenic Mobility. Environmental Science & Technology 2003; 37: 4182-4189.

Filella M. Freshwaters: which NOM matters? Environmental chemistry letters 2009; 7: 21-35.

Fritzsche A, Rennert T, Totsche KU. Arsenic strongly associates with ferrihydrite colloids formed in a soil effluent. Environmental Pollution 2011; 159: 1398-1405.

Gaffney JW. Role of natural organic matter in controlling the behaviour of Fe in natural waters. School of Earth, Atmospheric and Environmental Science. University of Manchester, 2008.

Gaffney JW, White KN, Boult S. Oxidation state and size of Fe controlled by organic matter in natural waters. Environmental Science & Technology 2008; 42: 3575-3581.

Garnier JM, Hurel C, Garnier J, Lenoble V, Garnier C, Ahmed KM, et al. Strong chemical evidence for high Fe(II)-colloids and low As-bearing colloids (200 nm-10 kDa) contents in groundwater and flooded paddy fields in Bangladesh: A size fractionation approach. Applied Geochemistry 2011; 26: 1665-1672.

Ghosh MM, Yuan JR. Adsorption of inorganic arsenic and organoarsenicals on hydrous oxides. Environmental Progress 1987; 6: 150-157.

Gonzalez Z, Krachler M, Cheburkin A, Shotyk W. Spatial distribution of natural enrichments of arsenic, selenium, and uranium in a minerotrophic peatland, Gola di Lago, Canton Ticino, Switzerland. Environmental Science & Technology 2006; 40: 6568-6574.

Grafe M, Eick M, Grossl P, Saunders A. Adsorption of arsenate and arsenite on ferrihydrite in the presence and absence of dissolved organic carbon. Journal of Environmental Quality 2002; 31: 1115-1123.

Guo H, Zhang B, Zhang Y. Control of organic and iron colloids on arsenic partition and transport in high arsenic groundwaters in the Hetao basin, Inner Mongolia. Applied Geochemistry 2011; 26: 360-370.

Haque S, Ji JF, Johannesson KH. Evaluating mobilization and transport of arsenic in sediments and groundwaters of Aquia aquifer, Maryland, USA. Journal of Contaminant Hydrology 2008; 99: 68-84.

Haque SE, Tang J, Bounds WJ, Burdige DJ, Johannesson KH. Arsenic geochemistry of the great dismal swamp, Virginia, USA: Possible organic matter controls. Aquatic Geochemistry 2007; 13: 289-308.

Huang J-H, Matzner E. Mobile arsenic species in unpolluted and polluted soils. Science of the Total Environment 2007; 377: 308-318.

Islam FS, Gault AG, Boothman C, Polya DA, Charnock JM, Chatterjee D, et al. Role of metal-reducing bacteria in arsenic release from Bengal delta sediments. Nature 2004; 430: 68-71.

Krachler M, Emons H, Barbante C, Cozzi G, Cescon P, Shotyk W. Inter-method comparison for the determination of antimony and arsenic in peat samples. Analytica Chimica Acta 2002; 458: 387-396.

Lee JA, Tallis JH. Regional and historical aspects of lead pollution in Britain. Nature 1973; 245: 216-218.

Liang L, Morgan JJ. Chemical aspects of iron oxide coagulation in water: laboratory studies and implications for natural systems. Aquatic Sciences 1990; 51: 32-55.

Liu G, Fernandez A, Cai Y. Complexation of Arsenite with Humic Acid in the Presence of Ferric Iron. Environmental Science & Technology 2011; 45: 3210-3216.

Macalady DL, Ranville JF. The chemistry and geochemistry of natural organic matter (NOM). In: Macalady DL, editor. Perspectives in Environmental Chemistry. Oxford Press, New York, 1998.

Mandal BK, Suzuki KT. Arsenic round the world: a review. Talanta 2002; 58: 201-235.

Manning BA, Fendorf SE, Goldberg S. Surface structures and stability of arsenic(III) on goethite: spectroscopic evidence for inner-sphere complexes. Environmental Science & Technology 1998; 32: 2382-2388.

Masscheleyn PH, Delaune RD, Patrick WH. Effect of redox potential and pH on arsenic speciation and solubility in a contaminated soil. Environmental Science & Technology 1991; 25: 1414-1419.

Morel B, Durand P, Jaffrezic A, Gruau G, Molenat J. Sources of dissolved organic carbon during stormflow in a headwater agricultural catchment. Hydrological Processes 2009; 23: 2888-2901.

Pédrot M, Boudec AL, Davranche M, Dia A, Henin O. How does organic matter constrain the nature, size and availability of Fe nanoparticles for biological reduction? Journal of colloid and interface science 2011; 359: 75-85.

Pfeifer H-R, Gueye-Girardet A, Reymond D, Schlegel C, Temgoua E, Hesterberg DL, et al. Dispersion of natural arsenic in the Malcantone watershed, Southern Switzerland: field evidence for repeated sorption-desorption and oxidation-reduction processes. Geoderma 2004; 122: 205-234.

Pullin MJ, Cabaniss SE. The effects of pH, ionic strength, and iron-fulvic acid interactions on the kinetics of photochemical iron transformations. I. Iron(II) oxidation and iron(III) colloid formation. . Geochimica et Cosmochimica Acta 2003; 67: 4067-4077.

Puls RW, Powell RM. Transport of inorganic colloids through natural aquifer material: implications for contaminant transport. Environmental Science & Technology 1992; 26: 614-621.

Raven KP, Jain A, Loeppert RH. Arsenite and Arsenate Adsorption on Ferrihydrite: Kinetics, Equilibrium, and Adsorption Envelopes. Environmental Science & Technology 1998; 32: 344-349.

Ravenscroft P, Richards K, Brammer H. Arsenic Pollution: A Global Synthesis. Chichester, UK: Wiley-Blackwell, 2009.

Redman A, Macalady D, Ahmann D. Natural organic matter affects arsenic speciation and sorption onto hematite. Environmental Science & Technology 2002; 36: 2889-2896.

Ritter K, Aiken G, Ranville J, Bauer M, Macalady D. Evidence for the aquatic binding of arsenate by natural organic matter-suspended Fe(III). Environmental Science & Technology 2006; 40: 5380-5387.

Rothwell JJ, Evans MG, Daniels SM, Allott TEH. Baseflow and stormflow metal concentrations in streams draining contaminated peat moorlands in the Peak District National Park. Journal of Hydrology 2007; 341: 90-104.

Rothwell JJ, Taylor KG, Ander EL, Evans MG, Daniels SM, Allott TEH. Arsenic retention and release in ombrotrophic peatlands. Science of the Total Environment 2009; 407: 1405-1417.

Rothwell JJ, Taylor KG, Chenery SRN, Cundy AB, Evans MG, Allott TEH. Storage and Behavior of As, Sb, Pb, and Cu in Ombrotrophic Peat Bogs under Contrasting Water Table Conditions. Environmental Science & Technology 2010; 44: 8497-8502.

Rowland HAL, Pederick RL, Polya DA, Pancost RD, Van Dongen BE, Gault AG, et al. The control of organic matter on microbially mediated iron reduction and arsenic release in shallow alluvial aquifers, Cambodia. Geobiology 2007; 5: 281-292.

Seidel H, Mattusch J, Wennrich R, Morgenstern P, Ondruschka J. Mobilization of arsenic and heavy metals from contaminated sediments by changing the environmental conditions. Meeting on Phytoremediation. Wiley-V C H Verlag Gmbh, Leipzig, Germany, 2001, pp. 153-160.

Sharma P, Ofner J, Kappler A. Formation of Binary and Ternary Colloids and Dissolved Complexes of Organic Matter, Fe and As. Environmental Science & Technology 2010; 44: 4479-4485.

Sharma P, Rolle M, Kocar B, Fendorf S, Kappler A. Influence of Natural Organic Matter on As Transport and Retention. Environmental Science & Technology 2011; 45: 546-553.

Signes-Pastor A, Burlo F, Mitra K, Carbonell-Barrachina AA. Arsenic biogeochemistry as affected by phosphorus fertilizer addition, redox potential and pH in a west Bengal (India) soil. Geoderma 2007; 137: 504-510.

Smedley PL, Kinniburgh DG. A review of the source, behaviour and distribution of arsenic in natural waters. Applied Geochemistry 2002; 17: 517-568.

Stanger G, VanTruong T, Ngoc LTM, Luyen TV, Thanh TT. Arsenic in groundwaters of the Lower Mekong. Environmental Geochemistry and Health 2005; 27: 341-357.

Taylor G, Owens PN, Batalla RJ, Celso G. Sediment and contaminant sources and transfers in river basins. Sustainable Management of Sediment Resources. Volume 4. Elsevier, 2008, pp. 83-135.

Thanabalasingam P, Pickering WF. Arsenic sorption by humic acids. Environmental Pollution 1986; B: 233-246.

Tipping E, Smith EJ, Lawlor AJ, Hughes S, Stevens PA. Predicting the release of metals from ombrotrophic peat due to drought-induced acidification. Environmental Pollution 2003; 123: 239-253.

Todman M. Controls on water chemistry in an upland catchment. School of Earth, Atmospheric and Enviromental Sciences. PhD. University of Manchester, 2005.

Warwick PI, E.; Evans, N. . Environ. Chem. 2005, 2, 119–124. Arsenic's interaction with humic acid. Environmental Chemistry 2005; 2: 119-124.

WHO. Guidelines for drinking water quality. Vol. 1: Recommendations. World Health Organization, Geneva, 2004.

Williams PN, Zhang H, Davison W, Meharg AA, Hossain M, Norton GJ, et al. Organic Matter - Solid Phase Interactions Are Critical for Predicting Arsenic Release and Plant Uptake in Bangladesh Paddy Soils. Environmental Science & Technology 2011; 45: 6080-6087.

Worrall F, Burt T, Jaeban R, Warburton J, Shedden R. Release of dissolved organic carbon from upland peat. Hydrological processes 2002; 16: 3487-3504.

Xu H, Allard B, Grimvall A. Influence of pH and organic substance on the adsorption of As(V) on geologic materials. Water, Air and Soil Pollution 1988; 40: 293-305.

CHAPTER 7

Conclusions

7.1 The Occurrence and Mobility of As

This study has investigated the controls on arsenic (As) occurrence and mobility within two diverse environments (including both river environments and upland peat catchments) to further constrain controls on the mobility, behaviour, and ultimately transport of As. The four manuscripts contained within this thesis examine not only the total concentration of As within the solid phase, but using sequential extraction procedures (SEPs) have investigated the potential for mobilisation of As, through solid-phase associations. Variability in the controls on the mobility of As in both river sediments and upland peats under changing environmental conditions has been supported by a number of key observations, the making of which formed the objectives of this study.

These objectives, first presented in Chapter One, will each be revisited in this concluding Chapter.

7.1.1 To determine the retention and binding mechanisms of As within contrasting soils and sediments

The biogeochemical cycling of As within sediments of rivers and within organic rich upland environments is of concern due to the widespread occurrence of As within the natural environment and its toxicity. Within the studied field areas, As was found to not only be present above global averages for sediments and soils, but also was found to be contained within the labile, or more available part of the solid phase. However the phases responsible for storage of As within the solid phase have been found to vary depending on the environment.

Within both the Allier-Apremont and Loire-Imphy Rivers (France), As concentrations were above global averages for sediments, with the total As content of the sediment found to reflect the upstream geogenic contributions. Consistent with previous work on sediments (Blute et al., 2009; Dixit and Hering, 2003; Haque et al., 2008; Linge and Oldham, 2002; Masscheleyn et al., 1991). Iron (Fe) was found to play a key role in the retention of As within the sediment, with As found to be predominantly within the reducible phases associated with Fe-(oxy)hydroxide minerals in the sediments from both sites.

Seasonal changes in mineralogy may play a role in the mobility of As, with the storage of As found to redistribute between sequential extraction procedure's (SEPs) operationally defined phases targeting amorphous and then, crystalline Fe-(oxy)hydroxide minerals. During winter,

more As was associated with the fraction targeting amorphous Fe-(oxy)hydroxide minerals in the Allier-Apremont sediment, while in summer more As was found within the crystalline Fe-(oxy)hydroxide minerals. In the Loire-Imphy sediments a similar relationship is evident, with the amount of As associated with crystalline mineral phases increasing in summer

Within the peat of two upland subcatchments within Crowden Great Brook, Peak District (UK), considerable variability was found in both maximum total As concentration and its vertical distribution within apparently homogeneous microenvironments. Within the more vegetated subcatchment (site 30) peak As concentrations were considerably higher in one of the five sampled cores (core A, 50 $\mu g\ g^{-1}$) than in the others. Within the more eroded site 50, loss of peat was apparent from its thickness and the trace element profiles were similarly truncated compared to the uneroded cores. Of the three measured cores, two showed no evidence of accumulation of As, likely due to the losses through the physical act of erosion. However, one core was similar in its concentration profile to those observed at the vegetated site, showing the erosion process to be spatially heterogeneous.

The partitioning of As was found to be in contrast to lead (Pb). While Pb was found within the SEPs reducible fraction, As was found within the oxidisible fraction of the peat across both vegetated and degraded catchments. The exchangeable fraction was also highlighted as a key phase retaining As, indicating a possible role for Fe-minerals in As adsorption, although the reducible As contained likely within Fe-minerals was small. The importance of the oxidisible fraction suggested that organic matter is key to the retention of As within the ombrotrophic peat. From analysis of core A, the partitioning of As was found to vary with depth, with the exchangeable and reducible As present showing signs of post-depositional movement (PDM), whilst oxidisible and reducible As remained in a profile similar to that of Pb. This suggests that a proportion of As is being held by Fe/OM at the original deposition depth of peat.

7.1.2 Examine the potential for the use of Sr and Pb isotopes to provide insight into the mineralogical source of trace elements including As within riverbed sediment

Chapter 4 provided a first order basis on which to better understand the application of isotopic analysis in order to determine the mineralogical origins of sediments. The combination of isotopic analysis and SEP was able to provide information on the nature of both Pb and strontium (Sr) within the sediments, with important implications for understanding the

mobility of As within the studied systems. Although there was considerable difference in the partitioning of As within the sediments from the Loire and Allier Rivers (France), compared to both Sr and Pb, correlations between both As/Sr and As/Pb within each fraction were found, allowing the further investigation of isotopic composition.

As natural processes do not fractionate $^{87}Sr/^{86}Sr$ isotope ratios, the $^{87}Sr/^{86}Sr$ isotope ratios were used to provide information on the formation of important As storage phases within the sediment. Comparison of labile $^{87}Sr/^{86}Sr$ ratios to the reducible fractions showed that the formation of the crystalline Fe-minerals was occurring downstream from the more amorphous minerals, indicating the occurrence of the cyclic redox conditions required for ferrihydrite crystallisation. The degree to which this mineral transformation is taking place could have important implications for the transport of As, given the importance of reducible As within the sediments.

Use of Pb isotopes was also able to provide information on the geological contributions to the sediment. The variable Pb isotopic ratios obtained for the SEP indicated the presence of different reservoirs of Pb within the sediment, likely to be granites and basalts, with the composition affected by weathering processes. Anthropogenic Pb was not found to be significant within the sediments by comparison of $^{208}Pb/^{204}Pb$ vs. $^{206}Pb/^{204}Pb$ to known anthropogenic Pb domains, and by the lack of Pb associated with carbonates in the Allier-Apremont sediment. The source of other contaminants, including As is therefore more likely to be of geogenic origin.

7.1.3 Identify environmental processes contributing to the mobilisation of As from within both riverbed sediment and upland peat.

The labile nature of As stored within the solid phase of both studied sites indicates the importance of dynamic environmental processes in controlling the ongoing storage of As within the solid phase. Within the studied fluvial environments in France, riverbed sediments contained a reservoir of As able to be released under seasonal changes in environmental conditions. Use of batch incubation experiments were able to show how that the sediments are capable of the rapid release of As through both dissolution and desorption processes. Release of exchangeable and OM-associated As was seen under short term fluctuations in alkaline pH conditions, at pH values commonly experienced in both rivers during summer

months. Analysis of river sediments during summer supported the loss of labile As from the bed sediment, with minimal exchangeable As present. Both desorption and dissolution were found to be occurring within the sediments under anaerobic conditions. However, despite the importance of Fe in storage of As within the sediment, the Fe content of the sediment (as an indicator of the mineral content of the sediment), was not the only contributing factor to the release of As. Consideration of the composition of the sediments, including organic matter (OM) content, and microbiological factors is required in order to predict As mobilisation, in addition to the changes in environmental conditions.

Within the upland peat of Crowden Great Brook (UK), As was found to exhibit concentration profiles showing enrichment in surface layers, suggestive of PDM linked to the redox cycling of Fe. However, evidence of PDM was not apparent in all sampled cores within a subcatchment, as clear subsurface peaks, suggestive of the retention of As within the peat, were also found. Within subcatchments of similar topography, the difference in observed As profiles were found to be in correlation with the profiles of either Fe and Pb, two elements known for their divergent mobility behaviour. These observations suggest that the processes controlling the PDM of Fe and As are subject to local conditions not apparent from surface topography, with prediction of the occurrence of PDM not possible based on site location and surface conditions alone.

7.1.4 Assess transportation of As within organic-rich stream environments in order to understand the factors controlling size and therefore mobility of As in the aqueous phase.

Measurements of As concentrations under a range of hydrological conditions downstream of ombrotrophic peatlands in the Peak District, UK, illustrated the variability of the magnitude and composition of As flux within organic-rich stream environments. High temporal resolution monitoring was able to show that As export from the peat catchments was not a function of the physical erodibility of the peat. Calculated fluxes for two sites experiencing different levels of degradation were found to be comparable, with transport of soluble (<0.2 μm) As predominant for both sites. The transport of soluble As, as opposed to particulate As suggested that chemical transformation was the dominant control on mobilisation of As, specific transformations probably being those associated with the redox cycling of Fe within the peat. Given this, the role of antecedent conditions is an important factor controlling the storage of As within porewaters. While no direct relationship was found between As

concentration and discharge (Q), analysis of particular Q events illustrated the importance of these events in the movement of significant proportions of As into the stream(s).

Arsenic was correlated with both Fe and organic carbon (OC) to varying degrees dependent on both particle size and Q conditions. This general correlation with Q, directed further high temporal resolution monitoring of water chemistry during changing Q. During this Q event, the ratio of Fe:OC within the aqueous phase was found to vary, with ratios below 0.02 not exerting any control over the size of either Fe or As. Above this value increasing Fe size was evident with increasing Fe:OC ratio. Despite the high concentrations of OC present, in Fe-rich waters the particle size distribution (PSD) of As was closely coupled to Fe. However, despite the importance of particulate transport of both As and Fe under these conditions, As was never found solely within the particulate fraction, with the presence of dissolved and colloidal As found even above Fe:OC ratios of 0.2.

In addition to the role of Fe:OC ratio, the form of the Fe was also a key factor in the size of the transported As. Previously pooled particulate Fe becoming mobilised and Fe(II) oxidising altered the relationship between As and the Fe:OC ratio in the initial flush of water through the catchment following precipitation. After peak Q was experienced, the likely mobilisation of more soluble Fe(II) showed a different relationship between As and Fe:OC ratio indicating that information other then total concentration is required in order to assess the likely transport of As.

7.2 Future Research

The sediments of the Loire and Allier River, France, and the upland peat of the Peak District, United Kingdom, were shown to contain variable reservoirs of As able to be released into the aqueous phase. An understanding of the factors affecting mobilisation transport of As through fluvial systems is of key concern due to the need for safe drinking water supplies. Given the variability observed within this thesis, and the potential range of environmental processes controlling the mobility of As within the both environments, the following recommendations are made for future research:

- Further work exploring the storage of As within environments undergoing physical environmental changes, such as those occurring through the ongoing climate change: including erosion, acidification, increased precipitation and temperature (Atkinson et al., 2007; Taylor et al., 2008; Tipping et al., 2003). Additional batch experiments

utilising likely climate extremes may be useful in providing a potential range of behaviours likely to be experienced in the environment.

- The use of automatic water samplers on the Loire and Allier Rivers to achieve high resolution sampling would provide a better understanding of these rivers contribution to the transport of As to the Bay of Biscay, France. Investigations into the diurnal transport of As could provide more insight into rapid response of rivers sediments to changes in environmental conditions and therefore, the ongoing transport of As within the rivers.
- Given the association of As with Fe(oxy)hydroxides, the role of microbially assisted mineral dissolution should be explored. The contribution of microorganisms to As release with the soils/sediments can be evaluated initially through simple polymerase chain reaction (PCR) characterisation methods (Islam et al., 2004; Pederick et al., 2007).
- Given the importance of both Fe and OC in the transport of As, further work to determine the role of OC in controlling the PSD/behaviour of Fe(II) under low redox subsurface conditions is necessary. Use of laboratory simulations to monitor the role of NOM in controlling the oxidation rate of Fe(II) following exposure to air, and explore the importance of the order of mixing of OC, Fe and As, with analysis of field samples used to determine the validity of laboratory simulations.
- Additional characterisation of the OC present in the aqueous phase may provide information to explain the observed relationships between As and OC under different Q conditions.
- Future research utilising Sr and Pb isotopic analysis should look to build a database of sediments and waters in a wider range of aquatic environments. In order to advance understanding of the interchange occurring between phases, and the role of physicochemical changes on Sr and Pb isotopic composition, samples should cover a wide range of conditions, incorporating both source and downstream samples. Work to constrain the ratios of different endmembers, including minerals from As anomaly areas would also enable further exploration of obtained ratios.

7.3 References

Atkinson CA, Jolley DF, Simpson SL. Effect of overlying water pH, dissolved oxygen, salinity and sediment disturbances on metal release and sequestration from metal contaminated marine sediments. Chemosphere 2007; 69: 1428-1437.

Blute NK, Jay JA, Swartz CH, Brabander DJ, Hemond HF. Aqueous and solid phase arsenic speciation in the sediments of a contaminated wetland and riverbed. Applied Geochemistry 2009; 24: 346-358.

Dixit S, Hering JG. Comparison of Arsenic(V) and Arsenic(III) Sorption onto Iron Oxide Minerals: Implications for Arsenic Mobility. Environmental Science & Technology 2003; 37: 4182-4189.

Haque S, Ji JF, Johannesson KH. Evaluating mobilization and transport of arsenic in sediments and groundwaters of Aquia aquifer, Maryland, USA. Journal of Contaminant Hydrology 2008; 99: 68-84.

Islam FS, Gault AG, Boothman C, Polya DA, Charnock JM, Chatterjee D, et al. Role of metal-reducing bacteria in arsenic release from Bengal delta sediments. Nature 2004; 430: 68-71.

Linge K, Oldham C. Arsenic remobilization in a shallow lake: The role of sediment resuspension. Journal of Environmental Quality 2002; 31: 822-828.

Masscheleyn PH, Delaune RD, Patrick WH. Effect of redox potential and pH on arsenic speciation and solubility in a contaminated soil. Environmental Science & Technology 1991; 25: 1414-1419.

Pederick RL, Gault AG, Charnock JM, Polya DA, Lloyd JR. Probing the biogeochemistry of arsenic: Response of two contrasting aquifer sediments from Cambodia to stimulation by arsenate and ferric iron. Journal of Environmental Science and Health Part A 2007; 42: 1763-1774.

Taylor G, Owens PN, Batalla RJ, Celso G. Sediment and contaminant sources and transfers in river basins. Sustainable Management of Sediment Resources. Volume 4. Elsevier, 2008, pp. 83-135.

Tipping E, Smith EJ, Lawlor AJ, Hughes S, Stevens PA. Predicting the release of metals from ombrotrophic peat due to drought-induced acidification. Environmental Pollution 2003; 123: 239-253.

Appendix 1

Publications and Presentations

Publications

Hegan, A., Polya, D.A., 2008. Report on best practice for sampling and analytical protocols. Technical Report to the European Commission. Deliverable 5: AquaTRAIN (MRTN-CT-2006-035420) Geogenic Chemicals in Groundwaters and Soils: a Research Training Network

Millot, R., Hegan, A., Négrel, Ph. Geothermal waters from the Taupo Volcanic Zone, New Zealand: Li, B and Sr isotopes characterization. Applied Geochemistry. Submitted.

Mondal, D., Hegan, A., Rodriguez-Lado, L., Banerjee, M., Giri, A.K., Polya, D.A. 2008. Multiple regression analysis of As ground-water hazard and assessment of As-attributable human health risks in Chakdha Block, West Bengal. Mineralogical Magazine 72: 461-465.

Rodríguez Lado, L., Polya, D., Winkel, L., Berg, M. and Hegan, A., 2008. Modelling arsenic hazard in Cambodia: A geostatistical approach using ancillary data. Applied Geochemistry, 23: 3010-3018.

Rodríguez Lado, L., Polya, D.A. and Hegan, A., 2008. A logistic regression method for mapping the As hazard risk in shallow, reducing groundwaters in Cambodia. Mineralogical Magazine, 72(1): 437-440.

Presentations

Lado, L. R., Polya, D. A. & Hegan, A. (2008) A logistic regression method for mapping the As hazard risk in shallow, reducing groundwaters in Cambodia. Geochemistry of the Earths Surface, 8-12 August 2008, London, UK.

Rodríguez Lado, Luis., Hegan, Aimee., Polya, David (2008) Environmental Hazard Mapping using Auxiliary Variables and Logistic Regression Modelling: Arsenic Hazard in Shallow Reducing Groundwaters in Cambodia. The Central and Eastern Europe Conference on Health and the Environment (CEECHE) October 2008. Cluj Napoca, Romania

Hegan, A., Gaffney, J., and Boult, S. (2010) Controls on the mobility of As in natural waters: The role of the Fe/OC ratio. AquaTRAIN International Conference on Geogenic Chemicals in Groundwaters and Soils. July 2010. Orléans, France.

Hegan, A., Millot, R., Négrel, Ph., and Polya D.A. (2010) Occurrence of Arsenic in River Sediments: The use of isotopic analysis as a possible tracer of the mineralogical source. AquaTRAIN International Conference on Geogenic Chemicals in Groundwaters and Soils. July 2010. Orléans, France.

Appendix 2

Chapter 3 Supplementary data

Table S3-1 As release data- pH_{stat} incubation

WINTER	ALLIER	A		B		C		D		IMPHY	A		B		C		D	
	hours	As	pH	As	pH	As	pH	As	pH	hours	As	pH	As	pH	As	pH	As	pH
	2	1.9	6.49	12.1	7.97	26.7	8.64	138.3	9.81	2	10.8	7.15	8.8	7.70	34.4	9.12	52.0	9.99
	5	4.1	6.43	31.5	7.92	43.5	8.44	277.5	10.09	5	12.2	7.26	13.9	7.82	26.8	8.87	62.1	9.97
	24	4.8	6.73	16.4	7.95	43.9	8.44	434.2	9.99	24	13.8	7.53	17.0	7.94	38.4	8.68	83.3	9.87
	48	8.7	6.61	17.7	7.58	53.8	8.16	475.3	9.59	48	12.6	7.28	19.5	7.95	39.7	8.75	105.8	9.88
	72	4.3	6.65	19.5	7.85	91.2	8.60	559.1	9.82	72	11.8	7.39	18.6	7.94	46.0	8.60	116.3	9.87
	120	11.8	6.61	31.3	7.55	118.4	8.70	624.3	9.82	120	10.5	7.38	20.6	8.00	42.7	8.59	135.4	9.91
	168	22.6	6.74	28.5	7.63	129.6	8.54	502.2	9.79	168	8.2	7.18	14.0	7.55	52.3	8.50	142.4	10.01
	240	7.9	6.89	24.9	7.74	189.3	8.46	592.1	9.93	240	8.2	7.28	11.1	7.99	46.3	8.58	145.9	9.90
	336	8.6	6.78	24.5	7.54	148.5	8.26	547.5	9.61	336	7.1	7.31	13.4	7.71	67.0	8.81	194.7	10.30

SUMMER	ALLIER	A		B		C		D		IMPHY	A		B		C		D	
	hours	As	pH	As	pH	As	pH	As	pH	hours	As	pH	As	pH	As	pH	As	pH
	2	61.9	6.94	35.11	7.36	26.42	8.26	47.60	10.23	2	7.8	7.01	7.4	7.91	5.8	7.37	13.6	9.60
	5	17.57	7.00	14.43	7.99	173.6	8.47	96.15	9.91	5	4.7	7.12	14.0	7.55	37.4	7.94	39.1	10.03
	24	23.29	7.04	20.42	7.52	31.04	8.25	86.68	10.05	24	11.2	6.97	12.3	7.71	14.2	8.02	49.3	9.86
	48	35.92	7.20	25.7	7.44	35.77	8.31	100.2	9.91	48	8.4	6.88	11.1	7.44	57.6	8.53	88.5	10.01
	72	12.82	7.40	162.3	7.65	64.6	8.28	153.7	10.81	72	12.1	7.01	16.5	7.63	34.4	8.60	81.0	10.00
	120	11.57	7.14	15.87	7.64	36.33	8.34	159.6	10.41	120	10.4	6.91	15.8	7.58	38.0	8.60	85.7	9.85
	168	17.96	7.14	22.06	7.53	39.94	8.32	162.7	10.19	168	8.8	6.87	17.2	7.67	40.2	8.56	98.4	10.15
	240	17.44	7.05	62.31	7.82	82.6	9.43	185.3	10.42	240	4.7	6.81	15.9	7.62	87.6	8.34	124.5	9.91
	336	10.95	7.28	28.86	7.60	80.23	8.80	356.4	10.25	336	11.0	7.03	27.3	7.70	52.6	8.37	127.4	9.97

Table S3-2 **Summary of sequential extraction results**

		Arsenic (μg g^{-1})											
SAMPLE	**SAMPLE TREATMENT**	**XRF**	**F1**		**F2**		**F3**		**F4**		**F5**		**SUM**	**ERROR**
Imphy - Winter		6.4 ± 1.2	0.031 ±	0.001	0.566 ±	0.028	1.97 ±	0.05	**2.77 ±**	**0.33**	0.13 ±	0.03	5.46 ±	0.34
	pHstat (8)		0.011 ±	0.001	0.288 ±	0.010	1.67 ±	0.16	**4.09 ±**	**0.43**	0.06 ±	0.01	6.12 ±	0.46
	pHstat (10)		0.019 ±	0.001	0.227 ±	0.012	1.40 ±	0.13	**4.22 ±**	**0.55**	0.12 ±	0.00	5.99 ±	0.57
	microcosm (anaerobic)		0.044 ±	0.002	0.418 ±	0.028	**2.94 ±**	**0.02**	1.86 ±	0.05	0.02 ±	0.00	5.28 ±	0.06
	microcosm (aerobic)		0.034 ±	0.002	0.22 ±	0.004	**2.78 ±**	**0.52**	2.57 ±	0.33	0.08 ±	0.02	5.70 ±	0.16
Allier - Winter		15.8 ± 1.2	0.364 ±	0.060	3.600 ±	0.087	**5.46 ±**	**0.19**	3.08 ±	0.19	1.71 ±	0.05	14.22 ±	0.29
	pHstat (8)		0.009 ±	0.003	1.417 ±	0.129	3.95 ±	0.25	**6.56 ±**	**0.73**	0.06 ±	0.01	12.00 ±	0.78
	pHstat (10)		0.076 ±	0.002	1.377 ±	0.042	3.30 ±	0.24	**5.12 ±**	**0.24**	0.15 ±	0.02	10.02 ±	0.34
	microcosm (anaerobic)		0.015 ±	0.005	2.570 ±	0.183	**4.81 ±**	**0.10**	2.66 ±	0.17	0.37 ±	0.01	10.42 ±	0.27
	microcosm (aerobic)		0.015 ±	0.002	1.829 ±	0.020	5.23 ±	0.94	**4.19 ±**	**0.36**	1.82 ±	0.19	13.07 ±	1.02
Imphy - Summer		9.4 ± 1.2	0.011 ±	0.004	0.496 ±	0.026	2.71 ±	0.41	**4.26 ±**	**0.18**	1.12 ±	0.11	8.60 ±	0.46
Allier - Summer		12.4 ± 1.2	0.046 ±	0.015	0.609 ±	0.094	2.93 ±	0.21	**5.86 ±**	**0.86**	1.99 ±	0.56	11.43 ±	1.06

bold indicates major phase

Table S3-3 As release data- microcosm

Allier-winter

	As			
	Anaerobic		Aerobic	
hours		±error		±error
5	4.5	0.5	4.0	1.1
24	8.7	1.4	2.9	0.3
48	10.5	4.0	5.6	0.1
72	13.0	4.4	5.7	1.1
120	29.5	4.4	8.9	2.4
168	27.5	3.5	7.6	2.0
264	47.8	7.9	7.2	1.7
336	48.7	14.0	5.1	1.0

Imphy-winter

	As			
	Anaerobic		Aerobic	
hours		±error		±error
5	13.3	1.9	0.8	0.4
24	15.2	1.5	14.1	1.8
48	24.0	2.9	17.3	3.3
72	24.9	4.1	21.1	3.5
120	28.3	3.4	23.1	4.3
168	26.1	1.3	22.8	1.0
264	29.9	1.2	20.2	0.4
336	45.0	4.2	22.5	0.9

Allier-summer

	As			
	Anaerobic		Aerobic	
hours		±error		±error
5	12.8	0.4	10.2	0.6
24	16.1	0.8	13.1	0.3
48	26.8	2.9	15.1	0.8
72	36.9	1.3	14.9	0.7
120	44.1	4.4	17.8	0.7
168	63.0	0.9	17.3	0.6
264	72.4	1.9	21.1	0.3
336	77.0	2.4	24.0	0.4

Imphy-summer

	As			
	Anaerobic		Aerobic	
hours		±error		±error
5	8.3	0.1	6.9	0.1
24	10.6	0.2	7.3	0.2
48	13.3	0.4	8.1	0.1
72	15.3	0.1	8.6	0.2
120	16.7	0.5	10.2	0.2
168	19.6	0.4	10.3	0.2
264	22.8	0.6	8.7	1.9
336	26.9	0.5	12.7	0.6

Appendix 3

Chapter 5 Supplementary data

Table S5-1 Total digest and XRF full dataset

		As µg g^{-1}		Fe mg g^{-1}		Pb µg g^{-1}	
		XRF	digest	XRF	digest	XRF	Digest
	cm						
A	0-3	65.1	50.1	14.8	10.1	395.9	341.3
	3-6	28.7	24.1	4.8	2.4	651.5	543.7
	6-9	28.5	29.3	3.4	2.0	824.4	738.1
	9-12	15.5	16.9	3.3	2.2	367.6	329.3
	12-15	13.9		3.1		256.8	
	15-18	10.2	12.1	2.9	2.1	201.4	208.3
	18-21	9.4	14.4	2.8	2.0	165.7	137.5
	21-24	10.9	10.1	2.7	2.0	97.5	82.6
	24-27	12.3	8.0	2.5	1.7	64.6	53.4
	27-30	9.4	7.0	2.7	2.0	45.8	37.1
	30-33	10.8	7.4	2.6	1.9	27.2	28.6
B	0-3	26.5	28.6	9.1	1.9	701.6	219.2
	3-6	24.1	21.9	7.5	3.7	1018.1	671.7
	6-9	9.1	12.3	3.8	2.5	532.5	453.8
	9-12	8.5	7.3	3.6	2.9	350.7	296.4
	12-15	8.9	8.8	3.4	2.0	220.8	221.9
	15-18	12.3	7.9	2.0	1.4	98.6	124.8
	18-21	13	7.9	1.9	1.3	90.1	61.0
	21-24	9.8	6.3	2.1	1.5	50.1	44.5
	24-27	8	5.1	2.2	1.3	44.4	51.9
	27-30	8.5	4.4	2.2	1.3	32.2	27.9
	30-33	7.8	3.3	1.7	1.1	23.7	18.6
C	0-3	33.8	22.2	14.1	8.2	436.3	321.4
	3-6	19.6	18.6	6.2	3.4	921.1	966.5
	6-9	5.2		3.6		906.1	
	9-12	5.4	9.3	3.4	2.6	620.7	561.6
	12-15	6.4	7.5	2.9	2.1	332.1	297.4
	15-18	7.5	7.0	2.7	2.1	224.2	210.0
	18-21	9.2	8.1	2.7	2.0	191.5	137.4
	21-24	8.9		2.2		73.6	
	24-27		8.1		1.6		82.5
	27-30	10.9	8.9	1.6	1.3	27.0	27.5
	30-33	12.1	7.6	1.4	0.9	17.5	14.5

		As µg g^{-1}		Fe mg g^{-1}		Pb µg g^{-1}	
		XRF	digest	XRF	digest	XRF	digest
D	**0-3**	32.1	31.8	12.6	10.2	526.5	671.6
	3-6	7.3		11.2		805.7	
	6-9	4.3	10.5	2.7	1.9	542.5	806.3
	9-12	15.5		4.8		926.0	
	12-15	4		2.0		292.6	
	15-18		6.6		1.0		179.0
	18-21	8.3	6.0	1.0	0.8	69.9	105.9
	21-24	7.7		1.0		49.2	
	24-27	6.9	4.5	1.1	0.8	29.5	37.2
	27-30	8.2	5.3	1.0	0.8	36.9	46.7
	30-33	10.3	5.6	1.3	0.9	36.3	48.5
E	**0-3**	11.2		6.2		368.8	
	3-6	21.9	22.8	12.5	9.2	547.0	803.9
	6-9	25	26.2	4.8	2.5	827.0	734.1
	9-12	16.9	20.8	3.6	2.2	752.4	692.5
	12-15	11.2	16.2	3.8	2.7	660.3	652.5
	15-18	7.5	10.7	2.7	2.0	508.5	488.8
	18-21	6.6	7.2	2.2	1.7	264.6	248.2
	21-24	5.9	5.4	2.3	1.8	179.2	171.2
	24-27	5.8	5.5	2.1	1.6	132.4	122.4
	27-30		6.6		1.5		76.6
	30-33		6.7		1.2		48.6
F	**0-3**	2.3[a]	4.2	5.1	4.1	264.4	275.3
	3-6	1.1[a]	8.3	8.5	5.2	688.3	595.3
	6-9	4	12.4	10.8	6.4	893.0	807.4
	9-12	4.5	14.9	2.4	8.0	349.3	788.0
	12-15		11.8		6.6		647.6
	15-18	3.2	7.7	4.2	4.2	381.7	568.6
	18-21		5.2		3.3		264.0
	21-24	5.4		4.1		192.3	
	24-27	5.1	3.0	3.5	2.6	124.6	115.3
	27-30	4.4	2.2	2.4	1.7	73.9	59.2
	30-33		3.7		2.4		174.1

		As µg g^{-1}		Fe mg g^{-1}		Pb µg g^{-1}	
		XRF	digest	XRF	digest	XRF	Digest
G	0-3	4.2	3.0	2.6	1.8	173.0	161.6
	3-6	3	2.9	2.4	1.7	152.0	139.7
	6-9	3.9	2.8	2.2	1.5	137.1	107.7
	9-12	4	3.2	3.1	2.0	174.6	146.0
	12-15		1.0	3.6	2.6	15.1	13.8
	15-18	4.3	3.6	3.4	2.3	199.6	187.7
	18-21	4.2	3.4	2.8	2.0	174.2	172.5
	21-24	4	3.8	3.6	2.6	208.4	196.9
	24-27	3.4	3.5	3.6	2.4	243.7	221.9
	27-30	4.6	3.8	3.7	2.5	246.2	227.5
	30-33	2.4	4.4	3.5	2.8	256.9	250.6
H	0-3	3.3		3.1		25.4	
	3-6	2.7		3.5		13.7	
	6-9	4.3		3.4		168.6	
	9-12	3		1.8		8.9	
	12-15	2.3		1.8		5.8	
	15-18	1.6		1.9		5.6	
	18-21	2.5		1.5		3.7	
	21-24	2.4		0.9		2.9	
	24-27	1.9		0.8		3.4	
	27-30	1.7		0.8		1.7	
	30-33	1.9		0.6		1.7	

[a] Below XRF detection level

Table S5-2 Total digest replicate analysis

Sample			As µg g^{-1}	Pb µg g^{-1}	S mg g^{-1}	Fe mg g^{-1}
Core A	(0-3 cm)	1	57.0	547.1	4.0	12.3
		2	60.5	556.3	4.8	12.8
		3	56.4	577.0	4.2	12.4
		average	**58.0**	**560**	**4.4**	**12.5**
		sd	**2.2**	**15**	**0.4**	**0.3**
Core B	(30-33 cm)	1	4.8	38.0	3.5	1.3
		2	4.2	36.6	3.4	1.3
		3	4.7	41.8	4.1	1.5
		average	**4.6**	**39**	**3.7**	**1.4**
		sd	**0.3**	**3**	**0.4**	**0.1**
Core C	(9-12 cm)	1	11.9	1206	6.5	3.0
		2	10.0	981	5.2	2.5
		3	10.2	1031	5.4	2.6
		average	**10.7**	**1073**	**5.7**	**2.7**
		sd	**1.0**	**118**	**0.7**	**0.3**
Core B	(0-3 cm)	1	28.7	218	6.0	1.9
		2	28.4	221	5.4	1.9
		3	28.7	219	5.7	1.9
		average	**28.6**	**219**	**5.7**	**1.9**
		sd	**0.1**	**1**	**0.3**	**0.04**
Core A	(0-3 cm)	1	51.1	348	3.9	10.3
		2	49.1	334	3.8	10.0
		3	50.1	341	3.6	10.2
		average	**50.1**	**341**	**3.8**	**10.1**
		sd	**1.0**	**7**	**0.1**	**0.2**
Core C	(0-3 cm)	1	22.8	334	4.2	8.3
		2	21.6	309	3.9	8.1
		3	22.2	322	3.9	8.1
		average	**22.2**	**321**	**4.0**	**8.2**
		sd	**0.6**	**13**	**0.2**	**0.1**

			As µg g^{-1}	Pb µg g^{-1}	S mg g^{-1}	Fe mg g^{-1}
grit	basement	1	2.4	34.9	0.1	7.1
		2	2.3	36.9	0.1	7.0
		3	2.5	37.9	0.1	7.5

		average	**2.4**	**36.6**	**0.1**	**7.2**
		sd	**0.1**	**1.6**	**0.0**	**0.3**
Shale	basement	1	3.4	38.6	0.6	33.5
		2	3.2	36.9	0.5	32.8
		3	3.3	36.1	0.6	32.5
		average	**3.3**	**37.2**	**0.6**	**32.9**
		sd	**0.1**	**1.3**	**0.0**	**0.5**

			As	Pb	S	Fe
CRM	**NIMT/UOE/FM/001**		µg g^{-1}	µg g^{-1}	mg g^{-1}	mg g^{-1}
	Certified Value		2.44	174	-	921
		±	0.55	8	-	84
	Total digest 1		3.0	175	4158	940
	Total digest 2		3.3	183	4546	901
	Total digest 3		3.1	175	4284	877
		average	**3.1**	**178**	**4329**	**906**
		sd	**0.1**	**5**	**198**	**32**
	XRF		6.0	180		1189
		±	0.8	0.5		85